Université du Québec en Abitibi-Témiscamingue

CHANGEMENTS GLOBAUX ET DYNAMIQUES DES PESSIÈRES DU QUÉBEC-LABRADOR AU COURS DE L'HOLOCÈNE. APPROCHE RÉTROSPECTIVE DES INTERACTIONS FEU-CLIMAT-VEGETATION

Thèse
présentée
comme exigence partielle
du doctorat sur mesure en écologie forestière

Par
Jonathan Lesven

Août 2024

THÈSE DE DOCTORAT DE L'ÉTABLISSEMENT UNIVERSITÉ BOURGOGNE FRANCHE-COMTÉ

PREPARÉE AU LABORATOIRE CHRONO-ENVIRONNEMENT

École doctorale n°554

Environnements - Santé

Doctorat en Biologie des populations et écologie, par

Jonathan LESVEN

Changements globaux et dynamiques des pessières du Québec-Labrador au cours de l'Holocène. Approche rétrospective des interactions feu-climat-végétation.

Thèse présentée et soutenue à Besançon, le 03 juillet 2024

Composition du Jury :

Dr. Hugo ASSELIN, Professeur à l'UQAT, Rouyn-Noranda	Président du jury
Dr. Odile PEYRON, Directrice de recherche CNRS à l'ISEM, Montpellier	Rapportrice
Dr. Guillaume DE LAFONTAINE, Professeur à l'UQAR	Rapporteur
Dr. Florence MAZIER, Chargée de recherche CNRS, Toulouse	Examinatrice
Dr. François GILLET, Professeur à l'UFC, Besançon	Directeur
Dr. Yves BERGERON, Professeur à l'UQAT/UQAM, Rouyn-Noranda, Montréal	Directeur
Dr. Damien RIUS, Chargé de recherche CNRS à l'UFC, Besançon	Co-directeur
Dr. ANDRÉ ARSENAULT, Chercheur au Service Canadien des Forêts, Corner	Co-directeur

REMERCIEMENTS

La thèse de doctorat est souvent perçue comme l'accomplissement de quatre années d'un travail de recherche plus qu'exigeant, bien que passionnant. Pour moi, elle représente surtout la concrétisation de dix années de dévouement intense et d'efforts soutenus dans mes études universitaires, marquées par des joies, des peurs, des doutes, mais surtout par des aventures extraordinaires. Chaque étape de ce périple universitaire m'a façonné, enrichi, et m'a permis de repousser mes limites intellectuelles. Chaque obstacle surmonté, chaque découverte réalisée, chaque brin de connaissance acquis a contribué à forger ma détermination et ma passion pour la recherche. Ainsi, cette thèse incarne bien plus qu'un simple travail de recherche; elle symbolise l'aboutissement d'une décennie de dévouement, de persévérance et d'exploration intellectuelle, et elle représente un jalon significatif dans mes vies académique, professionnelle comme personnelle.

--- D'un intérêt scientifique à une passion paléoclimatique ---

Bien qu'attiré depuis toujours par les sciences et la recherche scientifique au sens large, cette thèse de doctorat n'aurait pu exister sans la passion qui m'anime pour les paléoclimats et l'histoire évolutive de notre planète.

Je tiens tout d'abord à remercier l'ensemble du personnel et des chercheurs de l'Université de Bretagne Occidentale (UBO), de l'Institut Universitaire Européen de la Mer (IUEM) et de l'Institut Français de Recherche pour l'Exploitation de la Mer (IFREMER) pour avoir enrichi mon parcours universitaire. Ces années ont largement contribué à développer ma passion pour les sciences naturelles lato sensu, au travers de la biologie et la géologie. Leur engagement envers l'excellence académique et la recherche a été une source d'inspiration constante.

Plus spécifiquement, l'année de licence 2 à Brest a largement contribué à changer ma vie, marquée en particulier par les enseignements passionnants d'Aurélie Penaud et

de Muriel Vidal. Je les remercie chaleureusement par la transmission de leur savoir et de leur passion, mais également pour ces trois semaines de stage qui m'auront fait découvrir le monde merveilleux de la palynologie aux côtés de Clément Lambert, que je tiens également à remercier chaleureusement.

--- *Vers l'Europe* ---

Brest est une ville bien connue pour être le départ des tours du monde maritimes. Le mien ne se sera pas fait à la tête d'un trimaran, mais plutôt à pied, en voiture, bus, car, canoë, train et avion. Ceux-ci m'ont amené à découvrir différents laboratoires, mais aussi différents écosystèmes à travers la France, l'Angleterre puis la péninsule ibérique.

Je remercie l'équipe du Department of Geography and Planning de l'Université de Liverpool – Fabienne Marret, Andrew Hacket-Pain, Abbie Wood, Paul Chavasse et l'ensemble des étudiants rencontrés – pour cette découverte de la dendrochronologie et pour mes premières reconstitutions de l'histoire passée de notre climat à l'été 2018. Merci pour cet accueil chaleureux en Angleterre, et bien sûr pour les quelques bières dans les pubs !

Mon périple paléoclimatique n'aurait bien sûr pas eu la même saveur sans ces stages de Master 1 et 2 au laboratoire EPOC de l'Université de Bordeaux en 2019 et 2020. Je tiens tout d'abord à adresser mes plus sincères reconnaissances à Maria-Fernanda Sánchez Goñi pour ses précieux conseils et sa formation rigoureuse en matière d'analyse pollinique, pour m'avoir accordé sa confiance sur les deux séquences sédimentaires étudiées, mais également pour avoir su garder le cap de l'encadrement malgré le confinement de 2020. Je tiens également à remercier Stéphanie Desprat et Anne-Laure Daniau pour les discussions constructives, et plus largement l'ensemble du laboratoire EPOC pour ces mois merveilleux et ce soutien.

Au-delà de l'encadrement, ce voyage au laboratoire EPOC a été marqué par des rencontres extraordinaires. Merci particulièrement à mes chères amies Tiffanie Fourcade (oui tu étais co-encadrante en M1, je ne l'oublie pas !) et Marion Genet (la reine des microcharbons et de l'enseignement) pour leur soutien indéfectible au cours de ces stages, et pour leurs encouragements perpétuels en période de concours. Tiff', j'espère que ton pied se remet progressivement du choc gravitationnel avec l'œuvre de Maurice Reille ! Je remercie également toutes les rencontres que j'ai pu rencontrer durant ces séjours, Charlotte, Coralie, Maëva, Baptiste, Audrey, pour ces bons moments que je n'oublierai jamais.

--- Un envol physique et intellectuel outre Atlantique ---

À la suite de mon Master 2 devaient se succéder de nombreux concours dans les écoles doctorales de France, afin d'espérer décrocher le Saint-Graal : une bourse de thèse. Ce voyage n'a pas été celui qui était prévu. Un seul concours à Besançon, et me voilà avec trois ans de financement en poche dans des thématiques qui me sont littéralement inconnues : paléoécologie, forêt boréale, Labrador, chironome ? Et l'océan alors ? De quoi dessécher le bon Breton que je suis !

Ce projet n'aurait bien évidemment pas été possible sans l'aide de mes quatre directeurs et codirecteurs. Merci à François Gillet pour sa disponibilité, sa réactivité, et surtout sa grande patience et ses conseils avisés avec un étudiant qui n'avait quasiment jamais touché à R il y a de cela quatre ans. Merci à Damien Rius pour sa confiance en moi, pour m'avoir accompagné, guidé et soutenu tout au long de ce doctorat, tout en me formant sur le comptage des (dizaines de milliers de) macrocharbons comptés au cours de cette thèse. Merci à André Arsenault pour ses conseils, ses suggestions pertinentes dans les différentes étapes de ce travail doctoral, mais également pour m'avoir fait découvrir les incroyables forêts labradoriennes au cours de dix jours de périple intense et de rencontres avec les communautés autochtones de la région, à l'été 2022. Enfin, cette thèse aurait eu un goût d'inachevé sans les remarques toujours pertinentes et la bienveillance propres à

Yves Bergeron, et sans ce suivi intellectuel rapproché, tout en étant souvent loin géographiquement. Bien que n'étant pas dans mon encadrement officiel, je tiens également à remercier dans ces quelques lignes Laurent Millet pour son enseignement en matière de paléoclimats nord-américains, de paléolimnologie, et pour sa formation sur les capsules céphaliques de chironomes. Malgré mes craintes, l'expertise de mes quatre (cinq) encadrants s'est révélée être un véritable atout pour mener à bien cette thèse de doctorat. Je les remercie tous pour leur disponibilité constante, leur rigueur scientifique et leur humanisme.

Je souhaite vivement remercier Odile Peyron, Florence Mazier, Guillaume de Lafontaine et Hugo Asselin pour avoir accepté, en tant que membres du jury, d'évaluer avec intérêt mes travaux de recherche. Merci également pour ces questions pertinentes et leur bienveillance au cours de la soutenance.

Je tiens également à remercier les membres de mes comités d'encadrement français et québécois – Adam A. Ali, Erwan Messager et Fabio Gennaretti – pour leur aide, leurs nombreux conseils et leur soutien au cours de l'ensemble des rencontres scientifiques qui ont jalonné ce parcours de thèse. J'adresse tout particulièrement à Adam A. Ali un grand merci pour les nombreuses discussions passionnées autour de nos thématiques de recherche, pour m'avoir fait confiance, encouragé, et plus simplement pour ces moments agréables partagés à la station de recherche de la Forêt d'Enseignement et de Recherche du Lac Duparquet (FERLD).

Merci à l'équipe du laboratoire Chrono-environnement pour son accueil, pour les nombreuses discussions au coin d'un couloir, et pour leur soutien sans faille durant ces quatre années. Un merci particulier à Isabelle, Émilie, Fanny, Charles-Henri, Estelle, Hélène pour ces discussions scientifiques – ou non – et pour leur aide et leurs encouragements permanents.

Je tiens à remercier l'ensemble de l'école doctorale Environnement-Santé (ED ES) de Besançon pour m'avoir accueilli en tant que doctorant, puis représentant des doctorants durant ces quelques années. Un merci particulier à Martine Gautheron,

Christelle Caillot et Nadine Bernard pour leur dévouement perpétuel et leur gentillesse.

Impossible de terminer cette thèse sans remercier mes camarades représentants des doctorants à l'ED ES de Besançon et chargés d'organisation du Forum des Jeunes Chercheurs (FJC) – Susie Gaillot, Eline Dubois et Sophie Cot – pour ces bons moments (de galère), mais aussi et surtout de plaisir. Merci à elles pour avoir toléré avec gentillesse ma non-présence pendant mes séjours outre-Atlantique. Plus largement, merci à tous les organisateurs du FJC pour ces deux jours mémorables, et pour ces bons moments passés au bar bien entendu !

Un merci particulier à Cécile C. Remy pour sa patience et sa bienveillance lors des séances d'explication de traitement des données de feux sur CharAnalysis ou tapas. Merci également pour ton aide précieuse tout au long de ce doctorat et des articles qui l'ont jalonné, et pour la préparation aux questions avant la soutenance.

Du côté québécois, je tiens évidemment à remercier Danièle Laporte et Marie-Hélène Longpré pour leur bonne humeur communicative, et pour avoir facilité mon périple dans les dédales de l'administration qu'une cotutelle de thèse exige, dont elles seules détiennent les secrets. Je ne pourrai jamais remercier suffisamment l'équipe de la FERLD – Yvan Poirier, Marie-Robin Myler, Danielle Charron, Raynald Julien – pour leur accueil dans cet endroit que j'apprécie tant, et pour ces bons moments de rire et d'échanges quotidiens. Je tiens également à remercier Marc-André Gemme pour son dévouement pour l'UQAT durant toutes ces années, qui nous manque grandement.

Je remercie chaleureusement l'équipe du laboratoire GEODE de l'Université Toulouse - Jean Jaurès pour leur accueil durant ces quelques semaines de comptage pollinique, en particulier Florence Mazier et Vanessa Py-Saragaglia. J'ai bien sûr une pensée pour Didier Galop, qui manque aujourd'hui cruellement au monde de la palynologie. Plus légèrement, merci à Gilbert pour les moments sympathiques passés autour d'un microscope, ou d'une bonne bière !

Merci également aux nombreux partenaires qui ont soutenu financièrement ce projet de recherche, mais également les déplacements et participations aux divers congrès et colloques scientifiques. Dans ce cadre, je remercie l'ED ES, l'ANR « Interarctic » (coord. Émilie Gauthier), le Belmont Forum « NICH-Arctic » (coord. Anne de Vernal), le projet de recherche international « Cold Forests » (coord. Adam A. Ali), le programme PEPS-INEE EPIDERME (coord. Damien Rius), le centre d'étude de la forêt (CEF), le programme Mitacs Globalink, ainsi que la Fondation J.A. DeSève et la Fondation de l'UQAT.

Un grand merci à l'Association des Palynologues de Langue Française (APLF) pour ces bons moments, pour ces rencontres scientifiques passionnantes, et tout simplement pour permettre à tous ces jeunes chercheurs de participer à des congrès à travers le monde au travers de leurs financements. Je retiendrai bien sûr cette belle rencontre à Paris en janvier 2022, même si cette aventure palynologique est loin d'être terminée.

Merci à l'extraordinaire équipe d'organisation du concours « Ma thèse en 180 secondes » à Besançon – Jeanne-Antide Léqué, Lionel Maillot, Robin Drieu, Jérémy Querenet –, à tous ceux qui ont vécu cette aventure avec moi, ainsi qu'au comité d'organisation de la demi-finale nationale à Paris. Une pensée particulière pour Rémi Dorgnier qui a vécu l'aventure parisienne avec moi. Des moments stressants, mais magiques, que je n'oublierai jamais.

J'adresse un remerciement sincère aux Premières Nations de l'est du Québec et du Labrador pour les échanges au cours de l'été 2022, ainsi que pour leur intérêt pour mes travaux de recherche.

J'aimerais également remercier tous les chercheurs des universités nord-américaines avec qui j'ai eu l'occasion d'échanger au cours de ces années sur des sujets tous plus passionnants et diversifiés les uns que les autres : Miguel Montoro-Girona, Guillaume Grosbois, Pierre Grondin, Pierre J.H. Richard, Pierre Drapeau, Fabio Gennaretti, Alain Leduc, Maxence Martin, Carsten Meyer-Jacob, Matthew Hurteau. Enfin, merci à

l'équipe du Groupe de Recherche en Écologie de la MRC-Abitibi (GREMA) pour leur accueil durant ces quelques jours à l'été 2022.

Cette thèse n'aurait pas été possible sans ceux qui m'ont entouré tout au long de l'avancement de ce projet de recherche, côté français comme québécois. Cette thèse n'aurait jamais vu le jour sans l'aide, les encouragements et le soutien indéfectible de Milva Druguet Dayras, ma chère co-bureau qui a traversé avec moi les épreuves du proposé de recherche, des revues de littérature interminables, et de l'examen doctoral, ainsi que quelques moments peu stables sur des rafiots québécois. Même si tu m'as lancé des stylos, obligé à faire des pauses 38 fois par jour, et soufflé ta fumée de cigarette au visage, cette thèse n'aurait jamais été ce qu'elle est aujourd'hui sans toi. Merci pour tout. Je remercie bien évidemment tous les copains de Besançon – Pierre, Cyril, Céline, Clara, Ariane, Elia, Claude, Aerine, Rémy, Alexandra, Ségolène, Anthony, Jordan, Romain, Laurie, Joshua, Léa, Augustin, Thomas, Justine, Anne-Lise, Victor, Kilian, Alexandre, Lorraine, Olivier, Lise, Mellina, et j'en oublie certainement, pour ces bons moments partagés au quotidien.

Côté québécois, mon séjour aurait été nettement moins agréable sans les précieuses rencontres faites à Rouyn-Noranda, Amos ou la FERLD : Marion B., Dorian, Aurélie, Corentin, Marianne, Nils, Marion L., Alex, Manon, Amélie, Maëlis, Thibaut, Jonathan, Amélie, Solène, Gabriel, Julie, Alexandre, Perrine, Lisa, et les autres étudiants. Je n'oublierai jamais ces moments passés en votre compagnie, à naviguer sur le lac Hébécourt, explorer les grands espaces québécois, et flâner sous les aurores boréales.

Je ne peux continuer ces remerciements sans mes brestois qui ont été inconditionnellement encourageants et représentent un support émotionnel depuis de si nombreuses années. À mes meilleurs amis Corentin et Jérémy qui ont partagé la quasi-intégralité de ma vie, à tous les copains depuis si longtemps que je ne peux compter les années – Geoffrey, Zazouille, Léna, Lisa, Marie-Anne – merci à tous pour simplement être vous-même.

Cette thèse n'aurait pas été possible sans le soutien et l'amour perpétuel de ma famille – tous les Lesven, Joussaume et apparentés – qui m'ont offert un cadre d'épanouissement personnel qui a tant contribué à la réussite de mes études primaires, secondaires comme universitaires, un énorme merci.

Enfin, cette thèse n'aurait jamais existé sans mes parents et mon frère Lucas qui, sans forcément comprendre mes choix et activités académiques (non maman, je n'étudie pas des grains de pollen du Jurassique !), m'ont perpétuellement soutenu et porté jusqu'à ce niveau d'étude. Bien évidemment à Élodie, qui me soutient depuis tant d'années et qui m'a encouragé perpétuellement à me dépasser et dépasser les limites de ce que je croyais possible, merci. Cette thèse vous est dédiée à tous les quatre.

Finalement, à tous les lecteurs de cette thèse qui trouveront un intérêt à mes travaux doctoraux, et qui peut-être un jour les continueront, merci.

Jonathan

ÉPIGRAPHE

"What you do makes a difference, and you have to decide what kind of difference you want to make."

J. Goodall

AVANT-PROPOS

Le corps de cette thèse de doctorat se décline en quatre chapitres centraux, faisant chacun l'objet d'une publication scientifique dans une revue internationale avec comité de lecture par les pairs. Ces différents articles scientifiques sont précédés d'une introduction générale elle-même constituée d'un état de l'art, des questions de recherche et objectifs traités dans ce travail doctoral, ainsi que du matériel et des méthodes utilisés. Les deux premiers articles (chapitre I et chapitre II) sont publiés, et les deux suivants (chapitre III et chapitre IV) sont en cours de finalisation avant soumission. La forme de ces différents chapitres peut par conséquent varier selon les revues visées. Les chapitres I à IV de cette thèse sont rédigés en anglais, alors que l'introduction et la conclusion sont rédigées en français. Ils sont suivis d'une conclusion résumant les travaux présentés et discutant leurs implications et limites, ainsi que les perspectives de recherche pour le futur. Chaque article scientifique devant être complet et se suffire à lui-même, certaines parties introductives ou méthodologiques peuvent apparaître redondantes au lecteur entre les différents chapitres de cette thèse.

Je suis le premier auteur de l'ensemble des chapitres présentés ci-après, et ai été le principal responsable des études, de l'échantillonnage des carottes sédimentaires, de leur analyse, et de la rédaction des articles. Chacun d'entre-eux résulte d'une étroite collaboration avec les différents coauteurs de chacun de ces travaux. Toutes les étapes de cette thèse, de la collecte des données à la soumission des articles, ont été possibles grâce à mes directeurs de recherche François Gillet et Yves Bergeron ainsi que mes co-directeurs Damien Rius et André Arsenault, qui sont par conséquent coauteurs de l'ensemble des articles. Le chercheur Laurent Millet, bien qu'extérieur à mon encadrement officiel, a également contribué à l'encadrement général de la thèse et aux réflexions autour des problématiques de recherche.

Le matériel étudié dans cette thèse a été prélevé au cours d'une campagne de terrain réalisée à l'été 2019 (*i.e.* plus d'un an avant le début de cette thèse de doctorat) par mes encadrants Damien Rius et Laurent Millet. Je n'ai par conséquent pas pu

participer au choix des sites, à la méthodologie de carottage utilisée, ni au transport des séquences prélevées. Parmi les coauteurs extérieurs à mes encadrants, Milva Druguet Dayras et Jonathan Cazabonne ont contribué au chapitre I en apportant leur expertise sur les épidémies d'insectes et maladies/parasites affectant l'épinette noire, respectivement. Milva Druguet Dayras a également participé à l'acquisition des données anthracologiques nécessaires aux chapitres II à IV. Romain Borne a apporté ses connaissances en codage Java pour développer la macro utilisée dans le chapitre II, de même que Cécile C. Remy pour les analyses des données de feux qui sont largement utilisées dans les chapitres suivants. Thomas Suranyi, Augustin Feussom-Tcheumeleu et Lisa Bajolle ont contribué au chapitre III en apportant les données de chironomes modernes et/ou fossiles, et Adam A. Ali a joué un rôle de supervision externe et de réflexion quant aux questions de recherches. De nombreux coauteurs sont également associés au chapitre IV en raison de leurs implications précédemment évoquées pour les reconstitutions des paramètres de feu ou du climat. Tous les coauteurs ont également contribué aux différents articles scientifiques en relisant et modifiant les manuscrits aux différentes étapes du processus de publication. Ce travail de doctorat n'aurait par conséquent pas été possible sans l'ensemble d'entre eux.

Introduction générale

Chapitre I. Lesven, J. A., Druguet Dayras, M., Cazabonne, J., Gillet, F., Arsenault, A., Rius, D., Bergeron, Y. (2024). Future impacts of climate change on black spruce growth and mortality: Review and challenges. *Environmental Reviews*, 32-(2), 214-230. https://doi.org/10.1139/er-2023-0075

Chapitre II. Lesven, J., Druguet Dayras, M., Borne, R., Remy, C. C., Gillet, F., Bergeron, Y., Arsenault, A., Millet, L., Rius, D. (2022). Testing a new automated macrocharcoal detection method applied to a transect of lacustrine sediment cores in eastern Canada. *Quaternary Science Reviews*, 295, 107780. https://doi.org/10.1016/j.quascirev.2022.107780

Chapitre III. Lesven, J., Millet, L., Gillet, F., Suranyi, T., Feussom-Tcheumeleu, A., Bajolle, L., Bergeron, Y., Arsenault, A., Remy, C. C., Ali, A. A., Rius, D. (*en préparation*

pour Geophysical Research Letters). Influence of environmental factors on pollen- and chironomid-based Holocene temperature inferences: a multisite comparison in eastern Canada.

Chapitre IV. Lesven, J., Gillet, F., Bergeron, Y., Arsenault, A., Ali, A. A., Druguet Dayras, M., Millet, L., Remy, C. C., Rius, D. (*en préparation pour Journal of Ecology*). Deciphering the roles of temperature and fire on vegetation dynamics along a North-South transect in eastern Québec and Labrador.

Conclusion générale

TABLE DES MATIÈRES

LISTE DES FIGURES

LISTE DES TABLEAUX

LISTE DES SIGLES ET DES ABRÉVIATIONS

AMS : Accelerator mass spectrometry

ANOVA : Analysis of variance

AUR : Lac Aurélie

BB : Biomasse brûlée

BCI : Bootstrap confidence intervals

BIL : Lac Billy

BLH : Lac Blow Hole

BP : Before present (ref. 1950)

CAZ : Chironomid assemblage zone

CA : Correspondence analysis

CCA : Canonical correspondence analysis

CHAR : Charcoal accumulation rate

CONISS : Constrained incremental sum of squares

CMI : Climate moisture index

CRS : Constant rate of supply

DCA : Detrended correspondence analysis

ESB : Eastern spruce budworm

FACE : Free-air CO_2 enrichment

FF : Fire frequency

FRI : Fire return interval

FS : Fire size

GAM : Generalised additive model

GIEC : Intergovernmental Panel on Climate Change

GDP : Gross domestic product

GOF : Goodness-of-fit

HTM : Holocene thermal maximum

LOESS : Locally weighted scatterplot smothing

ka cal BP : kilo calibrated years before present

MAT : Modern analogue technique

MIS : Lac Mista

MSAT : Mean summer air temperature

NA : North America

NPP : Net primary productivity

PAZ : Pollen assemblage zone

PEA : Petit Anne Lake

PCA : Principal component analysis

PIMA : *Picea mariana* (épinette noire)

ppm : Parties par million

RCP : Representative concentration pathway

RegFF : Regional fire frequency

RGB : Red-green-blue

RMSE : Root mean square error

SNI : Signal to noise index

SqRL : Squared residual length

TRE : Lac Tremblay

WA-PLS : Weighted average – Partial least squares

yr cal BP : Calibrated years before present

ΔT : Différence de température

xxx

LISTE DES SYMBOLES ET DES UNITÉS

mm^2 : Millimètre carré

km^2 : Kilomètre carré

µm : Micromètre

cm : Centimètre

m : Mètre

km : Kilomètre

yr : Année

°C : Degré Celsius

RÉSUMÉ

Les changements climatiques représentent désormais une réalité indéniable, et leurs conséquences sur l'environnement sont plus tangibles chaque jour. Les écosystèmes boréaux représentent un enjeu considérable d'un point de vue climatique, économique comme écologique. Émerge ainsi l'importance de mieux comprendre leur dynamique, afin de garantir leur résilience face aux défis climatiques actuels et futurs. Les approches rétrospectives apparaissent alors comme essentielles afin de fournir une banque d'expériences passées servant de point de référence pour le futur. Cependant, la régionalité du climat, des régimes de perturbations et par conséquent de la végétation dans l'est du Canada empêche une généralisation des données à des échelles supra-régionales. Comparativement aux régions plus occidentales, l'est du Québec et le Labrador sont marqués par un climat plus océanique, des fréquences de feu plus faibles, un relief plus vallonné, et une végétation différente. Bien qu'un intérêt croissant ait été porté à l'étude des forêts boréales dans les dernières décennies, l'est du Québec et le Labrador restent peu étudiés à l'échelle millénaire. L'ambition générale de cette thèse de doctorat est d'examiner les dynamiques passées de la végétation au cours du temps – en particulier celle de l'épinette noire (*Picea mariana* (Mill.) B.S.P.) – en lien avec l'évolution des régimes de perturbations et du climat, le long d'un transect nord-sud situé dans l'est du Québec et au Labrador. Plus spécifiquement, elle vise à apporter de nouvelles connaissances sur la réponse de ces régions aux changements climatiques au travers d'approches synthétiques, méthodologiques comme analytiques.

La première partie de cette thèse révèle à partir d'une synthèse bibliographique que les régions de l'ouest et du centre du Canada vont subir les plus importants épisodes de mortalité et les plus fortes réductions de croissance, en particulier dû à l'accroissement du déficit hydrique. À l'inverse, les forêts de l'est du Canada apparaissent comme moins impactées et donc plus résilientes, en particulier dans les régions septentrionales. Cependant, notre étude révèle que d'autres facteurs comme les épidémies d'insectes, les maladies et le gel pourraient également induire des réductions de croissance et des épisodes de mortalité importants dans ces régions. Dans un second temps, une étude paléoécologique en trois chapitres a permis de reconstituer l'histoire des feux, du climat et de la végétation à l'est du Québec et au Labrador. L'analyse des macrocharbons, des capsules céphaliques de chironomes et des grains de pollen a permis de décrypter les rôles respectifs des températures estivales de l'air, de la fréquence et de la taille des feux sur les trajectoires de végétation le long d'un transect Nord-Sud à l'est du Canada. Le partitionnement de variation et les modèles additifs généralisés utilisés montrent une réponse différentielle en fonction de la latitude. La toundra forestière du Labrador présente des épisodes de densification des peuplements lors des périodes chaudes avec des fréquences d'incendies élevées, mais à l'inverse une ouverture des peuplements durant les périodes froides marquées par des évènements de feu. Dans les pessières ouvertes, aux latitudes intermédiaires, les températures jouent un rôle négligeable sur la dynamique de végétation, contrôlée majoritairement par les feux de forêt (fréquence et taille). À l'inverse, la température joue un rôle substantiel dans les pessières

fermées au sud du transect. Enfin, nos données soulignent une augmentation récente de la taille des feux, associée à une diminution de l'abondance relative de l'épinette noire et une augmentation des taxons typiques de milieux ouverts. Dans un contexte de changements climatiques et d'accroissement de la fréquence et de la taille des feux, différentes trajectoires de végétation peuvent ainsi être envisagées selon la latitude.

Mots-clés : Forêt boréale, Holocène, Sédiments lacustres, Feu, Macrocharbon, Végétation, Pollen, Climat, Chironome, Québec, Labrador, Paléoécologie.

Keywords: Boreal forest, Holocene, Lake sediments, Fire, Macrocharcoal, Vegetation, Pollen, Climate, Chironomid, Quebec, Labrador, Paleoecology.

INTRODUCTION

En l'espace de quelques décennies, le changement climatique d'origine anthropique s'est révélé comme l'enjeu le plus urgent et universel de notre époque. Les chercheurs du monde entier s'accordent presque unanimement sur le fait que les activités humaines, en particulier les émissions de gaz à effet de serre résultant de l'utilisation des combustibles fossiles, sont le principal moteur des modifications récentes du climat (IPCC, 2022). De l'augmentation des perturbations naturelles affectant la sécurité alimentaire de plusieurs milliards d'êtres humains à l'extinction massive d'espèces ou la montée rapide du niveau marin, le récent rapport de synthèse du Groupe d'experts Intergouvernemental sur l'Évolution du Climat (GIEC) (IPCC, 2022) a mis en exergue le fait que les impacts du changement climatique seront pires qu'évalués précédemment (voir IPCC, 2007; Field et al., 2014). Ils ont et auront des répercussions profondes et irréversibles sur les humains comme les écosystèmes à l'échelle mondiale, soulignant l'importance de mesures d'adaptation rapides (IPCC, 2022).

Parmi ces écosystèmes, les forêts constituent un enjeu majeur. Elles abritent près des trois quarts de la biodiversité terrestre (Thompson, 2009), contribuent à l'économie mondiale (Pearce, 2001) à hauteur de 145.10^{18}\$/an (Costanza et al., 2014), et stockent 861 ± 66 Pg de carbone à l'échelle planétaire (Pan et al., 2011). Cependant, les écosystèmes forestiers sont aujourd'hui largement menacés par les pressions naturelles comme anthropiques (McDowell et al., 2020), mettant ainsi en exergue l'importance cruciale de leur gestion, préservation et réhabilitation (FAO, 2012; Field et al., 2014). Mais malgré les menaces auxquelles elles sont soumises, les forêts démontrent une remarquable capacité naturelle à maintenir leurs structures et fonctions écologiques après les perturbations (Thompson, 2009). Cette aptitude définit la résilience des écosystèmes. Une perte de résilience implique la possibilité de changements brusques et irréversibles des trajectoires écologiques, qui pourraient par conséquent altérer profondément les biens et services rendus par les écosystèmes forestiers. Cependant, les changements climatiques prévus dépassent largement l'expérience humaine et la portée des données instrumentales disponibles

(Hayhoe et al., 2017; IPCC, 2022), et pourraient en conséquence surpasser les capacités d'adaptation et de résistance connues des écosystèmes (Rockström et al., 2009). Émerge alors la nécessité d'explorer l'histoire des forêts, afin d'en retracer leur dynamique passée et d'apporter des connaissances sur la manière dont les changements climatiques ont affecté les capacités d'adaptation des écosystèmes forestiers au cours du temps (Johnstone et al., 2016). Cependant, cette tâche demeure complexe en raison d'une « compréhension inégale des échelles temporelles et spatiales interdépendantes des réponses des écosystèmes » (IPCC, 2007).

Dans ce contexte, la paléoécologie permet de reconstituer la composition et la structure de la végétation ainsi que les régimes climatiques ou de perturbation les affectant, en couvrant différentes intensités d'impacts anthropiques (Lindbladh et al., 2013). À la différence des inventaires forestiers traditionnels, de la télédétection ou de la dendroécologie, dont la portée temporelle est généralement limitée aux dernières années ou décennies ou aux derniers siècles, cette discipline adopte une approche multi-indicateurs permettant d'explorer des échelles de temps plurimillénaires (Figure 1). C'est dans ce contexte que s'inscrit cette thèse de doctorat, dont le but est d'améliorer notre compréhension de la dynamique forestière sous l'influence du climat et des régimes de perturbations de l'est du Canada au cours des derniers milliers d'années.

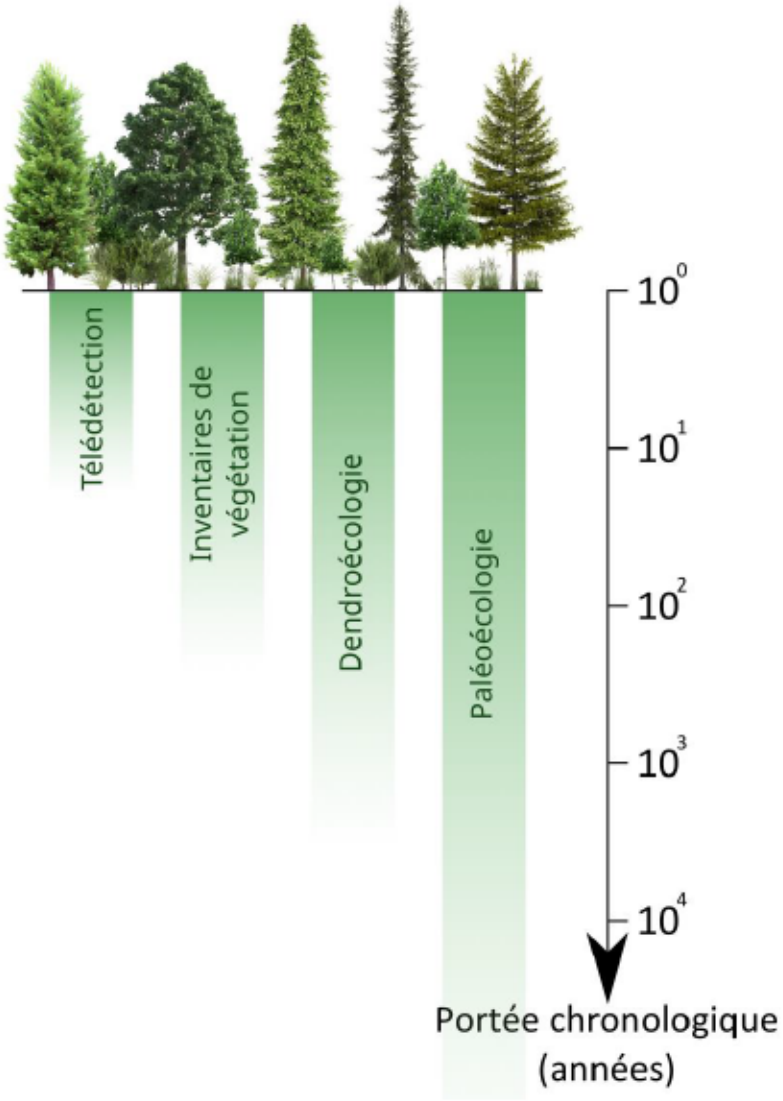

Figure 1
Portée chronologique de différentes méthodes d'étude de la dynamique des forêts et de leur environnement au cours du temps.

Le biome boréal. ***Importance et enjeux.*** Formant une large ceinture dans les latitudes circumpolaires de l'hémisphère nord, le biome boréal s'étend approximativement entre 47 et 70 degrés de latitude nord (Gauthier et al., 2015). Les forêts boréales recouvrent quelque 12 millions de km², correspondant à 11% de la surface terrestre mondiale (Burton et al., 2003) ou environ un tiers (30%) de la surface

forestière mondiale (Gauthier et al., 2015). En conséquence, elles constituent l'un des biomes les plus vastes de la planète, bien que parmi les plus jeunes, ayant évolué depuis le retrait des inlandsis à la fin de la dernière période glaciaire (Brandt et al., 2013), dont les plus récents ont disparu il y a environ 5700 ans cal BP (Dalton et al., 2020). Elles sont aujourd'hui considérées comme parmi les derniers grands biomes intacts pouvant encore être protégés (Ministère des Ressources naturelles et de la Faune, 2008). En plus de leur importance écologique indéniable, elles présentent une valeur traditionnelle majeure pour les peuples autochtones (Berkes et Davidson-Hunt, 2006; Oberndorfer, 2020), comme économique, sociale et culturelle pour le reste des populations humaines (Hassan et al., 2005; Johnson et Miyanishi, 2012).

Bien que relativement peu peuplés, les écosystèmes boréaux jouent un rôle crucial en fournissant de multiples biens et services essentiels aux activités humaines. Parmi ceux-ci, ils contribuent à plus de 33% de l'approvisionnement mondial en bois (construction, chauffage) ainsi qu'à 25% de la production mondiale de papier (Mery et al., 2010). Ils assurent également la régulation des phénomènes naturels (inondations, maladies) (Brandt et al., 2013), limitent l'érosion par le maintien des sols (Costanza et Limburg, 1997), et offrent un espace privilégié pour la pratique d'activités culturelles (Hassan et al., 2005). L'extraction de ressources naturelles non renouvelables (e.g. nickel, platine, uranium, cobalt, or, fer), comme la production d'énergies renouvelables (hydroélectricité) y est également pratiquée (Roberts et al., 2006; Bogdanski, 2008). En outre, les forêts boréales agissent comme un puits de carbone, absorbant environ 500 Tg de carbone par an, et jouent par conséquent un rôle majeur dans l'aide au maintien de l'équilibre climatique mondial par le biais du cycle du carbone (Pan et al., 2011). Bien que souvent perçues comme de vastes étendues sauvages inhabitées (Johnson et Miyanishi, 2012), ces forêts ont été et continuent d'être habitées par de nombreuses communautés autochtones, qui bénéficient des ressources des écosystèmes forestiers pour la chasse, la pêche, la cueillette ou les activités culturelles (Teitelbaum et al., 2023). Dans un contexte de changements globaux, il devient impératif de comprendre la dynamique de ces écosystèmes à des échelles de temps pluriséculaires à plurimillénaires. Cette

compréhension s'avère essentielle afin d'aider les gestionnaires à anticiper et à orienter l'atténuation des changements climatiques dans les écosystèmes boréaux, avec des cibles et des objectifs réalistes (Lindbladh et al., 2013).

Des entités dynamiques. À travers les variations de température, de précipitation et de dioxyde de carbone, le climat représente le forçage majeur de la variabilité naturelle et la dynamique des écosystèmes boréaux (Brooks et al., 1998; Barber et al., 2000; Yin et Berger, 2012; PAGES, 2016), et influence la répartition spatiale et la reproduction des espèces végétales (Hamann et Wang, 2006; Messaoud et al., 2007; Soja et al., 2007). Cependant, d'autres facteurs abiotiques tels que la topographie, le régime des vents, l'épaisseur du couvert nival ou les inondations influent également sur la composition, la structure comme la dynamique de la végétation boréale (Irland, 2000; Denneler et al., 2008; Gauthier et al., 2015). Surimposée à cela, la dynamique des écosystèmes boréaux est étroitement liée aux régimes de perturbations naturelles, tels que les incendies, les épidémies d'insectes ravageurs et les maladies, opérant à différentes échelles spatiales et temporelles (Johnson, 1996; McCullough et al., 1998; Kneeshaw et Bergeron, 1998; Brandt et al., 2013). Parmi ceux-ci, les feux de forêt représentent des processus écologiques majeurs contribuant au développement spatial comme temporel d'une mosaïque de végétation variant en âge, en structure et en composition (Stocks et al., 2002; Gillett et al., 2004; Hanes et al., 2019). Les études montrent cependant d'importantes différences intercontinentales dans la dynamique des incendies. Alors que les feux de surface de faible intensité affectent principalement le sous-bois des forêts boréales eurasiennes (Aakala et al., 2018), les forêts boréales nord-américaines sont principalement dynamisées par des feux de cime de haute intensité, induisant le renouvellement des peuplements (Kneeshaw et al., 2011; Shorohova et al., 2011).

Par conséquent, les incendies représentent le principal facteur de perturbation influençant le paysage des forêts boréales nord-américaines (Payette, 1992; Johnson, 1996; Kuuluvainen et Aakala, 2011) et permettent leur fonctionnement physique

comme biologique (Girardin et al., 2013b). Ils influent sur la formation et le modelage des paysages (Filion et al., 1991), le maintien de la diversité biologique (Burton et al., 2008), les flux d'énergie du milieu (Stocks et al., 2002) et permettent également de renouveler la disponibilité des minéraux dans les sols (Giovanni, 1994). En Amérique du Nord, ces feux de forêt surviennent principalement dans les peuplements d'épinette noire mature (*Picea mariana* (Mill.) B.S.P.) (Viereck et al., 1990). Cette espèce produit des cônes faiblement sérotineux, c'est-à-dire s'ouvrant graduellement avec le temps, mais dont les graines sont rapidement dispersées quand soumises à la chaleur d'un incendie (Johnstone et al., 2009). En éliminant la compétition et en enlevant la couche organique de sol, les fréquences et sévérités de feux holocènes ont ainsi permis son renouvellement et son maintien au cours du temps (Johnstone et al., 2004; Drobyshev et al., 2010). Plus généralement, les perturbations en forêt boréale initient les successions écologiques et offrent l'occasion à certaines espèces de coloniser le milieu, tout en dépendant largement de l'héritage laissé par la végétation antérieure (Johnstone et al., 2010). La traversée de ces processus cycliques de perturbation, de réorganisation et de renouvellement est définie comme un cycle adaptatif (Holling, 1973), et peut s'exprimer à différentes échelles spatiales comme temporelles. Le cadre du modèle conceptuel de la panarchie (voir Allen et al., 2014) relie les cycles adaptatifs s'exprimant et évoluant à différentes échelles de temps et d'espace. Ainsi, les niveaux les plus grands, mais les plus lents (e.g. climat, paysage) régissent les conditions dans lesquelles les plus petits, mais les plus rapides (*e.g.* feuilles des arbres) s'expriment.

Les écosystèmes boréaux dans un contexte de changement climatique. Les températures ont augmenté d'environ 1°C à l'échelle mondiale depuis l'ère préindustrielle, une tendance qui devrait s'accentuer considérablement dans les décennies à venir (IPCC, 2022). En raison de l'incertitude entourant les rejets futurs de gaz à effet de serre, plusieurs scénarios ont été élaborés (van Vuuren et al., 2011). Par exemple, le scénario RCP2.6 estime une augmentation des températures d'environ +1,8°C à l'échelle mondiale d'ici à 2100 comparé à l'ère préindustrielle, alors

que le scénario RCP8.5 prédit la plus forte augmentation des températures, atteignant +4,3°C (IPCC, 2022). Bien que cette augmentation des températures moyennes représente déjà un défi majeur pour les écosystèmes mondiaux, celle-ci sera loin d'être uniforme (Field et al., 2014). Le phénomène d'amplification polaire, initialement décrit par Arrhenius (1896), devrait mener à un impact disproportionné sur les écosystèmes du nord de la planète (Holland et Bitz, 2003). Cette augmentation plus prononcée des températures aux pôles est attribuable, entre autres, à des rétroactions locales impliquant la fonte des glaces polaires et à des modifications dans les transports d'énergie vers les pôles, entraînant un réchauffement estimé à environ deux fois la moyenne mondiale (Previdi et al., 2021). Dans les écosystèmes boréaux nord-américains, cette élévation des températures pourrait atteindre près de 10°C (Gauthier et al., 2015), alors que les précipitations ne devraient augmenter, en comparaison, que de 20 à 30% à l'horizon 2100 (IPCC, 2022), ce qui ne sera pas suffisant pour compenser l'évapotranspiration croissante (He et Pomeroy, 2023).

Les transformations climatiques en cours sont sans précédent dans l'histoire humaine (Kusunoki et al., 2020). Elles induisent des répercussions majeures dans les écosystèmes, avec des effets bénéfiques ou néfastes pour les espèces végétales. Par exemple, l'élévation des températures et de la concentration atmosphérique en CO_2 allonge la saison de croissance des arbres (Bronson et al., 2009; Ols et al., 2016), et stimule positivement la photosynthèse (Bigras et Bertrand, 2006; Sniderhan et al., 2021; Pau et al., 2022), et est par conséquent bénéfique à leur croissance. Cependant, les changements climatiques entraînent également une augmentation notable des épisodes de sécheresse (Tam et al., 2018), des épidémies d'insectes ravageurs (Régnière et al., 2012), de la fonte du pergélisol (Chasmer et Hopkinson, 2017), ainsi que des modifications dans les relations de compétition (Oboite et Comeau, 2020). À l'échelle individuelle, ces modifications des facteurs biotiques et abiotiques auront des répercussions importantes sur la croissance et les taux de mortalité des arbres. Plus particulièrement, l'épinette noire devrait être particulièrement impactée en raison de son réseau racinaire superficiel et de sa sensibilité aux modifications des facteurs biotiques et abiotiques (Burns et al., 1990).

Ces conséquences seront cependant loin d'être uniformes, en raison d'importants gradients longitudinaux comme latitudinaux à travers sa zone de répartition, qui sont encore aujourd'hui mal caractérisés.

Au-delà de ces impacts au niveau de l'arbre, l'augmentation prévue des régimes de perturbations (voir Flannigan et Wotton, 2001; Flannigan et al., 2005; Wotton et al., 2010) pourrait entraîner des modifications importantes des populations, des communautés et des écosystèmes (Baltzer et al., 2021). Bien que l'épinette noire soit naturellement adaptée aux perturbations naturelles, plusieurs décennies sont nécessaires pour que les peuplements deviennent matures et établissent une banque de graines suffisante pour leur régénération (Viereck et al., 1990; Johnstone et Chapin, 2006b; Johnstone et al., 2010). Ainsi, des incendies de trop forte sévérité, des intervalles de retour du feu trop courts, des changements climatiques majeurs ou la combinaison de ces facteurs peuvent compromettre sa capacité de régénération, entraînant progressivement une transition vers une dominance de feuillus ou d'espèces de pins (Johnstone et Chapin, 2006b; Baltzer et al., 2021), voire à la formation de landes à lichens en l'absence de régénération (Splawinski et al., 2019a). Ces échecs de régénération peuvent également être favorisés lorsque la couche de sol organique n'est plus suffisamment importante après un incendie pour permettre la germination des graines (Greene et al., 2007; Johnstone et al., 2010), lorsque des feux de forte intensité brûlent les cônes dans la canopée (Zasada et al., 1979; Johnstone et al., 2009), ou à l'inverse lorsque des feux de trop faible intensité au sol ne permettent pas de fournir de bons lits de germination (Jayen et al., 2006; Johnstone et Chapin, 2006a).

Les forêts canadiennes démontrent une résilience importante face à des perturbations spécifiques et à des schémas établis (Hart et al., 2019; Couillard et al., 2021). Cependant, le dépassement de ces seuils de résilience ou l'introduction de facteurs anthropiques tels que la foresterie peuvent compromettre la pérennité des forêts et la durabilité de leurs services (Trumbore et al., 2015). L'identification des forçages sous-jacents aux modifications de la composition de la végétation au cours du temps devient par conséquent un enjeu majeur, afin de permettre le développement de

stratégies de gestion forestière appropriées et durables, permettant de prévenir de tels dépassements.

L'est du Québec et le Labrador : une dynamique spatiale et temporelle complexe. ***Histoire climatique du Québec-Labrador.*** Des nombreuses archives glaciaires (Jouzel et al., 2007), terrestres (Tzedakis et al., 2006) ou encore marines (Lisiecki and Raymo, 2005; Sánchez Goñi et al., 2021; Fourcade et al., 2024) à travers le monde montrent que le climat du Quaternaire est caractérisé par des oscillations répétées et relativement régulières entre périodes glaciaires et interglaciaires, reflétant d'importants changements du volume de glace stocké aux pôles ainsi que du niveau marin associé. Au cours du dernier million d'années, les cycles glaciaires-interglaciaires atteignent une cyclicité d'environ 100 ka (Yin et Berger, 2012; PAGES, 2016), et sont produits à l'origine par les variations d'insolation (Milankovitch, 1941; Shackleton et Opdyke, 1973; Hays et al., 1976; Berger et Loutre, 1991; Ruddiman, 2006), elles-mêmes déterminées par les variations des trois paramètres orbitaux que sont l'excentricité, l'obliquité et la précession des équinoxes (Milankovitch, 1941). À une échelle plus fine, la dernière période glaciaire (~115 à 11,7 ka BP) se termine par un réchauffement rapide du climat induit par l'augmentation de l'insolation estivale (Berger et Loutre, 1991), entrainant le retrait de l'inlandsis laurentidien (Laurentide Ice-Sheet, LIS) (Carlson et al., 2008). Ce retrait initie la vidange des grands lacs proglaciaires et la colonisation rapide des espèces végétales situées aux marges des inlandsis ou sur les îles des lacs proglaciaires (Vogel et al., 2023). Cependant, alors que l'ouest de l'Amérique du Nord a été déglacé tôt dans son histoire (Dyke, 2004; Dalton et al., 2020), les derniers vestiges de la LIS ont persisté jusqu'à environ 5700 ans avant aujourd'hui au Québec-Labrador, exerçant ainsi un effet de refroidissement sur ces régions (Viau et Gajewski, 2009; Fréchette et al., 2021). Surimposé à cela, la vidange des grands lacs proglaciaires Agassiz et Ojibway ainsi que la fonte de la calotte ont modifié les conditions de température et de salinité des eaux de surface dans le golfe du Saint-Laurent (de Vernal et al., 1993) et la mer du Labrador (Kolling et al., 2023), influençant par conséquent le climat et l'afforestation des sites à

proximité (Anderson et al., 2007). Ainsi, le cumul des forçages internes et externes a entraîné des divergences spatiales et temporelles majeures dans l'histoire climatique holocène du Québec-Labrador (Renssen et al., 2009). Plus particulièrement, l'initiation, la durée et l'amplitude du maximum thermique de l'Holocène (Holocene Thermal Maximum, HTM) restent aujourd'hui relativement mal contraints à l'est de l'Amérique du Nord, de même que l'initiation de la période néoglaciaire subséquente (Kaplan et Wolfe, 2006; Viau et Gajewski, 2009; Gajewski, 2015; Bajolle et al., 2018). Cependant, une meilleure caractérisation spatiale et temporelle des évènements climatiques majeurs de l'Holocène semble aujourd'hui nécessaire, afin d'améliorer notre compréhension des relations avec les dynamiques long terme de la végétation et des feux.

Dynamique spatiale de la végétation actuelle. La forêt boréale du nord-est américain se divise en trois régions principales selon la latitude. Elle comprend une région de forêts denses au sud, une transition vers des forêts clairsemées aux latitudes intermédiaires, et une toundra forestière dans sa partie la plus septentrionale. Entre approximativement 48 et 52°N (Figure 2) s'étendent les pessières fermées (75% de couvert forestier, Scheffer et al., 2012) dominées par l'épinette noire, le sapin baumier (*Abies balsamea* (L.) Mill.), le bouleau à papier (*Betula papyrifera* Marsh.), le peuplier faux-tremble (*Populus tremuloides* Michx.), l'épinette blanche (*Picea glauca* (Moench) Voss) et le pin gris (*Pinus banksiana* Lamb.) (Baldwin et al., 2020). Entre le 55^{e} et le 52^{e} parallèles s'étendent les pessières ouvertes (Figure 2), principalement caractérisées par des peuplements clairsemés d'épinettes noire et blanche (10 à 40% de couvert forestier, Scheffer et al., 2012), sous lesquels prospère un dense tapis de lichen. Le sapin baumier, le bouleau à papier, le peuplier faux-tremble, l'épinette blanche et le pin gris y sont également présents en moindres proportions (Baldwin et al., 2020). Les forêts fermées et ouvertes sont considérées comme des états alternatifs stables (Jasinski et Payette, 2005; Côté et al., 2013; Payette et Delwaide, 2018), c'est-à-dire des écosystèmes stables pouvant persister dans deux configurations différentes sous des conditions environnementales similaires (Suding

et al., 2004; Suding et Hobbs, 2009). Le passage d'une pessière fermée à ouverte reflète la plupart du temps le dépassement d'un seuil de résilience en raison de la récurrence, de la taille ou de la sévérité importante de perturbations naturelles ou anthropiques - ou de leur concomitance - incluant les feux de forêt (Splawinski et al., 2019a), les épidémies d'insectes (Jasinski et Payette, 2005), ou encore l'exploitation forestière (Girard et al., 2008).

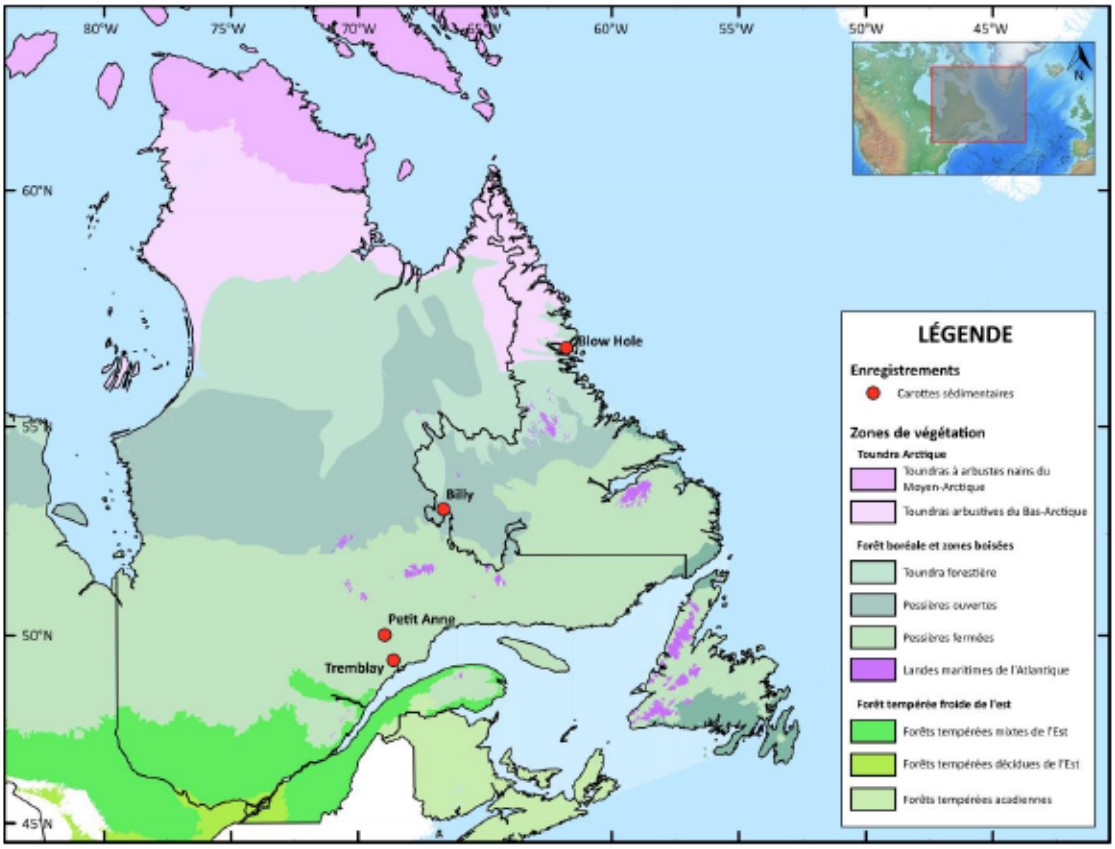

Figure 2
Localisation des sites d'étude à travers les zones de végétation du Canada.
Source : Baldwin et al., (2020)

Enfin, au nord du 55^{e} parallèle, la toundra forestière (Figure 2) se présente sous la forme d'îlots boisés souvent espacés, composés principalement d'épinettes noire et blanche, se développant généralement sous des formes de croissance altérées dites

en "krummholz". Ces îlots, également formés de mélèze laricin (*Larix laricina* (Du Roi) K. Koch), sont séparés par une matrice constituée de bouleaux (*Betula* spp.) et de saules (*Salix* spp.) arbustifs, d'aulne vert (*Alnus viridis* ssp. *crispa*), ainsi que de diverses espèces d'Ericaceae, de Poaceae, de Cyperaceae et de lichens (Baldwin et al., 2020).

À ce gradient latitudinal s'ajoute un gradient longitudinal prononcé. La partie occidentale de la région présente un climat continental relativement sec, alors que l'est du Québec-Labrador est influencé par la proximité du golfe du Saint-Laurent et de l'océan Atlantique, lui conférant un climat sous influence maritime (Mackay et al., 2021). L'épinette noire, le pin gris et le peuplier faux-tremble dominent à l'ouest du Québec, en partie en raison d'intervalles de retour du feu courts, entre 80 et 150 ans en moyenne (Lesieur et al., 2002). A l'est du Québec et au Labrador, les précipitations importantes induites par la proximité de l'océan Atlantique maintiennent une humidité élevée dans les sous-bois, particulièrement défavorable au développement d'incendies (Foster, 1983a). Les intervalles de retour de feu y sont par conséquent parmi les plus longs du Canada (Zhang et Chen, 2007), estimés entre 250 et 350 ans dans les forêts mixtes de la région Côte-Nord (Québec) (Couillard et al., 2021), à environ 350 ans dans les pessières fermées du centre du Labrador (Miranda et al., 2016), et dépassant 500 ans plus proche de la côte Atlantique (Foster, 1983b, 1983a), voire plusieurs milliers d'années (Coops et al., 2018). Ces forêts sont en conséquence dominées par les épinettes noire et blanche, le sapin baumier et le bouleau à papier, tandis que le pin gris ne peut y prospérer en raison d'intervalles de retour du feu trop longs (Asselin et al., 2003). Cependant, la plupart des études réalisées dans ces régions couvrent des échelles de temps courtes, inférieures à 100 ans, soulignant la nécessité d'études à plus long terme.

Dynamiques actuelle et future en contexte de changements climatiques. Au Québec, 9% des pessières fermées ont basculé vers des états stables ouverts en raison de l'accroissement des perturbations naturelles et anthropiques dans la

seconde moitié du XX^{e} siècle (Girard et al., 2008). Plus au nord, de nombreuses pessières ouvertes ont également basculé vers des communautés végétales caractéristiques de la toundra (Payette et Delwaide, 2018), soulignant une perte récente de résilience des forêts boréales à l'est du Canada. Ces changements résultent souvent de la combinaison de perturbations naturelles ou anthropiques telles que les incendies, les épidémies d'insectes ou l'exploitation forestière (Payette et al., 2000; Jasinski et Payette, 2005; Girard et al., 2008; Côté et al., 2013; Payette et Delwaide, 2018). La question de la résilience future des forêts de l'est du Canada, en particulier celle de l'épinette noire, apparait par conséquent comme cruciale d'un point de vue économique, écologique comme climatique. Cette essence représente en effet l'une des ressources économiques principale associée à l'industrie forestière au Canada (Natural Resources Canada, 2022b), un secteur évalué à 1,7% du produit intérieur brut du pays (39,2 milliards de dollars, Government of Canada, 2023). Une réduction de la densité forestière pourrait également engendrer un stockage de carbone réduit, posant ainsi un défi majeur sur le plan climatique.

A l'est du Québec et au Labrador, les intervalles de retour du feu plus longs (*i.e.* feux de forêt plus espacés dans le temps) laissent théoriquement penser que la végétation est moins susceptible aux échecs de régénération. Cependant, le climat y est également plus froid (Fréchette et al., 2021). Cela se traduit par une réduction du nombre de graines viables (Sirois, 2000; Meunier et al., 2007), une maturation des cônes plus longue et une difficulté de germination plus importante (Sirois, 2000), entrainant des conditions de régénération post-feu plus difficiles (Lavoie et Arseneault, 2001). En conséquence, le climat, combiné à l'impact des feux de forêt, pourrait jouer un rôle dans l'ouverture des peuplements dans ces régions.

Bien que les régions à l'ouest du Québec aient fait l'objet de nombreuses études (Payette et al., 2000; Jasinski et Payette, 2005; Girard et al., 2008; Veilleux-Nolin et Payette, 2012; Côté et al., 2013; Payette et Delwaide, 2018), les régions de l'est du Québec et du Labrador restent aujourd'hui peu explorées à l'échelle plurimillénaire. De plus, les forçages de la dynamique de la végétation dans ces régions restent encore largement méconnus. Dans le cadre de la lutte contre le réchauffement

climatique initiée à la fin du XX^{e} siècle, ce projet de thèse vise à améliorer notre compréhension des dynamiques forestières passée et actuelle en relation avec les régimes de perturbations naturelles, afin de mieux guider les mesures de gestion durable et de conservation de ces écosystèmes.

Questions de recherche, objectifs et hypothèses. L'objectif principal de cette thèse est de caractériser l'impact respectif des feux de forêt et du climat sur la dynamique de la végétation, en particulier celle de l'épinette noire, à travers les diverses zones de végétation boréale à l'est du Québec et au Labrador. Elle vise ainsi à appréhender l'impact des changements climatiques dans les forêts boréales d'Amérique du Nord. Sous cet objectif général se déclinent différentes approches synthétiques, méthodologiques comme analytiques, visant chacune à enrichir les connaissances existantes et à générer de nouvelles informations sur la manière dont les écosystèmes boréaux du nord-est de l'Amérique du Nord ont réagi et réagiront aux variations climatiques passées et futures.

Quels seront les impacts des changements climatiques futurs sur la croissance et la mortalité de l'épinette noire à travers sa zone de répartition ? Les changements climatiques auront des répercussions majeures sur l'épinette noire, à différents niveaux. A l'échelle individuelle, cette espèce devrait subir de profondes modifications de sa croissance et de ses taux de mortalité, entrainant des conséquences majeures pour la foresterie comme le stockage de carbone. Cependant, en plus de dépendre des scénarios climatiques futurs, l'existence de gradients latitudinaux (Baldwin et al., 2020) comme longitudinaux (Couillard et al., 2019) devrait mener à une réponse différentielle à travers la zone de distribution de l'épinette noire. Par exemple, l'accroissement de la saison de croissance et des températures pourrait augmenter la productivité de l'épinette noire sur l'ensemble de sa zone de répartition (Strömgren et Linder, 2002; Bronson et al., 2009), alors que le déplacement progressif des isothermes vers le nord devrait réduire ses taux de

mortalité à sa limite septentrionale (Gamache et Payette, 2004). À l'inverse, l'accroissement du stress hydrique, prévu pour augmenter particulièrement au centre et à l'est de l'Amérique du Nord (Bonsal et al., 2011; Price et al., 2013), pourrait largement limiter la capacité de photosynthèse de cette espèce au système racinaire peu profond (Farrar, 1995), et par conséquent son potentiel de croissance (Girardin et al., 2008; Ma et al., 2012; Girardin et al., 2016b).

Le premier chapitre de cette thèse (Figure 3) est une synthèse bibliographique, visant à dresser un état des connaissances de l'impact des changements climatiques sur la croissance et les taux de mortalité de l'épinette noire à l'horizon 2100, dans l'ensemble de sa zone de répartition. À travers cette étude, nous avons pour objectif a) de synthétiser l'impact des modifications de différents facteurs abiotiques (températures, précipitations, gel, paramètres édaphiques) comme biotiques (épidémies d'insectes, compétition, maladies et parasitisme) le long des gradients latitudinaux, longitudinaux et altitudinaux d'Amérique du Nord, b) d'identifier les zones les plus à risque à travers la zone de répartition de l'épinette noire, et c) de discuter les enjeux liés à la gestion durable de cette espèce d'intérêt majeur.

La détection des macrocharbons présents dans les échantillons des carottes sédimentaires est-elle possible de manière entièrement automatisée ? Au-delà du niveau individuel, les changements climatiques auront également des répercussions à des échelles plus larges (Genet et al., 2021). L'étude des relations feu-climat-végétation à l'échelle de l'écosystème requiert en particulier la reconstitution des régimes de feu (fréquence, taille) au cours du temps. Dans les carottes sédimentaires lacustres, la méthode la plus utilisée pour reconstituer les fréquences de feu locales (i.e. < 3 km des berges du lac, Clark, 1990; Clark et Royall, 1996; Higuera et al., 2007; Oris et al., 2014) implique l'analyse numérique des taux d'accumulation de macrocharbons (Oris et al., 2014b). Dans ces approches, les macrocharbons sont généralement quantifiés (Gavin et al., 2006; Leys et al., 2013) ou leur aire mesurée (Carcaillet et al., 2001; Ali et al., 2009b; Halsall et al., 2018) en

utilisant des méthodes visuelles (*e.g.* Rius et al., 2012) ou semi-automatisées (*e.g.* Lestienne et al., 2020; Gaboriau et al., 2020). Cependant, celles-ci sont généralement coûteuses en temps ou développées sur des logiciels sous licence. Comme les macrocharbons peuvent être distingués visuellement par un utilisateur après tamisage, un algorithme devrait être en mesure de les différencier, de les dénombrer, et de mesurer automatiquement leur surface.

Dans le deuxième chapitre de cette thèse (Figure 3), nous développons et testons une nouvelle méthode de comptage entièrement automatisée développée sur le logiciel open-source ImageJ (Abràmoff et al., 2004). Dans ce chapitre, nous comparons notre méthode avec la méthode visuelle traditionnelle, en utilisant les données de flux, et de fréquences de feu locales et régionales afin d'identifier et d'expliquer les différences observées.

L'histoire climatique holocène du Québec-Labrador peut-elle être reconstituée de manière fiable à partir des grains de pollen et des assemblages de chironomes ? L'étude des interactions entre feu, végétation et climat au cours du temps implique la nécessité de reconstitutions paléoclimatiques fiables à long terme. Cependant, les changements climatiques de l'Holocène dans l'est de l'Amérique du Nord présentent une variabilité temporelle et spatiale complexe (Viau et Gajewski, 2009; Renssen et al., 2009; Gajewski, 2015) et ne peuvent donc être généralisés. Au Québec-Labrador, la plupart des enregistrements paléoclimatiques et des synthèses des températures de l'Holocène reposent sur l'analyse des grains de pollen (*e.g.* Kerwin et al., 2004; Viau et Gajewski, 2009; Fréchette et al., 2018, 2021). Cependant, bien que la végétation soit théoriquement en équilibre dynamique avec le climat (Webb, 1986), d'autres facteurs tels que les feux de forêt ou les épidémies d'insectes peuvent avoir un impact sur sa structure et sa composition (Brandt et al., 2013; Hanes et al., 2019), affectant par conséquent les assemblages polliniques et pouvant interférer avec le signal climatique. Dans ce contexte, les capsules céphaliques de chironomes permettent des reconstitutions particulièrement précises des

températures estivales de l'air (<1°C d'erreur par rapport aux mesures instrumentales, Larocque et al., 2009; Larocque-Tobler et al., 2015). Bien qu'également sujettes à des biais, elles peuvent par conséquent être utilisées pour renforcer ou remettre en question les reconstitutions issues des grains de pollen.

Afin d'évaluer les biais inhérents aux deux reconstitutions, notre objectif dans ce troisième chapitre (Figure 3) est de comparer les reconstitutions issues des grains de pollen et de chironomes sur cinq sites répartis à l'est du Canada, en utilisant la Technique des Analogues Modernes (MAT) et une fonction de transfert (fxtWA-PLS). Nous émettons l'hypothèse que les grains de pollen et les chironomes permettent des reconstitutions de températures similaires, sauf durant les périodes d'activité (fréquence et taille) de feux importantes. À partir de ces reconstitutions, nous discutons ensuite l'histoire climatique holocène du Québec-Labrador. Nous supposons que les sites les plus septentrionaux montrent un maximum thermique de l'Holocène plus tardif et court comparé aux sites plus méridionaux, avant d'être marqués par une diminution de température caractéristique de la période Néoglaciaire.

Quelle a été la part respective du climat et des régimes de feu sur la dynamique de la végétation du Québec-Labrador au cours de l'Holocène ? Le climat ainsi que les fréquences et tailles de feux sont les forçages majeurs de la dynamique de la végétation dans les pessières fermées du Canada. En particulier, des études récentes ont suggéré que la taille des feux représentait le forçage principal de la dynamique de la végétation dans les pessières du Québec-Labrador (Remy et al., 2017a, 2017b). Cependant, la part respective du climat et des incendies a pu varier temporellement, comme spatialement.

Dans ce quatrième et dernier chapitre (Figure 3), nous avons pour objectif de décrypter les rôles respectifs du climat et des feux sur la dynamique de la végétation au cours de l'Holocène, le long d'un transect nord-sud situé à l'est du Québec et au Labrador. Pour cela, nous utilisons une approche innovante basée sur l'utilisation de

modèles additifs généralisés afin d'évaluer les relations entre climat, feux de forêt et végétation au cours du temps. Nous émettons dans un premier temps l'hypothèse que la température a joué un rôle majeur dans la dynamique de la végétation des écosystèmes les plus nordiques, alors que la taille des feux a été le paramètre principal au sud (Remy et al., 2017b). Dans un second temps, nous souhaitons déterminer si, comme plus à l'ouest, des changements de trajectoire de végétation ont été observés durant les derniers siècles, et identifier les causes de ces changements. Nous supposons que contrairement aux régions situées plus à l'ouest, l'est du Québec-Labrador n'a pas été marqué par des changements récents de dynamique de végétation, à cause d'intervalles de retour du feu plus longs.

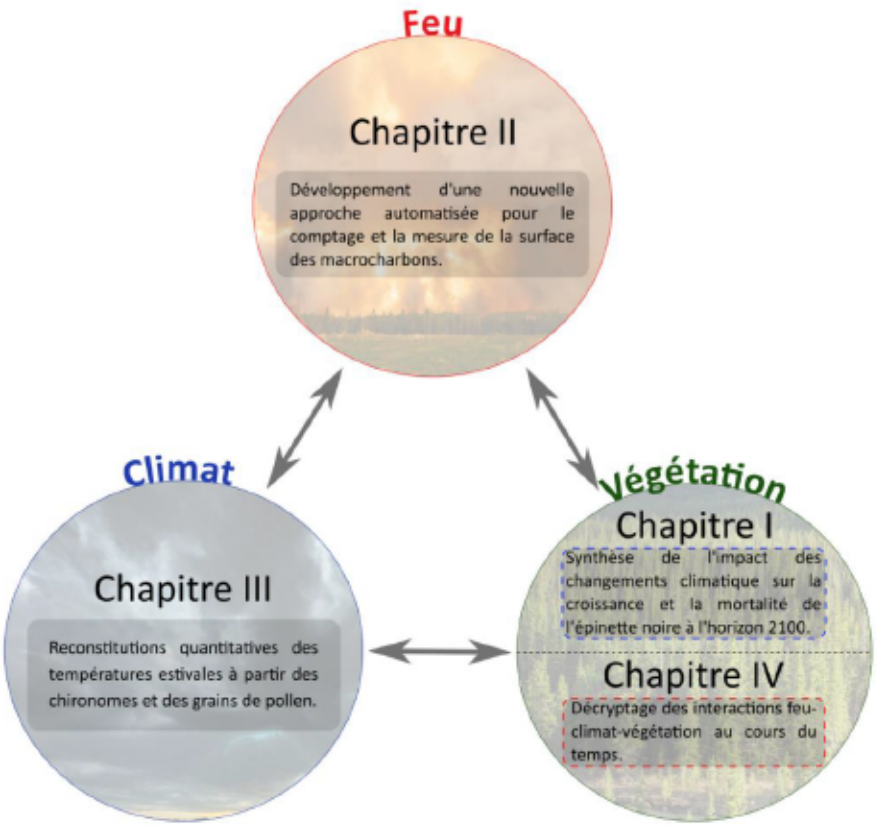

Figure 3
Représentation schématique des relations entre les chapitres traités dans cette thèse. La ligne en pointillés bleus représente l'échelle de l'individu, la ligne en pointillés rouges l'échelle de l'écosystème.

Matériel et méthodes : une approche paléoécologique multi-indicatrice. ***Intérêts et principes de la paléoécologie.*** Il est aujourd'hui impératif que les nouveaux plans d'aménagement forestiers soient élaborés à long terme, en tenant compte des risques liés aux perturbations et à la migration des espèces induits par les changements climatiques (Niemelä, 1999; Bergeron et al., 2002; Chapin et al., 2004). Une manière d'appréhender les relations complexes entre les régimes de perturbations, le climat et la végétation à long terme repose sur l'étude d'indicateurs paléoécologiques tels que les macrocharbons, les capsules céphaliques de chironomes ou les grains de pollen (Whitlock et Larsen, 2002; Velle et al., 2005; Birks et Birks, 2006). La paléoécologie est une discipline permettant de fournir un aperçu des conditions environnementales passées ayant prévalu dans un espace défini, en apportant des informations sur la structure, la composition et les régimes de perturbations ayant joué sur les écosystèmes dans le passé (Lindbladh et al., 2013). Elle offre une perspective unique sur les trajectoires écologiques à des échelles de temps plurimillénaires, permettant ainsi de mieux quantifier la réponse des écosystèmes face aux régimes de perturbations et du climat, que les méthodes d'observation actuelles ne permettent pas de couvrir. Par conséquent, elle permet de compléter les observations actuelles, en apportant des données sur la variabilité naturelle des écosystèmes (i.e. avec un impact anthropique négligeable, mais voir Johnson et Miyanishi, 2012).

La plupart des études paléoécologiques s'appuie sur des archives sédimentaires lacustres, permettant de fournir des informations fiables sur le climat, la végétation ou les régimes de perturbations au cours du temps. Dans le cadre des pessières fermées de l'Amérique du Nord, la genèse des lacs remonte à la fin de la dernière glaciation ou au retrait des lacs proglaciaires, datés entre 11.000 ans cal BP au sud du Québec, et environ 5700 ans cal BP dans sa partie septentrionale (voir Dyke, 2004; Dalton et al., 2020). L'accumulation progressive et continue des sédiments résultant de l'érosion de leur bassin versant a permis la séquestration dans les sédiments organiques de nombreux bioindicateurs passés de la végétation (macrorestes végétaux, grains de pollen, ADN sédimentaire), des régimes de perturbations (micro- et macrocharbons,

capsules céphaliques d'insectes, écailles de lépidoptères), du climat (capsules céphaliques de Chironomidae) (Figure 4), ainsi que de signaux géophysiques et géochimiques. L'intégration d'une approche multi-indicatrice permet par conséquent d'obtenir une vision plus complète et nuancée que celle qui pourrait être obtenue à partir de l'étude d'un seul indicateur, en raison du réseau complexe d'interactions influant sur la dynamique des écosystèmes (Birks et Birks, 2006).

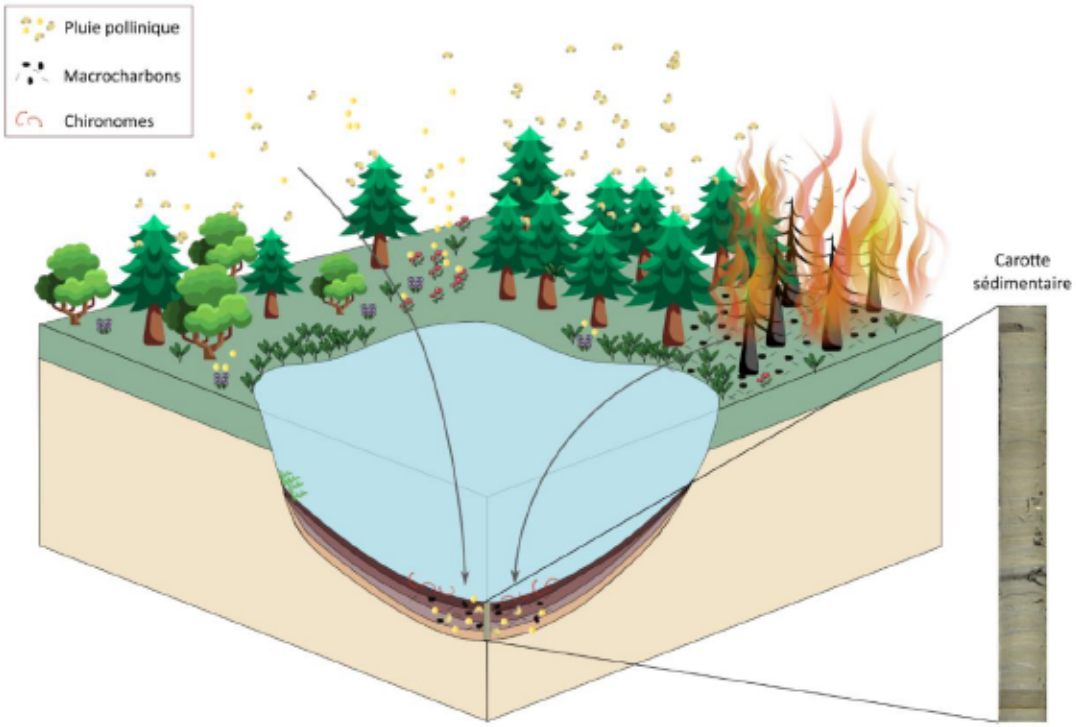

Figure 4
Illustration du dépôt de différents indicateurs (grains de pollen, macrocharbons, chironomes) dans les sédiments lacustres.

Les archives lacustres représentent des outils de choix afin de reconstituer la dynamique de la végétation, du climat et des régimes de feux, de par plusieurs aspects. Tout d'abord, elles sont formées de sédiments stratifiés possédant généralement un taux de sédimentation stable à long terme, permettant d'obtenir des modèles âge-profondeur relativement fiables avec peu de datations radiocarbone (Carcaillet et al., 2001; Conedera et al., 2009). Elles permettent également des

reconstitutions à l'échelle de l'Holocène tout en offrant des résolutions temporelles de l'ordre de la décennie (*e.g.* Bastianelli, 2018), et enregistrent des informations locales comme régionales (Conedera et al., 2009). Les sédiments lacustres représentent par conséquent des outils de choix afin d'améliorer notre compréhension de la dynamique des forêts boréales est-canadiennes (*i.e.* Blarquez et al., 2015; Remy et al., 2018; Feussom Tcheumeleu et al., 2023).

Stratégie d'échantillonnage et datations. Cette thèse s'appuie sur l'étude d'un transect de carottes sédimentaires lacustres orienté globalement sud-ouest/nord-est, permettant ainsi de couvrir les gradients écologiques et climatiques de l'est du Québec et du Labrador. Plus spécifiquement, ce transect se compose de quatre sites d'étude répartis de la côte nord du fleuve Saint-laurent à la côte atlantique du Labrador. Ces lacs, nommés de manière formelle (Lac Georges Tremblay) ou informelle (Lac Petit Anne, Lac Billy, Lac Blow Hole), ont été échantillonnés à l'été 2019, soit environ un an avant le début de cette thèse de doctorat. Ils sont placés à des endroits stratégiques, afin de permettre la reconstitution des trajectoires de végétation dans différentes zones au cours de l'Holocène. Plus spécifiquement, le site Petit Anne (PEA, 49°50'14"N, 68°43'30"W, 148 cm de longueur de carotte) est localisé dans les pessières fermées, proche de la transition avec les forêts mixtes situées plus au sud (Figure 2, Tableau 1). Légèrement plus au nord, le site Tremblay (TRE, 49°24'44"N, 68°28'27"W, 116 cm de longueur de carotte) est également situé dans les pessières fermées (Figure 2, Tableau 1). Le site Billy (BIL, 53°04'60"N, 66°57'87"W, 89 cm de longueur de carotte) se situe à la transition entre les pessières fermées et ouvertes (Figure 2). Enfin, le site Blow Hole (BLH, 56°31'25"N, 61°41'49"W, 113 cm de longueur de carotte), est situé sur la côte du Labrador, dans la toundra forestière, à environ 2 km au sud du village de Nain (Figure 2, Tableau 1).

Le modèle âge-profondeur de chaque séquence lacustre a été établi à partir d'une méthode de datation bayésienne (Blaauw et al., 2021), intégrant différents radioisotopes. L'âge des sédiments les plus récents a été obtenu à partir de la mesure

de l'activité du ^{210}Pb et du ^{137}Cs (Appleby et al., 1979; Le Roux et Marshall, 2011), et les sédiments plus anciens à partir de datations au radiocarbone réalisées sur des macrorestes végétaux.

Tableau 1
Caractéristiques principales des quatre lacs étudiés et de leurs conditions climatiques respectives.
Source : Ressources Naturelles Canada (2010).

Exemple de tableau	Blow Hole	Billy	Petit Anne	Tremblay
Zone de végétation	Toundra forestière	Pessière ouverte	Pessière fermée	Pessière fermée
Latitude	56°31'25"N	53°04'60"N	49°50'14"N	49°24'44"N
Longitude	61°41'49"W	66°57'87"W	68°43'30"W	68°28'27"N
Élévation (m a.s.l.)	122	541	323	332
Surface (ha)	7.0	9.7	9.1	3.5
Profondeur d'eau maximum	4.8	3.8	2.4	16.0
Longueur de carotte sédimentaire (cm)	113	91	138	113
Apports fluviaux	Absents	Absents	Absents	Absents
Bordure du lac	Pentu	Plat	Pentu	Pentu
Station météorologique la plus proche (distance en km)	NAIN A (3.05)	WABUSH LAKE A (23.79)	BAIE-COMEAU A (86.97)	BAIE-COMEAU A (33.49)
Température estivale de l'air en °C en juin/juillet/août (moyenne)	6.4/10.1/11.0 (9.7)	10.3/13.8/12.5 (12.2)	12.4/15.6/14.7 (14.2)	12.4/15.6/14.7 (14.2)
Précipitations annuelles moyennes en mm	925.4	839.5	1001.0	1001.0

Reconstitution des régimes de feu passés à partir des macrocharbons. Durant les dernières décennies, un grand nombre d'études a montré que les macrocharbons (*i.e.* >150 µm) préservés dans les archives lacustres sont des preuves directes des évènements de feu, et fournissent par conséquent de nombreuses informations sur la dynamique des incendies au cours du temps (Whitlock et Larsen, 2002; Higuera et al., 2007; Jensen et al., 2007; Belcher et al., 2018). Leurs propriétés optiques, formes et tailles peuvent en effet renseigner sur les caractéristiques du feu qui les a générés (Bird et al., 2008; McBeath et al., 2013; Belcher et al., 2018), mais aussi sur leur taille (Whitlock et Larsen, 2002), fréquence, intervalle de retour de feu (FRI) (Gavin et al., 2007; Ali et al., 2008, 2012; Conedera et al., 2009), ainsi que sur la quantité de biomasse brûlée et la taille/sévérité des feux (Ali et al., 2012).

Dans ces approches, les macrocharbons sont extraits de la matrice sédimentaire par traitement chimique (NaOH, H_2O_2), puis observés à la loupe binoculaire après tamisage avant d'être quantifiés par dénombrement (*e.g.* Gavin et al., 2006; Leys et al., 2013), estimation de leur surface (*e.g.* Carcaillet et al., 2001; Lynch et al., 2004; Halsall et al., 2018) ou de leur volume (*e.g.* Weng, 2005; Ali et al., 2009; Belcher et al., 2018). Avec l'aide du modèle d'âge, ces comptages ont ensuite été transformés en taux d'accumulation de charbons ($mm^2.cm^{-2}.an^{-1}$). En suivant la méthode décrite par Higuera (2009), la détection des évènements de feux a ensuite été réalisée à partir de ces taux d'accumulation de charbons en séparant, entre autres, les composantes à basse et à haute fréquence, cette dernière étant assumée comme représentant les évènements de feux locaux. Ainsi, à partir de ces évènements de feu, les fréquences de feu (FF) et quantité de biomasse brûlée (BB) ont pu être reconstituées à l'échelle locale (Blarquez et al., 2013, 2014). Le rapport entre BB et FF a ensuite été utilisé afin d'estimer la taille et/ou la sévérité des feux (Ali et al., 2012; Hennebelle et al., 2020) au cours du temps. Par souci de simplicité, cet indice sera nommé « indice de taille de feu » dans la suite du manuscrit.

Reconstitution de la végétation : une étude palynologique. La palynologie correspond à la discipline scientifique s'adressant à l'étude des palynomorphes, c'est-à-dire l'ensemble des microfossiles à paroi organique (e.g. grains de pollen, spores,

acritarches, diatomées, dinokystes, etc…) préservés dans les archives sédimentaires. Leur résistance importante leur permet d'être conservés, et par conséquent de représenter des témoins uniques de l'histoire, de la composition et la dynamique de la végétation au cours du temps. Ainsi, l'identification des grains de pollen et l'estimation des taux d'accumulation pollinique permettent d'estimer la proportion relative des différent(e)s familles, genres ou espèces ayant caractérisés les écosystèmes passés (Faegri et al., 1989). En se basant sur le principe d'uniformitarisme, selon lequel la pluie pollinique reflète le contexte de végétation, les enregistrements polliniques permettent de suivre les trajectoires de végétation au cours du temps, ainsi que leurs relations avec le climat et les régimes de perturbations (Faegri et al., 1989; Moore et al., 1991; Reille, 1995). Cependant, la représentation pollinique peut varier selon différents processus, allant de la production du pollen à son transport et sa préservation dans les sédiments lacustres (Campbell, 1999; Lebreton et al., 2010). Démêler ces facteurs nécessite par conséquent un effort d'interprétation, afin d'identifier dans quelle mesure ils reflètent la végétation passée.

Dans notre étude, des échantillons sédimentaires ont été extraits à intervalles réguliers sur les séquences sédimentaires, avant d'être traités à l'aide d'un protocole chimique, intégrant des attaques longues aux acides chlorhydrique et fluorhydrique, un tamisage, une digestion de la matière organique, et une coloration par acétolyse. Les lames ont ensuite été montées entre lame et lamelle mobile, et un minimum de 500 grains de pollen identifié à chaque niveau pour reconstituer l'histoire de la végétation au cours de l'Holocène. Un nombre connu de spores exotiques de Lycopodium clavatum L. a également été ajouté à chaque échantillon afin de calculer les concentrations absolues en palynomorphes (#.grains.cm^{-3}), puis les taux d'accumulation pollinique au cours du temps (#.cm^{-2}.yr^{-1}).

Reconstitution des températures estivales à partir des assemblages de Chironomidae. Les reconstitutions quantitatives des changements de températures passés peuvent aider à comprendre l'ampleur des changements climatiques et leurs liens avec les régimes de perturbations. Cependant, l'asynchronisme des évènements climatiques majeurs de l'Holocène et la variabilité spatiale empêchent une

généralisation de l'histoire climatique du Québec-Labrador. En conséquence, les enregistrements paléoclimatiques fournissent une base solide pour étudier les interactions avec la végétation régionale et les régimes de perturbations au cours du temps (Girardin et al., 2019). Dans ce contexte, les capsules de chironomes peuvent être préservées pendant plusieurs centaines de milliers d'années dans les sédiments lacustres (Axford et al., 2009), et permettent des reconstitutions précises des températures de l'air (<1°C d'erreur par rapport aux mesures instrumentales) (Larocque et al., 2009; Larocque-Tobler et al., 2015). Plusieurs études en Amérique du Nord (*e.g.* Hausmann et al., 2011; Fortin et al., 2015; Bajolle et al., 2018; Medeiros et al., 2022) ont montré leur sensibilité aux changements de température de l'air, soulignant l'importance de leur étude pour une meilleure compréhension de la variabilité climatique Holocène.

Pour cela, des échantillons sédimentaires ont été prélevés à intervalles réguliers sur les différentes séquences sédimentaires, et les capsules céphaliques de chironomes isolées par défloculation de la matière organique puis filtration. Chaque capsule céphalique a ensuite été montée entre lame et lamelle fixes en position ventrale, puis observée au microscope optique afin de permettre l'identification des différents morphotypes. Un minimum de 50 capsules céphalique a été identifié par échantillon pour assurer la représentativité statistique des échantillons par rapport aux tendances climatiques locales (Quinlan et Smol, 2001; Larocque, 2001; Heiri et Lotter, 2010). Par la suite, les températures moyennes estivales de l'air ont été reconstituées à partir des assemblages de chironomes à l'aide d'un modèle de moyenne pondérée des moindres carrés partiels avec correction des fréquences des variables climatiques (weighted average-partial least squares with frequency correction of the training set climate variables, fxtWA-PLS) appliqué au jeu de données modernes de Suranyi et al., (*in prep.*).

1. FUTURE IMPACTS OF CLIMATE CHANGE ON BLACK SPRUCE GROWTH AND MORTALITY: REVIEW AND CHALLENGES

Jonathan Lesven, Milva Druguet Dayras, Jonathan Cazabonne, François Gillet, André Arsenault, Damien Rius, Yves Bergeron

Published in Environmental Reviews – February 2024

DOI: 10.1139/er-2023-0075

1.1 Abstract

Black spruce (*Picea mariana* (Mill.) B.S.P.) is the dominant conifer species across a large part of North American boreal forests, providing many goods and services essential to human activities, and playing a major climatic role through the global carbon cycle. However, a comprehensive synthesis of the effects of climate change on black spruce has not yet been undertaken. The dynamics of black spruce are influenced by various living (biotic) and non-living (abiotic) factors, as well as their combined effects, which are particularly responsive to changes in climate. Climate change predictions suggest that northern ecosystems will experience the world's most significant impact. Therefore, black spruce is likely to undergo profound disruptions in its growth and mortality rate in the next few decades, resulting in significant changes in forestry and carbon storage. However, these changes will not be uniform throughout the entire distribution of the species. Future changes in temperature and precipitation will create more stress for water availability in the boreal forests of western and central North America than in their eastern counterparts. Thus, significant longitudinal and latitudinal gradients in tree growth and mortality variability are expected throughout the range of the species. This literature review aims to summarise the impacts of climate change on individual tree growth and mortality of this major species. While enhanced black spruce productivity could occur through both increased air temperature and nitrogen mineralisation in the soil, moisture limitation in central and western North America will result in significant growth reduction and mortality events across these regions. Conversely, under the expected climate change scenarios, black spruce forests may be more resilient in eastern North America, where climatic conditions appear more suitable, particularly in their northernmost range. In this review, we identify current research gaps for some disturbances, which should be addressed to better understand the impact of climate change on black spruce. Finally, we identify issues associated with sustainable forest management and the maintenance of black spruce under projected future climate changes.

Keywords: Black spruce, Growth, Mortality, Climate change, Sustainable Forest Management

1.2 Résumé

L'épinette noire (*Picea mariana* (Mill.) B.S.P.) est l'espèce de conifère dominante dans la majeure partie des forêts boréales d'Amérique du Nord. Elle fournit de nombreux biens et services indispensables aux activités humaines, et joue un rôle climatique majeur dans le cycle mondial du carbone. Cependant, aucune synthèse complète des effets du changement climatique sur l'épinette noire n'a été réalisée à ce jour. La dynamique de l'épinette noire est influencée par divers facteurs vivants (biotiques) et non-vivants (abiotiques), ainsi que par leurs effets combinés, particulièrement sensibles aux changements climatiques. Les prévisions suggèrent que les écosystèmes nordiques subiront l'impact le plus important au monde. Par conséquent, l'épinette noire noire est susceptible de subir de profondes perturbations de sa croissance et de ses taux de mortalité au cours des prochaines décennies, entrainant des changements significatifs pour la sylviculture et le stockage du carbone. Cependant, ces changements ne seront pas uniformes à travers l'aire de répartition de l'espèce. Les changements futurs de température et de précipitations créeront plus de stress pour la disponibilité en eau dans les forêts boréales de l'ouest et du centre de l'Amérique du Nord qu'à l'est. Des gradients longitudinaux et latitudinaux significatifs dans la variabilité de la croissance et de la mortalité des arbres sont par conséquent attendus sur l'ensemble de l'aire de répartition de l'espèce. Si l'augmentation de la température de l'air et la minéralisation de l'azote dans le sol pourraient améliorer la productivité de l'épinette noire, l'humidité limitée dans le centre et l'ouest de l'Amérique du Nord entraînera une réduction significative de la croissance et des épisodes de mortalité. À l'inverse, dans les scénarios de changement climatique prévus, les forêts d'épinette noire pourraient être plus résistantes dans l'est de l'Amérique du Nord, où les conditions climatiques semblent plus appropriées, en particulier dans leur aire de répartition la plus septentrionale. Dans cette étude, nous identifions les lacunes actuelles de la recherche, qui devraient être comblées afin de mieux comprendre l'impact du changement climatique sur l'épinette noire. Enfin, nous identifions les questions liées à la gestion durable des forêts et au maintien de l'épinette noire dans le cadre des changements climatiques futurs prévus.

Mots-clés : Épinette noire, Croissance, Mortalité, Changements climatiques, Gestion forestière durable

1.3 Introduction

Global temperature has increased by an average of 1°C since the preindustrial era, a pattern that is likely to be exacerbated as a result of human-induced rising atmospheric CO_2 concentrations (hereafter [CO_2]) (Field et al., 2014; Pörtner et al., 2022). As the magnitude of future greenhouse gas emissions is still uncertain, several scenarios have been developed (van Vuuren et al., 2011). For example, the RCP2.6 scenario model predicts a +1.8°C temperature increase at the global scale under the lowest estimated 2100 [CO_2] equivalent, whereas the RCP8.5 scenario projects the highest temperature increase, estimated at +4.3°C, under the highest estimated concentrations (Pörtner et al., 2022). Exponential anthropogenic forcing is projected to have a tremendous impact on northern biomes, estimated at more than twice the global average (Field et al., 2014). This could reach up to 10°C compared to the pre-industrial era at high latitudes under the RPC8.5 scenario, with precipitation also being expected to increase by 20 to 30% (Field et al., 2014; Pörtner et al., 2022). The estimated temperature increases will result in higher rates of evapotranspiration that will not be fully compensated for, despite concurrent increases in precipitation (Tam et al., 2018), leading to major vegetation shifts and mortality episodes. Shrinking individual growth, reduced stand density and the resulting large-scale boreal forests dieback have consequently been defined as a tipping point, *i.e.* a critical threshold at which a small perturbation in forcing can fundamentally and irreversibly alter the ecosystem state (Rao et al., 2023). This threshold may be crossed under a global warming scenario of 3°C (Lenton et al., 2008). In turn, global warming has the potential to considerably impact individual tree growth and survival, resulting in either positive or negative effects for both carbon storage (Kurz et al., 2008) and timber supply (Gauthier et al., 2015). Our ability to anticipate the impact of these changes is of major interest to land managers and stakeholders in order to develop realistic targets and goals for sustainable forest management strategies that promote the long-term resilience of these ecosystems.

Black spruce (*Picea mariana* (Mill.) B.S.P. - hereafter PIMA) is a conifer species endemic to North America (hereafter NA), that is currently widely distributed throughout Canada, the northeastern U.S.A., and Alaska (Viereck et al., 1990). It

represents a major economic resource, especially in eastern and central Canada, as it is widely used for both wood and paper pulp supply (Natural Resources Canada, 2022b). PIMA forests also serve multiple important societal functions, by being frequently utilised for spiritual, educational, and recreational activities (Hassan et al., 2005). Additionally, these forests hold significant traditional value for Indigenous Peoples (Clément, 1995) and have a crucial climatic role in storing substantial amounts of biogenic carbon (Pan et al., 2011).

As a shallow-rooted species, PIMA is particularly sensitive to water stress and grows mainly on nutrient-poor soils in cold and humid to dry subhumid environments (Girardin et al., 2016b), although it can also be found on more mesic sites. As a fire-adapted species due to its semi-serotinous cones, PIMA life-history at the landscape scale is also largely related to the historical occurrence and severity of fires, which allows for its post-fire renewal and maintenance over time (Johnstone et al., 2004). However, PIMA also reproduces by layering, particularly in regions of high moisture where fires are less frequent or where temperature do not allow for viable seed production, thus emphasising its wide ecological range (Viereck et al., 1990). Future climate changes, through their capacity to modify evaporative balances and disturbance regimes, have a significant potential to alter PIMA growth and mortality rate, as well as its spatial distribution and interactions with other species. These changes will ultimately result in a balance of effects that may or may not be favourable to its maintenance in the future. For example, longer growing seasons and warmer temperatures may favour PIMA productivity and increase soil nutrient availability (Strömgren and Linder, 2002; Bronson et al., 2009), while its mortality rate may be reduced at the northern limit of its distribution through the northward displacement of isotherms (Gamache and Payette, 2004). On the other hand, enhanced water stress may limit its photosynthetic capacity and consequently decrease its growth potential (Goetz et al., 2005). In addition, mortality rate may increase by shifting the range of insect pests and pathogens outbreaks to regions where PIMA was previously protected by harsh winter conditions (Régnière et al., 2012).

While these changes in the growth and mortality rate of PIMA will have wide economic, ecological, and climatic implications across North American ecosystems, they are predicted to be far from uniform, leading to significant regional discrepancies in the severity and direction of the expected impacts. Western and central NA are already experiencing longer and more frequent droughts than eastern Canadian regions (Bonsal et al., 2011), a pattern that is likely to be particularly exacerbated under high anthropogenic forcing scenarios (Tam et al., 2018). This increase will likely lead to enhanced wildfire activity in western and central NA (Flannigan et al., 2005; de Groot et al., 2013), resulting in shifts from PIMA-dominated to broadleaf-dominated forests, induced by too short fire return intervals (Baltzer et al., 2021). Superimposed on these disturbance-mediated changes in forest stand composition, permafrost thaw is also expected to lead to geographic changes in tree growth conditions that will vary according to longitude, latitude, elevation and expected disturbances (Duveneck et al., 2014).

Understanding the spatial variability of individual responses of PIMA trees to climate change is thus of major interest for projections of future global carbon sequestration and timber production, and to inform climate change mitigation and sustainable forest management strategies in northern ecosystems. In this context, our review summarises the main findings from the last decades on the major abiotic and biotic factors affecting PIMA growth, *i.e.,* changes in basal area, diameter at breast height, and tree height, shoot elongation, net primary productivity (NPP), and mortality rate by the end of the 21st century, under the current climate and predicted climate scenarios. Our intention in emphasising these effects was to evaluate the impact of climate change at the individual level, separately from broader processes at the population, stand, or ecosystem levels such as regeneration, although the latter may be discussed as contextual elements. Our review was conducted across the current range of PIMA, which we divided into four main areas (western, central, southeastern, and northeastern NA) for analysis. Our specific objectives were to examine the existing understanding of how climate change affects the growth and mortality rate of individual PIMA trees differently and identify the most-at-risk areas. We then discuss the

combined effects of these factors on PIMA productivity and mortality rate in the future and link them to the challenges facing future sustainable forest management.

1.4 Approach

1.4.1 Study area and climatic data

In order to accurately identify regional climatic trends in NA, we used the Terrestrial Ecozones of Canada Classification (Ecological Stratification Working Group, 1995) modified by Price et al. (2013), on which we overlaid the current distribution of PIMA (Figure 5). This allowed us to refer to the projections of Price et al. (2013), which used the same geographical areas as a baseline for identifying future climate trends in our study area. We first classified the ecozones into three distinct groups or study zones, western, central and eastern NA, to easily identify the major discrepancies in future PIMA growth and mortality rate. As eastern NA represents a more straightforward latitudinal gradient (D'Orangeville et al., 2016, 2018) than their central and western counterparts, we chose to subdivide this zone into northeastern and southeastern NA (Figure 5). A summary of the main climatic data of the ecozones studied is presented in Table 2. We finally overlaid the extent of continuous and discontinuous permafrost over our study area, based on the data of Natural Resources Canada (2022a), in order to easily identify the zones that could be impacted by their respective thaw over the next decades (Figure 5).

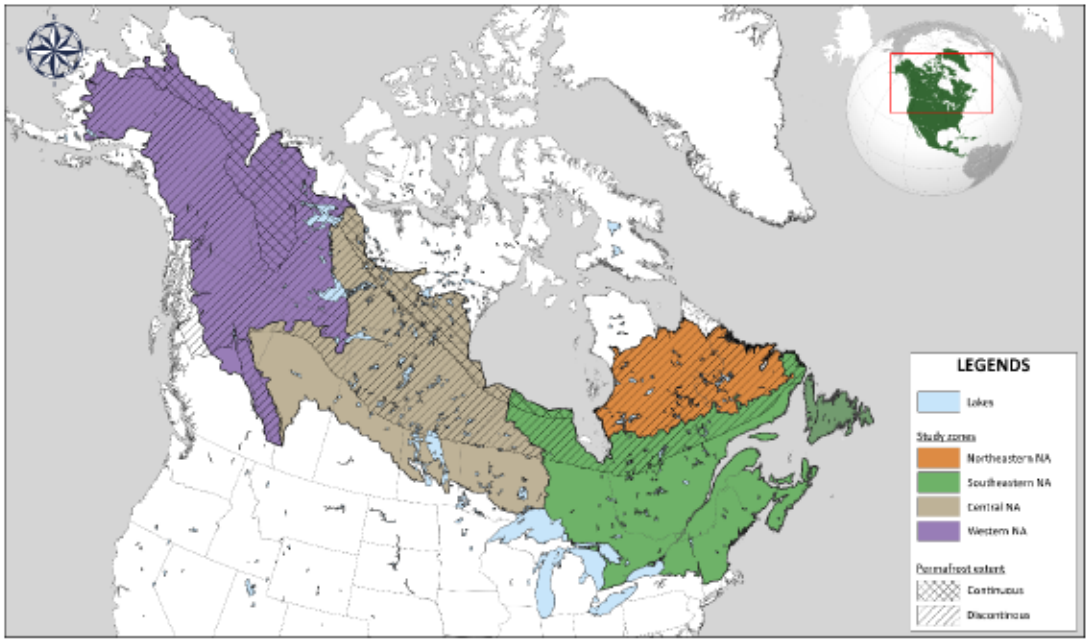

Figure 5
Map of the study area across North America. The extent of the four zones was defined by overlaying the Canadian terrestrial ecozone boundaries to the range of black spruce across North America. The distributions of discontinuous and continuous permafrost within the black spruce range are shown in simple and double dashed lines, respectively.
Sources : Ecological Stratification Working Group, (1995); Price et al., (2013); Natural Resources Canada (2022a).

Table 2
Summary of the ecozones included in each study zone and their respective climatic parameters.
Source : Price et al., (2013).

Study zones	Ecozones	Mean July (January) air temperature (°C)	Mean annual precipitation (mm)	Mean growing (non-growing) season precipitation (mm)	Growing season length (days)
Western NA	Taiga Plains	13.8 (-27.2)	347	184 (163)	127
	Taiga Cordillera	10.2 (-27.6)	401	172 (229)	94

	Boreal Cordillera	10.6 (-21.3)	446	195 (251)	113
	Montane Cordillera	*N.A.*	*N.A.*	*N.A.*	*N.A.*
Central NA	Boreal Shield (West)	16.1 (-22.6)	579	371 (208)	159
	Boreal Plains	15.4 (-19.2)	472	316 (156)	163
	Aspen Parkland	17.0 (-16.6)	451	323 (128)	176
	Taiga Shield (West)	12.8 (-29.7)	340	174 (166)	117
South-eastern NA	Boreal Shield (East)	14.9 (-16.7)	1000	519 (481)	161
	Hudson Plains	13.6 (-24.2)	555	337 (218)	144
North-eastern NA	Taiga Shield (East)	10.8 (-22.8)	747	335 (412)	118

1.4.2 Literature review

We used a twofold filtering process for our literature review. We first conducted an extensive review of the literature using major electronic databases (e.g., Google Scholar, Scopus®, and Web of Science™) to gather published, peer-reviewed articles and reports. The search includes three parameters with the first being terms "black spruce" or "*Picea mariana*", the second being "climate change" or "temperature" or "precipitation" or "CO_2" and "snow" or "frost" or "wind" or "soil temperature" or "mineralisation" or "insect" or "competition" or "pathogen" or "parasite" or "disease", and the third being "growth" or "mortality". Due to recent advances in these areas of forest science in the last few decades which were used in our search parameters, we focused primarily on papers published from 1990 onward. Studies that do not address the direct relationships between the various biotic and abiotic factors and PIMA growth or mortality and various biotic and abiotic factors were removed from the initial list. In addition, bibliographies were also scanned to add peer-reviewed articles that passed

our first research filter. The final dataset comprised 436 peer-reviewed articles that were selected as relevant for this literature review.

1.5 Climate change-induced abiotic risks on black spruce growth and mortality rate

1.5.1 Cumulative impacts of temperature and precipitation

From a physiological point of view, variations in air temperature and precipitation are generally considered as the most limiting factors for tree growth (Subedi and Sharma, 2013). Depending on the depth of the water table (see Lieffers and Rothwell, 1987), PIMA is mostly shallow-rooted and thus has limited access to deep water resources, making it particularly sensitive to water stress. It also occurs on drought-sensitive organic soils, therefore increasing its vulnerability to drought events (Marchand et al., 2021). While the PIMA range is currently subject to a double climatic gradient along both east-west and north-south axes, the respective influences of temperature and precipitation depend highly on the specific geographic location being considered.

In eastern Canada, cold temperatures in the northernmost latitudes exercise a major constraint on PIMA growth, whereas, further south, increased solar radiation results in higher evapotranspiration, leading to a moisture-limited environment (Sniderhan, 2018). Currently, the boundary between temperature- and precipitation-limited environments in eastern Canada is approximately situated between 49°N and 50°N (D'Orangeville et al., 2016, 2018). In contrast, western and central North America receives about half as much precipitation as their eastern counterparts (Table 2), resulting in an imbalance between evapotranspiration and available moisture (Price et al., 2013). Central and western NA are thus almost exclusively moisture-limited until their northernmost extent (Wilmking et al., 2004), and temperature consequently exerts a minor constraint on tree growth in these regions. Indeed, while low temperatures also largely prevail in these regions and might intuitively suggest that a large part of these regions could be temperature-limited, many studies have shown a negative relationship between temperature and tree growth in central (Peng et al., 2011) and western NA (Cahoon et al., 2018). This paradoxical response, often referred

to as the '*divergence problem*' (see D'Arrigo et al., 2008 for a review), mainly involves temperature-induced drought stress as the factor explaining reduced tree growth. One exception is found in the high elevations of central and western NA (Youngblut and Luckman, 2008; Flower and Smith, 2011), where topographic gradients, mainly in the Rocky Mountains and Alaska Range, lead to the development of stunted or non-arboreal growth forms resulting from harsh climatic conditions (see Gamache and Payette, 2004).

When viewed independently of precipitation (Table 2), the projected increase in temperatures by 2100 has the potential to positively affect basal area (Sniderhan et al., 2021) and height growth (Pau et al., 2022) of PIMA through their effects on photosynthetic activity (D'Orangeville et al., 2018). In northeastern NA, Price et al. (2013) predict an increase in the growing season length by 33 (RCP2.6) to 44 (RCP8.5) days by 2100 and an increase in mean July air temperature by 3.1°C (RCP2.6) to 4.8°C (RCP8.5), with increasing precipitation expected to fully compensate higher evapotranspiration (Climate Moisture Index (CMI): +5.5 to 8.5 cm under RCP2.6 and RCP8.5, respectively, Table 3). The resulting enhanced photosynthetic rates north of 50°N should highly promote PIMA growth in terms of both height and basal area (D'Orangeville et al., 2016, 2018; Pau et al., 2022), up to +65% under a +4°C/+15% precipitation scenario. Model-based studies estimate a more modest increase in PIMA growth under a x2 CO_2 scenario, estimated at a maximum of +25% north of 49°N (Huang et al., 2013). Payette et al. (1995) and MacDonald et al. (1998) also suggest a future increase in upright growth forms at the PIMA treeline in eastern and central Canada, due to increasing temperature. More importantly, Pau et al. (2022) demonstrated that even under the RCP8.5 scenario, the increase in air temperature is not expected to exceed the threshold at which warming has a negative impact on radial and height growth in northeastern Canada. In contrast, increasing evapotranspiration (CMI: -1.2 to -3.5 cm, Price et al., 2013, Table 3) and the strong dependence of autotrophic respiration on temperatures in southeastern Canada should be mostly detrimental to PIMA growth but will depend on the climatic scenario considered (Girardin et al., 2016b; Chaste et al., 2019). A study conducted by

D'Orangeville et al. (2018) in eastern NA revealed that under a +2°C temperature increase associated with a 15% increase in precipitation, enhanced growth of PIMA is expected over its entire range except for a thin band covering its southern limit. Conversely, a +4°C global increase with associated increased evapotranspiration would lead to a severe growth decline south of 50°N, with decreases in basal area of up to 45% (D'Orangeville et al., 2018).

Currently, central and western NA receive about half as much precipitation as their eastern counterparts (Table 2; Price et al., 2013). Despite the low temperatures prevailing in these regions, particularly in western NA (Table 2; Price et al., 2013), most studies revealed that drought is currently the main factor involved in spruce growth reduction and dieback episodes across western (Hogg and Bernier, 2005) and central (Kljun et al., 2006) NA. An overall decrease in soil water availability is predicted by 2100, with CMI decreases of 8.2 and 1.4 cm being estimated for central and western NA, respectively (Table 3, Price et al., 2013). These regions should thus experience the strongest increase in the frequency and intensity of drought events across the entire PIMA range (Price et al., 2013; Tam et al., 2018). This should lead to severe declines in black spruce NPP (Girardin et al., 2008; Ma et al., 2012; Girardin et al., 2016b), reaching up to 25% under the RCP8.5 scenario by the end of the century (Girardin et al., 2016b). It seems important to note that western NA also possesses significant topographic gradients due to the presence of mountainous areas, particularly in the Rocky Mountains and Alaska. These high-altitude regions are dominated by wetter and colder conditions, thus suggesting a control of PIMA growth by temperature and consequently a positive future response to climate change (Hogg and Bernier, 2005; Walker and Johnstone, 2014). Surprisingly, studies conducted in the interior of the Alaska Range and in the northern Yukon revealed that the PIMA growth response to increased temperature was negative, and largely independent of latitudinal or elevation gradients (Walker and Johnstone, 2014; Walker et al., 2015). These studies suggest that PIMA in central and western North America will become increasingly susceptible to drought stress by the end of the century, independent of temperature gradients related to altitude or elevation.

1.5.2 CO_2 concentration

CO_2 concentrations have increased from 310 ppm in 1950 to 421 ppm in 2023, mainly due to the burning of fossil fuels by human activities. According to current projections, these emissions may remain stable (RCP2.6), increase moderately to 670 ppm (RCP6), or, in the most pessimistic scenario, reach up to 936 ppm (RCP8.5) by the year 2100 (Table 3, Pörtner et al., 2022). Under the present climate policies, recent projections suggest that the latter two are currently the most likely (Capellán-Pérez et al., 2016), thus suggesting high atmospheric [CO_2] enrichment by 2100. As photosynthetic uptakes of carbon-driving NPP are not saturated at current atmospheric levels (Long et al., 2004), CO_2 fertilisation may have a net positive effect on PIMA growth. At a physiological level, it is predicted that elevated [CO_2] would allow for better net carbon fixation and shade tolerance through more efficient use of light energy (Drake et al., 1997). In this sense, CO_2-enrichment experiments realised under a 710 ppm [CO_2] scenario increased the NPP, height, diameter, shoot, and root dry mass of PIMA seedlings by 23% (Bigras and Bertrand, 2006), while similar experiments suggest a 55% NPP increase under the same atmospheric conditions (Johnsen and Seiler, 1996). Other theoretical experiments on PIMA seedlings also suggest an increase in PIMA growth over its entire range as a consequence of rising [CO_2] as compared to the preindustrial era (Table 2, Li et al., 2015).

However, several studies using tree rings have not been able to objectively show this increase in tree growth at the global scale (Gedalof and Berg, 2010), and more specifically for boreal species (Price et al., 2013; Girardin et al., 2016a). Indeed, the response of mature trees may differ from that of seedlings, but is also more challenging to study due to numerous confounding factors. As a result, our understanding of the response of mature PIMA trees compared to seedlings remains limited at present. Recent tree-ring studies over the last 50 years have struggled to identify any significant impact of increased atmospheric [CO_2] levels, mainly due to these confounding factors and the relatively modest rise in [CO_2] levels (Gedalof and Berg, 2010), while a study conducted in British Columbia by Messaoud and Chen (2011) on mature PIMA trees suggest a positive response to recent increases in [CO_2]. Free-Air CO_2 Enrichment (FACE) experiments have the potential to improve our

knowledge of mature trees, but have so far rarely been carried out on mature trees, and to our knowledge, not on PIMA. In addition to the direct impact of [CO_2] on the growth of PIMA, Bigras and Bertrand (2006) showed that higher atmospheric [CO_2] was related to earlier bud set in fall. As an earlier bud set reduces the likelihood of damage from early frost events, [CO_2] enrichment also has the potential to decrease frost damage to PIMA buds in the upcoming decades.

1.5.3 Interactions between snow and frost

Boreal trees have naturally evolved to cope with intense winter stress, characterised by long frost periods and substantial snow accumulation that largely affect their phenology. The decreasing photoperiod and reduced temperatures in fall induce the development of buds and enable cold hardiness, while warmer temperatures and the longer photoperiod in spring initiate budburst and trigger annual shoot growth (Chang et al., 2021). Under a warming climate, the photoperiod will remain unchanged while predicted temperatures will rise, resulting in an increasing mismatch between these two parameters that may happen more frequently. This will modify the phenological cycles of trees, making them increasingly vulnerable to future freezing conditions. Indeed, earlier dehardening of PIMA buds followed by below-freezing temperatures can induce injuries to meristems, leaves or roots in spring (Man et al., 2021). Early frost conditions in fall may have similar impacts or create xylem cavitation (Sperry and Robson, 2001), ultimately leading to reduced PIMA growth. In addition to these impacts on the apical apparatus, prolonged ground freeze can also damage the fine roots of seedlings or mature trees. When there is insufficient snow cover in winter, roots are particularly vulnerable, as snow acts as an insulator and protects PIMA roots against frost in spring and fall (Fréchette et al., 2011). Consequently, frost can largely hinder PIMA growth, cause permanent damage, and even lead to individual death several years following a frost event (Gaumont-Guay et al., 2008).

Winter conditions as a determinant of tree growth have often been overlooked during the past decades despite their major impact in northern environments (Gamache and

Payette, 2004), due to the uncertainties related to future winter conditions. Snow and frost responses to global warming will indeed vary greatly with latitude, longitude, elevation, and seasonality, inducing complex predictions for their respective influences on PIMA growth. For example, the model of Brown and Mote (2009) predicts a large decrease in the snow cover by the year 2070 south of 60°N in western and central NA, while in eastern NA this transition occurs between 51 and 53°N (Table 3). Snow cover is also predicted to significantly decrease in the coastal areas of western and eastern NA, and conversely increase north of the Great Lakes (Table 3; Brown and Mote, 2009).

As snow is a significant ground insulator, several hypotheses have been suggested for how predicted changes will affect PIMA growth. Firstly, freeze events are likely to become increasingly frequent in the NA regions where significant decreases in snow cover are predicted (Groffman et al., 2001). Root damage is thus more likely to occur and may induce reductions in PIMA growth or mortality episodes. In contrast, the potential for root damage is not likely to be different from current conditions in regions that are expected to experience an increase in snow cover. Secondly, higher temperatures and longer growing seasons across the entire PIMA range should induce an earlier emergence from winter dormancy, during which sub-zero temperatures are still common (Ma et al., 2019), but at a time when new needles have low frost resistance. Even though PIMA is highly adapted to below-freezing temperatures (Girardin et al., 2022), the average number of frost days during the growing season has increased by more than two weeks between 1982 and 2012, a tendency that is likely to continue over the next decades (Liu et al., 2018). Since PIMA is an early leaf-out species (Girardin et al., 2022), we can anticipate increased damage to the buds and shoots of both mature trees and seedlings due to climate change, likely leading to significant reductions in individual growth (Groffman et al., 2001; Marquis et al., 2022).

Currently, harsh winter conditions, characterised by thick snowpatches, frost desiccation of needles and buds, and mechanical damage associated with high wind speeds, prevail towards the forest-tundra ecotone (Truchon-Savard et al., 2019;

Maher et al., 2020). These conditions hinder the development of erect PIMA forms due to damage caused by snow and ice, resulting in the development of stunted ("krummholz") growth forms (Truchon-Savard et al., 2019). In the next decades, climate change at the northern range of PIMA is expected to results in an amelioration of climatic conditions through reduced ice crystal abrasion and thicker snow cover during winter (Brown and Mote, 2009), thus resulting in significant growth gains at the individual level. An increased development of upright PIMA growth forms has already been identified at the treeline in northern Quebec in response to 20th-century global warming, a tendency that is likely to continue in the future with increasing mean annual temperatures (Gamache and Payette, 2004).

1.5.4 Edaphic parameters

PIMA forest ecosystems are largely dominated by cold, nutrient-poor, permafrost-dominated soils, which induce an overall low NPP (Cleve et al., 1993). Combined with short growing seasons and limited decomposition rates due to cold air temperatures, it partly explains why boreal forests store important quantities of biogenic carbon, and play a major role in climate regulation through the carbon cycle (Snyder et al., 2004). Soil warming due to climate change and increased wildfire activity may affect many chemical processes in forested ecosystems and is also expected to stimulate permafrost thaw, ultimately leading to major changes in PIMA growth and mortality rate.

Most of the boreal zone is currently subject to nitrogen limitations (Norby et al., 2010). Soil temperature is indeed a key factor affecting processes such as litter decomposition, soil respiration, nutrient acquisition by plant species, and fine root growth dynamics (Rustad et al., 2001). At a physiological level, high soil temperatures improve xylem activity and water uptake of gymnosperms (Alvarez-Uria and Körner, 2007), and are also positively correlated to the decomposition and mineralisation rates of organic materials, themselves driven by temperature-limited microbial activity (Rustad et al., 2001; Lafleur et al., 2015). Consequently, the predicted increase in soil

temperatures over the upcoming decades is expected to stimulate the overall growth of boreal trees. This will occur through the enhancement of nitrogen mineralisation and nitrification processes in organic soils (Campbell et al., 2009; Price et al., 2013). More particularly, Moore et al. (1999) predict a 4-7% increase in litter decomposition rates under a 500-700 ppm [CO_2] scenario, which could stimulate PIMA growth across its entire range. However, few studies have been carried out on the specific response of spruce compared with other conifer species. Peng and Dang (2003) and Dang and Cheng (2004) have shown from soil warming experiments conducted on PIMA seedlings that its optimum soil temperature for total biomass is around 16.0°C. When summer soil temperatures reach approximately 15°C in southeastern NA (Lupi et al., 2012), with projected increases between 1.9 to 3.3°C by the year 2080 (Houle et al., 2012), PIMA productivity across its entire range is expected to be positively impacted, as the temperatures will be reaching a beneficial threshold an extended part of the year. Moreover, a study conducted in eastern Canada by Lafleur et al. (2015) suggests a decrease in peat production rates by the end of the century under increasing frequency of high-severity fires. The related decrease in peat production rates may also reduce the area covered by paludified forests in southeastern NA, thus increasing the general productivity of eastern Canadian forests in permafrost-free areas.

With the disappearance of permafrost expected within the next 50-100 years (Price et al., 2013), large offsets of positive effects related to warmer soils can also be expected. Currently, most of central and western North America is covered by discontinuous permafrost, although continuous permafrost covers a thin strip north of the PIMA range (Figure 5). In eastern NA, discontinuous permafrost covers the entire region above 52°N (Figure 5) and is often surrounded by saturated, permafrost-free wetlands with few trees (Zhang et al., 2003). Currently, peat plateaus cover between 30 and 70% of peatlands in the discontinuous permafrost zone where PIMA is the more common species (Olefeldt et al., 2021). Due to warming soils, permafrost was estimated to thaw by approximately 0.58% per year between 2000 and 2015 in western Canada, a tendency that is predicted to continue in the upcoming decades (Chasmer and Hopkinson, 2017). The resulting deepening of the active layer will lead to major

hydrological changes, including increased waterlogged conditions due to the transformation of discontinuous permafrost into thermokarst (Olefeldt et al., 2021), to which PIMA is poorly adapted (Islam and Macdonald, 2004). At the physiological level, flooding conditions impair root functions and water uptake, thus reduced PIMA growth could be largely expected in these areas (Baltzer et al., 2014). Moreover, the intolerance of PIMA to flooding (Islam and Macdonald, 2004) and the increased transformation of dry peat plateaus to inundated wetlands should result in large-scale PIMA mortality episodes in the next decades (Haynes et al., 2021). This negative effect could even be amplified by the increasing soil instability due to permafrost thaw (Van Cleve et al., 1990), resulting in increased PIMA mortality rate across the current permafrost zone. Observations of this effect are already visible in eastern (Pelletier et al., 2019), central (Camill et al., 2001), and western NA (Baltzer et al., 2014). Additionally, recent studies have shown that wildfire activity is tightly linked to permafrost thaw, in part due to the low albedo of the burned zone, which leads to higher soil temperature. About 25% of the peat plateaus of western Canada have burned in the last 30 years (Gibson et al., 2018), and this tendency is predicted to increase in the next decades, particularly in central and western NA (de Groot et al., 2013). Regions where wildfire activity is predicted to increase could thus become increasingly vulnerable to permafrost thaw in the next decades (Turetsky et al., 2011).

1.6 Climate change-induced biotic risks

1.6.1 Eastern spruce budworm

Insect outbreaks are, with fire, among the most severe ecological disturbances in NA boreal forests (Jardon et al., 2003). Among these, the eastern spruce budworm (*Choristoneura fumiferana* (Clem.), hereafter ESB), a conifer defoliating moth widely distributed across PIMA range, is considered the main insect pest for PIMA (Fierravanti et al., 2015). It feeds on the young needles of fir (*Abies* spp.) and spruce (*Picea* spp.), inducing tree damage ranging from simple annual growth reduction to the death of large stands after repeated major defoliation years (Chen et al., 2017). As a flush feeder, ESB larvae begin to feed on the newest annual foliage. The

phenology between larvae emergence from diapause and the timing of budburst of its hosts thus highly determine its specific impact. Historically, balsam fir (*Abies balsamea* (L.) Mill.) budburst occurred a few days after the emergence of the 2nd ESB instar from winter diapause, and on average 13 days later for PIMA (Nealis and Régnière, 2004). While PIMA remains an attractive host in terms of nutritional value for the ESB (Pureswaran et al., 2015), this phenological asynchrony largely explains the reduced impact of defoliation on this species during 20th-century outbreaks. However, as insect species are extremely sensitive to changes in spring temperatures, many defoliating insects show an advanced phenology in response to temperature increases (Pureswaran et al., 2015; Fuentealba et al., 2017; Bellemin-Noël et al., 2021). While an even earlier emergence of ESB could increase the phenological lag for PIMA budburst, rising temperatures in boreal ecosystems also affect tree species phenology (Wolkovich et al., 2012). Currently, field experiments (see Bronson et al., 2009; Bellemin-Noël et al., 2021) have shown that warmer temperatures will probably improve ESB-PIMA phenological synchrony and increase caterpillar growth rates. As a result, PIMA could experience defoliation rates close to those of balsam fir in the next decades (Fuentealba et al., 2017; Bellemin-Noël et al., 2021), although defoliation rates may also be moderated by the increase in mixed stands due to a growing impact of ESB (Cappuccino et al., 1998).

While its hosts range currently extends beyond the 60th parallel, the northern limit of the ESB in eastern NA rarely reaches the ecotone between closed-crown forest and open-canopy woodlands, which is situated at approximately 52°N (Gray, 2008). Despite the presence of their hosts, short summers in the high latitudes prevent ESB larvae from completing their development cycle and limit their northern distribution. Thus, the spatial variability of ESB distribution is not only related to forest composition but also depends on climatic conditions necessary for its development, particularly temperature. In eastern Canada, recent climatic models suggest a reduction in the prevalence of epidemics at the southernmost limit of ESB distribution (Régnière et al., 2012; Pureswaran et al., 2019). Conversely, northernmost ESB populations will no longer be limited by summers too short to complete their life cycle. In consequence,

an extension of the northern limit of defoliation and a shift to higher elevations is likely to happen (Gray, 2008; Pureswaran et al., 2015; Régnière et al., 2012). As ESB population dynamics are impacted by many climatic, biological, and physical factors, its future extension to the north remains uncertain. For example, Gray (2008) suggests an increase in the severity and duration of outbreaks northwards by the end of the century. On the other hand, Régnière et al. (2012) remain less skeptical, and suggest that the low density of PIMA in the lichen woodlands of eastern Canada should prevent the increasing prevalence of outbreaks until the year 2100. In this sense, further studies (see Cappuccino et al., 1998) have also shown that climate-induced northward shift in ESB epidemics could be moderated by the predicted increase in mixed stands.

Similar to their eastern counterparts, the model of Régnière et al. (2012) suggests a decreasing prevalence of outbreaks in the southern part of western and central NA, due to unsuitable climatic conditions. However, higher densities of white (*Picea glauca* (Moench) Voss) and black spruce currently prevail at the northernmost latitudes in these regions. Consequently, this model predicts that the higher density of ESB's host plants in northern latitudes may largely enhance the prevalence of outbreaks in these regions due to climate change. However, to our knowledge the specific response of PIMA has not been studied in these regions, and the question of the duration of ESB outbreaks remains uncertain. While Price et al. (2013) suggest longer epidemics in the future, the models of Boulanger et al. (2016) in central and eastern Canada suggest little change in their duration under the RCP2.6 scenario, while the RCP8.5 would induce a shortening of epidemic duration. At the same time, ESB epidemics are expected to develop at higher altitudes in the mountainous regions of western Canada, where harsh conditions currently limit its spatial distribution (Régnière et al., 2012). This increased impact of ESB in western and central NA may also be moderated by a rise in the proportion of deciduous species in western and central NA stands, caused both by increasing frequency, size and severity of fires and insect outbreaks (Cappuccino et al., 1998).

1.6.2 Competition

Competitive relationships for water, nutrients, or light have been shown to exert a major impact on PIMA growth (Légaré et al., 2004; Montoro Girona et al., 2017). More specifically, recent studies (*e.g.* Ettinger and HilleRisLambers, 2013; Oboite and Comeau, 2020) demonstrated that competition may have a greater impact than climate on the radial and height growth of tree species, making it one of the most influential natural processes in NA boreal forests. PIMA growth and mortality rate indeed do not only depend on climate or disturbance regimes but also on the surrounding environment, including species diversity. As ecosystem dynamics are shaped by patterns and processes of disturbance and recovery, particularly fire, they are likely to be largely modified under predicted climate change. PIMA responses may thus strongly depend on future system states (Trugman et al., 2018), including resilience-driven ecosystem composition. However, strong regional differences in the recovery patterns of PIMA are expected (Baltzer et al., 2021), which may modify their competitive relationships.

Although they are largely dependent on future climate scenarios, large-scale studies conducted in southeastern Canada show that future changes in fire regimes (+33% in fire occurrence (Wotton et al., 2010) and +39 to 157% in area burned (Price et al., 2013) by the year 2100) and intensifying forest management are expected to affect the regeneration potential of PIMA and lead to an increasing number of regeneration failures (Boulanger et al., 2017; Molina et al., 2021; Baltzer et al., 2021). Through reversion from closed-crown forest to open lichen woodland, the decrease in general PIMA stand density (Splawinski et al., 2019) should reduce intraspecific competition, particularly for ground water (Ameray et al., 2023), and conversely largely promote PIMA growth at the individual level (Oboite and Comeau, 2020). For example, the models of Augustin et al. (2022) state that more than 30% of southeastern Canada will be covered by open woodlands under the RCP4.5 and RCP8.5 scenarios by year 2100. On the other hand, a transcontinental-scale study conducted by Baltzer et al. (2021) suggests that replacement of PIMA by jack pine (*Pinus banksiana* Lamb.) is the most probable outcome in northeastern and southeastern NA.

Different scenarios are forecast for central and western NA. Due to shorter fire cycles (typically <100 years), and a predicted larger burned area (up to +124% in western NA and +143% in central NA by 2100, Price et al., 2013), it is predicted that pure PIMA stands will shift to a deciduous dominance in western (Johnstone et al., 2010; Walker et al., 2017; Mack et al., 2021) and central NA (Baltzer et al., 2021). More specifically, mixed PIMA-broadleaves stands dominated by aspen (*Populus* spp.) and birch (*Betula* spp.) should dominate, especially on moderately to well-drained sites (Johnstone et al., 2010). Studies conducted in eastern Canada (see Légaré et al., 2004; Chavardès et al., 2021, 2023) pointed out that aspen tends to increase the nutrient mineralisation rate in mixed aspen-PIMA stands, thus increasing radial and height growth of the latter. Positive effects on PIMA related to interspecific relationships are thus likely to occur in western and central NA.

Superimposed on these longitudinal gradients, permafrost-thaw could also induce major changes in PIMA competitive relationships. For example, Nicklen et al. (2021) emphasised that the faster-growing and deeper-rooted white spruce may outcompete PIMA in areas currently underlain by permafrost through a better use of the active layer under permafrost thaw, resulting in increased drought stress for PIMA. In consequence, interspecific competition should be largely detrimental to PIMA in regions currently underlain by permafrost (Figure 5) (Trugman et al., 2018). However, intra- and interspecific competition mechanisms linked to PIMA remain currently poorly investigated in boreal forest (Chavardès et al., 2023) and are intrinsic to complex interactions with other disturbance factors. Further research is required to better assess their impacts on PIMA individual growth.

1.6.3 Diseases and parasites

Diseases and parasites are major components of forest ecosystems, and thus have significant consequences that range from individual tree growth to stand-level structure, composition and dynamics (Skay et al., 2021). Currently, about 20 species of pathogens endemic to North America attack PIMA (Canadian Forest Service, 2010).

For example, fungi belonging to the genus *Armillaria* (Fr.) Staude infects over 200 million hectares across Canada (Canadian Forest Service, 2010), with a 116,000 m^3 of PIMA growth loss per year estimated in the Canadian province of Manitoba (Brandt, 1995). Another example is eastern dwarf mistletoe (*Arceuthobium pusillum* Peck, hereafter ESDM), which is a parasitic vascular plant on conifers that extends across eastern and central NA, causing large growth declines in infested trees. After about 15 years, 75% of trees succumb to the effects of the parasite (Ostry and Nicholls, 1979). Despite their major impact on stand dynamics, the interaction between pathogens, parasites, and climate change has surprisingly received little attention in boreal forests. Consequently, their future evolution remains highly uncertain and further research is definitely needed. As climate change affects pathogens, hosts, and their interactions, various general hypotheses can however be put forward, although their longitudinal and latitudinal variability remain difficult to interpret.

Firstly, climatic constraints currently limit the ranges of many diseases and parasites such as ESDM (Kliejunas et al., 2009). Longer growing seasons and decreasing annual duration of snow or frost in the soil will likely result in an extension of their range to higher latitudes and elevations, thus exacerbating their impact on PIMA in regions where they were previously limited (Gray et al., 2021). Secondly, infection potential and the spread of diseases and parasites are highly related to tree stress (Zhang and Sutton, 2011). An increasing frequency of drought events, particularly over the central and western parts of PIMA range, may result in increasingly stressful conditions, thus enhancing the impact of diseases and parasites on its growth and mortality rate over these regions. These stressful conditions are likely to be reduced in the northeastern regions of Canada where moisture is less limited. However, Kliejunas et al. (2009) remind us that increasing precipitation in spring may consequently increase the impact of foliar diseases, while enhanced precipitation during fall may promote PIMA stem rusts. Finally, Westwood et al. (2012) propose that the area infected by *Armillaria* spp. could triple in the next 50 years under climate change scenarios in central Canada, suggesting an increasing impact of these fungi on PIMA.

1.7 Complex relationships between factors and their link with ecosystem-scale disturbances

Our review highlights the importance of available moisture on the growth and mortality rate of PIMA, which will largely vary over its entire range. These changes will be particularly striking in western and central NA, where they are predicted to translate into sharp decreases in PIMA growth and abrupt increases in mortality episodes by 2100 (Ma et al., 2012; Peng et al., 2011), notably under severe human-forcing scenarios (Table 3). In southeastern NA, these changes will be more moderate, but will nevertheless result in significant PIMA growth reductions and mortality episodes (Girardin et al., 2016b; Chaste et al., 2019). On the other hand, eastern Québec and Labrador are predicted to become a potential climatic refugium for PIMA in the upcoming decades, due to increased temperatures and the absence of moisture limitation (D'Orangeville et al., 2016). While some factors such as increased air and soil temperatures may enhance PIMA productivity over its range and partially compensate for growth reductions due to moisture limitations, the increased impact of late frosts, ESB, diseases, and parasites will introduce additional constraints on PIMA. These constraints should largely result in abrupt growth declines and mortality episodes over the majority of its range (Table 3). As all factors discussed in this review are largely interrelated, they can also have many cascading impacts, and make the response of PIMA to climate change much more complex. For example, warmer soils may lead to earlier budburst and thus increase frost damage (Li et al., 2015) or enhance the impact of pathogens (Kliejunas et al., 2009). Increasing ESB outbreaks could enhance the impact of diseases and pathogens (Hudak and Singh, 1970). Furthermore, diseases and pathogens may reciprocally increase the severity of ESB epidemics, but this mechanism has been poorly investigated in NA boreal forests. Disease damage may also be enhanced due to a decrease in soil insulation caused by a thinner and shorter snow cover (Battles et al., 2006). As the majority of these factors seem to reinforce a negative effect or, at the very least, reduce a positive effect on growth and mortality rates, collectively they should bring an additional constraint on PIMA growth with climate change. Recent continental-scale modelling studies confirms these assumptions, with a very large reduction in suitable habitats for PIMA

by the year 2100, particularly under the RCP8.5 scenario (Prasad et al., 2020). A meta-analysis conducted on all the species range could however help to more precisely assess the future impact of all the factors discussed on PIMA growth and mortality rate in this review.

Although this review focuses on the impacts of climate change at the scale of the individual tree, we must mention that climate-induced PIMA growth declines and mortality episodes will likely combine with ecosystem-scale disturbances, particularly fire, and reduce the potential productivity of NA boreal forests. In this sense, western and central NA should again be the most impacted with a large increase in area burned (Flannigan et al., 2005), fire occurrence (Wotton et al., 2010) and fire season length (Flannigan and Wotton, 2001) that may exceed PIMA resilience threshold and induce shift away from conifer to mixed and deciduous stands mainly dominated by aspen and birch (Baltzer et al., 2021). In eastern Canada, shorter fire return intervals should result in a different postfire pattern and promote the transition from closed-crown to open-canopy forests (Girard et al., 2008), making PIMA less likely to be affected by growth reduction due to lower intraspecific competition (Ameray et al., 2023) and less severe ESB outbreaks (Régnière et al., 2012). The exceedance of resilience thresholds by PIMA may also be exacerbated in areas under active forest management, where logging followed by fire may also increase the regeneration failure of PIMA (Splawinski et al., 2019). This species currently provides over 35% of the merchantable wood volume for the Canadian provinces of Québec and Ontario (Chagnon et al., 2022). Thus, human-related stressors, such as forestry, are considered major disturbances in these regions (Burton, 2003), and are expected to have a significant impact on the resilience of PIMA forests. For example, clearcutting practices with short rotations may increase regeneration failures, especially in regions marked by short fire cycles or insect outbreaks, thereby exacerbating the loss of PIMA resilience to disturbances (Splawinski et al., 2019). More effective fire suppression, initiated in the 1970s (Lefort et al., 2003), may at the same time mitigate increasing fire frequency, but also enhance ericaceous competition with PIMA seedlings (Mallik and Bloom, 2005). Finally, as globalisation and global trade accelerate, North

American forests are increasingly vulnerable to a growing number of biological invasions. Among them, animal and plant species as well as diseases also have the potential to directly affect PIMA tree growth and mortality rate, or work with previously described biotic and abiotic factors, as well as forest management (Dukes et al., 2009). While North American boreal forests currently face fewer biological invasions than southern regions, Weltzin et al. (2003) suggest that climate change could also intensify invasive species issues in the upcoming decades.

Taken as a whole, our synthesis largely supports the idea that future climate change will deeply and lastingly disrupt the growth and mortality rate of PIMA, depending on its spatial distribution. Although the entire PIMA range will be affected, the predicted large decrease in water availability in central and western Canada is expected to lead to significant growth reduction and mortality events. While some similar drought conditions may occur in its southern range (D'Orangeville et al., 2018), the majority of eastern Canada is expected to undergo a smaller water deficit resulting from a lower precipitation-evapotranspiration ratio (Price et al., 2013; D'Orangeville et al., 2016), and thus be less impacted than their central and western counterparts. However, there will likely be latitudinal and longitudinal differences in how the Canadian provinces of Quebec and Newfoundland-and-Labrador will be impacted. While southeastern NA should be marked by the increased impacts of water stress, spring frosts, and more frequent fire events and pathogen outbreaks, the more northern regions should be spared. At the same time, higher precipitation rates in the easternmost regions of eastern Canada (particularly the Labrador Peninsula and the Côte-Nord region of Québec) are projected to mitigate the increase in temperature, and therefore the region should remain favourable to the development of PIMA. Thus, our synthesis supports the hypothesis proposed by D'Orangeville et al. (2016) that the less moisture-limited regions of northeastern NA may serve as a potential PIMA refugium in the upcoming decades. However, these refugia may be temporary if future climate change becomes too severe, as the conditions in northeastern Canada could become comparable to their western counterparts (D'Orangeville et al., 2018).

1.8 Challenges for sustainable forest management

Forestry is currently one of the most important economic sectors in Canada, representing 1.7% of the national GDP in 2021 (*i.e.* $39.2 billion) (Government of Canada, 2023), among which PIMA represents one of the main economic resources (Natural Resources Canada, 2022b). The predicted major transformations of the North American boreal forests, as described in this paper, are unprecedented in human history and pose major challenges to policymakers and forest managers from ecological, climatic, and economical perspectives. Sustainable forest management practices will likely need to adapt to meet the increasing pressure of predicted climate change on boreal forests over the next decades, particularly in the southernmost forest regions. Thus, proactive forest management strategies should be implemented to mitigate growth reductions and mortality episodes of PIMA, while reducing the risk of fire exposure (Splawinski et al., 2019). As emphasised by our synthesis, these changes in silvicultural practises must be region-specific, since the impacts of climate change will be far more significant in the central and western ranges of PIMA as compared to their eastern counterparts. Mixed plantations of PIMA and jack pine and an increase in seed tree retention have been proposed as an interesting strategy to maintain economically viable forest productivity (Cyr et al., 2022), but are only profitable in areas where the mean fire return interval is over 300 years (Splawinski et al., 2019), which will not be the case over the majority of the PIMA distribution according to recent models (Wotton et al., 2010). Thus, in areas where it is possible, the promotion of broadleaf species in mixed stands is known to induce negative feedback and mitigate fire risk (Astrup et al., 2018), while increasing the productivity of PIMA during periods of water limitation (Augustin et al., 2022; Ameray et al., 2023). However, Boulanger and Pascual Puigdevall (2021) emphasize that since conifers are typically preferred over broadleaves for wood supply, changes in forest composition will significantly impact the forest industry, necessitating adaptation.

This review provides a good baseline to identify the challenges inherent in maintaining the resilience of PIMA and adjusting sustainable forest management practices in NA boreal forests. It highlights the importance of both retrospective and current studies to identify the vulnerabilities of PIMA to climate change and demonstrates that the effects

of climate change will be significantly more negative for PIMA growth and mortality rate under the RCP8.5 scenario than lower anthropogenic forcing scenarios, particularly in western and central NA. Therefore, it underscores the increasing importance of mitigating anthropogenic climate influences to achieve temperatures lower than the predicted levels by the end of the century. This action is essential to minimize the impact of climate change on black spruce and, more broadly, on NA ecosystems.

1.9 Acknowledgments

We thank the two anonymous reviewers for improving the first version of the manuscript through their useful comments and suggestions. We also would like to thank Paul Jasinski for proof-reading this article.

1.10 Author statements

1.10.1 Competing interests statement

The authors declare there are no competing interests.

1.10.2 Author contribution statement

Jonathan Lesven: Investigation, Data Curation, Writing - Original Draft, Writing - Review & Editing, Project administration; Milva Druguet Dayras: Investigation, Data Curation, Writing - Review & Editing; Jonathan Cazabonne: Investigation, Writing - Review & Editing; François Gillet: Resources, Writing - Review & Editing, Supervision, Project administration; André Arsenault: Resources, Writing - Review & Editing, Supervision, Project administration; Damien Rius: Resources, Writing - Review & Editing, Supervision, Project administration, Funding acquisition; Yves Bergeron: Conceptualization, Resources, Writing - Review & Editing, Supervision, Project administration, Funding acquisition.

Table 3
Summary of the projected changes in selected study zones by 2100 and their individual effects on BS growth and mortality. MAT: Mean Annual Temperatures ; MAP: Mean Annual Precipitation ; GSL: Growing Season Length ; WAI: Water Availabilitv Index : CMI: Climate Moisture Index

Parameters	Location	Prediction by 2100	Effect on black spruce
Temperature	West	Increase of MAT by up to 5.5°C (1961-1990 baseline) (Price et al., 2013) Increase of GSL by 24 to 46 days (1961-1990 baseline) (Price et al., 2013)	Increase in basal area (Sniderhan et al., 2021) and height growth (Pau et al., 2022), but constrained by moisture (Pau et al., 2022)
	Centre	Increase of MAT by 5.5°C (1961-1990 baseline) (Price et al., 2013) Increase of GSL by 21 to 35 days (1961-1990 baseline) (Price et al., 2013)	Increase in basal area (Sniderhan et al., 2021) and height growth (Pau et al., 2022), but constrained by moisture (Pau et al., 2022)
	South-east	Increase of MAT by 5.5°C (1961-1990 baseline) (Price et al., 2013) Increase of GSL by 31 to 43 days (1961-1990 baseline) (Price et al., 2013)	Increase in basal area (Sniderhan et al., 2021) and height growth (Pau et al., 2022) due to longer growing season, but limited due to a moisture-limited environment (Pau et al., 2022)
	North-east	Increase of MAT by 3.5 to 6°C (1961-1990 baseline) (Price et al., 2013) Increase of GSL by 33 to 44 days (1961-1990 baseline) (Price et al., 2013)	Increase in height (Gamache & Payette, 2004; Pau et al., 2022) and basal area growth (D'Orangeville et al., 2016; Silva et al., 2010) and leader shoot elongation (Gamache & Payette, 2004) due to a currently temperature-limited environment associated to longer growing season (D'Orangeville et al., 2016; Pau et al., 2022; Sniderhan et al., 2021)

Precipitation and water availability	West	Increase in MAP by 10 to 25% (Price et al., 2013) Low water availability: WAI < 1 (1950-2000 baseline) (D'Orangeville et al., 2016) / CMI: +2.8 to -1.4 cm (1961-1990 baseline) (Price et al., 2013)	Decrease in general BS growth (D'Orangeville et al., 2016), net primary productivity (Z. Ma et al., 2012) and basal area growth (D'Orangeville et al., 2018; Z. Ma et al., 2012; Sniderhan et al., 2021)
	Centre	Increase in MAP by 11% (Price et al., 2013) Low water availability: WAI < 1 (1950-2000 baseline) (D'Orangeville et al., 2016) / CMI: -2.4 to -8.2 cm (1961-1990 baseline) (Price et al., 2013)	Decrease in general BS growth (D'Orangeville et al., 2016), net primary productivity (Z. Ma et al., 2012) and basal area growth (D'Orangeville et al., 2018; Z. Ma et al., 2012; Sniderhan et al., 2021)
	South-east	Increase in MAP by 13% (Price et al., 2013) Moderate water availability: 1.0 < WAI < 2.0 (1950-2000 baseline) (D'Orangeville et al., 2016) / CMI: -1.2 to -3.5 cm (1961-1990 baseline) (Price et al., 2013)	Decrease in general BS growth (D'Orangeville et al., 2016), net primary productivity (Z. Ma et al., 2012) and basal area growth (D'Orangeville et al., 2018; Z. Ma et al., 2012)
	North-east	Increase in MAP by 10 to 22% (Price et al., 2013) High water availability: WAI > 1.5 (1950-2000 baseline) (D'Orangeville et al., 2016) / CMI: +5.5 to 8.5 cm (1961-1990 baseline) (Price et al., 2013)	Increase in general BS (D'Orangeville et al., 2016) and basal area growth (D'Orangeville et al., 2018)

Atmospheric CO_2 concentration	West	421 ppm (RCP2.6) to 936 ppm (RCP8.5) (Pörtner et al., 2022)	Increased water-used efficiency (Girardin, Hogg, et al., 2016). Theorical increase in net primary productivity by 20 to 25% (Girardin, Hogg, et al., 2016; Li et al., 2015; Norby et al., 2005), and radial and height growth (Messaoud & Chen, 2011), but may be more moderate in reality (Girardin, Bouriaud, et al., 2016; Price et al., 2013)
	Centre	421 ppm (RCP2.6) to 936 ppm (RCP8.5) (Pörtner et al., 2022)	Increased water-used efficiency (Girardin, Hogg, et al., 2016). Theorical increase in net primary productivity by 20 to 25% (Girardin, Hogg, et al., 2016; Li et al., 2015; Norby et al., 2005), and radial and height growth (Messaoud & Chen, 2011), but may be more moderate in reality (Girardin, Bouriaud, et al., 2016; Price et al., 2013)
	South-east	421 ppm (RCP2.6) to 936 ppm (RCP8.5) (Pörtner et al., 2022)	Increased water-used efficiency (Girardin, Hogg, et al., 2016). Theorical increase in net primary productivity by 20 to 25% (Girardin, Hogg, et al., 2016; Li et al., 2015; Norby et al., 2005), and radial and height growth (Messaoud & Chen, 2011), but may be more moderate in reality (Girardin, Bouriaud, et al., 2016; Price et al., 2013)
	North-east	421 ppm (RCP2.6) to 936 ppm (RCP8.5) (Pörtner et al., 2022)	Increased water-used efficiency (Girardin, Hogg, et al., 2016). Theorical increase in net primary productivity by 20 to 25% (Girardin, Hogg, et al., 2016; Li et al., 2015; Norby et al., 2005), and radial and height growth (Messaoud & Chen, 2011), but may be more moderate in reality (Girardin, Bouriaud, et al., 2016; Price et al., 2013)

Snow	West	Increase in snow cover by 1 to 50% (1961-1990 baseline) (Brown & Mote, 2009) Increase in soil insulation during winter or no change (Groffman et al., 2001)	Poorly studied in NA boreal forests (Fréchette et al., 2011). More research needed.
	Centre	Decrease in snow cover by 1 to 50% (1961-1990 baseline) (Brown & Mote, 2009) Decrease in soil insulation during winter (Groffman et al., 2001)	Poorly studied in NA boreal forests (Fréchette et al., 2011). More research needed.
	South-east	Decrease in snow cover by 1 to 10% (1961-1990 baseline) (Brown & Mote, 2009) Decrease in soil insulation during winter (Groffman et al., 2001)	Decreased net primary productivity of BS stands (Fréchette et al., 2011)
	North-east	Stable snow cover or increase by up to 10% (1961-1990 baseline) (Brown & Mote, 2009) Increase in soil insulation during winter or no change (Groffman et al., 2001)	Poorly studied in NA boreal forests (Fréchette et al., 2011). More research needed.

Frost	West	Decrease in snow crystal abrasion Decreasing probability of frost damages (Nitschke & Innes, 2008)	40% probably of decreasing frost damages during growing season (early 21st century baseline) (Nitschke & Innes, 2008)
	Centre	Increase in snow crystal abrasion Increase of frost damages during growing season (Liu et al., 2018)	Increase in fine root mortality (Groffman et al., 2001)
	South-east	Increase in snow crystal abrasion Increase of frost damages during growing season (Groffman et al., 2001)	Increase in fine root mortality (Groffman et al., 2001)
	North-east	Decrease in snow crystal abrasion (Gamache & Payette, 2005)	Increase in height growth (Gamache & Payette, 2005) Development of upright growth forms at the northern limit of BS (Gamache & Payette, 2004)

Edaphic parameters	West	Increased soil temperature (Dao et al., 2015) Increased nitrogen mineralization and nitrification (Rustad et al., 2001) in permafrost-free areas Permafrost thaw in northernmost environments (Wisser et al., 2011)	Increased tree growth in permafrost-free areas (Melillo et al., 2011) Increase in freezing injuries due to earlier budbreak (Li et al., 2015) Decreased tree growth in areas underlained by permafrost (Baltzer et al., 2014)
	Centre	Increased soil temperature (Dao et al., 2015) Increased nitrogen mineralization and nitrification (Rustad et al., 2001) in permafrost-free areas Permafrost thaw in northernmost environments (Wisser et al., 2011)	Increased tree growth in permafrost-free areas (Melillo et al., 2011) Increase in freezing injuries due to earlier budbreak (Li et al., 2015) Decreased tree growth in areas underlained by permafrost (Baltzer et al., 2014)
	South-east	Increased soil temperature (Dao et al., 2015) Increased nitrogen mineralization and nitrification (Rustad et al., 2001) in permafrost-free areas	Increased tree growth (Melillo et al., 2011) Increase in freezing injuries due to earlier budbreak (Li et al., 2015)
	North-east	Increased soil temperature (Dao et al., 2015) Increased nitrogen mineralization and nitrification (Rustad et al., 2001) in permafrost-free areas Permafrost thaw in northernmost environments (Wisser et al., 2011)	Increased tree growth in permafrost-free areas (Melillo et al., 2011) Increase in freezing injuries due to earlier budbreak (Li et al., 2015) Decreased tree in areas underlained by permafrost (Baltzer et al., 2014)

SBW outbreaks	West	Reduced defoliation at the southern limit of SBW distribution, but expansion northward (Régnière et al., 2012) Increased severity and duration of outbreaks on BS (Bellemin-Noël et al., 2021; Fuentealba et al., 2017)	Increased phenological synchrony between SBW and BS budburst (Bellemin-Noël et al., 2021; Bronson et al., 2009) Increased BS growth reduction and mortality episodes (Pureswaran et al., 2015)
	Centre	Reduced defoliation at the southern limit of SBW distribution, but expansion northward (Régnière et al., 2012) Increased severity and duration of outbreaks on BS (Bellemin-Noël et al., 2021; Fuentealba et al., 2017)	Increased phenological synchrony between SBW and BS budburst (Bellemin-Noël et al., 2021; Bronson et al., 2009) Increased BS growth reduction and mortality episodes (Pureswaran et al., 2015)
	South-east	Reduced impact at the southern limit of SBW distribution (Régnière et al., 2012)	Increased phenological synchrony between SBW and BS budburst (Bellemin-Noël et al., 2021; Bronson et al., 2009) Increased BS growth reduction and mortality episodes (Bellemin-Noël et al., 2021; Fuentealba et al., 2017)
	North-east	Increased severity of outbreaks at the northern limit of SBW distribution (D. R. Gray, 2008; Régnière et al., 2012) Increased duration of outbreaks at the northern limit of SBW distribution (D. R. Gray, 2008)	Increased phenological synchrony between SBW and BS budburst (Bellemin-Noël et al., 2021; Bronson et al., 2009) Increased BS growth reduction and mortality episodes (Bellemin-Noël et al., 2021; Fuentealba et al., 2017)

Competition	West	Increased proportion of broadleaf (mainly Populus and Betula) taxa (Baltzer et al., 2021) Increased proportion of white spruce in area subjected to permafrost thaw (Nicklen et al., 2021)	Growth reductions (Young-Robertson et al., 2016) or increased radial and height growth (Chavardès et al., 2021, 2023; Légaré et al., 2004). More research needed.
	Centre	Increased proportion of broadleaf (mainly Populus and Betula) taxa (Baltzer et al., 2021) Increased proportion of white spruce in area subjected to permafrost thaw (Nicklen et al., 2021)	Growth reductions (Young-Robertson et al., 2016) or increased radial and height growth (Chavardès et al., 2021, 2023; Légaré et al., 2004). More research needed.
	South-east	Increased proportion of broadleaf taxa (mainly Populus and Betula) (Ameray et al., 2023) and jack pine (Baltzer et al., 2021)	Decreased productivity of BS stands (Ameray et al., 2023). More research needed.
	North-east	Increased proportion of jack pine (Baltzer et al., 2021)	More research needed.

Diseases and parasites	West	Northward expansion of diseases and parasites (Kliejunas et al., 2009) Increased impact of diseases and parasites through increased drought stress	Increased growth reductions and mortality rates in areas infected by diseases and parasites. More research needed.
	Centre	Northward expansion of ESDM and more generally of diseases and parasites (Kliejunas et al., 2009) Increase by 200% of the area infected by ESDM (Westwood et al., 2012) Increased impact of diseases and parasites through increased drought stress	Increased growth reductions and mortality rates in areas infected by ESDM (Westwood et al., 2012) or other diseases and parasites. More research needed.
	South-east	Northward expansion of ESDM and more generally of diseases and parasites (Kliejunas et al., 2009)	Increased growth reductions and mortality rates in areas infected by ESDM (Westwood et al., 2012) or other diseases and parasites. More research needed.
	North-east	Northward expansion of ESDM and more generally of diseases and parasites (Kliejunas et al., 2009)	Increased growth reductions and mortality rates in areas infected by ESDM (Westwood et al., 2012) or other diseases and parasites. More research needed.

2. TESTING A NEW AUTOMATED MACROCHARCOAL DETECTION METHOD APPLIED TO A TRANSECT OF LACUSTRINE SEDIMENT CORES IN EASTERN CANADA

Jonathan Lesven, Milva Druguet Dayras, Romain Borne, Cécile C. Remy, François Gillet, Yves Bergeron, André Arsenault, Laurent Millet, Damien Rius

Published in Quaternary Science Reviews – October 2022

DOI: 10.1016/j.quascirev.2022.107780

2.1 Abstract

Over the past decades, the abundance and area of macrocharcoal (*i.e.* ≥ 150 mm in diameter) fragments from sedimentary sequences have been quantified using visual or semi-automated methods to reconstruct fire histories. However, the lack of uniformity between counting methods used in each study could introduce methodological biases influencing fire frequency reconstructions, and therefore impact their interpretation and limit their comparisons. To overcome this issue, we propose here a new automated method to quantify the number of macrocharcoal fragments and measure their areas from high-definition image capture, based on the analysis of colorimetric parameters. We tested the efficiency of our method and reconstructed charcoal influx over the last 8000 years by comparing visual and automatic counting methods along a north-south transect from eastern Canada, estimating number and size, and the associated local and regional fire frequencies. Results show that our automated method is efficient in detecting charcoal particles, except for highly minerogenic samples, and suggest that the traditional visual inspection tends to overestimate the size of macrocharcoal fragments. Local fire frequencies varied greatly depending on the macrocharcoal detection method used. At the regional scale they seem closer, and our automated method reproduces similar trends to published studies in our study area. However, it does represent a methodological advancement, particularly for recent centuries, that should be considered for future paleoecological studies.

Keywords: Charcoal, Methodology, Holocene, Wildfire, Sediment core, Influx, Fire frequencies

2.2 Résumé

Au cours des dernières décennies, l'abondance et la surface des fragments de macrocharbons (*i.e.* ≥ 150 µm de diamètre) provenant de séquences sédimentaires ont été quantifiées à l'aide de méthodes visuelles ou semi-automatisées afin de reconstituer l'histoire des incendies. Cependant, le manque d'uniformité entre les méthodes de comptage utilisées dans chaque étude pourrait introduire des biais méthodologiques influençant les reconstitutions de la fréquence des incendies, et donc impacter leur interprétation et limiter leurs comparaisons. Pour résoudre ce problème, nous proposons ici une nouvelle méthode automatisée pour quantifier le nombre de macrocharbons et mesurer leur surface à partir d'une capture d'image haute définition, basée sur l'analyse de paramètres colorimétriques. Nous avons testé l'efficacité de notre méthode et reconstitué les flux de charbon de bois au cours des 8000 dernières années en comparant les méthodes de comptage visuel et automatique le long d'un transect nord-sud de l'est du Canada, en estimant le nombre et la surface, ainsi que les fréquences d'incendie locales et régionales associées. Les résultats montrent que notre méthode automatisée est efficace pour détecter les macrocharbons, à l'exception des échantillons hautement minérogéniques, et suggèrent que l'inspection visuelle traditionnelle tend à surestimer la taille des fragments de macrocharbon. Les fréquences des incendies locaux varient fortement en fonction de la méthode de détection des macrocharbons utilisée. À l'échelle régionale, elles semblent plus proches, et notre méthode automatisée reproduit des tendances similaires à celles des études publiées dans notre zone d'étude. Cependant, elle représente une avancée méthodologique, en particulier pour les derniers siècles, qui devrait être prise en compte dans les futures études paléoécologiques.

Mots-clés : Charbon, Méthodologie, Holocène, Feux de forêt, Carotte sédimentaire, Flux, Fréquence de feu

2.3 Introduction

Fire is a natural disturbance with a major influence on terrestrial ecosystems (Wright, 1974; Bergeron et al., 2004; Bond et al., 2005). It is widely accepted that in the upcoming decades climate change will threaten the carbon sink of boreal ecosystems and lead to numerous disturbances worldwide (Hauer et al., 2001; Chapin et al., 2004; Flannigan et al., 2005, 2009; Tymstra et al., 2007), including an increase in the occurrence, size and severity of forest fires in circumboreal areas (Shvidenko and Schepaschenko, 2013; Rogers et al., 2015; Walker et al., 2019). Paleoecological approaches allows to document disturbance regimes and the response of ecosystems over multimillennial periods for which observational data are not available. As our understanding of fire regimes across the world is still fragmentary, paleoecology provides the baselines for a better understanding of fire regimes in a context of climate change (Bergeron et al., 2006; Pardi and Smith, 2012). Therefore, charcoal records in soils or lakes can be used to infer explicit short- or long-term reconstructions of fire regimes, which is a major controlling factor in the structure and functioning of boreal forests (Swain, 1973; Clark, 1990; Higuera et al., 2007).

In lacustrine sediment cores, a widely used method for reconstructing local fire frequencies, *i.e.* ~1-3 km from the lakeshores (Clark, 1990; Clark and Royall, 1996; Higuera et al., 2007; Oris et al., 2014), involves numerical analysis of macroscopic charcoal accumulation records (CHAR), generally defined as ≥ 150 mm in diameter (Oris et al., 2014a). For this, the decomposition approach relies on dissociating the macrocharcoal records into "charcoal peaks", assumed to represent local fire events, from the "charcoal background", resulting from secondary deposition of charcoals or inputs of a regional origin (Long et al., 1998; Hallett and Walker, 2000; Carcaillet et al., 2001; Long and Whitlock, 2002; Lynch et al., 2002; Oris et al., 2014a). In this approach, macrocharcoal particles are usually quantified by simple counting (*e.g.* Long et al., 1998; Gavin et al., 2006; Leys et al., 2013), by an estimation of their area (*e.g.* Carcaillet et al., 2001; Lynch et al., 2004; Leys et al., 2013; Halsall et al., 2018), or more recently calculating their volume using various methods (see Weng, 2005; Ali et al., 2009; Crawford and Belcher, 2016; Halsall et al., 2018; Belcher et al., 2018) after chemical treatments and sieving of sediment samples (Rhodes, 1998). These

methods can be easily performed by using a binocular microscope (see Rius et al., 2012; Bobek et al., 2019 for example); nevertheless, the measurement of total area, *i.e.* the sum of the areas of all charcoal particles in a sample, is often made visually from a known-size grid placed in the objective of a binocular microscope. It is therefore dependent of the charcoal particle's shape and of the observer bias, thus accuracy of this method may vary. To overcome this problem, semi-automatic measurements of macrocharcoals have been developed, such as the WinSEEDLE™ Software (Regent Instruments Canada Inc. Software, 2009) (see Remy et al., 2017, 2018) or others colorimetric-based macrocharcoal detection methods (see Bobek et al., 2019; Lestienne et al., 2020), but requires a systematic visual inspection of detected particles. These methods remain highly time-consuming for the most charcoal-rich samples, and have often been developed on licensed software; consequently these could be improved with both the development of a more automated, time-efficient approach and the use of open-source softwares. To overcome this latter problem, automated charcoal analysis methods have also been developed on open-source softwares such as ImageJ, based on pixel grayscale value thresholds and particle grayscale standard deviation threshold, but have only been applied to microcharcoals (*i.e.* 150 mm in diameter) from pollen slides (Zou et al., 2021). Moreover, to our knowledge, no study comparing "manual" (*i.e.* visual) to "automatic" (*i.e.* automated) counting methods for macrocharcoal analysis has been carried out to date. We therefore propose to assess the impact of manual versus automatic counting for number and area measurements of macrocharcoal particles from sediment samples in order to evaluate the impact of both methods on fire regime reconstructions in eastern Canada using lacustrine sediment cores.

In this study, we present and test a new automated method to quantify the number of charcoal fragments and measure their size, developed on the open-source ImageJ software (Abràmoff et al., 2004), to improve the detection of historical local fire events for paleoecological studies. This method is based on the definition of filters from macrocharcoal colorimetric parameters, that allow the detection of charcoal particles over a series of Z-stack pictures. We tested our new method by comparing it with the

standard visual method for charcoal detection to reconstruct historical fire frequencies at local and regional scales, from three sites located along a bioclimatic gradient in the boreal forest of Eastern Canada. Finally, we compared our reconstructions of regional fire frequencies with previously published data that used semi-automatic measurement, in order to point the relevant differences with our method. Testing our new approach in this way is crucial to study the effectiveness and the potential biases of the different fire regime reconstruction methods, and in consequence improve our understanding of fire-climate interactions in anticipation of the current climate change.

2.4 Material and methods

2.4.1 Environmental settings

For the purpose of the study, three small freshwater lakes were selected to provide locally robust fire sediment records. The studied lakes are located between 49°N and 56°N across the eastern Canadian regions of Quebec and Labrador (Figure 6). These lakes were chosen both for their small surface area (less than 10 ha) and sufficiently long sediment cores - thus providing robust records of fires at the local scale - and because they encompass varied vegetation zones, allowing a wide range of fire records and vegetation compositions to be covered. Georges Tremblay Lake (TRE; 49°24'44"N, 68°28'27"W, 332 m a.s.l.) is located in the eastern boreal forests of southern Quebec. Billy Lake (BIL; 53°04'60"N, 66°57'87"W, 541 m a.s.l.) is located in southwestern Labrador, 25 km from Labrador City, in the northern boreal woodlands. Finally, Blow Hole Lake (BLH; 56°31'25"N, 61°41'49"W, 122 m a.s.l.) is located on the Atlantic coast of northeastern Labrador, in the subarctic woodlands and tundras.

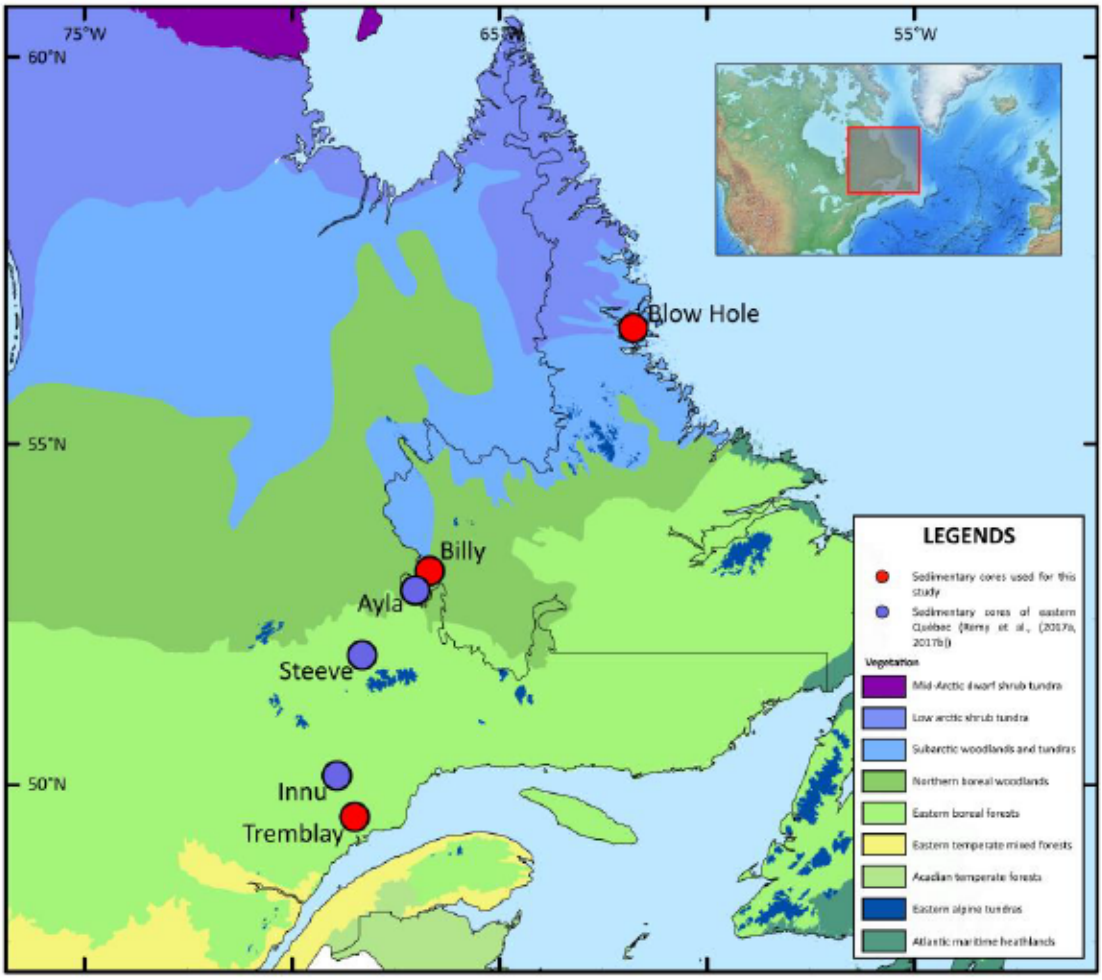

Figure 6
Location of the study sites across the vegetation zones of Canada in Québec-Labrador regions. The three lakes used for this study (Tremblay, Billy, Blow Hole) are represented in red, the three lakes used by the other studies in blue.
Source : Remy et al., (2017a, 2017b); Baldwin et al., (2020).

2.4.2 Coring and chronology

Short sedimentary sequences of 116 (TRE), 91 (BIL), and 113 (BLH) cm in length were collected in August 2019 using a Uwitec gravity corer, 9 cm in diameter, at the deepest point of each lake. The Georges Tremblay Lake is divided in two parts; a large (~40 ha) basin in a southern position, and a smaller (~3.5 ha) basin in a northern position, both separated by a peat bog. For this study, TRE core was retrieved from the northern basin of the lake.

Chronologies of each sediment record were based on the combination of two dating methods. In order to get robust chronology for the last 150 years, the first 10 cm of each core were measured for ^{210}Pb and ^{137}Cs activity activities (Le Roux and Marshall, 2011). In order to obtain the ages, a Constant Rate of Supply (CRS) model was applied (Appleby et al., 1979). To complete this chronology, three to four ^{14}C AMS radiocarbon dates based on plant macroremains (needles, wood, Bryophytes) were obtained for each lake and calibrated at 2σ to calendar years (Table 4) using the IntCal20 Northern Hemisphere Radiocarbon Age Calibration Curve (Reimer et al., 2020). Age-depth models were obtained with a smoothing spline function using the 'Clam' package version 2.3.9 (Blaauw, 2010) in R environment version 4.1.0 (R Core Team). All dates are expressed in calibrated kilo years before present, hereafter referred as ka cal BP. The sediment cores consisted of uniformly dark-brown sediments and were sliced into 0.5-1 cm thick samples representing a median temporal resolution of 40, 60 and 64 years for TRE, BIL and BLH sites, respectively. Age models are available in Supplementary Information 1, 2 and 3 for TRE, BIL and BLH sites, respectively.

Table 4
Radiocarbon (^{14}C) age determination for cores TRE, BIL and BLH. The ^{14}C analyses were performed both at the Poznań Radiocarbon Laboratory at Poznań, Poland, and at the Radiochronology Laboratory at Laval (QC), Canada. The ^{14}C ages were calibrated at 2σ using the IntCal20 Northern Hemisphere Radiocarbon Age Calibration Curve.

Core	Depth in record (cm)	Type	Sample number	Age (Cal yr BP)	Range of calibration (cal yr BP; 2σ)
Tremblay	16.5	Needles	TRE 16-17	155 ± 30	144 (9-278)
Tremblay	25.5	Wood and needles	TRE 25-26	1960 ± 15	1887 (1834-1940)
Tremblay	63.5	Wood and needles	TRE 63-64	3210 ± 15	3419 (3384-3453)
Billy	35.5	Bryophytes	BIL 35-36	1715 ± 30	1602 (1536-1635)
Billy	55.5	Bryophytes	BIL 55-56	2735 ± 35	2823 (2759-2883)

Billy	75.5	Bryophytes	BIL 75-76	4040 ± 15	4475 (4438-4475)
Billy	81.5	Bryophytes	BIL 81-82	4510 ± 15	5149 (5052-5193)
Blow Hole	20.5	Leaves and wood	BLH 20-21	1800 ± 30	2208 (2225-2297)
Blow Hole	53.5	Leaves and wood	BLH 53-54	3795 ± 35	4181 (4084-4295)
Blow Hole	93.5	Wood	BLH 93-94	6205 ± 15	7084 (7008-7133)
Blow Hole	109.5	Needles and wood	BLH 109-110	6910 ± 40	7739 (7669-7838)

2.4.3 Sampling and chemical treatments

The cores were sliced with a step of 0.5 cm for the top-10 cm of each core to get a high-resolution record during the last centuries, then every cm for deeper sediments. One subsample of ~0.435 or 0.87 cm^3 for each 0.5 or 1 cm thick slice, respectively, was taken using a needleless syringe. These were immersed in 20 ml of a 10% NaOH solution for 24 h, followed by 6% H_2O_2 for the same period of time in order to isolate the charcoal particles, by facilitating deflocculation and bleaching the dark organic matter, following the protocol of Rhodes (1998).

2.4.4 Manual estimation of charcoal counts and area

The wet residue was passed through a 4-cm-diameter, 150-mm mesh of a 3D-printed sieve to retain only macrocharcoals, assumed to represent local fire events. To fit with microscope dimensions, a sieve holder was additionally 3D-printed. Charcoals counts and area were then visually estimated under a binocular microscope at x50 magnification, using a grid of 10 x 10 squares of $62.5.10^3$ mm^2 each (Figure 7). This represents the so-called "manual" count, hereafter called C_M.

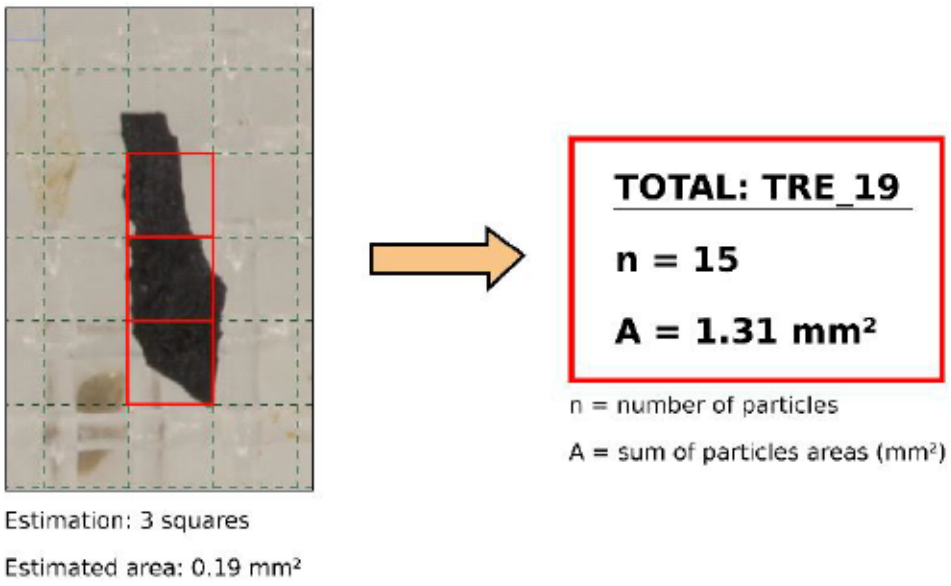

Figure 7
Schematic representation of charcoal manual estimation.
Charcoal particle can be estimated to cover approximately three or four squares, depending on the observer. Here, we estimated that it was covering three squares with a projected area of 0.0625 mm² each, so about 0.19 mm². TRE_19 image, part of the calibration images, was taken as a template: 15 charcoal particles were detected, covering a total area of 1.31 mm².

2.4.5 Automatic estimation of charcoal counts and area

The sieves were scanned and Z-stacked as RGB digital images at x50 magnification using a Keyence VHX-7000 microscope at the Chrono-Environnement Laboratory (UMR 6249 CNRS, Besançon, France). The images obtained were then individually saved as TIFF files about 1.2 GB in size. They were imported into a macro developed under the ImageJ software, allowing the automatic quantification of charcoals and measurement of their area. This represents the so-called "automatic" count, hereafter called C_A. Script was developed in ImageJ Macro language (Abràmoff et al., 2004).

Red-Green-Blue (RGB) image channels were split into individual 8-bit images, and a correction was applied to homogenize the series global luminosity (Supplementary Information 4). Split B channel always displayed a higher number of dark particles than R and G channels. Since charcoal particles are dark on every R, G or B channel, the process operation R + G - B increased intensity of non-charcoal particles, and thus global contrast (Figure 8a). Image segmentation with threshold upper limit of 75 mean intensity and minimum area of 0.015 mm² was defined to select the darker particles and eliminate too small particles (Figure 8b). This selection allowed to extract several information such as area, aspect ratio parameters, position, R, G, or B mean or minimum and maximum values.

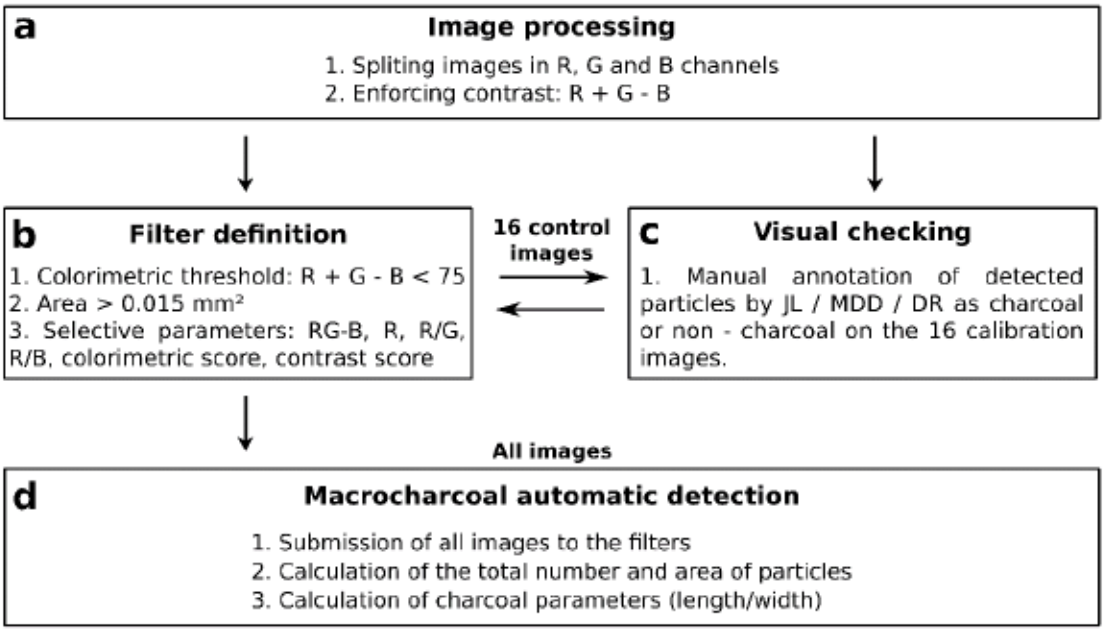

Figure 8
Schematic representation of charcoal automatic detection process. Automatic detection of charcoal particles was processed according to the following steps.
a. Image processing. Red, Green, and Blue channels were split from the RGB image and image process (R+G-B) was performed to enforce contrast of dark particles including charcoals.
b. Filter definition. A segmentation based on a threshold with an upper limit of 75 was performed on all particles of at least 0.015 mm² on the 16 calibration

images. Colorimetric parameters (RG-B, R, R/G, R/B, colorimetric score and contrast score) were measured for each particle.
c. Visual checking. Detected particles were annotated as charcoal or not by Jonathan Lesven (JL), Milva Druguet Dayras (MDD) and Damien Rius (DR) to calibrate the filters defined of the step b. on the 16 calibration images. Then, selective parameters were defined to discriminate both particles populations.
d. Macrocharcoal detection. Particles were filtered according to the limit path of the defined parameters on all images, and non-satisfying particles deleted.

Particles overlays were applied to the original RGB picture from TRE or BIL calibration series of 16 images to allow a manual annotation of these particles by Jonathan Lesven (JL), Milva Druguet Dayras (MDD) or Damien Rius (DR) as true charcoal or not (Figure 8c). Several colorimetric parameters, including ratio of colors, were compared for both populations of particles (Figure 9), resulting in a filter definition composed of six levels. The filter selectivity was tested to validate the ability of keeping annotated particles (Annexe B). Finally, the whole series of images from TRE, BIL and BLH were submitted to this filter analysis (Figure 8d). Every segmentation dataset was filtered considering that a true charcoal particle has to correspond to the whole 6 parameters of the filter. Every particle missing only one parameter was excluded (Figure 8d). The number and area of the remaining particles were then calculated (Figure 8d).

ImageJ macro script is available in Annexe C.

2.4.6 Comparison of the two methods

We compared the distribution of the number and area of macrocharcoal particles in sediment samples obtained by manual and automatic quantifications by means of boxplots separately for each site. For a better visualisation, data were log_{10}-transformed ($y = \log_{10}(x+1)$). A non-parametric Wilcoxon signed-rank test for paired data was used to evaluate the null hypothesis that the distribution of the difference between values obtained by the two methods is symmetric about the mean, and thus, to detect a possible methodological bias. In addition, we computed Spearman's rank correlations between the count or area values estimated by the two methods, as a simple assessment of synchronicity along each series.

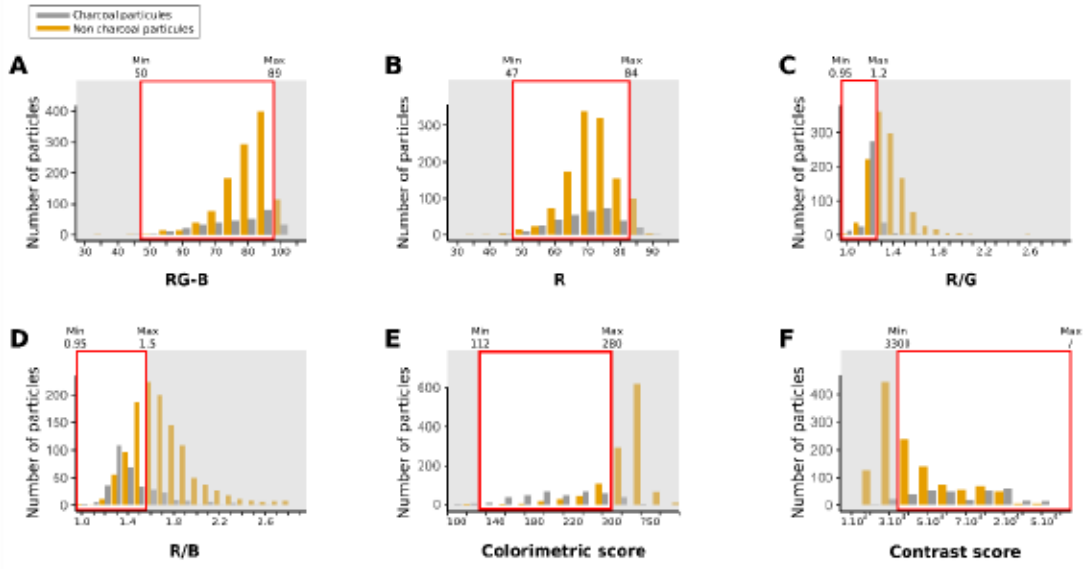

Figure 9
Filter definition on annotated particles from TRE and BIL series.
Histograms show the sum of particles annotated from TRE and BIL series (1639 particles). Particles annotated as charcoal (417) are displayed in grey histograms, particles annotated as non-charcoal (1222) are displayed in orange histograms. Band pass filters are indicated for each parameter in red: a. RG-B mean (processed image); b. R value; c. R/G (Green mean value) ratio; d. R (Red mean value)/B (Blue mean value) ratio; e. Colorimetric score: (R+(R+G-B))*R/G*R/B ; f. Contrast score : G_{min}*B_{min}+$\Delta G_{max-min}$* $\Delta B_{max-min}$.

2.4.7 Numerical and statistical treatments of charcoal records

Several studies have shown that charcoal particles can be quantified in number or area (Tinner and Hu, 2003; Carcaillet, 2007; Ali et al., 2009b) to provide accurate fire regime reconstructions. To compare manual and automatic results, these counts were transformed into charcoal accumulation rates (CHAR) in number (#.cm^{-2}.yr^{-1}, hereafter $CHAR_{\#}$) or area (mm^2.cm^{-2}.yr^{-1}, hereafter $CHAR_A$) based on numerical age-depth models, thus providing a continuous record of fire activity over the three cores. Automatic area ($CHAR_{Aa}$) and number ($CHAR_{An}$), and manual area ($CHAR_{Ma}$) and number ($CHAR_{Mn}$) reconstructions can then be compared statistically to estimate the accuracy of both methods on the interpretation of fire frequency.

Following Higuera (2009), the identification of fire events is based on the separation of the high (C_{peak}) from the low ($C_{background}$) frequency component. To reduce the impact of abrupt changes in sedimentation rate over time, charcoal datasets were interpolated to the median temporal resolution of each record (Gavin et al., 2006). The resulting datasets was named $C_{interpolated}$. The estimation of $C_{background}$ was performed using a lowess function that is robust to outliers. The resulting $C_{background}$ series is then smoothed over a 500-to-750-year time window, and C_{peak} calculated as $C_{peak} = C_{interpolated} - C_{background}$. This C_{peak} signal is composed of two subpopulations: (1) C_{noise}, reflecting the variability due to site sampling, to the noise inherent to statistical and numerical analyses performed, and to the portion of the background that would not have been removed in the previous step; and (2) C_{fire}, which represents the occurrence of one or more local fires (Aleman et al., 2013; Leys et al., 2017). The C_{fire} component is then separated from C_{noise} by using a Gaussian mixture model and applying a locally defined threshold, corresponding to the 99th percentile of the C_{noise} distribution.

All of these steps were performed using the CharAnalysis program (Higuera, 2009) freely available at https://sites.google.com/site/charanalysis/.

2.4.8 Fire frequency reconstruction at local and regional scales

From fire events at each site, local fire frequencies were reconstructed by smoothing using a kernel density function (Mudelsee et al., 2004; Ali et al., 2012) based on a 500-year defined bandwidth. To get regional fire frequencies (hereafter RegFF, Ali et al., 2012), composite curves were reconstructed by pooling the smoothed series of each site based on $CHAR_{Aa}$, $CHAR_{An}$, $CHAR_{Ma}$ and $CHAR_{Mn}$ series respectively, using the version 1.2.4 of the 'Paleofire' R package (Blarquez et al., 2014). The significance of changes in RegFF was assessed by repeating the bootstrap procedure 1000 times (BCI; 90%). Finally, intercomparisons between local – and then regional – fire frequencies were computed using Pearson's correlations for each 500-year time window along the record.

2.5 Results

2.5.1 Calibration and efficiency of the automatic approach

Before reconstructing charcoal influx and fire frequencies over the whole cores, it is important to ensure that our automatic detection method is able to detect charcoal particles efficiently on a calibration series (16 images on TRE and BIL series). For this purpose, filters need to be defined and therefore relies on the JL/DR or MDD/DR pairs of observers checking on RGB images after threshold selection. The manual counting method has detected 421 particles for a total area of 50.63 mm² over the 16 calibration images, while the annotation by at least one author on the RGB images after threshold selection has identified a total of 417 charcoal particles for a total area of 32.00 mm² on all 16 calibration images. Therefore, Z-stacked RGB images allows a very close (99% ± 20%) identification of charcoal particles by human eyes compared to manual identification under binocular microscope.

To define the filters, populations of charcoal (n = 417) and non-charcoal (n = 1212) particles of the calibration series are compared for successive colorimetric parameters (Figure 9). Even if several of these are tested to compare the populations, some parameters (RGB; R; R/G; R/B; Colorimetric score; Contrast score) show critical

differences between both populations, so only these six were kept for the filter definition. Therefore, the applied filters on calibration series identified a total of 374 particles for a total area of 30.36 mm². This selection represents an efficiency of 90% (±26%) and 95% (±21%) for the number and area of charcoals respectively compared to the manual annotation performed on detected particles after threshold selection.

2.5.2 Comparison of the two methods

The distribution of the $\log_{10}$-transformed data over the whole three sequences shows slightly lower values of C_A compared to C_M at TRE and BIL sites for both the number and area counts (Figure 10A-D). The non-parametric Wilcoxon signed-rank test for paired data shows that these differences are highly significant. Conversely, the BLH counts and areas show a radically different pattern marked by more similar distributions and *p*-values of 0.8332 and 0.0272, respectively (Figure 10E and F). However, a closer examination of the raw data reveals large differences of C_M and C_A between 7.9 and 6.6 ka cal BP (data not shown). We then chose to exclude the 7.9-to-6.6 time period (BLH excluding, hereafter BLHe), that is to say the last 21 values of the BLH series, and to compare the distribution of the last 6.6 ka cal BP (Figure 10G and H). Similarly to the other sites, this truncated series reveals significant lower values of C_A compared to C_M, in both number and area.

Finally, Spearman's rank correlations between the four counting methods were performed after merging the data of the three sites (Figure 11). Highly significant correlations between C_M and C_A are observed ($p = 0.605$ and $p = 0.624$ for number and area, respectively, $P < 0.001$), revealing an overall monotonic relationship between manual and automatic detection methods despite statistically different distributions. However, strong differences may appear for some series, especially BLH. A close-to-linear positive relationship is obtained for all sites beyond about ten visual counts after log transformation but the relationship tends to be negative when less macrocharcoal particles were detected with the manual method (Figure 11A). This U-shaped pattern is less pronounced for log-transformed area measurements, whose

distribution remains very skewed (Figure 11B). In both cases however, most of the points are below the diagonal, especially for area measurements.

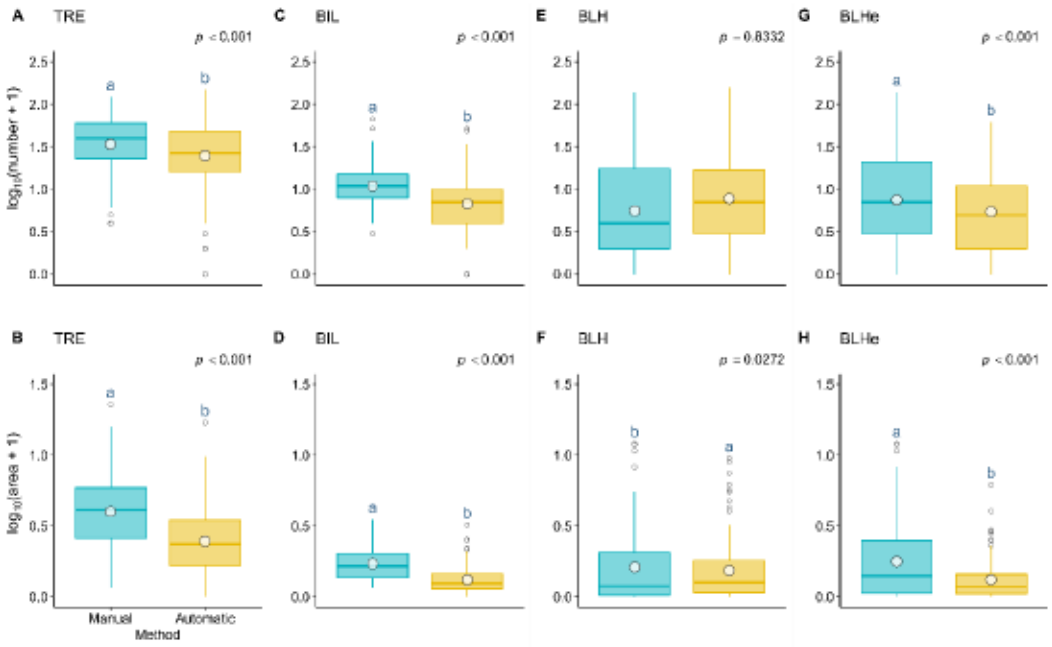

Figure 10
Boxplots of the total number of charcoals per sample (A, C, E, G) and of the total area of macrocharcoal particles per sample (B, D, F, H) for TRE (n = 125), BIL (n = 98), BLH (n = 118) and BLHe (n = 97) series, based on manual (blue) or automatic (yellow) counting (log10-transformed data). Big white points represent means. Results of paired Wilcoxon signed-rank tests are shown with p-values and letters indicating the rank when differences are significant (a > b).

2.5.3 Comparison of the four series

Figure 12 displays $CHAR_{Aa}$, $CHAR_{An}$ (left panels), $CHAR_{Ma}$ and $CHAR_{Mn}$ (right panels) trends to compare the C_M and C_A methods at each study site. At TRE, the visual comparison of C_M and C_A suggests close results over the whole core (Figure 12A), and indicates a similar and probably efficient charcoal particle detection by both methods. This observation is supported by the highly significant Pearson's correlation between $CHAR_{Mn}$ and $CHAR_{An}$ (r = 0.809). Similar observations can be made between $CHAR_{Ma}$ and $CHAR_{Aa}$ series (r = 0.828), however Figure 12D shows lower values of

C_A compared to C_M, similarly to the boxplot representations (Figure 10A and B). Finally, it is important to note that each charcoal peak of TRE identified by C_M, in number or area, was identified by C_A.

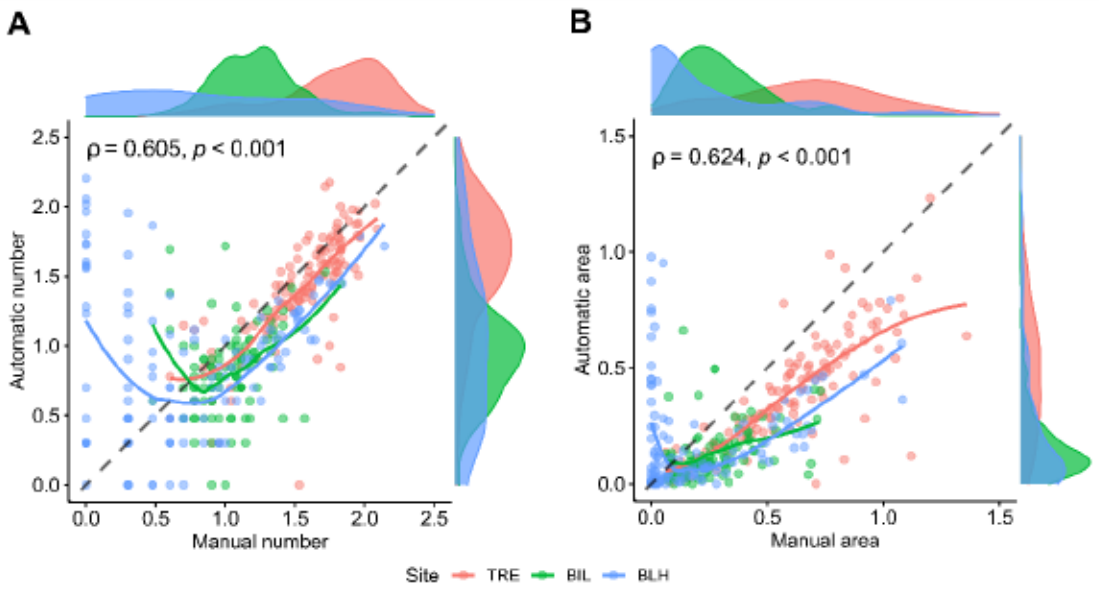

Figure 11
Pairwise relationships between manual and automatic measurements of number (A) and total area (B) of macrocharcoal particles in the three sites (coloured points) with Spearman's rank correlations. Scatter plots are drawn from log10-transformed data with lowess fitted curves (coloured lines). Density plots in the margins show the distribution of each variable. The grey dashed lines represent expected perfect fit (y = x).

Similar observations can be made in Figure 12B and E, representing the four series at BIL. Pearson's correlation shows greater differences between the pairs $CHAR_{Mn}$-$CHAR_{An}$ and $CHAR_{Ma}$-$CHAR_{Aa}$ (r = 0.358 and 0.497, respectively) than for TRE site, but stay highly significant. Although similar trends are displayed in number and area across the whole core, the automatic analysis appears to create an artefact charcoal peak around 1.6 ka cal BP. Conversely, in both series, two peaks (around 4.9 and 4.7 ka cal BP) identified by C_M were not identified by C_A. These discrepancies in BIL CHAR series suggest that reconstructions of fire frequency would differ, depending on the reconstruction method used.

BLH series show the greatest differences between C_M and C_A. While between about 6.6 and 0 ka cal BP the reconstructions show similar trends, C_A reveals a very large overestimation of charcoals between 7.9 and 6.6 ka cal BP (Figure 12C and F), based on the visual inspection of the sieves that reveal only a few charcoal particles. Consequently, we can easily assume that distribution of the raw data between C_A and C_M in Figure 10E and F would be radically different; however, this is not the case. While the values of C_A are lower than C_M from 6.6 to 0 ka cal BP, the very large overestimation of C_A at the bottom of the core increases the automatic values, explaining the relatively close distributions observed in Figure 10E and F. Therefore, Pearson's correlations between C_M and C_A had low significance ($r = 0.153$ and 0.192 for the pairs $CHAR_{Mn}$-$CHAR_{An}$ and $CHAR_{Ma}$-$CHAR_{Aa}$, respectively). However, while excluding the 7.9- to-6.6 ka cal BP time period, Pearson's correlation values increase to 0.725 and 0.712 for the pairs $CHAR_{Mn}$-$CHAR_{An}$ and $CHAR_{Ma}$-$CHAR_{Aa}$, respectively. Finally, over this period, all charcoal peaks identified by C_M were identified by C_A.

In conclusion, the comparison between C_M and C_A displays an effective detection of charcoal peaks by the automatic detection for TRE and BIL sites. At BLH, although the period between 7.9 and 6.6 ka cal BP seems strongly overestimated by the manual analysis, the period between 6.6 ka cal BP and the present also shows an effective detection of charcoals. Finally, on all sites, C_M displays a higher distribution than C_A, particularly in charcoal area estimates.

2.5.4 Local fire frequencies

Fire events were identified and local fire frequencies (FF) were reconstructed at the three study sites. To produce comparable results, the same smoothing and peak analysis parameters were used in the CharAnalysis program within a given study site. At TRE, charcoal peak analysis based on $CHAR_{Aa}$, $CHAR_{An}$, $CHAR_{Ma}$ and $CHAR_{Mn}$ identified 14, 13, 13 and 9 fire events respectively. At BIL, this analysis identified 12, 15, 14 and 10 fire events, respectively, while 11, 17, 8 and 12 were found at BLH. In order to check whether each record can be used for peak analysis to reconstruct local

fires, the signal to noise index (SNI) (*e.g.* Kelly et al., 2011) was used for each reconstruction method. Although $CHAR_{Ma}$ and $CHAR_{Mn}$ records from BLH site have a SNI of 2.87 and 2.65, respectively, the majority of records have a SNI greater than 3, critical value considered as appropriate for peak detection (Kelly et al., 2011). Only one record, $CHAR_{Mn}$ at TRE site, showed a value of 2.01 and requires caution in its interpretation.

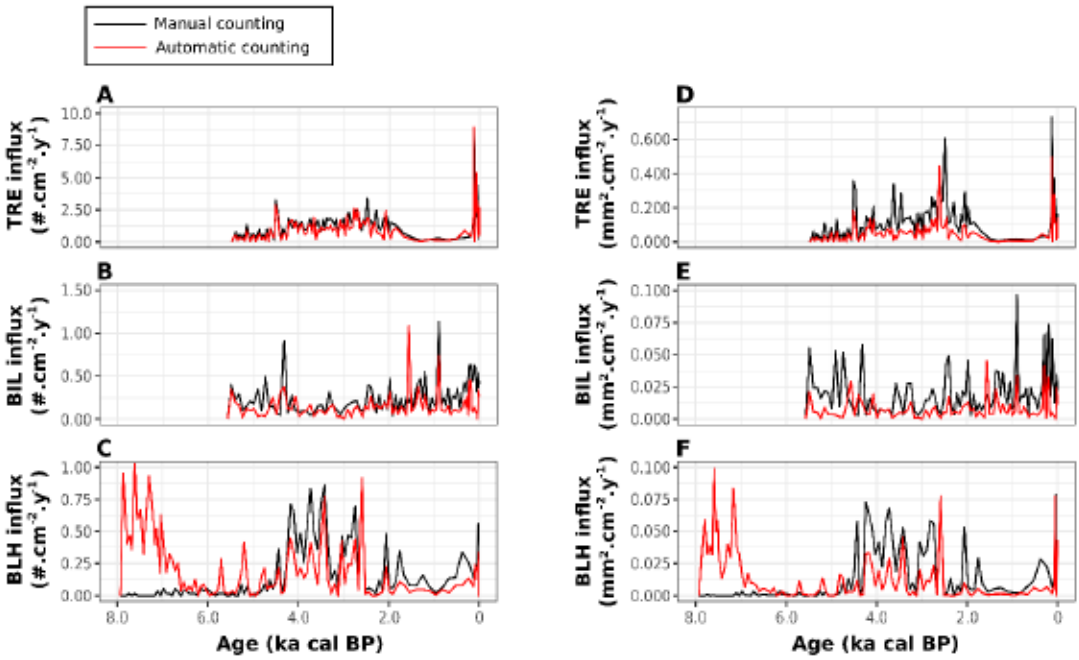

Figure 12
Charcoal influx calculated for TRE, BIL et BLH series as a function of age (ka cal BP). Black curves represent charcoal influxes calculated from manual counting, red curves represent charcoal influxes calculated from automatic counting. All ages are expressed in ka cal BP. (A-C) Number of charcoals per cm^{-2} per year ($\#.cm^{-2}.y^{-1}$) for TRE, BIL and BLH series, respectively ; (D-F) Total area of charcoals per cm^{-2} per year ($mm^2.cm^{-2}.y^{-1}$) for TRE, BIL and BLH series, respectively.

Reconstructed fire frequencies show significantly different pattern within the three study sites, depending on the reconstruction method used. At TRE, FF based on $CHAR_{An}$, $CHAR_{Mn}$, and $CHAR_{Aa}$ reveal similar long-term trends, characterized by a decrease of FF at the end of the Holocene Climatic Optimum (~5.0 ka cal BP), a slight

increase around 2.0 ka cal BP followed by a decrease until about 1.0 ka cal BP, before increasing up to the present period (Figure 13A and B), even if the latter is marked by a significant variability among reconstruction methods (from 1.8 to 4 fire.ka^{-1}). The similar patterns of FF are reflected in the high Pearson correlation coefficients calculated between the four reconstruction methods (Figure 14). Although the $CHAR_{Ma}$ based reconstruction displays similar variations to the others over the last 1000 years, the overall trend shows a decrease of FF from until 1.0 ka cal BP, falling from ~4 to ~2 fire.ka^{-1}, without a decrease around 3.5 ka cal BP (Figure 13B). This divergence is reflected in the either negative or low correlation appearing at the same period in Figure 14, when $CHAR_{Ma}$-based reconstructions are compared with the others methods. Finally, fire frequencies based on all reconstruction methods in TRE are, on the whole, well positively correlated over the studied period; however negative correlation appears punctually over the studied period (Figure 14).

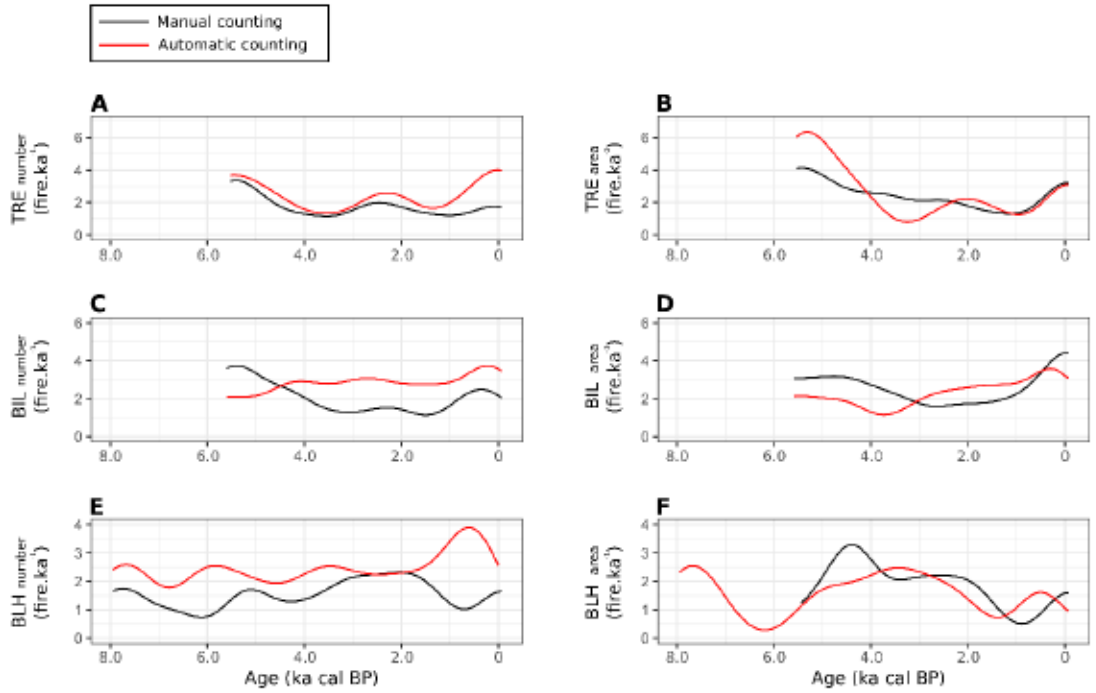

Figure 13
Reconstructed local fire frequencies (number of fires.ka^{-1}) based on number or area CHAR series for (A-B) TRE, (C-D) BIL and (E-F) BLH sites against age. Black curves represent manual counts, red curves represent automatic counts. All ages are expressed in ka cal BP.

At BIL, the reconstructions display more contrasting results (Figure 13C and D). Indeed, between 6.0 and 3.5 ka cal BP, fire frequencies reconstructed from $CHAR_{Mn}$ decrease from 3.8 to 1.5 fire.ka^{-1}, while they increase from 2.1 to 2.8 fires.ka^{-1} for $CHAR_{An}$ (Figure 13C). Then, both methods show similar patterns, although the $CHAR_{An}$-based FF are lower than $CHAR_{Mn}$ by an average of 1.2 fires per year. Figure 14 shows similar results, marked by a negative correlation from 5.5 to 3.0 ka cal BP, followed by high positive correlations until the current period. In area (Figure 13D), the variations of the FF are asynchronous and may lead to different interpretations: on the one hand, FF reconstructed from $CHAR_{Ma}$ first decrease between 4.0 and 3.0 ka cal BP, then remain constant until 1.0 ka cal BP and finally increase until the present period, while the $CHAR_{Aa}$ based FF increase from 3.8 to ~0.2 ka cal BP, before decreasing slightly until today. When comparing all reconstructions on BIL, median correlations are always greater than 0.5, except the comparison between $CHAR_{An}$ and $CHAR_{Ma}$.

Finally, the FF reconstructed on BLH show highly contrasted patterns (Figs. 8E, F and 9). Although all reconstructions display FF between 2 and 3 fire.ka^{-1} around 3.0 ka cal BP, the top and bottom of the core show radically different fire frequencies, supported by the high variability among correlations coefficients, varying positively and negatively along the whole core (Figure 14). Except the couple $CHAR_{Aa}$ - $CHAR_{Mn}$, all median correlations remain however highly positive ($r > 0.9$).

In summary, FF based on the four reconstruction methods show distinct patterns across the study sites. While the reconstructed FF on TRE display similar fire frequencies, BIL and BLH sites show more contrasting results. This suggests that the interpretation of local fire frequency can greatly vary within a same site, depending on the method (manual *versus* automatic count) and on the type of macrocharcoal measurement (number *versus* area) used.

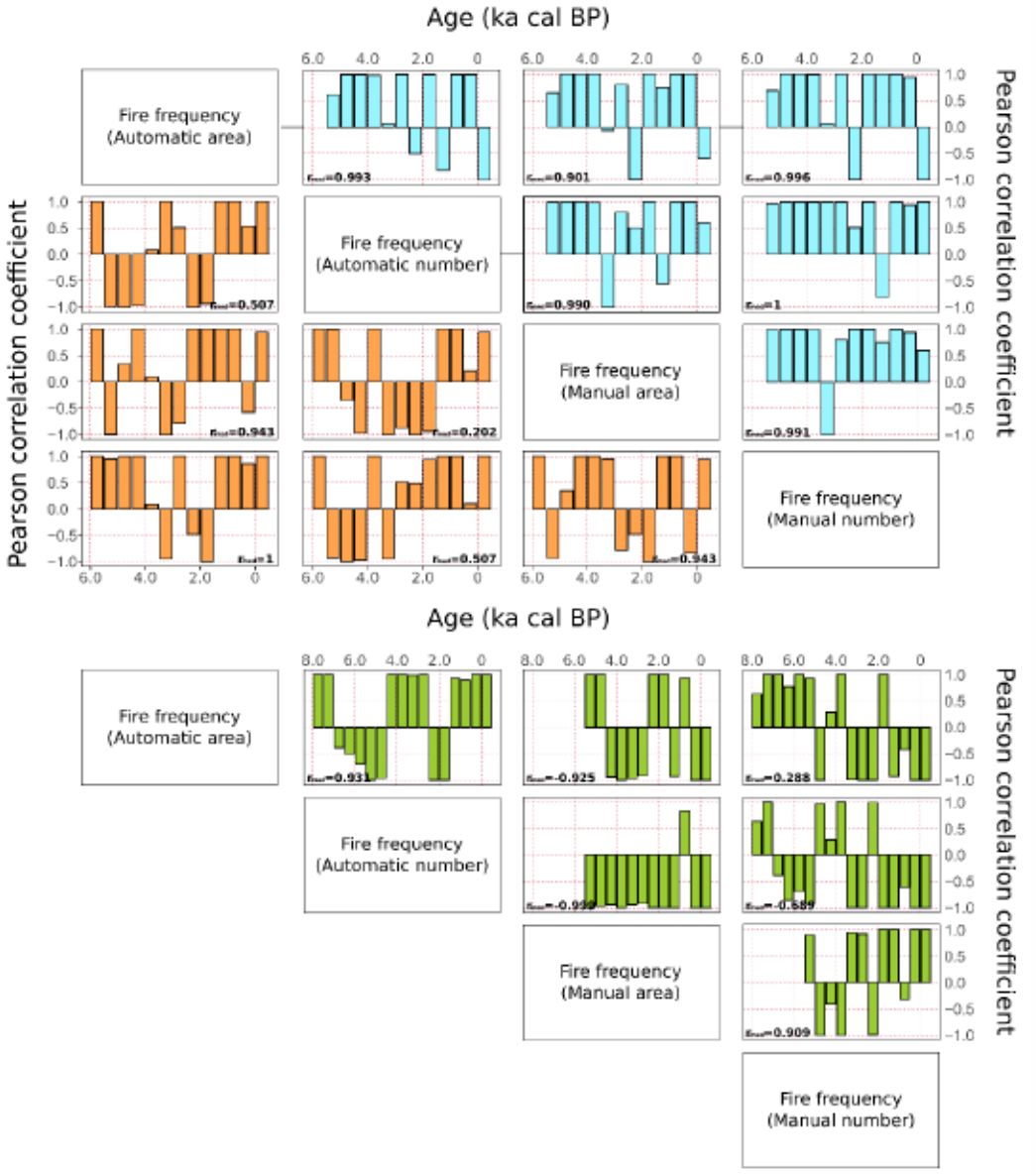

Figure 14
Comparison of Pearson correlation coefficient (1 = perfect correlation; −1 = negative correlation; 0 = no correlation) of fire frequencies calculated every 500-year time steps for each counting method against age. All ages are expressed in ka cal BP. Median Pearson correlation coefficients are displayed on the bottom of each panel. TRE is represented in blue, BIL in orange and BLH in green.

2.5.5 Regional fire frequencies

Reconstructions of past RegFF based on the four reconstruction methods were performed, and begin at ~5.4 ka cal BP for all CHAR series because of the length of TRE record (Figure 15) dating back in time no further than this period. Similar long-term trends are observed over the whole cores, with a pattern characterized by a decrease of RegFF from the 5.4-4.6 ka cal BP period - depending on the record - until about 3.5 ka cal BP, a plateau or an increase until 2.2 ka cal BP, and a second decrease until the 1.4-1.2 period (Figure 15). Finally, all reconstructions are marked by a significant increase of RegFF during the last millennium, varying however greatly in amplitude (Figure 15). This similarity in long-term trends is reflected in the high positive median Pearson correlation coefficient (r_{med}>0.99) between all counting methods, except those using $CHAR_{Ma}$ (Figure 16).

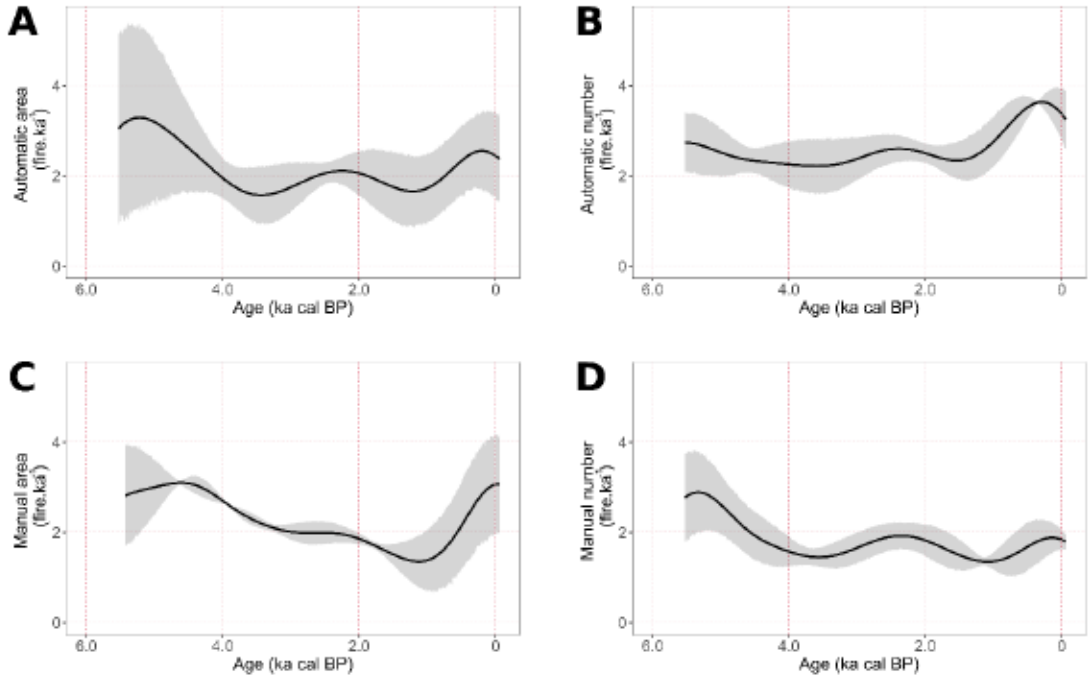

Figure 15
Reconstructed regional fire frequencies (number of fires.ka^{-1}, black line) based on (A) $CHAR_{Aa}$, (B) $CHAR_{An}$, (C) $CHAR_{Ma}$ and (D) $CHAR_{Mn}$ against age (ka cal BP). RegFF are calculated for a 500-year bandwidth. Shaded areas indicate 90% bootstrap confidence intervals (BCI; 90%). All ages are expressed in ka cal BP.

On a smaller timescale, greater variability in RegFF is apparent. The four sequences are marked by a high fire frequency at the end of the Holocene Climatic Optimum (~5.0 ka cal BP), but the highest values of RegFF are reached at the beginning of the record for $CHAR_{An}$, at 5.4 ka cal BP for the reconstructions based on $CHAR_{Aa}$ and $CHAR_{Mn}$, and at 4.6 ka cal BP for $CHAR_{Ma}$; however, they all reached ~3 fire.ka^{-1}. All reconstructions are then marked by a decrease of RegFF until about 3.5 ka cal BP, reaching a minimum RegFF value varying between 2.2 and 1.4 fire.ka^{-1}. From this period, while $CHAR_{Aa}$, $CHAR_{An}$ and $CHAR_{Mn}$-based RegFF reconstructions increase to a maximum RegFF value of 2.1, 2.6 and 1.9 fire.ky^{-1}, respectively, at 2.2 ka cal BP, $CHAR_{Ma}$ is not marked by this increase and reaches a plateau. The poor correlations during the 5.4-to-3.0 period (except from 4.5 to 3.5) between $CHAR_{Ma}$-based reconstructions and the three other methods are probably the consequence of these discrepancies (Figure 16). Finally, after a last decrease of RegFF until the 1.4-1.2 ka cal BP period reaching 1.7, 2.3, 1.3 and 1.4 fire.ka^{-1} for $CHAR_{Aa}$, $CHAR_{An}$, $CHAR_{Ma}$ and $CHAR_{Mn}$, respectively, all reconstructions are characterized by a high increase of RegFF until the present day. This period shows the highest variability between the records, reaching a maximum value of 3.6 fire.ka^{-1} for $CHAR_{An}$, and a minimum value of 1.9 for $CHAR_{Mn}$. Only $CHAR_{Ma}$-based reconstructions are not followed by a decrease of RegFF during the last centuries (Figure 15); it is therefore the only record showing a poor correlation during this period (Figure 16).

2.6 Discussion

2.6.1 Automatic approach

Our results show that direct manual counting of macrocharcoal particles under binocular microscope and their identification on Z-stacked RGB images of the calibration series by human eyes give similar number of macrocharcoals (421 *versus* 417 particles); consequently, charcoal versus non-charcoal particles details are clearly identifiable on Z-stacked images. This highly supports the idea that automatic detection is possible.

Efficient filters have been defined to optimize the selection of true charcoal particles when using the automatic approach. Other colorimetric parameters were also investigated but they were not able to provide a sufficient selectivity among both populations of particles. We also applied the methodology of Zou et al., (2021) based on grayscale images, such as the median grayscale value, but surprisingly both types of particles had similar greyscale ranges (data not shown). This criterion has been developed for the observation of charcoal on pollen slides, which generate much more contrasted pictures than ours. Furthermore, colorimetric properties of charcoal particles and other elements may be very different, preventing the application of similar filters on different type of generated pictures.

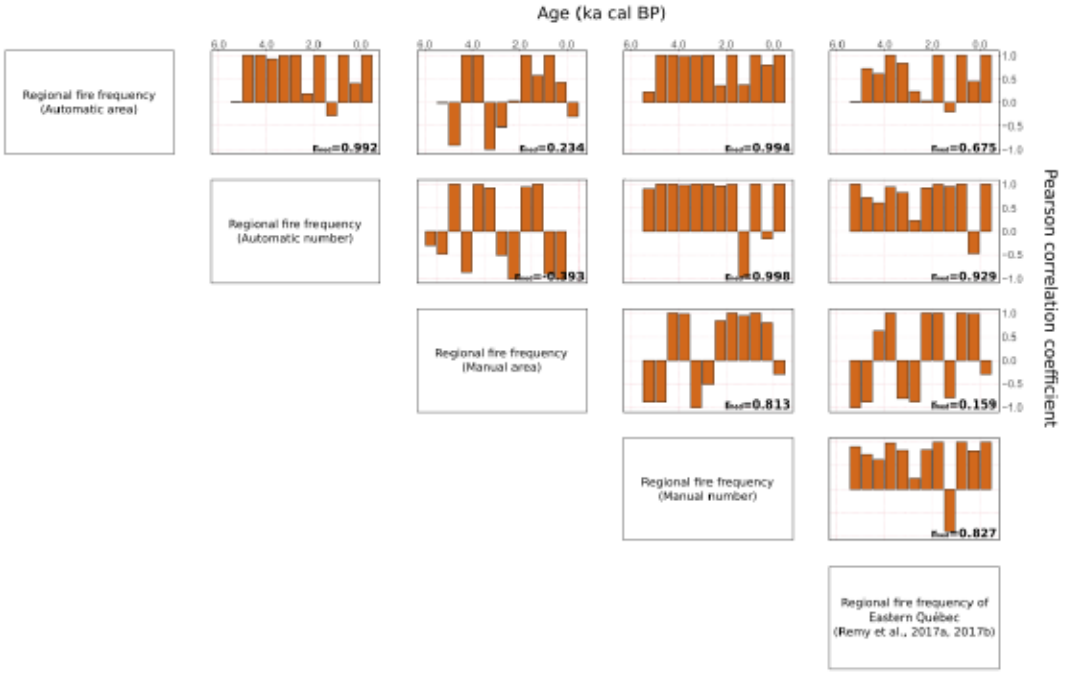

Figure 16
Comparison of Pearson correlation coefficient (1 = perfect correlation; -1 = negative correlation; 0 = no correlation) between regional fire frequencies (RegFF) reconstructed in this study for each counting method and reconstructed RegFF of eastern Québec against age (ka cal BP). All RegFF were calculated using 500-year time steps. Median Pearson correlation coefficients are displayed on the bottom right of each panel.
Source : Remy et al., (2017a, 2017b).

While the identification of macrocharcoals on Z-stacked pictures of the calibration series by human eyes found a total of 417 particles for a total area of 32.00 mm^2, the global selection of particles by the filters on the same images after threshold selection found a total number of 374 particles for a total area of 30.36 mm^2. This represents an efficiency of 90% (±26%) and 95% (±21%) for the number and area of charcoals, respectively. We therefore conclude that this margin of error is acceptable, and that our macro allows sufficient detection of charcoal particles in the calibration images. Consequently, it has been applied to the whole series to reconstruct local and regional fire frequencies.

2.6.2 Differences observed in local fire frequency reconstruction

Reconstructions of the CHAR series on TRE display the same charcoal influx trends, whereas the area has a higher amplitude of charcoal peaks. Although the area counting method is assumed to be more accurate than number (Leys et al., 2013; Zou et al., 2021) due to the risk of fragmentation of charcoal particles by transport, taphonomic processes and laboratory treatments, several studies have shown that number- versus area-based CHAR series closely matched (Tinner and Hu, 2003; Carcaillet, 2007; Ali et al., 2009b), particularly in boreal biomes (Leys et al., 2013). However, while FF reconstructions on TRE using $CHAR_{An}$, $CHAR_{Mn}$ and $CHAR_{Aa}$ are similar in trends (Figure 13A) and highly correlated (Figure 14), $CHAR_{Ma}$ indicates a slightly different local fire frequency marked by the absence of decrease of FF around 3.5 ka cal BP (Figure 13B). This discrepancy could be explained by the differences between C_A and C_M distributions (Figs. 10B and 12D), induced by the overestimation of the area of charcoal particles by C_M due to the lack of precision of the measurements while using a binocular microscope. As the total area of a sample results from the sum of the areas of each individual charcoal particle, it is likely to suppose that the overestimation of the total area is greater in the most charcoal-rich samples. High amplitude charcoal peaks detected by $CHAR_{Ma}$ at ~3.6 and 3.5 ka cal BP (Figure 12) explain the lack of FF decline during this period (Figure 13), and is reflected in the either negative or poor correlation with the other reconstruction methods in Figure 14

at the same period. Although manual area counting method is assumed to be better than manual number counting method to reconstruct local FF (Ali et al., 2009b), we can hypothesise that it could create additional charcoal peaks due to this overestimation, and therefore result in a less reliable fire frequency reconstruction. This bias, induced by the difficulty to visually estimate the area of charcoal particles due to the variability in particle size distribution and particle morphology, has already been highlighted by Clark and Hussey (1996). Finally, as $C_{background}$ conditions the ability to detect fire events via the widely used CHAR series decomposition approach (Carcaillet et al., 2001; Gavin et al., 2006; Higuera et al., 2007; Higuera, 2009), we hypothesise that increasing the total area of successive samples in manual counts may lead to an increase of $C_{background}$, and consequently decrease the ability to differentiate from C_{peak}, *i.e.* to detect fire events. Thus, although the reconstructions of CHAR series give visually similar trends, local FF reconstructed from these series may reflect significantly different local fire frequencies.

However, although similar charcoal peaks appear to occur in the $CHAR_{Ma}$ series from BIL site at 4.9 and 4.7 ka cal BP (Figure 12B) and may explain the differences observed between the reconstructed fire frequencies in Figure 13C and D, an artefact charcoal peak is detected at 1.6 ka cal BP by C_A, both in number and area series, thus suggesting a large overestimation of C_A. Similarly, at BLH site, the 7.9-to-6.6-ka-cal-BP period shows significant differences between CHAR series both in number and area, induced by the very large overestimation of C_A. This overestimation of the number and area of charcoal particles by our method could be explained by the presence of a large supply of charcoal-like particles, making it difficult to automatically detect real charcoal particles. This observation is confirmed by the visual inspection of the 3D-printed sieves, showing an important quantity of dark minerals, and therefore making it difficult to automatically discriminate charcoal from non-charcoal particles. It is thus directly related to the paleoclimatic context of the study site, indicating that the timing of the deglaciation occurred between ~8.5 and ~7.0 ka cal BP in the BLH region (Dyke, 2004). These particles probably result from the sudden increase of freshwater inflow during the melting of the Laurentide ice sheet, leading to extensive soil leaching

and consequently high coarse mineral deposition rate (Christoffersen et al., 2008). When using our automated counting method, we therefore recommend paying particular attention to highly minerogenic samples, and by extension to the sedimentological and environmental context of the study site. Perhaps for these sites, a hybrid approach of visual and automated charcoal detection would be optimal.

2.6.3 Regional fire frequency in eastern Canada during the Holocene

While several studies have examined the regional fire frequency of the Ontario-Quebec boundary (Hély et al., 2010, 2020; Ali et al., 2012; Girardin et al., 2013a), only few studies have focused on eastern Quebec and Labrador (see Remy et al., (2017a, 2017b)) on a multimillennial timescale. These regions are also marked by a strong east-west climatic, topographic and vegetation variability, leading to major RegFF differences during the Holocene between eastern and western regions (Ali et al., 2012; Remy et al., 2017a, 2017b). While western Quebec is marked by a continental climate and a relatively flat topography, eastern Quebec and Labrador are dominated by a more oceanic influence resulting from their proximity to the Atlantic Ocean, and show a hillier relief. Consequently, the latest long-term regional studies in eastern Quebec and Labrador showed major variability in fire regimes (regional fire frequency, size and amount of biomass burned) between eastern and western Quebec Remy et al., (2017a, 2017b). In this paper, we therefore compared our reconstructions of RegFF using the four CHAR series to those reconstructed in eastern Quebec (Figure 16) - *i.e.* both studies of Remy et al., (2017a, 2017b) - to check the reliability of our reconstruction methods and the eventual biases. These studies, based on three lakes in eastern Quebec (Figure 6), used WinSEEDLE™ semi-automatic measurement, and may therefore be considered as highly precise in terms of charcoal particles measurements, and thus relevant for the comparison of regional fire frequencies.

When comparing our records, all reconstructions except $CHAR_{Ma}$ indicate maximum RegFF values (around 3 fire.ka^{-1}) at 5.2 ka cal BP (Figure 15). These three reconstructions are consequently similar to the studies of eastern Quebec by Remy et

al., (2017a, 2017b), showing the highest RegFF (6 fire.ka^{-1} on average) of the last 6000 years, induced by warm climatic conditions and dry summers, characteristic of the Holocene Climatic Optimum (Viau and Gajewski, 2009). These differences in the amplitude of RegFF are probably explained by the geographical position of our records, extending further east than the reconstructions of Remy et al., (2017a, 2017b). Indeed, fire return intervals of the Labrador region are among the lowest of Canada, in particular because of the high precipitations (Foster, 1983a; Coops et al., 2018); it is therefore likely that RegFF are lower when using records retrieved further east. Until 3.5 ka cal BP, a large decrease of RegFF reconstructed from the four counting methods is then observed similarly to Remy et al., (2017a, 2017b), suggesting relevant reconstruction of the four CHAR series during this period. However, after 3.5 ka cal BP, $CHAR_{Aa}$, $CHAR_{An}$ and $CHAR_{Mn}$-based reconstructions coincide and show highly positive correlation with the increase of RegFF at 2.7 ka cal BP from eastern Quebec. At the opposite $CHAR_{Ma}$-based reconstruction is negatively correlated and do not follow the same pattern.

Then, while reconstructions of eastern Quebec show a peak of RegFF at 2.7 ka cal BP, reconstructions based on $CHAR_{Aa}$, $CHAR_{An}$ and $CHAR_{Mn}$ follow the same pattern, but 500 years later. This time lag, explaining the poor Spearman correlation between all our records and those of eastern Quebec, could be explained by the spatial heterogeneity of our records. Indeed, Quebec and Labrador regions were marked by significant climatic variability during the Holocene, resulting in highly variable temperature and drought patterns (Viau and Gajewski, 2009), therefore probably leading to regional variations of fire synchronicity. Thus, whereas the studies of Remy et al., (2017a, 2017b) were based on spruce-moss forest and spruce-lichen woodlands bioclimatic domains of the Quebec region, our data encompass a broader latitudinal gradient, extending from the white birch fir stand to the forest tundra; it therefore seems likely that RegFFs differ according to the spatial gradient studied. Then, the reconstructions of Remy et al., (2017a, 2017b) show the lowest values of the last 6000 years at 1.4 ka cal BP (4.0 fire.ka1) followed by an increase up to the present period. Again, while $CHAR_{Aa}$, $CHAR_{An}$ and $CHAR_{Mn}$-based reconstructions follow the same

pattern and show highly positive correlations, $CHAR_{Ma}$ is poorly correlated with all other reconstructions.

Our study highlights the role of methodological choice while reconstructing regional fire frequency. Although charcoal influx appears strongly correlated between the different reconstruction methods (Figs. 11 and 12), they may lead to large differences in fire frequency reconstructions. According to our results, three counting methods - manual and automatic number, and automatic area - seem to be appropriate to reconstruct reliable regional fire frequencies; conversely, biases related to manual area measurement under binocular microscope induce significant differences with previously published studies, and potentially provide less reliable fire frequency reconstructions.

2.6.4 Guidelines and perspectives for the use of ImageJ software automatic counting method

Our study aims to investigate the biases of charcoal counts from a methodological point of view, complementary to studies carried out and discussed in numerous papers (Clark and Hussey, 1996; Tinner and Hu, 2003; Ali et al., 2009b; Leys et al., 2013; Finsinger et al., 2014; Hawthorne and Mitchell, 2016; Zou et al., 2021). Our macro developed on ImageJ software has several advantages, making its use interesting for the analysis of macrocharcoal sequences. While semi-automated methods such as WinSEEDLE™ Software are used in many studies for counting and measuring macrocharcoal area (see Senici et al., 2013, 2015; Oris et al., 2014; Remy et al., 2017, 2018, 2019; Blarquez et al., 2018; Magne et al., 2020; Hennebelle et al., 2020) and are found to be relatively accurate, the necessity of visual inspection of each detected charcoal particle makes the analysis of the most charcoal-rich samples relatively constraining and time-consuming. Our method on the ImageJ software thus offers an open-source, fully automated measurement, without post-processing inspection of the detected particles, and offers complementary measurements (length/width ratio via Feret diameter, data not shown) similarly to the WinSEEDLE™ software. As the inter-observer bias for area estimation by the manual method could also be a high source

of error but to our knowledge has not been tested in the literature, the use of our ImageJ macro alleviates the need to use these estimates like in other semi-automated softwares.

Although our area estimation method does not provide a significant time benefit compared to manual counting (~15-20 min per sample, considering the sieving and high-resolution Z-stacked image capture time), it indicates a lower number but more accurate measurement of macrocharcoal particles area than the estimation performed under a binocular microscope. As background conditions the ability to detect fire events via the widely used CHAR series decomposition approach (Carcaillet et al., 2001; Gavin et al., 2006; Higuera et al., 2007; Higuera, 2009), we hypothesise that increasing the total area of successive samples in manual counts may lead to an increase in the CHAR background, and consequently decrease the ability to detect fire events. This variability between C_M and C_A created large fluctuations in local and regional FF across the three study sites, and thus suggests that reconstructions of fire frequency may vary significantly depending on the methodological approach employed. This study is consequently crucial to better understand and correct potential biases of local fire reconstructions. It therefore suggests that reconstructions of fire frequency can vary significantly at both local and regional scales based on number or area measurements from manual or automated methods. However, many paleoecological studies still use different counting methods to reconstruct and compare fire frequency across the world; an evolution towards a standardisation of charcoal data acquisition seems therefore necessary in order to get the most comparable data and improve our global understanding of fire regimes.

Nonetheless, this automatic image analysis requires the use of a high-performance microscope, allowing the acquisition of high-resolution Z-stacked images while including a relatively precise measurement scale. It also requires a high-performance computer, allowing the program to efficiently process all the pictures, and has only been tested in boreal environment dominated by high intensity crown fires. As low intensity surface fires dominate Northern Europe, it would be interesting to test our method in these environments. However, our colorimetric-filter analysis is adaptable

to any image since the resolution is sufficient to identify charcoal particles; we then strongly support the idea that it can be used in any study as long as the mineral load is not too high. It also allows a reduced bias between observers, and thus offers an interesting opportunity to study fire regimes at large spatial and temporal scales, with limited methodological bias.

2.7 Conclusion

A new method for quantifying and measuring macrocharcoal area from Z-stacked high-definition pictures was developed and tested in this study. Based on the successive application of a detection threshold and of colorimetric filters to detect charcoal particles, the efficiency of this method developed on the ImageJ software was tested on three lakes in the eastern Canadian boreal forests based on pair-checking of detected particles by the authors. The results show a good detection of charcoal particles, except for the most minerogenic samples, and suggest that this method can be a powerful, fast and accurate tool for fire regime reconstructions. In order to verify its impact on the assessment of fire frequencies, we reconstructed charcoal influx, and then local and regional fire frequencies, respectively.

Influx reconstructions showed a large overestimation of charcoal particle areas by visual binocular counting methods, induced by the lack of precision of the measurements. While many previous studies have shown similar reconstructions of local and regional fire frequencies by the different reconstruction methods, our study reveals large differences, and suggests that methodological choice of charcoal identification can strongly impact fire reconstructions at both local and regional scales. Consequently, comparison between fire frequencies should be conducted with special attention given to the counting method in order to avoid possible misinterpretation related to methodological choices. However, our study suggests that at a regional scale, reconstructions based on manual number, automatic number and automatic area are statistically correlated to previously published studies and can provide reliable fire reconstructions.

2.8 Acknowledgements

The authors would like to thank Natasha Roy and Augustin Feussom Tcheumeleu for their assistance in the field. This work was supported by the grants of the ANR Interarctic, the Nich-Arctic Project, the PEPS-INEE EPIDERME program and the International Research Project "Cold forest".

3. INFLUENCE OF ENVIRONMENTAL FACTORS ON POLLEN- AND CHIRONOMID-BASED HOLOCENE TEMPERATURE INFERENCES: A MULTISITE COMPARISON IN EASTERN CANADA

Jonathan A. Lesven, Laurent Millet, François Gillet, Yves Bergeron, André Arsenault, Cécile C. Remy, Thomas Suranyi, Augustin Feussom-Tcheumeleu, Lisa Bajolle, Adam A. Ali, Damien Rius

3.1 Abstract

While pollen and chironomid assemblages are supposed to be primarily forced by climate, biases can arise from non-analogous paleoclimates or changes in environmental parameters affecting these proxies. Eastern Canada, characterised by local climatic variability due to both the influence of external and internal forcings, presents major challenges in reconstructing its climate history. In this study, we use pollen and chironomid assemblages from five sites in Quebec-Labrador to infer mean summer air temperatures, aiming to identify biases within each reconstruction and refine the Holocene climatic history of the region. We first assess the reliability of our inferences based on both proxies, to determine periods of good reliability. Subsequently, we show that pollen-based reconstructions are largely affected by fire regimes, and that the over-representation of some taxa can lead to biases in temperature inferences. Conversely, chironomid head capsules appear to better capture known climatic trends, albeit with potential influence from variable within-lake conditions. Finally, comparing these reconstructions allows us to discuss the spatial and temporal variability of the history of Quebec-Labrador during the Holocene, highlighting a strong spatial and temporal variability between sites. Our findings emphasise the importance of employing multi-proxy approaches in Holocene paleoclimatic reconstructions within boreal forests.

Keywords: Pollen, Chironomid, Climate, Fire, Holocene

3.2 Résumé

Alors que les assemblages de pollen et de chironomes sont censés être principalement influencés par le climat, des biais peuvent survenir en raison de paléoclimats non analogues ou de changements dans les paramètres environnementaux affectant ces indicateurs. L'est du Canada, caractérisé par une variabilité climatique locale due à la fois à l'influence de forçages externes et internes, présente des défis importants pour la reconstitution de son histoire climatique. Dans cette étude, nous utilisons les assemblages de pollen et de chironomes provenant de cinq sites au Québec-Labrador pour déduire les températures moyennes estivales de l'air, dans le but d'identifier les biais dans chaque reconstruction et d'affiner l'histoire climatique holocène de la région. Nous évaluons d'abord la fiabilité de nos inférences basées sur les deux proxys, afin de déterminer les périodes de bonne fiabilité. Ensuite, nous montrons que les reconstructions basées sur le pollen sont largement affectées par les régimes de feu, et que la surreprésentation de certains taxons peut conduire à des biais importants. À l'inverse, les capsules céphaliques des chironomes semblent mieux rendre compte des tendances climatiques connues, bien qu'elles puissent être influencées par les variables environnementales internes aux lacs. Enfin, la comparaison de ces reconstructions nous permet de discuter l'histoire du Québec-Labrador au cours de l'Holocène, mettant en évidence une importante variabilité spatiale et temporelle entre les sites. Nos résultats soulignent en particulier l'importance d'utiliser des approches multi-indicatrices dans les reconstructions paléoclimatiques de l'Holocène dans les forêts boréales.

Mots clés : Pollen, Chironomes, Climat, Feu, Holocène

3.3 Introduction

The scientific community widely acknowledges the unprecedented pace of earth warming, primarily attributed to human-induced greenhouse gas emissions. More precisely, recent projections suggest that the global mean annual temperature should reach +1.8 to +4.3°C by the end of the century compared to the preindustrial period (IPCC, 2022). These changes appear unprecedented over the Holocene – *i.e.* the last 11,700 years – and could even exceed the temperature optimum of the last interglacial, some ~115,000 years ago (Bova et al., 2021). However, boreal forests are anticipated to experience the most substantial temperature rise of all forest biomes, estimated between +4 and +11°C by the end of the century (Gauthier et al., 2015). This warming of high latitudes is projected to disrupt precipitation patterns (Rouhani and Leconte, 2018), with major implications for plant water availability (D'Orangeville et al., 2016) and landscape flammability (Flannigan and Wotton, 2001; Flannigan et al., 2005; Wotton et al., 2010). The interplay between climate, fire and anthropogenic activities thus have a large potential to shrink individual growth (Lesven et al., 2024) and induce major forest state changes (Splawinski et al., 2019b; Baltzer et al., 2021), both with critical implications for human economy and safety (Hassan et al., 2005; Brecka et al., 2018), carbon sequestration (Pan et al., 2011), and fundamental ecosystem services (Brandt et al., 2013) that North American boreal forests in particular provide.

Retrospective approaches are essential, since they allow the establishment of ecological benchmarks that enhance our understanding of climate variability and ecosystems change through space and time, and help resource managers to guide climate change mitigation with realistic targets and goals (Lindbladh et al., 2013). Consequently, there has been a significant emphasis on reconstructing Holocene temperatures using fossil-based quantitative inference methods in the last decades (Juggins and Birks, 2012). The high latitudes of eastern North America have indeed undergone high-amplitude climatic fluctuations since the deglaciation (Viau and Gajewski, 2009; Bajolle et al., 2018), with warming periods that could be considered as interesting reference points to explore the effects of future climate changes on boreal ecosystems. In eastern Canada, the predominant approach to reconstruct

Holocene temperature relies on the pollen-based modern analogue technique (MAT), as evidenced by numerous studies (*e.g.* Kerwin et al., 2004; Viau and Gajewski, 2009; Gajewski, 2015; Fréchette et al., 2018, 2021). Despite the theoretical assumption of vegetation-climate equilibrium (Webb, 1986), this method is, however, known to possess inherent limitations. In Eurasian forests, these weaknesses have been attributed to the over-representation of pollen taxa from wetland environments (Shala et al., 2017) or to late-glacial migrational lags (Peyron et al., 2005), introducing biases in temperature reconstruction. Although similar challenges may exist in North America, the dynamics of eastern Canadian boreal forests are largely influenced by natural disturbance regimes, particularly forest fires (Brandt et al., 2013; Hanes et al., 2019). Serotinous taxa like jack pine (*Pinus banksiana* Lamb.), and to a lesser extent black spruce (*Picea mariana* (Mill.) B.S.P.) can undergo substantial population expansion during periods of intense fire activity (Ali et al., *in prep.*; Remy et al., 2017b). Despite the anticipated impact of disturbance regimes on climate reconstructions, to our knowledge, this influence on pollen-based inferences has not yet been investigated.

More recently, several reconstructions involving chironomid head capsules started to emerge in eastern Canada (*e.g.* Bajolle et al., 2018, 2019; Feussom Tcheumeleu et al., 2023). Unlike traditional palynological studies, these reconstructions rely on transfer function approaches estimating taxa-climate relationships using entire modern datasets (Chevalier et al., 2020). This approach theoretically enhances robustness against spatial biases in the training set (Telford and Birks, 2005, 2011), while limiting fire influence. Chironomid head capsules offer highly precise reconstructions of summer air temperature, with an estimated error of less than 1°C compared to instrumental measurements (Larocque et al., 2009; Larocque-Tobler et al., 2015). This sensitivity to climate is attributed to their short generation time and the ease with which winged adults can disperse between breeding sites (Walker and Mathewes, 1987; Larocque-Tobler et al., 2015). However, non-climatic factors have been shown to also affect chironomid assemblage composition and temperature inferences (*e.g.* Millet et al., 2009; Velle et al., 2010; Bajolle et al., 2019).

Since neither method is without limitations, a potential approach to enrich our understanding of Holocene climate variability in eastern Canada involves evaluating the reliability of both reconstruction methods and elucidating their respective strengths and weaknesses. In this paper, we perform for the first time a comparative analysis of reconstructions of mean summer air temperatures (MSAT) based on pollen and chironomid assemblages at five sites in eastern Canadian boreal forests. We aim to identify common trends and notable disparities while shedding light on the factors contributing to discrepancies in light of regional and site-specific processes. We hypothesise that periods characterised by high fire activity (frequency/size) and the over-representation of taxa indicative of non-temperature-driven environments will lead to notable differences between reconstructions derived from pollen grains and chironomid head capsules. Additionally, we suppose that these identified differences may reflect a Holocene climatic history divergent from what was previously known while being based mainly on pollen assemblages.

3.4 Material & methods

3.4.1 Site selection and coring

To evaluate the accuracy of temperature inferences in different environments, five sites encompassing a broad vegetation and temperature gradient were selected across the boreal zone of eastern Canada (Baldwin et al., 2020). Petit Anne Lake (49°50'14"N, 68°43'30"W, 148 cm in length) is located at the transition between mixed and coniferous eastern boreal forests (Figure 17). Further north, Billy Lake (53°04'60"N, 66°57'87"W, 89 cm in length) lies at the transition between the closed eastern boreal forests and the open northern boreal woodlands (Figure 17). Finally, Blow Hole Lake (56°31'25"N, 61°41'49"W, 113 cm in length) is located in the subarctic woodlands and tundras (Figure 17). The three sites were cored in August 2019 using a Uwitec gravity corer, 9 cm in diameter, at the deepest point of the lakes. Additionally, the Mista and Aurélie sites, previously described by Bajolle et al., (2018) and Feussom Tcheumeleu et al., (2023), respectively, and located in the eastern boreal forests (Figure 17), were included in our study.

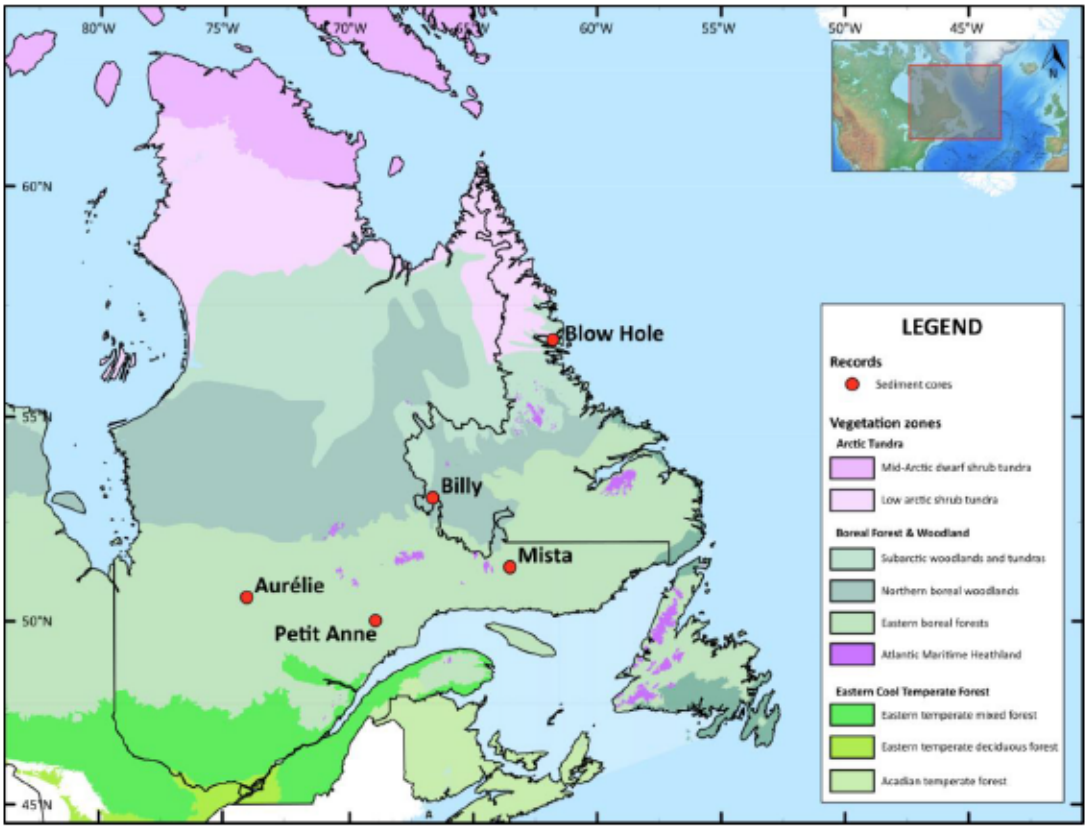

Figure 17
Location of the study sites across the vegetation zones of Canada in Québec and Newfoundland-and-Labrador provinces.
Source : Baldwin et al., (2020).

3.4.2 Chronologies

To establish reliable and comparable chronologies, Blow Hole, Billy and Petit Anne cores underwent dating procedures involving a minimum of four ^{14}C AMS radiocarbon dates based on plant macroremains (needles, wood, bryophytes) and charcoals (Table 5). Furthermore, the top 10 cm of these three cores were measured for ^{210}Pb and ^{137}Cs activities (Le Roux and Marshall, 2011), and a Constant Rate of Supply model (Appleby et al., 1979) applied to obtain calendar years. For Mista and Aurélie sites, we used dated levels as described by Bajolle et al., (2018) and Feussom Tcheumeleu et al., (2023). All radiocarbon dates were calibrated at 2σ to calendar

years using the IntCal20 Northern Hemisphere Radiocarbon Age Calibration Curve (Table 5, Reimer et al., 2020). The five bayesian age-depth models were developed using the 'rbacon' package v.3.1.1 (Blaauw et al., 2021) in R environment version 4.3.2 (R Core Team, 2023), and interpolated at contiguous 0.5-cm depth intervals. All dates were expressed in calibrated years before present, hereinafter referred to as 'yr cal BP'. Age-depth models are available in Annexe E.

Table 5
Radiocarbon (^{14}C) age determination for the five study sites. Radiocarbon analyses were performed both at the Poznań Radiocarbon Laboratory at Poznań, Poland, and at the Radiochronology Laboratory of the Centre d'Étude Nordique (CEN) at Laval (QC), Canada.

Core	Depth in record (cm)	Dated material	Sample code	Age 14C (year BP)	Calibrated 14C age ranges (yr cal BP; 2σ)
Blow Hole	20-21	Needles, wood	BLH 20-21	1800 ± 30	2208 (2225-2297)
Blow Hole	53-54	Needles, wood	BLH 53-54	3795 ± 35	4181 (4084-4295)
Blow Hole	70-71	Charcoals, needles	BLH 70-71	4815 ± 15	5557 (5482-5530)
Blow Hole	93-94	Wood	BLH 93-94	6205 ± 15	7084 (7008-7133)
Blow Hole	109-110	Needles and wood	BLH 109-110	6910 ± 40	7739 (7669-7838)
Billy	13-14	Needles, charcoals	BIL 13-14	415 ± 15	494 (471-508)
Billy	35-36	Bryophyta	BIL 35-36	1715 ± 30	1602 (1536-1635)
Billy	55-56	Bryophyta	BIL 55-56	2735 ± 35	2823 (2759-2883)
Billy	75-76	Bryophyta	BIL 75-76	4040 ± 15	4475 (4438-4475)
Billy	81-82	Bryophyta	BIL 81-82	4510 ± 15	5149 (5052-5193)
Petit Anne	20-22	Charcoals, wood	PEA 20-22	355 ± 15	388 (318-381)
Petit Anne	65-66	Needles	PEA 65-66	1585 ± 15	1562 (1569-1632)

Petit Anne	75-76	Needles	PEA 75-76	2160 ± 30	2150 (2047-2182)
Petit Anne	130-131	Needles	PEA 130-131	3315 ± 15	3526 (3484-3568)
Mista	69-74	Herbaceous stems	D-AMS 025608	2103 ± 21	2065 (1998–2124)
Mista	151-156	Herbaceous stems	D-AMS 025609	3694 ± 27	4036 (3928–4145)
Mista	229-234	Herbaceous stems	D-AMS 025610	5109 ± 27	5812 (5751–5923)
Mista	342-343	Picea glauca cone	D-AMS 025611	7472 ± 33	8283 (8193–8367)
Mista	359-360	Picea glauca cone	D-AMS 025612	7741 ± 32	8511 (8430–8590)
Aurélie	43-44	Plant macroremains	Poz-35983	2870 ± 30	2994 (2880–3076)
Aurélie	111-112	Plant macroremains	Poz-35984	3990 ± 35	4473 (4403-4532)
Aurélie	163-164	Plant macroremains	Poz-36014	4750 ± 35	5514 (5450-5585)
Aurélie	220-221	Plant macroremains	Poz-36016	6140 ± 40	7039 (6936-7162)
Aurélie	236-237	Plant macroremains	Poz-36017	6490 ± 40	7377 (7314-7436)
Aurélie	326-327	Plant macroremains	Poz-36018	7460 ± 50	8275 (8184-8372)

3.4.3 Chironomid analysis

1-cm^3 sediment samples were retrieved from the cores at regular interval, and chironomid head capsules were isolated by soaking them overnight in a 10%-concentrated KOH solution to bleach and deflocculate the organic matter. The residual solution was water-rinsed through a 100-µm-mesh sieve, and the upper fraction observed under a binocular microscope at x10 magnification. Each whole or half-broken head capsule was then individually picked using fine forceps and mounted ventral side up on a fixed microscope slide using Aquatex® mounting medium. Head capsules were then observed under a light microscope at x400 magnification to allow determination of chironomid morphotypes, based on the identification guides of Wiederholm (1983), Brooks et al., (2007) and Epler et al., (2013). A minimum of 50 capsules was identified per sample to provide an accurate representation of past

community composition (Quinlan and Smol, 2001; Larocque, 2001; Heiri and Lotter, 2010).

Temperatures were inferred from chironomid assemblages using northeastern Nearctic modern training set (Suranyi et al., *in prep.*), composed of 148 chironomid taxa from 182 lakes distributed along a latitudinal gradient from New-England to Baffin Island (Annexe F). To get the most accurate inferences, were removed from the training set: (1) taxa of too low taxonomic resolution (tribe level or higher), (2) taxa with a maximum occurrence lower than 2, (3) taxa with a maximum abundance lower than 2%, and (4) undetermined chironomids of the genus Psectrocladius and Heterotrissocladius, as several species groups exhibiting highly variable climatic optima and tolerances may be identified within these genera. Finally, the same criteria were applied to the fossil assemblages, resulting in final datasets consisting of 100 chironomid taxa.

3.4.4 Pollen analysis

Palynomorphs were extracted on each core at the same depths as for chironomid samples from about 1-cm^3 of wet sediments. Pollen samples were processed using the standard protocol for terrestrial samples, including long chemical treatments with hydrochloric and hydrofluoric acids, coarse-sieving (200-µm mesh), organic matter digestion with sodium hydroxide, acetolysis coloration, and slide preparation in glycerol. Each sample was mounted between slide and moving rectangular coverslip, and a minimum of two lines (one at the center and one at the edge of the coverslip) were counted on each slide to avoid any inherent bias in distribution due to pollen grain size (see Gottardini et al., 2009). Palynomorph counting was performed with an optic microscope at x400 magnification, using the Chrono-environnement (UMR 6249 CNRS-UFC) reference pollen collection and palynological guides (Beug, 1961; Richard, 1970; McAndrews, 1973; Reille, 1995). While a pollen assemblage may be considered as statistically representative once 150 to 300 pollen grains (excluding unidentified and aquatics) have been identified (Djamali and Cilleros, 2020; Chevalier

et al., 2020), a minimum of 500 pollen grains was identified in each sample of Blow Hole, Billy and Petit Anne cores, in order to allow the more accurate representation of the vegetation (Chevalier et al., 2020).

The modern training set used for pollen inferences was derived from the North American Pollen Database, compiled by Whitmore et al., (2005). We restricted this database to cover only sites above 45°N and east of 80°W to get a spatial coverage similar to the modern chironomid training set. Modern sites with a pollen sum below 300 grains were excluded, as well as aquatic taxa and non-pollen palynomorphs. The final modern calibration dataset consisted of 618 sites located in northeastern North America (Annexe FA-E), and harmonised in 89 pollen taxa.

3.4.5 Numerical analysis

All numerical analyses were performed in the R environment version 4.3.2 (R Core Team, 2023). Chironomid and pollen datasets were transformed to relative abundances summing to 1 for each site (modern datasets) or record (fossil datasets) before temperature inferences.

3.4.5.1 Stratigraphic diagrams and clustering

To allow visual interpretation of the records and abundance changes of pollen and chironomids over time, stratigraphic diagrams of relative abundance were produced for each lake using the strat.plot function of the 'rioja' package v.1.0-5 (Juggins and Juggins, 2020). Using the same package, statistically significant assemblage zones for pollen (PAZ) and chironomids (CAZ) were identified on Hellinger-transformed abundance data using constrained incremental sum of squares (CONISS) clustering (Grimm, 1987), and assessed by a broken stick model (Bennett, 1996). Stratigraphic diagrams are available in Annexe G to K, and their description in Annexe L-U.

3.4.5.2 Multivariate analysis

High-quality links between pollen assemblages and the surrounding environment are crucial to reconstruct post-glacial climate. A series of ordinations was therefore conducted to explore the relationships between 70 environmental variables and pollen assemblages of the modern training set and determine the most relevant. Environmental variables include – among others – air temperatures and precipitation for each month, averages for each season, and average sunshine for each season. The full list of parameters can be found in Whitmore et al., (2005). Separated Redundancy Analysis (RDA, Ter Braak and Prentice, 1988) and Canonical Correspondence Analysis (CCA, Ter Braak, 1986) were first carried out on the pollen training set, and the significance of each variable tested by means of permutations (999 times). Detrended Correspondence Analysis (DCA, Hill and Gauch Jr, 1980), Principal Component Analysis (PCA, Wold et al., 1987), and Correspondence Analysis (CA) were then applied to the pollen training set, and their first axis used as a predictor of the biological responses of pollen assemblages to environmental variables. Then, we ranked environmental variables using the R squared for each ordination. Their cumulative ranks identified mean summer air temperature (hereafter MSAT, June-July-August mean) as the most influential environmental variable in shaping pollen assemblages (Table S1).

Similar ordinations were performed by Suranyi et al., (in prep.) for the modern chironomid training set and yielded the same parameter as the most influential in explaining chironomid assemblages. As MSAT is the primary determinant of both pollen and chironomid modern assemblages in our study zone, modern analogue technique and inference models can be applied on both pollen and chironomid assemblages to predict past MSAT.

3.4.5.3 Quantitative reconstructions

MSAT were first inferred from pollen assemblages using the MAT, by calculating the squared Hellinger distance (Legendre and Gallagher, 2001) to the closest modern assemblage, a variant of chord distance commonly used in paleoecology (see Overpeck et al., 1985; Juggins, 2015). To assess model performances while considering the effect of spatial autocorrelation (Telford and Birks, 2005), a h-block cross-validation was used (Chevalier et al., 2020). Results are displayed is Table 6. To determine the optimal number of analogues from 1 to 20, various parameters (Root mean square error, R squared, skill score, and average and maximum biases) were systematically evaluated. Each parameter was assigned a rank based on its performance relative to the number of analogues, with a score of 1 assigned to the highest-performing parameter and 20 to the lowest. These scores were summed, and the number of analogues associated with the lowest total rank (8 analogues) was identified as indicating the best overall performance. MSAT were then estimated as the weighted average of their corresponding climatic values.

Table 6
Summary of modern training datasets, applied inference methods and model performance statistics for the two proxies.

Proxy	Pollen (MAT)	Chironomids (fxtWA-PLS)
Number of sites in the training set	618	182
Number of taxa in the training set	89	100
MSAT range (°C)	0.63-19.13	0.30-21.20
R^2	0.94	0.89
Maximum bias (°C)	2.12	4.97
RMSE (°C)	1.12	1.59

MSAT were reconstructed from chironomid assemblages using a tolerance weighted average-partial least square model with two components, with P-spline frequency correction of the training set climate variables (fxtWA-PLS; Liu et al., 2023). In order to take into account the effect of spatial autocorrelation, pseudo-removed leave-out cross-validation (999 permutations) was used to evaluate model performance statistics (Table 2).

To assess the causes of the discrepancies between pollen-based and chironomid-based inferences, we finally calculated the difference between both reconstructions. This difference was called ΔT.

3.4.5.4 Diagnostic of reconstructions

To evaluate whether the modern datasets provide reliable MSAT reconstructions or not, we calculated (1) the percentage of rare modern taxa per fossil sample, (2) the goodness-of-fit (hereafter GOF) of model prediction, and (3) the squared-chord distance of the fossil samples to the closest modern analogue. Following Heiri et al., (2003), taxa with a Hill's N2 (Hill, 1973) below 5 in the modern training set are identified as rare, and their optima and tolerances are likely to be poorly estimated. The percentage of rare modern taxa corresponds to the cumulative abundance of rare taxa in fossil samples. To evaluate the GOF, we calculated the squared residual length (SqRL) by passively fitting fossil samples to the redundancy analysis (RDA) axis of the modern training set (ter Braak and Prentice, 2004). The 90th and 95th percentiles of the modern residual distance of all modern samples were used as cut levels to assess whether a fossil sample had a 'poor fit' or 'very poor fit' to MSAT, respectively (Birks et al., 1990). Following Birks et al., (1990), the number of good and close analogues was calculated using the modern analogue technique and squared-chord distance. Indeed, reconstructed MSAT are considered as more reliable if the fossil sample has close modern analogues in the calibration dataset. To identify fossil samples with 'no close' and 'no good' modern analogue, we used the 5th and 10th percentile of all squared-chord distances within the modern calibration dataset,

respectively. As the fxTWA-PLS is intended to perform well even in situations of poor analogy, we did not use this criterion as a diagnostic element for chironomid inferences. GOF and Hill's N2 index were calculated using the 'compare' and 'residLen' functions of the 'analogue' R package (Simpson, 2007), and squared-chord distance was calculated using the 'analog' function of the same package.

3.4.6 Fire variables reconstructions

In order to reconstruct the fire regimes at each site, sediment samples of about 1 cm^3 were retrieved continuously at regular 1-cm intervals, with the exception of the top-10 cm of each core, which were sampled at 0.5-cm intervals. Macrocharcoal particles, assumed to originate from local fire events (Higuera et al., 2007; Oris et al., 2014a), were extracted from sediment samples, counted and their area measured, following the protocol described by Lesven et al., (2022).

Charcoal series were analysed using the 'tapas' package v.0.1.3 (Finsinger and Bonnici, 2022) to detect past fire events. This analysis includes interpolation of the charcoal data to the median temporal resolution of the samples, and decomposition of the records into background and peak components by applying a LOWESS-smoother technique robust to outliers, with a smoothing window varying within records between 300 and 750 years. Peaks were evaluated using a Gaussian mixture model, corresponding to the 95^{th} percentile of the modelled noise distribution (Higuera, 2009). Fire frequencies (hereafter FF) were reconstructed from detected significant fire events with a kernel density estimation procedure based on a 500-year smoothing bandwidth (Mudelsee et al., 2004; Ali et al., 2012), using a modified version of the 'paleofire' package v.1.2.4 (Blarquez et al., 2014). The amount of biomass burnt at each site was reconstructed from the individual charcoal accumulation rates, by (1) rescaling initial charcoal accumulation rates using a min-max transformation, (2) homogenising the variance using a Box-Cox transformation, and (3) rescaling the series to z-scores (Power et al., 2008), using a corrected version of the 'paleofire' package (Blarquez et al., 2014). A constant equal to 1 was added to biomass burned

and FF, and their ratio was calculated at each site to assess local fluctuations in fire size (hereafter FS) through time (Ali et al., 2012).

3.4.7 Fire-MSAT relationships

In order to assess the relationship between ΔT and fire parameters, linear and generalised additive models were tested using the 'mgcv' package (Wood and Wood, 2015). In these models, FF and FS served as explanatory variables, while ΔT was considered the response variable. Two linear models and two Generalised Additive Models (GAM), all assessed with and without interactions between FF and FS, were examined, and the deviance explained criterion used for model selection. Of the four tested models, the linear model without interaction between FF and FS exhibited the best performance for the five studied sites and was thus used for this study.

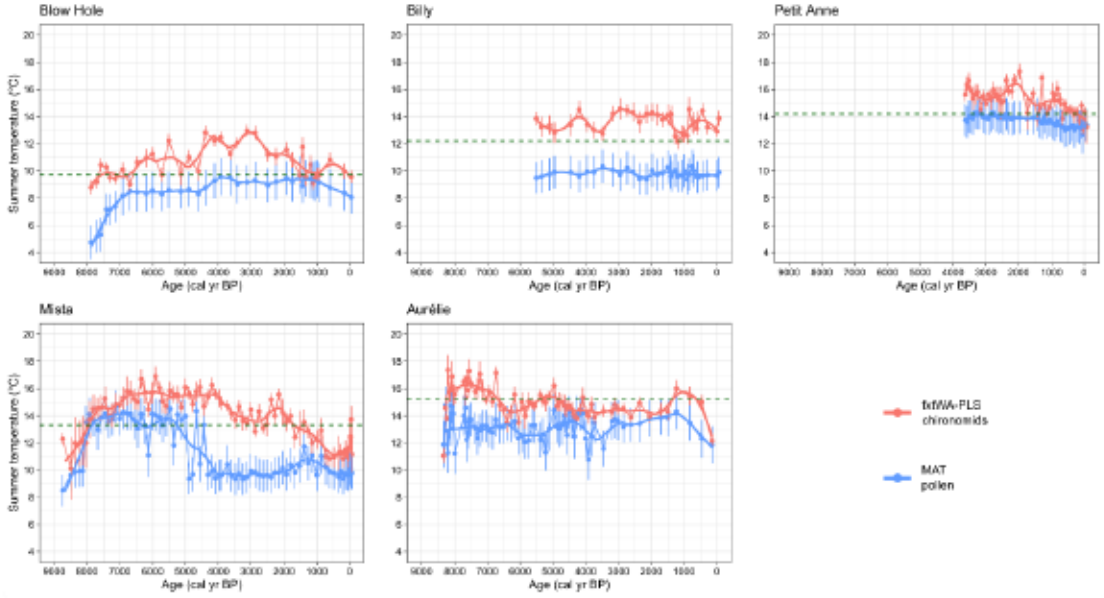

Figure 18
Comparison of paleoclimate reconstructions for the 5 studied sites over time, and smoothed over 1500 years using a loess regression.

3.5 Results

3.5.1 Chironomid-based reconstructions

The Mista and Aurélie records showed a period of rapid warming from the beginning of the record to ca. 9000-7500 yr cal BP (Figure 18). Although the number of rare taxa per sample was relatively high, all samples had less than 20% rare taxa in the training set, as required to obtain reliable reconstructions (Brooks and Birks, 2001; Larocque-Tobler, 2010) (Figure 19). Moreover, during this period, all samples were well fitted by MSAT. This warming phase appeared less distinct at Blow Hole. These samples had a poor or very poor fit with MSAT although there was no rare or missing taxa, suggesting that this period should be interpreted with caution. After this post-glacial warming phase, the Mista, Aurélie and Blow Hole records showed warm, stable conditions until *ca.* 5000-4000 years, with few rare taxa and a good fit with MSAT. This suggests a strong reliability of our inferences. From *ca.* 4500 yr cal BP, Blow Hole showed a warming phase of around 2-3°C, with an overall good reliability of reconstructions. Afterward, all sites exhibited a clear downward MSAT trend until the present day, starting *ca.* 5000 yr cal BP at Aurélie, *ca.* 4200 yr cal BP at Mista and ca. 3200 yr cal BP at Blow Hole. The pattern is less clear at Billy, but an overall decrease can be well distinguished after *ca.* 3000 yr cal BP. During this cooling phase, Mista and Petit Anne record showed a brief warming phase of about 1°C between *ca.* 2500 and 1800 yr cal BP, while Aurélie experienced a short warming between ca. 1500-800 yr cal BP. Overall, all samples showed less than 20% of rare taxa and therefore allowed reliable MSAT estimates (Brooks and Birks, 2001; Larocque-Tobler, 2010), although a few samples in each sequence had a poor fit with MSAT.

3.5.2 Pollen-based reconstructions

Similarly to chironomid-based inferences, pollen-based reconstructions indicated a rapid warming between *ca.* 8700 and 8000 yr cal BP at Mista (Figure 18), and between *ca.* 8000 and 6900 yr cal BP at Blow Hole. In contrast, Aurélie did not exhibit a warming period, therefore contradicting chironomid-based inferences. Despite a good fit to MSAT and a low occurrence of rare taxa (Figure 20), the Aurélie record showed almost

no analogues before *ca*. 8100 yr cal BP, and poor analogues for the majority of the sequence, suggesting a potential bias in MSAT inferences. Similarly, Blow Hole and Mista showed poor or no analogues following the deglaciation, while exhibiting a good fit with MSAT. Similarly to chironomid-based inferences, Mista record stagnated at high MSAT values (~13-14.3°C) until *ca*. 5500 yr cal BP, while displaying poor analogues but a good fit with MSAT. A trend comparable to that of chironomid-based inferences was observed up to ca. 4500 yr cal BP at Blow Hole, with high (~8.2°C) and stable MSAT. In parallel, Aurélie record displayed minimal MSAT fluctuations up to *ca*. 4500 yr cal BP. Similarly to chironomid-based inferences, Billy, Petit Anne and Mista records then revealed a general cooling trend from *ca*. 5500 yr cal BP up to the present day, while Aurélie showed a slight warming until *ca*. 1200 yr cal BP before following the same trend as a other sites. Blow Hole exhibited maximum MSAT (~9.0-9.6°C) after ca. 4000 yr cal BP. However, the subsequent decrease only began *ca*. 1000 yr cal BP. Throughout the entire period, Blow Hole exhibited good analogues, a good fit with MSAT, and no rare or missing taxa (Figure 20).

3.5.3 Fire histories

Mista and Aurélie exhibited relatively similar fire histories over the last 9000 years (Figure 21). At the onset of the sequence, both sites experienced maximum FF (9 and 15 fires per millennium, respectively), while FS demonstrated minimal values (~0.2). Subsequently, Aurélie showed a nearly continuous decline in FF to 2 fires per millennium until *ca*. 1200 yr cal BP, although a slight increase was noted in the recent period. Conversely, FS exhibited a continuous increase until reaching 1.8 in the recent period. Mista showed a continuous decline in FF until *ca*. 4200 yr cal BP, reaching 3.5 fires per millennium, followed by an increase to about 5.5 fires per millennium *ca*. 1800 yr cal BP, and finally a decrease to the present day. Conversely, FS at this site showed an opposite trend, increasing continuously until *ca*. 4200 yr cal BP, then gradually decreasing to the present day. The other sites displayed different patterns. Blow Hole had no recorded fire event until *ca*. 5500 yr cal BP, which then increased to 3 fires per millennium *ca*. 3000 yr cal BP, before decreasing to about 1.2 fires per millennium in

the current period. FS at Blow Hole showed minimal variation (0.7-1.3) throughout the sequence. At Billy, FS remained within a consistent range, with slightly higher values (1.75) at the beginning of the sequence. FF was initially low (<1 fire per millennium), gradually increasing until reaching 3.5 fires per millennium *ca*. 900 yr cal BP, and then decreasing to the present day. Finally, Petit Anne demonstrated a progressive increase in FF from 3 to 5.5 fires per millennium between *ca*. 3600 and 600 yr cal BP, before declining to the present day. FS exhibited high values (>1.5) at the beginning and end of the sequence, with little variation (0.7-1.3) between these boundaries.

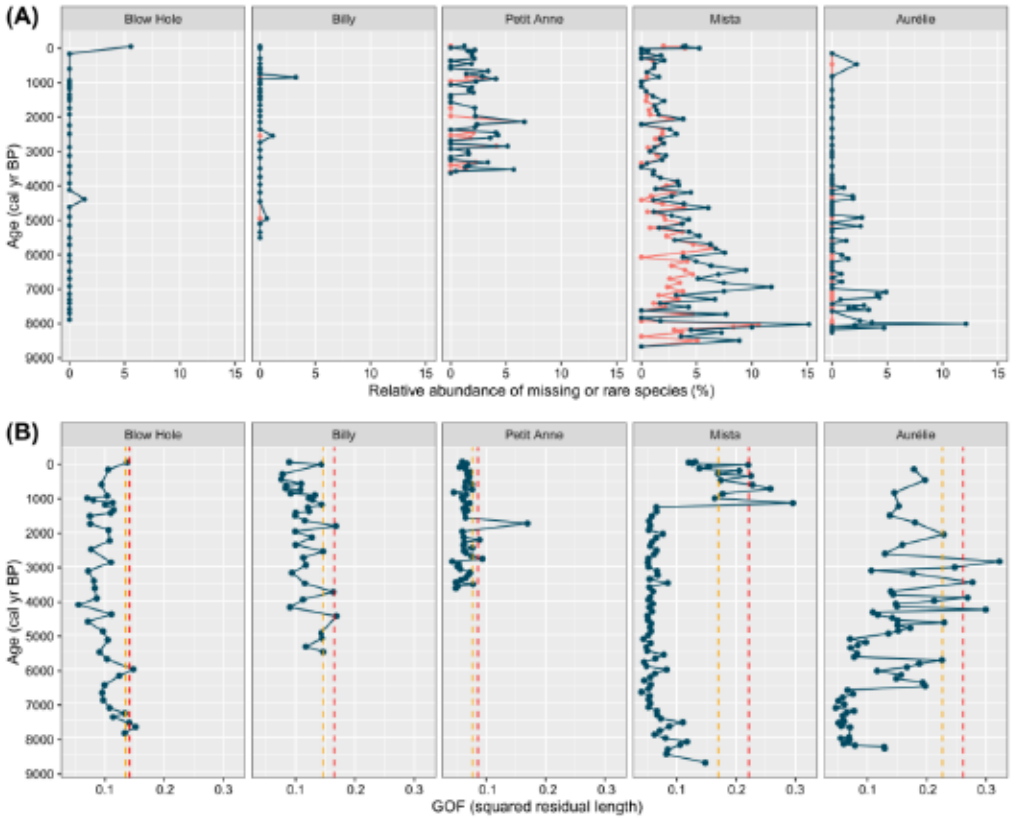

Figure 19
Reliability of chironomid inferences for Blow Hole, Billy, Petit Anne, Mista and Aurélie sites. Upper panels (A) display the relative abundance of missing (pink) or rare (dark blue) species in the modern training set (%), and lower panels (B) represents the goodness-of-fit (GOF) of fossil samples with temperature. Vertical dashed yellow and red lines represent the 90th and 95th percentiles of the modern residual distance of all modern samples, above which fossil samples are considered as a poor and very poor fit with temperature, respectively.

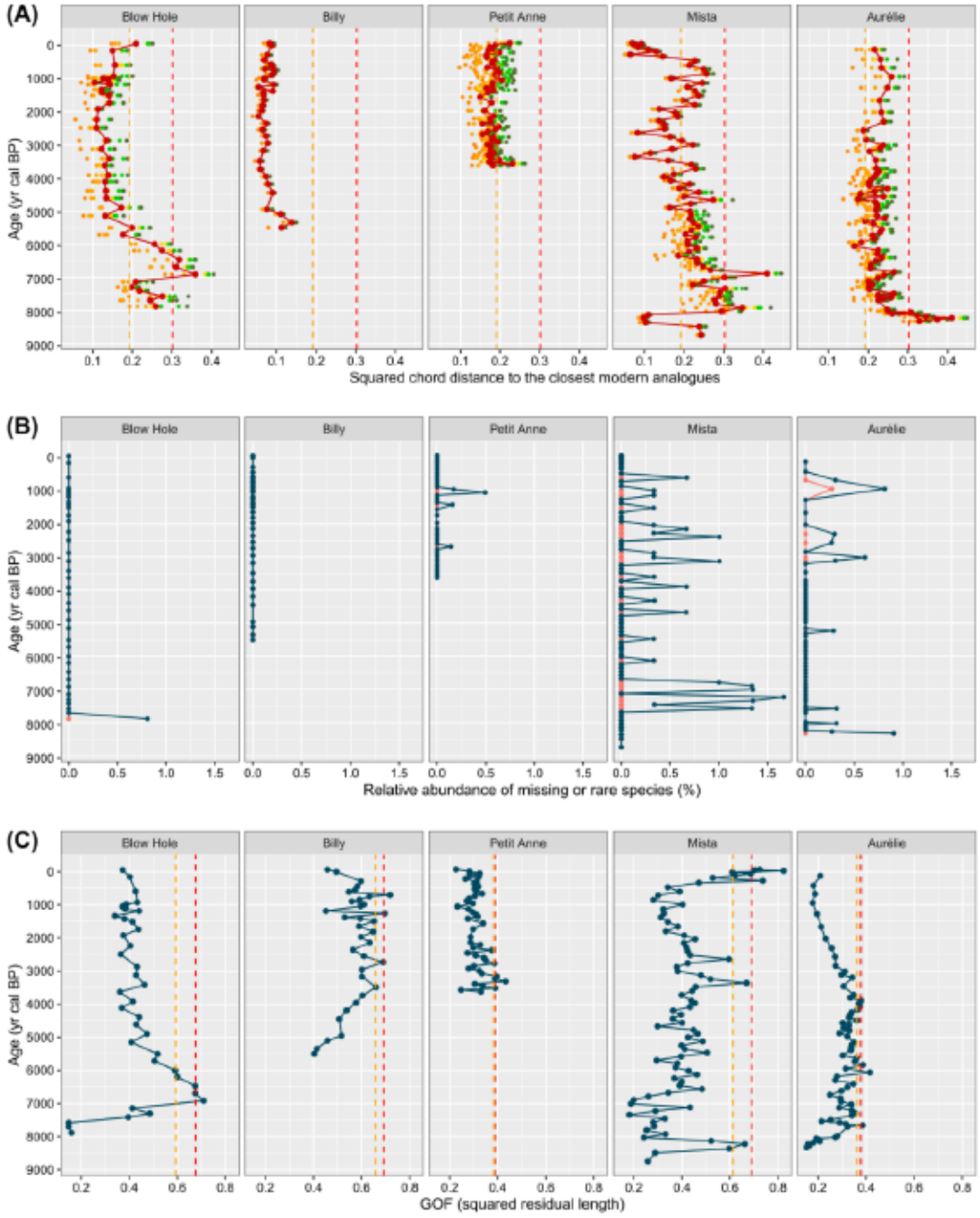

Figure 20
Reliability of pollen inferences for Blow Hole, Billy, Petit Anne, Mista and Aurélie sites. Upper panels (A) show the squared chord distance of the fossil samples to the 8 closest analogues (orange to dark green dots), and the red line represents their mean. Vertical dashed yellow and red lines represent cut

levels of the 5th and 10th percentile of all squared-chord distances within the modern calibration dataset, respectively. Middle panels (B) display the relative abundance of missing (pink) or rare (dark blue) species in the modern training set (%). Lower panels (C) represents the goodness-of-fit (GOF) of fossil samples with temperature. Vertical dashed yellow and red lines represent the 90th and 95th percentiles of the modern residual distance of all modern samples, above which fossil samples are considered as having a poor and very poor fit with temperature, respectively.

3.5.4 Link between ΔT and fire variables

The linear model unveiled varying relationships between ΔT and fire-related variables across the study sites. Significant correlations between ΔT and fire variables were observed only in the three longest sequences (Table 3). Among these, Mista exhibited the most conspicuous relationships. The model indeed demonstrated high significance for FS, with maximum ΔT during periods when the area burnt was maximum (Figures 21 and 22). In contrast, Aurélie displayed only a weak correlation between ΔT and FS (Table 3), while FF could appear more significant. As depicted in figure 21, the beginning of the record was characterised by notably high FF (~15 fires per millennium) coinciding with peak ΔT (~6°C), despite the absence of notable correlation. Blow Hole record indicated a moderately significant negative correlation between ΔT and both fire variables, indicating that as ΔT rises, FF and FS decline. Conversely, at Billy and Petit Anne, the model did not yield significance for either variable (Table 3). Nonetheless, Billy record exhibited elevated FS values during periods of high ΔT, while conversely displaying lower FS values during ΔT minima (Figures 21 and 22). This pattern was less pronounced at Petit Anne.

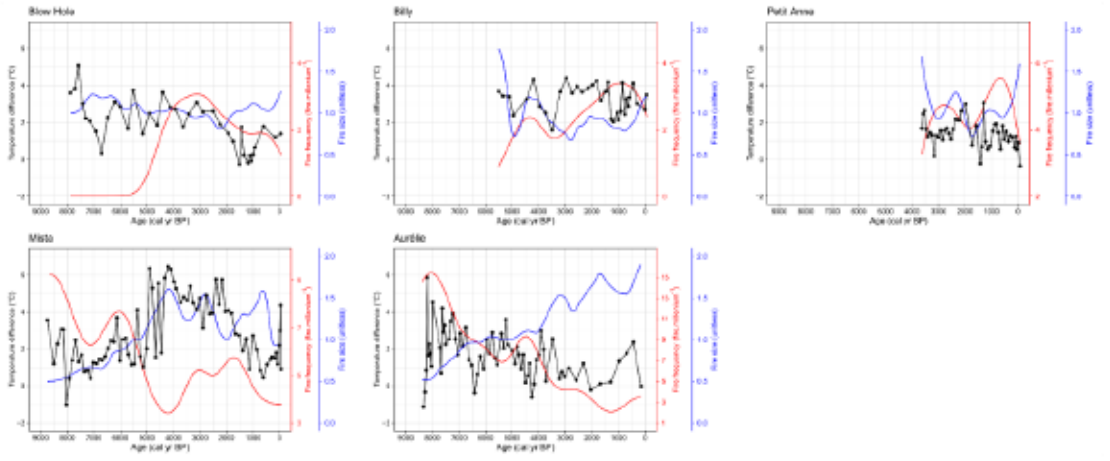

Figure 21
Comparison of ΔT and fire parameters (FF and FS) over time for the 5 studied sites.

Table 7
Performance and results of the models establishing the relationship between fire variables (model parameters) and ΔT for each studied site. ***p < 0.001, **p < 0.01 and *p < 0.05.

	BLH	BIL	PEA	MIS	AUR
p-value (fire frequency)	0.0033**	0.8368	0.6820	0.4679	0.1897
p-value (fire size)	0.0068**	0.6221	0.9290	0.0003***	0.0297*
R^2(adj) of the model	0.2080	-0.0427	-0.0371	0.2440	0.1300

3.6 Discussion

3.6.1 Causes of observed differences between pollen- and chironomid-based inferences

The comparison of temperature inferences revealed that not only absolute values, but also general trends extensively differed between pollen- and chironomid-based inferences across our study sites (Figure 18). These variations, potentially stemming from the low reliability of the reconstructions due to poor MSAT estimations, may be further exacerbated by internal forcings independent to climatic fluctuations.

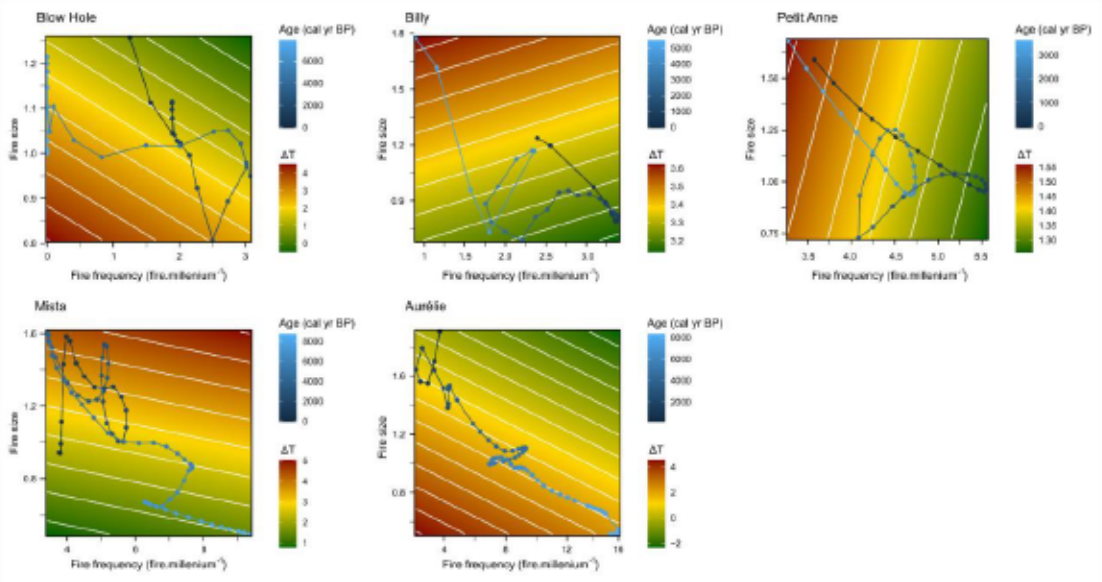

Figure 22
Heatmaps of the linear model representing the relationships between FF, FS and ΔT for each site studied. The predicted values of ΔT are represented by red, yellow and green colors. The trajectories of each site over time are shown in shades of blue.

3.6.1.1 Fire

The comparison of fire variables with ΔT through the GAM model highlights the major influence of forest fires on vegetation composition, mainly in closed-crown spruce-moss forests. Interestingly, vegetation changes in western Quebec appears to be driven by small but recurrent fires, whereas large fires have been major drivers of

change in the east (Figure 21), therefore aligning with recent studies suggesting similar longitudinal variation in the impact of wildfires (Remy et al., 2017).

In western Québec, the onset of the Aurélie record (*ca*. 8200-6700 yr cal BP) was characterised by its highest ΔT values (3-6°C, Figure 21). While chironomid-based MSAT remained reliable (Figure 19) and followed known climatic trends during this period (Viau and Gajewski, 2009; Gajewski, 2015; Fréchette et al., 2018), the unusually low temperature record inferred from pollen assemblages are related to high abundance of *Pinus banksiana*-type and *Picea*, leading to a situation of poor- or non-analogy with the training set (Figure 20). Previous studies have already documented a notable development of *Pinus banksiana*-type and *Picea mariana* during the early- to mid-Holocene period (Richard, 1980; Liu, 1990; Garralla and Gajewski, 1992; Gajewski et al., 1993; Carcaillet et al., 2001; Fréchette et al., 2021), whose rapid expansion may have been facilitated by recurrent fires (Carcaillet and Richard, 2000; Carcaillet et al., 2001) after the drainage of the proglacial lake Ojibway (Vogel et al., 2023). These serotinous conifers, particularly *Pinus banksiana*, depend on frequent fires but only little on temperature for their reproduction. Consequently, their analogues during this period are evenly distributed between 45 and 68°N (Annexe F) due to the poor response to temperature, leading to minor fluctuations in temperature inferences. It is therefore reasonable to assume that pollen-based inferences in the early Holocene may have been biased by short fire return intervals, favoring the development of coniferous taxa. Later, the reduction in fire frequency no longer favoured them, although they remained represented in the landscape, hence the non-significance of the model during periods of low fire frequency (Table 3).

At Mista, pollen- and chironomid-based inferences showed their main divergence during the mid-Holocene period (Figure 21). Pollen-based MSAT started to decline *ca*. 5500 yr cal BP, while chironomid-based inferences showed a downward trend only after *ca*. 4200 yr cal BP (Figure 18). Other regional-scale reconstructions have shown maximum temperatures up to *ca*. 4500 yr cal BP in south-western Quebec (Fréchette et al., 2018), and *ca*. 4000 yr cal BP in eastern Quebec and Labrador (Fréchette et al., 2021), thus supporting our chironomid inferences, whose reconstructions were

assessed as reliable (Figure 19). Comparatively, pollen assemblages showed few analogues during this period (Figure 20). The period between *ca*. 5500 and 4000 yr cal BP was characterised by a major transition from a mixed forest dominated by *Betula*, *Picea* and *Abies* to a spruce-moss forest largely dominated by *Picea* (Annexe J). The linear model is highly significant between ΔT and FS (Table 3), the latter showing its highest values during this period. It is likely that the serotinous *Picea mariana* was favoured by large and severe fires (Feussom Tcheumeleu et al., 2023), coinciding with wet climatic conditions in the region (Ali et al., 2012; Magnan and Garneau, 2014). Ali et al., (2012) showed a notable increase in annual precipitation *ca*. 5000 yr cal BP and a parallel decrease in fire ignition, leading to pronounced fuel accumulation. The persistently elevated temperatures at this period, combined with occasional dry spring conditions, facilitated the spread of large fires and concurrently spurred the expansion of conifers in the landscape (Bergeron et al., 2004). These fire-induced vegetation changes probably led to a coniferization of the region nearly one thousand years before the onset of the Neoglacial cooling. Accordingly, the apparent decline in pollen-based MSAT after *ca*. 5000 yr cal BP should not be interpreted as an indication of cooling.

3.6.1.2 Within-lake variables

The maximum ΔT at Blow Hole was recorded just following the deglaciation period (*ca*. 8000-7500 yr cal BP). Despite the small number of close analogues, pollen-based inferences showed an overall good reliability (Figure 20), marked by the classic afforestation sequence (Fréchette et al., 2021). Conversely, chironomid assemblages showed a combination of cold and warm affinity taxa, forming a mixture poorly to very poorly fitted with MSAT (Figure 19), whose majority have a particular affinity for acidophilic conditions. The post-deglaciation period has already been shown to be conducive to the rapid acidification of boreal lakes (Boyle et al., 2013; Sienkiewicz, 2016), due in particular to the absence of organic soil, leading to soil mineral depletion, as was the case at Blow Hole (Lesven et al., 2022). This suggests that factors beyond temperature may have influenced chironomids assemblages directly following the

deglaciation, before temperature gradually became the major forcing of chironomid assemblages after *ca*. 7500 yr cal BP.

Similarly, most of the Billy record showed a high ΔT along the whole sequence (~4°C, Figure 21). Once again, this appears to stem from inherent biases within chironomid assemblages, despite the apparent reliability of the reconstructions. The record is indeed largely dominated by taxa with a strong affinity for acidophilic environments and the presence of macrophytes in the lake, indicating a notable bias in reconstructions relying on chironomids. Despite major differences in absolute values, pollen- and chironomid-based MSAT inferences exhibit a consistent overall decline, characteristic of the Neoglacial period.

3.6.1.3 Over-representation of palynotaxa

Following the early-Holocene deglaciation period, Blow Hole record indicated a rapid increase in MSAT (Figure 18), mirroring the known tendencies of the region (Viau and Gajewski, 2009; Gajewski, 2015; Fréchette et al., 2018, 2021). However, the fit between the fossil samples and the training set sharply worsens, even leading to a situation of non-analogy between *ca*. 7000 and 6400 yr cal BP (Figure 20). This period appeared to be related to anomalously high values of *Alnus alnobetula* ssp. *crispa* (Annexe G), a taxa known for exhibiting a strong preference for open habitats (Gilbert and Payette, 1982) and for being a prolific pollen producer (Tinsley and Smith, 1974). In open environments like the Labrador coast, it may thus be disproportionately represented in pollen assemblages (Bradshaw, 1981). Presently, analogue sites are mainly located in the wet and cold conditions of northern Quebec, around Hudson and Ungava Bay (Annexe F). As a result, its high percentages throughout the sequence seem to lead to artificially low temperatures from *ca*. 7000 yr cal BP to today. The over-representation of this taxon is likely to have played a key role in shaping the temperature differences between pollen and chironomids throughout Blow Hole record, while tendencies remain relatively similar.

3.6.2 An updated Holocene climate history of eastern Canada

3.6.2.1 Deglaciation period

Despite the fact that the Holocene formally began 11,700 years ago, the presence of the Laurentide ice-sheet until *ca*. 5700 in Quebec-Labrador (Dalton et al., 2020) resulted in considerable regional variations in climate (Renssen et al., 2009), compensating for the strong orbitally-induced summer insolation (Berger and Loutre, 1991). The deglaciation occurred *ca*. 10,300 yr cal BP at Mista, and *ca*. 9600 yr cal BP at Blow Hole and Aurélie (Dalton et al., 2020), the latter having been covered by the proglacial Lake Ojibway until *ca*. 8200 cal BP. In accordance with pollen-based paleoclimatic syntheses of the region (Fréchette et al., 2021), both reconstructions of Mista showed a warming of about 5°C between *ca*. 8800 and 7500 yr cal BP. Inferences based on chironomids from Aurélie Lake showed warming of a similar magnitude between *ca*. 8200 and 7800 yr cal BP, while inferences based on pollen suggested warming of around 3.5°C between *ca*. 7800 and 6700 yr cal BP on the Labrador coast. Kerwin et al., (2004) and Gajewski, (2015) estimated a warming of around 2°C over the same period. These cold temperatures in the early Holocene were linked to the persistence of the Laurentide ice-sheet in the region Renssen et al., (2009) and the resulting clockwise anticyclonic atmospheric circulation due to cold katabatic winds Ullman et al., (2016).

3.6.2.2 Timing and duration of maximum temperatures

Following the post-glacial warming period, the retreat of the Laurentide ice-sheet marked the onset of the Holocene Thermal Maximum (HTM), a climatic phase whose initiation and duration varied extensively across North America (Gajewski and Atkinson, 2003; Kaufman, 2004; Miller et al., 2010). Indeed, the duration of the HTM in North America was largely dependent on both external and internal forcings, including orbital-induced summer insolation, the distance to the decaying ice-sheet, atmospheric greenhouse gas concentration (Renssen et al., 2009, 2012), but also ocean circulation changes in the Labrador Sea and Baffin Bay (Briner et al., 2016a). Our research provides novel insights into the timing of peak temperatures during this

period. While previous pollen-based reconstructions along the north shore of the St. Lawrence River indicated maximum temperatures *ca*. 3500 yr cal BP (Fréchette et al., 2021), our chironomid-based reconstructions showed this high-temperature phase until *ca*. 4200 yr cal BP. At Lake Aurélie, elevated temperatures persisted until *ca*. 5000-4500 yr cal BP, consistent with findings from other studies in the region (Viau and Gajewski, 2009; Fréchette et al., 2018). In contrast, the northern coast of Labrador exhibited a two-phase warming pattern, as revealed by our pollen- and chironomid-based reconstructions. Initially, there was a moderate stagnation in mean summer air temperatures (MSAT) from approximately 6700 yr cal BP (comparable to records from *ca*. 6000 yr cal BP south of Greenland by Gajewski (2015)), followed by a period of maximum temperatures after *ca*. 4200 yr cal BP (similar to findings in southern Greenland by Gajewski (2015)). The end of maximum temperature remains however unclear. While chironomids suggest a clear decreasing trend from *ca*. 3200 yr cal BP to the present, pollen-based inferences do not show this pattern until *ca*. 1500 yr cal BP (Figure 18). Gajewski (2015) and Viau and Gajewski (2009) reconstructed maximum temperatures in Quebec-Labrador up to the same period, while Kelly and Funder (1974) more closely agree with our chironomid data. Further studies are therefore needed to improve our understanding of recent climate dynamics around the Labrador Sea.

3.6.2.3 Mid- to late Holocene cooling: the Neoglacial period

Following the period of maximum temperatures, all five sites showed a notable decline in temperatures up to the present day. This cooling trend marks the gradual transition from the warm HTM to a colder neoglacial period, coinciding with reduced summer insolation consequent to the final retreat of the Laurentide ice-sheet (Kaplan and Wolfe, 2006; Fréchette et al., 2021). Along the North Shore of the St. Lawrence River, our chironomid reconstructions indicated a temperature decrease of approximately 4.5°C between *ca*. 4200 yr cal BP and present, estimated from ranging between 1 to 1.5°C based on previous pollen-based studies (Fréchette et al., 2021). These findings are corroborated by temperature reconstructions from Petit Anne, exhibiting variations

of a similar magnitude to those observed at Mista (Figure 18). At Aurélie, our chironomid-based data, in conjunction with synthesis by Fréchette et al., (2018) and reconstructions from Billy Lake, suggested a temperature decline of approximately 1.5°C. On the northern coast of Labrador, the neoglacial cooling trend was previously estimated at around 0.5°C between *ca*. 3200 yr cal BP and present Gajewski (2015). However, our chironomid data revealed a more substantial cooling of approximately 3.2°C, contrasting with a pollen-based reconstruction suggesting only a 1.5°C decrease after *ca*. 1000 yr cal BP. This Neoglacial period was probably characterised by higher amplitude events, *i.e.* the Roman Warm Period, the Medieval Climate Anomaly or the Little Ice Age. Although some of these events may be visible on our records, these variations remain within the margins of error of temperature inferences, and will therefore not be interpreted here.

3.7 Conclusion and guidelines

The holocene mean summer air temperatures of five sites in Quebec-Labrador were reconstructed using pollen and chironomid assemblages. While both proxies yielded reasonable inferences of past temperatures, our study revealed notable disparities, allowing discussions on potential enhancements for future studies. Pollen-based reconstructions appeared to be extensively influenced by fire regimes during periods of heightened fire frequency or size. In more northerly ecosystems, the over-representation of some taxa whose dynamics is not mainly related to temperature also appeared to bias the reconstructions. In this context, head capsules of chironomids can be used to reduce the bias inherent in pollen assemblages. Using chironomid assemblage help mitigate the biases inherent in pollen-based studies, and align particularly well with recent trends. However, they are also susceptible to within-lake variables, emphasising the need for ongoing reliability assessments. Furthermore, modern datasets in North America, particularly in eastern Canadian regions, are currently limited in spatial and climatic coverage. Expanding the number of modern dataset sites in the future would enhance their reliability, especially in poorly covered regions.

By highlighting the methodological challenges and potential biases in temperature inferences within eastern Canadian boreal forests, our study contributes to a deeper understanding of Holocene climate variability in this region. It enables a reevaluation of the Holocene climatic history, highlighting high spatial variability in warming and cooling periods. Moreover, it underscores the necessity for further multi-proxy studies to refine reconstructions and elucidate underlying mechanisms driving Holocene climate dynamics.

3.8 Author statements

3.8.1 Competing interests statement

The authors declare there are no competing interests.

3.8.2 Author contribution statement

Jonathan Lesven: Conceptualization, Methodology, Software, Investigation, Data curation, Writing - original draft, Writing - review & editing, Visualization, Project administration; Laurent Millet: Conceptualization; Methodology, Investigation, Writing - review & editing, Supervision, Project administration, Funding acquisition; François Gillet : Conceptualization, Methodology, Software, Data curation, Writing - review & editing, Visualization, Supervision, Project administration, Funding acquisition; Yves Bergeron: Conceptualization, Methodology, Writing - review & editing, Supervision, Project administration; André Arsenault: Conceptualization, Methodology, Writing - review & editing, Supervision, Project administration; Cécile C. Remy: Software, Writing - review & editing; Thomas Suranyi: Investigation, Data curation, Writing - review & editing; Augustin Feussom-Tcheumeleu: Investigation, Data curation, Writing - review & editing; Lisa Bajolle: Investigation, Data curation, Writing - review & editing; Adam A. Ali: Investigation, Writing - review & editing; Damien Rius: Conceptualization, Methodology, Investigation, Writing - review & editing, Supervision, Project administration, Funding acquisition

3.9 Funding statement

This work was supported by grants from the ANR Interarctic, the Nich-Arctic Project, the PEPS-INEE EPIDERME program, the Mitacs Globalink program, and the International Research Project “Cold forest”.

4. DECIPHERING THE ROLES OF TEMPERATURE AND FIRE ON VEGETATION DYNAMICS ALONG A NORTH-SOUTH TRANSECT IN EASTERN QUÉBEC AND LABRADOR

Jonathan A. Lesven, François Gillet, Yves Bergeron, André Arsenault, Adam A. Ali, Milva Druguet Dayras, Laurent Millet, Cécile C. Remy, Damien Rius

4.1 Abstract

In the upcoming decades, the boreal forests of eastern Canada are projected to undergo increased temperatures and heightened fire activity due to climate change, with numerous potential impacts on vegetation dynamics, and ultimately for carbon storage or economic activities. Despite these assumptions, there is a notable lack of millennial-scale studies focusing on eastern Quebec and Labrador, and existing research has not extensively explored the interplay between fire and temperature in shaping vegetation dynamics. As a result, our understanding of the influence of temperature fluctuations, fire frequency, and fire size on vegetation dynamics remains limited. This study addresses this gap by presenting three high-resolution multiproxy records along a north-south transect using pollen grains, chironomid head capsules and macrocharcoals, in order to explore changes in fire-climate-vegetation interactions during the Holocene in these regions. Through variation partitioning and generalised additive modelling, we discern differential impacts of temperature and fire across the latitudinal transect. Our analysis reveals major temperature effects in association to fire frequency on vegetation dynamics in the forest tundra and the closed-crown spruce-moss forests. Conversely, the influence of temperature appears to be limited in the open-crown lichen woodlands at mid-latitudes. Nevertheless, these variables, along with their interactions, displayed varied effects on black spruce over time. Notably, our study reveals an increasing impact of fire size over recent centuries along our transect, suggesting that the projected rise in fire activity due to climate change could have substantial future consequences. These results emphasise the critical need for implementing sustainable forest management strategies to mitigate the adverse effects of climate change on the boreal forests of eastern Canada.

Keywords: fire, climate, vegetation, *Picea mariana*, resilience, sustainable forest management

4.2 Résumé

Au cours des prochaines décennies, les pessières fermées du Canada devraient connaître une augmentation des températures et une intensification de l'activité des incendies en raison des changements climatiques, avec de nombreux impacts potentiels sur la dynamique de la végétation et, ultimement, sur le stockage du carbone et les activités économiques. Malgré cela, le nombre d'études portant sur l'est du Québec et du Labrador à l'échelle millénaire reste faible, et les recherches existantes n'ont pas exploré en profondeur les interactions entre les feux et la température dans le façonnement de la dynamique de la végétation. Par conséquent, notre compréhension de l'influence des fluctuations de température, de la fréquence et de la taille des feux sur la dynamique de la végétation reste limitée. Cette étude comble cette lacune en présentant trois enregistrements multi-indicateurs à haute résolution le long d'un transect nord-sud à l'aide de grains de pollen, de capsules céphaliques de chironomes et de macrocharbons, afin d'explorer les changements dans les interactions feu-climat-végétation au cours de l'Holocène dans ces régions. Grâce au partitionnement de variation et à des modèles additifs généralisés, nous discernons les impacts différentiels de la température et du feu sur le transect latitudinal. Notre analyse révèle des effets importants de la température de l'air en association avec la fréquence des incendies sur la dynamique de la végétation dans la toundra forestière de la côte du Labrador, et dans les pessières à mousses du sud-est du Québec. Inversement, l'influence de la température semble limitée dans les pessières à lichen de latitude intermédiaire. Néanmoins, ces variables, ainsi que leurs interactions, ont eu des effets variés sur l'épinette noire au cours du temps. Notre étude révèle notamment un impact croissant de la taille des incendies au cours des derniers siècles le long de notre transect, suggérant que l'augmentation prévue de l'activité des feux due au changement climatique pourrait avoir des conséquences importantes à l'avenir. Ces résultats soulignent la nécessité de mettre en place des stratégies de gestion forestière durable, afin d'atténuer les effets négatifs des changements climatiques sur les pessières fermées du Canada.

Mots-clés : incendie, climat, végétation, *Picea mariana*, résilience, gestion forestière durable

4.3 Introduction

Since the end of the 20th century, climate change has come to the forefront as one of the most significant challenges facing humanity (IPCC, 2022). The fast evolution of climatic conditions raises growing concerns worldwide, regarding its implications for biodiversity, biogeochemical cycles, and ecosystems sustainability (Thompson, 2009; FAO, 2012). While the most likely scenarios project a rise of approximately 4°C in mean global air temperature by the year 2100 (Capellán-Pérez et al., 2016), it is widely recognised that anthropogenic influences will disproportionately affect northern latitudes (Arrhenius, 1896; Holland and Bitz, 2003). In North American boreal ecosystems, this temperature rise could reach nearly 10°C (Gauthier et al., 2015), while precipitation is anticipated to increase by 20 to 30% (IPCC, 2022). The resulting rise in water stress and increased occurrence of lightning strikes (Janssen et al., 2023) is therefore expected to lead to enhanced wildfire activity (Flannigan et al., 2005; Wang et al., 2017; Wotton et al., 2017) in North American boreal landscapes.

However, changes in temperature and disturbance patterns resulting from shifts in climate conditions may serve as powerful catalysts for vegetation change (Flannigan et al., 2000; Baltzer et al., 2021). Specifically, high fire severity or short fire return intervals could jeopardise boreal forest resilience and gradually drive a transition towards deciduous tree dominance (Baltzer et al., 2021) or alternative stable states characterised by low tree density (Splawinski et al., 2019b). In Québec province, Girard et al., (2008) estimated that 9% of closed-crown spruce-moss forests transitioned to open conditions in the second half of the 20th century. Additionally, transitions from open-crown lichen woodlands to plant communities typical of forest tundra have been observed in northernmost ecosystems (Payette and Delwaide, 2018). In eastern Quebec and Labrador, long fire return intervals theoretically suggest reduced vulnerability to regeneration failures. However, the cold climate results in reduced seed viability (Sirois, 2000; Meunier et al., 2007), prolonged cone maturation, and increased difficulty in germination (Sirois, 2000), creating more challenging conditions for post-fire regeneration (Lavoie and Arseneault, 2001). Consequently, climatic conditions may play a major role in vegetation dynamics in these regions. To anticipate the potential future dynamics of boreal forests, it is therefore essential to

enhance our understanding of the interplay between fire regimes and climate on vegetation dynamics in eastern Quebec and Labrador.

Paleoecological records offer a unique opportunity to extend the temporal scope beyond historically documented data to encompass multimillennial timescales (Smol and Cumming, 2000; Battarbee et al., 2005; Rull, 2010). These records facilitate the exploration on how fire and temperature interact to influence vegetation dynamics across various geographical regions. Despite some studies conducted in eastern Quebec and Labrador (Remy et al., 2017a, 2017b; Feussom Tcheumeleu et al., 2023), existing research in eastern Canada has not fully examined the multifaceted interactions between fire and climate in affecting vegetation dynamics. The intricate nature of deciphering individual roles of each variable over time often leads to hypotheses on causality among different covariates, limiting the possible interpretations. In this context, variance partitioning (Borcard et al., 1992) may help identify the relative significance of different covariates in shaping vegetation dynamics across temporal scales. Nonetheless, this method solely provides the cumulative impact of each variable, precluding the precise identification of their temporal influence on changes in vegetation composition. Employing time-series analysis techniques (Simpson and Anderson, 2009) could offer enhanced understanding of the temporal and spatial dynamics of temperature and fire impacts on pollen assemblages. This approach enables the identification of particular periods when these factors influenced vegetation composition, as well as discerning periods of lesser importance. Furthermore, such techniques can help assess whether similar variables had a notable impact during corresponding periods across different latitudes. Underestimating the fire-climate-vegetation nexus therefore oversimplifies the complexity of the response of boreal forests to future changes (Gaboriau et al., 2023). This is especially important in a context where the effects of climate change spark discussions among scientists and policymakers, who strive to understand the forthcoming repercussions of temperature fluctuations and alterations in fire patterns on boreal forest dynamics. It is indeed essential for land managers and stakeholders to anticipate the impact of these changes, enabling the implementation of sustainable forest management

strategies that foster the long-term resilience of boreal ecosystems, with realistic targets and goals (Lindbladh et al., 2013).

In this study, we use three paleoecological records involving pollen grains, macrocharcoals, and chironomid head capsules along a north-south transect in eastern Québec and Labrador to reconstruct vegetation, fire history, and mean summer air temperature, respectively. Our study aimed to achieve two main objectives: (1) to disentangle the individual contributions of climate and fire to vegetation dynamics along our transect, and (2) to evaluate whether landscapes in eastern Canada have undergone substantial changes in recent centuries. We postulate that (1) temperature and fire frequency have a substantial influence on vegetation dynamics to the north of the transect, attributed to slow growth and reduced seed production, while fire regimes exercise the main role towards the south, and (2) contrary to their westernmost counterparts, the last few centuries in eastern Canada have not been marked by a decline in black spruce abundance due to long fire return intervals.

4.4 Material and methods

4.4.1 Study sites and current vegetation

For the purpose of this study, three freshwater lakes were selected along a Northeast-Southwest transect in eastern Québec province and Labrador (Figure 23). These lakes were chosen, among others, for their small area (<10 ha) and because they encompass varied vegetation zones, allowing a wide range of fire-climate-vegetation interactions to be covered. This latitudinal transect represents a climatic and vegetation gradient, extending from the subarctic woodlands and tundras on the Labrador coast to the eastern boreal forest of the northern shore of the St-Lawrence river in Quebec province (Baldwin et al., 2020, Figure 23). Blow Hole lake is located in the subarctic woodlands and tundras on the Labrador coast. The current flora comprises patches of black (*Picea mariana* (Mill.) B.S.P.) and white spruce (*Picea glauca* (Moench) Voss), often growing in stunted "krummholz" growth forms and

reproducing vegetatively. Tamarack (*Larix laricina* (Du Roi) K. Koch) is also present, with a shrubby birch (*Betula* spp.) understory associated to crowberry (*Empetrum nigrum* L.), blueberries and cranberries (*Vaccinium* spp.), fireweed (*Chamaenerion angustifolium* L.), and various species of mosses and lichens. Billy lake, is located at the transition between the northern boreal woodlands and the eastern boreal forests, in an open-canopy lichen woodland. Vegetation is largely dominated by black spruce, and to a lesser extend white spruce, birch, tamarack and balsam fir (*Abies balsamea* (L.) Mill.), in an open matrix dominated by lichens. Finally, hereafter *Petit Anne* lake, is located in the south-eastern boreal forests, in a closed-crown spruce-moss forest (Saucier et al., 2011). Black spruce is the dominant species, although balsam fir, white birch (*Betula papyrifera* Marsh.) and white spruce are also largely represented (Baldwin et al., 2020) due to the proximity of mixed white birch-balsam fir forest. The entire transect is characterised by long, cool winters and short, moist summers induced by the proximity of the Atlantic Ocean (Baldwin et al., 2020). A major temperature gradient is represented, with current mean summer air temperatures of around 9.7°C to the north of the transect and around 14.2°C toward the south (Table 8, Natural Resources Canada, 2010).

Table 8
Main characteristics of the three studied lakes and their respective climatic conditions.
Source : Ressources Naturelles Canada (2010).

	Blow Hole	Billy	Petit Anne
Latitude	56°31'25"N	53°04'60"N	49°50'14"N
Longitude	61°41'49"W	66°57'87"W	68°43'30"W
Elevation (m a.s.l.)	122	541	323
Surface area (ha)	7.0	9.7	9.1
Maximum water depth	4.8	3.8	2.4
Length of the sediment core (cm)	113	91	138

Fluvial inputs	Absent	Absent	Absent
Lakeshore (Flat/Abrupt)	A	F	A
Closest weather station (distance in km)	NAIN A (3.05)	WABUSH LAKE A (23.79)	BAIE-COMEAU A (86.97)
Summer air temperature in °C in June/July/August (mean)	6.4/10.1/11.0 (9.7)	10.3/13.8/12.5 (12.2)	12.4/15.6/14.7 (14.2)
Mean annual precipitation in mm	925.4	839.5	1001.0

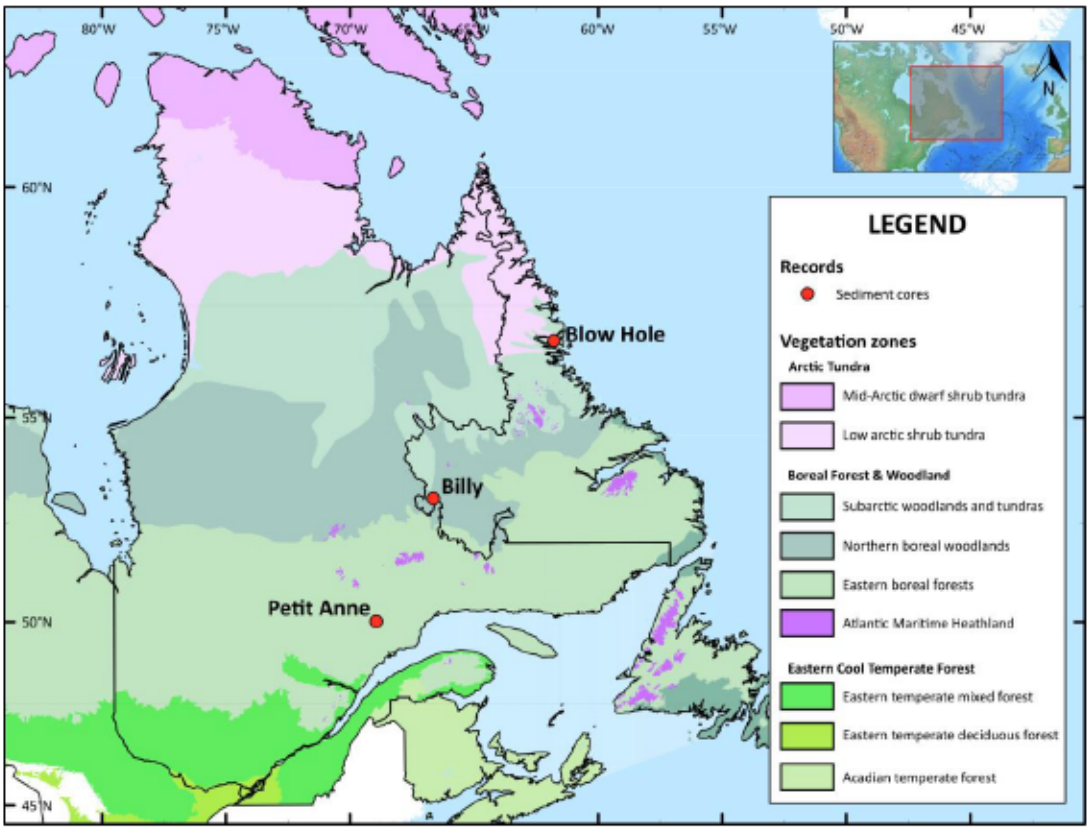

Figure 23
Location of the study sites across the vegetation zones of Canada in Québec and Newfoundland-and-Labrador provinces.
Source : Baldwin et al., (2020).

4.4.2 Sediment sampling and chronologies

Short sediment cores were retrieved at the deepest point of the three lakes in August 2019 using a 9-cm diameter Uwitec gravity corer. Once extracted, sediment cores were stored in plastic tubes and kept in cold conditions (4°C) until further analyses. The chronology of each site was established on a two-step dating method. The upper 10 cm of sediments were measured for ^{210}Pb and ^{137}Cs activities (Le Roux and Marshall, 2011), and a Constant Rate of Supply (CRS) model was applied to obtain an accurate chronology during the last 150 years (Appleby et al., 1979). The remaining sediments were dated by ^{14}C accelerator mass spectrometry (AMS) based on terrestrial plant macroremains. Each dated level was calibrated at 2σ (Table 9) using the IntCal20 Northern Hemisphere Radiocarbon Age Calibration Curve (Reimer et al., 2020) to obtain calibrated ages before the present (hereafter yr cal BP). Bayesian age-depth models were developed using dated levels, and ages interpolated at contiguous 0.5-cm depth intervals using the 'rbacon' package v.3.1.1. (Blaauw et al., 2021) in R environment version 4.3.2 (R Core Team, 2023).

Table 9
Radiocarbon (^{14}C) age determination for sites Blow Hole, Billy and Petit Anne. Radiocarbon analyses were performed both at the Poznań Radiocarbon Laboratory at Poznań, Poland, and at the Radiochronology Laboratory of the Centre d'Étude Nordique (CEN) at Laval (QC), Canada

Core	Depth in record (cm)	Type	Sample number	Age 14C (year BP)	Range of calibration (yr cal BP; 2σ)
Blow Hole	20.5	Needles, wood	BLH 20-21	1800 ± 30	2208 (2225-2297)
Blow Hole	53.5	Needles, wood	BLH 53-54	3795 ± 35	4181 (4084-4295)
Blow Hole	70.5	Charcoals, needles	BLH 70-71	4815 ± 15	5557 (5482-5530)
Blow Hole	93.5	Wood	BLH 93-94	6205 ± 15	7084 (7008-7133)
Blow Hole	109.5	Needles and wood	BLH 109-110	6910 ± 40	7739 (7669-7838)

Billy	13.5	Needles, charcoals	BIL 13-14	415 ± 15	494 (471-508)
Billy	35.5	Bryophytes	BIL 35-36	1715 ± 30	1602 (1536-1635)
Billy	55.5	Bryophytes	BIL 55-56	2735 ± 35	2823 (2759-2883)
Billy	75.5	Bryophytes	BIL 75-76	4040 ± 15	4475 (4438-4475)
Billy	81.5	Bryophytes	BIL 81-82	4510 ± 15	5149 (5052-5193)
Petit Anne	21	Charcoals, wood	PEA 20-22	355 ± 15	388 (318-381)
Petit Anne	65.5	Needles	PEA 65-66	1585 ± 15	1562 (1569-1632)
Petit Anne	75.5	Needles	PEA 75-76	2160 ± 30	2150 (2047-2182)
Petit Anne	130.5	Needles	PEA 130-131	3315 ± 15	3526 (3484-3568)

4.4.3 Mean summer air temperature inferences

We used chironomid-based mean summer (June, July, August) air temperatures, previously published by Lesven et al., (*in prep.*) at the three study sites, as a climate proxy. Summer temperatures were inferred using a tolerance weighted average-partial least square model with two components, with P-spline frequency correction of the training set climate variables (fxtWA-PLS) (Liu et al., 2023). Pseudo-removed leave-out cross-validation (999 permutations) was used to evaluate model performance statistics, and yielded a root mean square error of prediction of 1.59°C, a maximum bias of 4.97°C, with a R^2 of 0.89. Finally, summer temperatures were smoothed using a loess regression (span = 1500 years) for comparison with reconstructed fire and vegetation histories.

4.4.4 Pollen analysis

Samples of about 1 cm^3 were retrieved from the sediment cores at 1- to 2-cm intervals, in order to reach a high temporal resolution (usually <100 years). Sediment samples were chemically treated following a standard protocol for terrestrial samples to extract

palynomorphs, and a known number of exotic spores (*Lycopodium clavatum* L.) added to each sample. This protocol included long chemical attacks with hydrofluoric and hydrochloric acids, digestion of organic matter using sodium hydroxide, 200-µm coarse sieving, and acetolysis coloration. Each sample was then mounted between slide and moving rectangular coverslips in a drop of glycerol. To avoid distribution bias induced by palynomorph size in the slide (Gottardini et al., 2009), a minimum of two scans (one at the center and one at the edge of the coverslip) was realised. Palynomorphs were identified using a light microscope at x400 magnification, with the help of the reference collection of the Chrono-environnement laboratory (UMR 6249 CNRS-UFC) and various palynological guides (Beug, 1961; Richard, 1970; McAndrews, 1973; Reille, 1995). Although previous studies have shown that 150 to 300 pollen grains are considered as statistically representative of assemblages (Djamali and Cilleros, 2020), a minimum of 500 pollen grains and 100 *Lycopodium clavatum* spores were counted on each slide to obtain the most accurate representation of the pollen rain (Chevalier et al., 2020).

4.4.5 Fire regime reconstructions

Samples of about 1 cm^3 were retrieved at regular 1-cm intervals from the three studied sediment cores, with the exception of the first 10 cm, which were sampled every 0.5 cm. Each sample was chemically treated, sieved, and the residual macrocharcoals counted and their area measured using the protocol described by Lesven et al., (2022). From these datasets, fire events were detected for each series using the 'tapas' package v.0.1.3 (Finsinger and Bonnici, 2022), by separating high- and low-frequency components (Higuera, 2009). This process includes the interpolation of macrocharcoal datasets to the median temporal resolution of the samples to avoid the impact of changes in sedimentation rates over time (Gavin et al., 2006), and decomposition of the records in charcoal peaks and background by applying a LOWESS-smoother technique robust to outliers, with a smoothing window varying within records between 300 and 750 years. Charcoals peaks were then evaluated using a Gaussian mixture model corresponding to the 95th percentile of the modelled

noise distribution (Higuera, 2009). Once fire events were detected at each site, local fire frequencies were reconstructed using a kernel density function (Mudelsee et al., 2004; Ali et al., 2012) based on a 500-year defined bandwidth, using a modified version of the 'paleofire' package v.1.2.4 (Blarquez et al., 2014). We then reconstructed at each site the amount of biomass burnt using the same package, by rescaling initial CHAR values using a min-max transformation, homogenising the variance using a Box-Cox transformation, and rescaling the series to z-scores (Power et al., 2008). Finally, fluctuations in fire size through time were assessed from the ratio between biomass burnt and fire frequency, from which a constant equal to 1 was added (Ali et al., 2012).

4.4.6 Numerical analysis

All numerical analyses were performed using R environment version 4.3.2 (R Core Team, 2023).

4.4.6.1 Stratigraphic diagrams and clustering

For each core, relative abundance stratigraphic diagrams were produced using the 'rioja' package v.1.0-5 (Juggins and Juggins, 2020), in order to enable visual interpretation of the pollen records. Statistically significant pollen assemblage zones (PAZ) were then identified on Hellinger-transformed abundance data using constrained incremental sum of squares (CONISS) clustering (Grimm, 1987), and assessed by a broken stick model (Bennett, 1996).

4.4.6.2 Statistical analyses of climate-fire-vegetation interactions

To assess relationships with vegetation changes over time at each site, fire variables and smoothed summer temperatures were firstly interpolated at the same temporal resolution as pollen data. Only indigenous (*i.e.* currently represented in the neighboring vegetation of the lake) pollen taxa were considered in the analysis, excluding spores from pteridophytes, bryophytes and fungi because (1) their

occurrence is more often related to hydrological variables rather than fire or temperature (Fenton and Bergeron, 2006), and (2) their identification is generally possible only to low taxonomic level therefore limiting interpretations. To assess the individual and joint contribution of temperature and fire variables on pollen assemblages at each site, we determined the percentage of variance of the Hellinger-transformed abundance data (Legendre and Gallagher, 2001) explained by each environmental variable alone or in combination, based on partial redundancy analysis (RDA, Ter Braak and Prentice, 1988). This variance partitioning was made using the 'vegan' package (Borcard et al., 2018), and Euler diagrams were computed to visualise the results using the 'eulerr' package v.7.0.1 (Larsson et al., 2016). Patterns of pollen assemblage changes throughout the three cores were summarised at each site using a principal component analysis (PCA), performed on Hellinger-transformed pollen abundances, with environmental variables (summer temperatures, fire frequency and fire size) projected on the ordination plots. PCA and RDA were computed using the 'vegan' package v. 2.6-4 (Oksanen, 2015). Samples scores along PCA axis 1 (PC1) were extracted for subsequent modelling.

Generalised additive models (GAMs) were used because they allow the consideration of nonlinear relationships between an independent variable and multiple predictors (Wood, 2017), as this is the case for our study. PC1 scores of pollen samples were considered as the response variable for each tested GAM. To select the best model for each dataset, different GAMs including zero (null model), one, two and three environmental variables, all with or without interactions between them, were compared. Model performance was evaluated based on five selection criteria (Root Mean Square Error, Aikaike information criterion, Generalised Crossed Validation score, deviance explained and adjusted R^2). Each model was assigned a rank based on its performance relative to all tested criteria. Ranks were then summed, and the model associated to the lowest sum identified as exhibiting the best overall performance. Finally, we assessed the relative contribution of the three variables tested to the variation of PC1 scores, using a procedure similar to that of Simpson and Anderson (2009). This procedure involves the extraction of the specific contribution of

each variable to the GAM estimates, in order to assess the temporal and spatial variability of the response across our study transect.

4.5 Results

4.5.1 Dynamics in vegetation, fire and climate

4.5.1.1 Blow Hole

At Blow Hole, 47 pollen morphotypes were identified, among which 27 are considered as currently indigenous (*i.e.* currently represented in the neighboring vegetation of the lake). As displayed in the pollen diagram (Figure 24), sixteen taxa (excluding undetermined and unidentifiable) reached at least once a relative abundance of 1%.

The stratigraphically constrained cluster analysis of the pollen record indicated six significant pollen assemblage zones (PAZ1 to PAZ6, Figure 24). PAZ1 (*ca.* 8000-7500 yr cal BP) displayed a postglacial landscape with low temperature, dominated by herbaceous tundra, primarily consisting of herbs (Cyperaceae, Poaceae, Artemisia, Caryophyllaceae), dwarf shrubs (Ericaceae), and shrub taxa including *Salix*, *Betula*, and *Alnus alnobetula* ssp. *crispa*. These taxa decreased in abundance during the continuously cold period of PAZ2 (*ca.* 7500-7100 yr cal BP), with the exception of *Alnus alnobetula* ssp. *crispa* which registered a sharp increase, and *Betula*, which followed the same trend and peaked at around 60% relative abundance. *Picea mariana* and *Picea glauca* were almost not represented in the assemblage. Summer temperature then slightly increased in PAZ3 (*ca.* 7100-5900 yr cal BP), period during which *Betula* declined markedly, *Alnus alnobetula* ssp. *crispa* reached its maximum abundance (~76%), while herbaceous taxa reached their minimum in this zone. Concurrently, *Picea mariana* started to increase, reaching ~4% relative abundance, and then ~13% in PAZ4 (*ca.* 5900-4500 yr cal BP), during which summer temperature did not change compared to PAZ3. *Alnus alnobetula* ssp. *crispa* decreased in abundance in this zone, *Betula* displayed a second increase (~30% relative abundance), while herbaceous taxa remained in low proportions during this period. At the beginning of PAZ5 (*ca.* 4500-800 yr cal BP), *Picea mariana* showed a sharp

increase and reached a maximum (~22% relative abundance), while *Alnus alnobetula* ssp. *crispa* and *Betula* stabilised at around 50% and 15% relative abundance, respectively. This period was marked by a sharp increase in temperature, coinciding with a peak in fire frequency to three fires per millennium. *Picea glauca*, although poorly represented, also reached its maximum abundance during this period. PAZ5 was also marked by an increase of *Picea glauca* and taxa currently non-represented in the forest tundra of the Labrador such as *Abies balsamea*, *Pinus strobus*-type or *Alnus incana* ssp. *rugosa*. Finally, similarly to temperature and fire frequency, *Picea mariana* declined sharply at the end of PAZ5. At the same time, fire size began to increase rapidly. *Picea mariana* then stabilised at *ca.* 10-12% relative abundance in PAZ6 (*ca.* 900 yr cal BP to present) when temperature reached its lowest values such as fire frequency, while *Betula* and herbaceous taxa were marked by a notable increase. Opposingly, fire size reached its highest values of the record.

4.5.1.2 Billy

At Billy, a total of 37 pollen morphotypes was identified, among which 21 are currently indigenous. As displayed in the relative abundance pollen diagram, 12 taxa (excluding undetermined and unidentifiable) reached at least once a pollen percentage of 1% (Figure 24). This sequence covers the period from *ca.* 5500 yr cal BP to present.

The broken-stick model associated to the clustering revealed four significant zones, with relatively stable vegetation throughout the record. PAZ1 (*ca.* 5500-5250 yr cal BP) was largely dominated by *Picea mariana* (~50% relative abundance) and *Betula* (~35% relative abundance). *Abies balsamea* and *Alnus alnobetula* ssp. *crispa* were also represented in elevated proportions, along with herbs (Poaceae, Cyperaceae) in lesser proportions. Fire frequency was particularly low during this period, while fire size was the highest of the record. PAZ2 (*ca.* 5250-3600 yr cal BP) was characterised by an increase in fire frequency and a decrease in fire size, while temperature fluctuated between 12 and 13.5°C. This period was marked by a sharp decline in *Betula* relative abundance (from ~35 to 24%), while *Picea mariana* increased sharply,

from 50% to 70% relative abundance. *Abies balsamea* declined steadily in this zone, and then in PAZ3 (*ca*. 3600-1500 yr cal BP). In this third zone, *Betula*, *Picea glauca* and *Picea mariana* displayed minimal fluctuations. Conversely, *Alnus alnobetula* ssp. *crispa* and *Myrica gale* increased slightly in abundance, although they remained well less represented. In this zone, fire frequency began to increase to reach ~3 fire per millennium, while fire size reached its lowest values. Finally, PAZ4 (*ca*. 1500 yr cal BP to present) was marked by a gradual decline in temperature and in *Picea mariana* abundance, from ~70% to 57%, and *Abies balsamea*, from ~6 to 3%. Conversely, *Alnus alnobetula* ssp. *crispa* and exotic taxa increased sharply in abundance, while birch remained relatively stable compared to PAZ3. Interestingly, fire frequency and fire size reached high values during this period.

4.5.1.3 Petit Anne

At Petit Anne, a total of 46 different pollen morphotypes was found, among which 29 are currently indigenous. 16 pollen morphotypes reached a percentage of at least 1%, with 12 of them belonging to indigenous species (Figure 24). This sequence spans from *ca*. 3600 years ago to today.

Three pollen zones were distinguished by the clustering. PAZ1 (*ca*. 3629-2200 yr cal BP) was largely dominated by *Betula* (33-61% relative abundance) and *Picea mariana* (17-34% relative abundance), which varied markedly. *Abies balsamea*, *Alnus incana* spp. *rugosa* and *Picea glauca* were also well represented in the diagram, although the latter is not currently present in the study area. Summer temperature was the warmest of the record during this period (14.5-16.6°C), which was marked by a moderate fire frequency (3.2-4.7 fire per millenium). Then, *Picea mariana* gradually increased in abundance (from ~26 to 40% relative abundance) in PAZ2 (*ca*. 2200-700 yr cal BP), while *Betula* followed the opposite trend, dropping from around 45% to 30%. The other taxa remained relatively stable over time during this period which was marked by a progressive decrease in temperature and an increase in fire frequency. Finally, similarly to PAZ2, PAZ3 (*ca*. 700 yr cal BP - today) was characterized by a pronounced

decrease in *Betula* and an increase in *Picea mariana* relative abundance. At the same time, *Alnus incana* spp. *rugosa* and Poaceae increased sharply in abundance. In this zone, temperature reached progressively its lowest values, while fire frequency reached opposingly its highest values (5.5 fire per millennium). Finally, the last centuries of the record were marked by a sharp increase in fire size.

4.5.2 Partitioning the effects of fire and climate

Partitioning highlights considerable differences in how environmental variables (climate and fire) accounted for fractions of the variation in pollen assemblages among the three sites (Figure 25). At Blow Hole, fire frequency accounted for the largest fraction of the variation (34.5% in total, with 18.8% shared and 15.7% uniquely), followed by summer temperatures (20.7% in total, with 14.7% shared and 6% uniquely), and finally by fire size (15% in total, with 9.5% shared and 5.5% uniquely). Fire frequency and summer temperature jointly explained 9.3% of the variance, compared with 4.1% for fire frequency and fire size. Finally, the three variables together explained 5.4% of the variation in pollen composition. Similar to Blow Hole, fire frequency accounted for the main part of the variation in the pollen matrix at Billy (20.4% in total, with 11.3% shared with fire size). Fire size explained a total of 18.1% of the variance in the data, of which only 0.2% was shared with summer temperature. Finally, summer temperature explained the smallest fraction of the variation (only 0.6% in total, with 0.4% uniquely). At Petit Anne, partitioning of variation showed that summer temperature account for the largest fraction of the variation (19% in total, with 9.1% shared and 9.9% uniquely), followed by fire frequency (10.8% in total, with 6.5% shared with summer temperature and 4.3 uniquely), while fire size only account for 4.5% of the variation in the pollen matrix (2.6% shared with summer temperature, and 1.9% uniquely). It is interesting to note that the greater the chronological range, the smaller the unexplained variation.

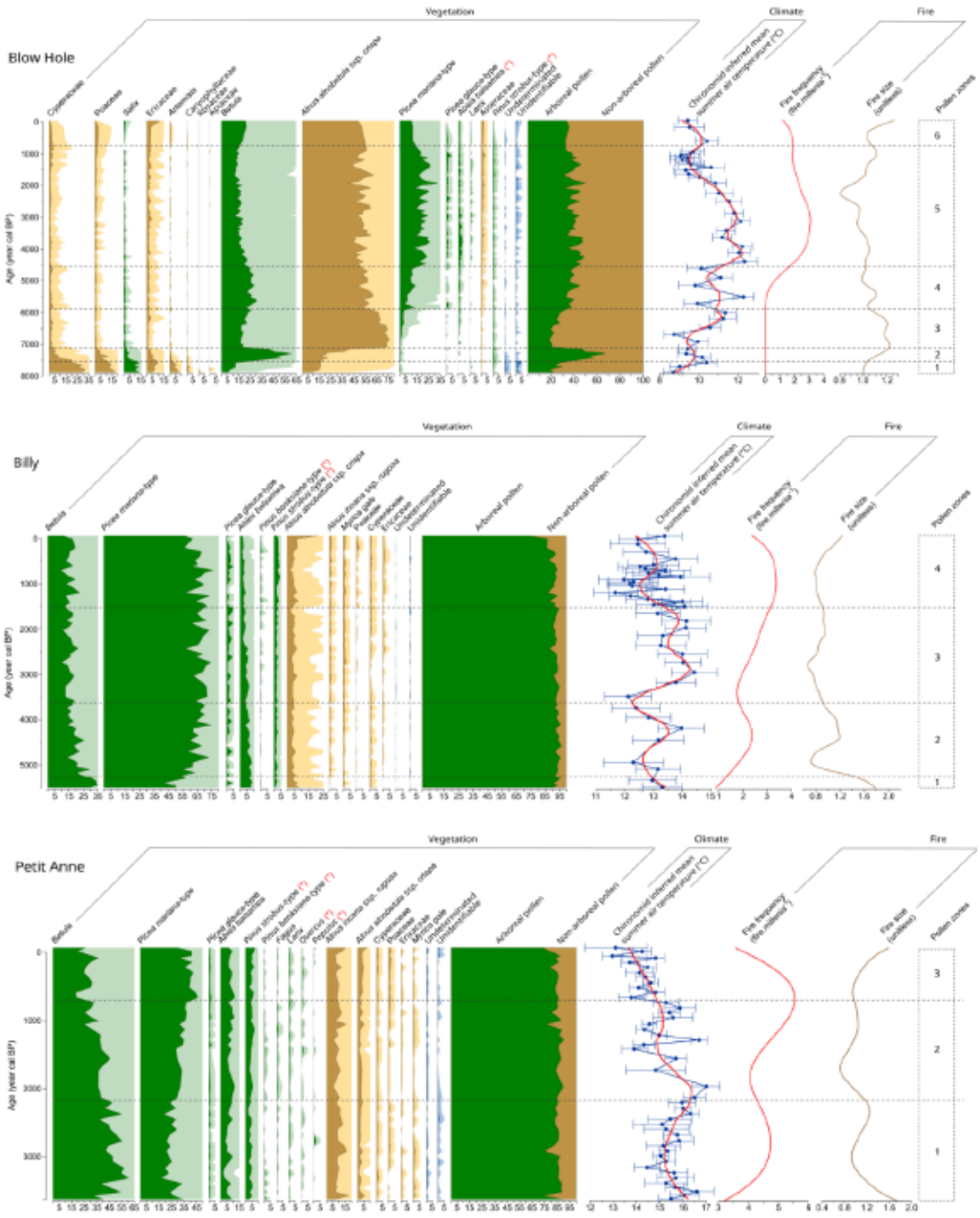

Figure 24
Simplified pollen diagrams for Blow Hole, Billy and Petit Anne, respectively, with their pollen assemblage zones. Pollen grains not currently represented

near the study site are indicated by a red asterisk. Arboreal taxa are represented in green, non-arboreal taxa in brown, each with their exaggeration curve (factor 5). Summer air temperature from chironomid assemblages is shown in blue with its sample-specific errors of prediction using 999-boostrap cycles, with a LOWESS smoothers in red (span = 1500 years). 500-year smoothed fire frequencies (fires per millennia) and fire size are represented by red and brown solid curves, respectively.

4.5.3 Ordinations

All ordinations were carried out with climate and fire variables considered as passive, as well as age. According to the series of PCAs, pollen assemblages and their relationships with environmental variables varied widely within our transect.

At Blow Hole, the ordination revealed that PC1 summarised well the major pollen assemblage changes and represented 58.1% of the variance in pollen assemblages, while the second axis captured 22.2% (Figure 26). Sample scores follow an inversed U-shape trajectory over time, with samples associated with strongly positive PC1 scores up to ca. 7100 yr cal BP, characterised by assemblages typical of herbaceous tundra (Cyperaceae, Poaceae, *Artemisia*, Ericaceae, *Salix*) followed by a broad dominance of *Betula*. After *ca*. 7100 yr cal BP, the assemblages shifted towards almost null PC1 scores associated with elevated abundance of *Alnus alnobetula* ssp. *crispa*. Then, PC1 scores evolved towards strongly negative values *ca*. 4500 yr cal BP associated with *Picea mariana* up to the present period, except the most recent 1300 years which were marked by a return towards null values. Fire size correlated positively with *Betula* and PC1, but express more along PC2. Conversely, *Picea mariana*, fire frequency and summer temperature express along the negative values of PC1 and PC2, thus showing an overall increase in fire frequency and summer temperature over time, but a decrease in fire size.

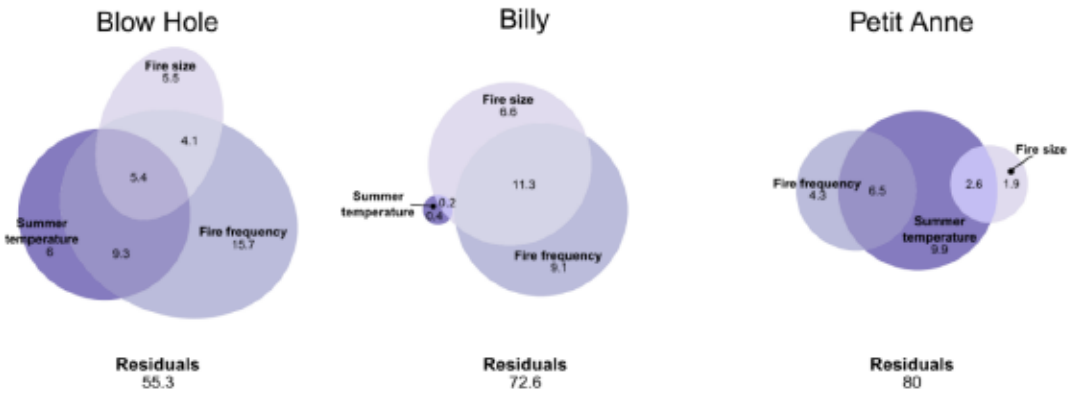

Figure 25
Partitioning of variation across the three explanatory variables displayed as area-proportional Euler diagrams. Values in the ellipses are the percentage of variation for each fraction.

At Billy, the ordination showed that PC1 captured 35.1% of the variance in pollen assemblages, while PC2 accounted for 17.1% (Figure 26). Sample scores followed a general trend from negative values along which *Betula* and *Abies balsamea* express, towards positive values characterised by *Picea mariana* after *ca.* 4200 yr cal BP. *Betula* and fire size were strongly positively correlated and showed higher values in the first period of the chronosequence. The relative abundance of *Betula* and *Abies balsamea* therefore decreased over time, whereas that of *Picea mariana* tended to increase. As fire frequency was positively correlated with PC1, the ordination showed an overall increase in fire frequency over time.

Finally, the ordination of Petit Anne showed that PC1 explained 48.7% of the variance in pollen assemblages, compared with 12.1% for PC2 (Figure 26). Samples scores followed a general evolution from negative to positive values, shifting between *ca.* 2100 and 1300 yr cal BP. *Picea mariana* and fire frequency were positively correlated to positive values of PC1, contrary to *Betula* and summer temperature, therefore suggesting an overall decrease in *Betula* and an increase in *Picea mariana* over time. Fire size expressed along negative values of PC2, and show a strong positive correlation with *Alnus incana* ssp. *rugosa*.

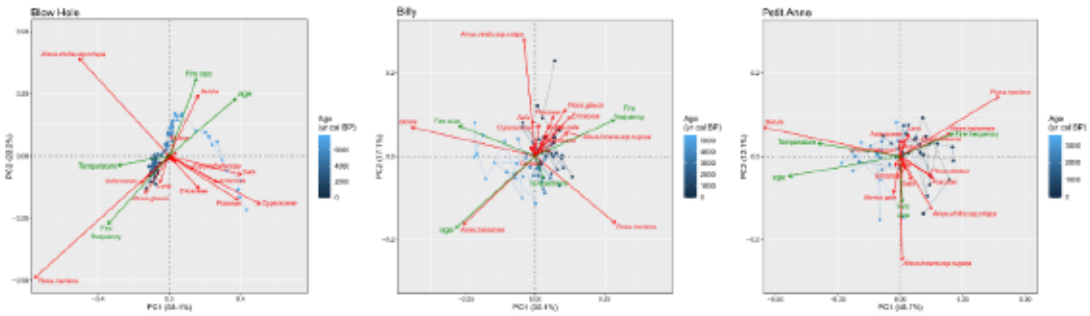

Figure 26
Principal component analysis depicting the relationships between pollen assemblages, summer air temperature, fire frequency, fire size and age. Only taxa with the most extreme PCA spores are represented to facilitate ecological interpretations. Observed trajectories are represented in shades of blue.

4.5.4 GAM selection and marginal effects of environmental variables

Among the tested models, those who performed best consistently incorporated all three variables to quantity the influence of fire regimes and climate on PC1 scores across the three sites. Interestingly, the best model differed across the study sites. For Blow Hole and Billy, it encompassed all three variables along with their interactions, whereas for Petit Anne, the model comprising the three variables without interactions yielded the best performances.

At Blow Hole, PC1 scores showed highly positive values from the start of the recording to *ca.* 6300 yr cal BP (Figure 27). The separation of marginal effects of each variable showed a positive effect of summer temperature and fire frequency up to this period, similarly to PC1 scores, suggesting a strong relationship between these variables. From this period until *ca.* 4500 yr cal BP, PC1 scores remained close to zero, before turning negative until today. Summer temperature showed a negative contribution to PC1 scores until *ca.* 2000 yr cal BP, underlining the importance of temperature in explaining pollen assemblages at this latitude. From *ca.* 4500 yr cal BP, the contribution of fire frequency displayed negative values until today, such as PC1 scores, also underlining its important contribution. Then, from *ca.* 2000 yr cal BP, the contribution of summer temperature shifted to positive values. Fire size always showed an opposite contribution to PC1 scores along the sequence, except from *ca.*

3500 to 1800 yr cal BP, and over the most recent period. This suggests that fire size plays a more important role in explaining PC1 scores than at the beginning of the sequence.

At Billy, the effect of fire frequency and fire size showed the greatest amplitude of variation, while that of summer temperature was much lower (Figure 27). Throughout the sequence, PC1 scores changed gradually from strongly negative to slightly positive values after *ca.* 4000 yr cal BP. Fire frequency and fire size showed a relatively similar pattern, suggesting a strong relationship between fire regimes and vegetation dynamics in the open-canopy lichen woodlands. The main differences between fire frequency and fire size appeared between *ca.* 4700 and 2700 yr cal BP, with scores alternating between positive and negative, but always remaining close to zero. In parallel, summer temperature showed a more complex contribution, alternating widely between positive and negative values throughout the sequence. Its positive relationships with PC1 scores are mainly situated between *ca.* 3800 and 1500 yr cal BP, as well as over the recent period.

At Petit Anne, PC1 scores exhibited a transition from null to negative values between *ca.* 3600 and 3200 yr cal BP, followed by a steady increase throughout the sequence, with scores nearing zero between *ca.* 2100 and 1300 yr cal BP (Figure 27). summer temperature displayed a relatively similar trend, indicating a positive correlation with PC1 scores across most of the sequence. Fire frequency demonstrated a similar pattern, although its contribution notably became predominantly negative over the recent period, implying a decreasing importance over the last few centuries. Conversely, fire size presented an opposite trend in its contribution to PC1 scores, except for the recent period where its influence appeared to have intensified compared to earlier periods.

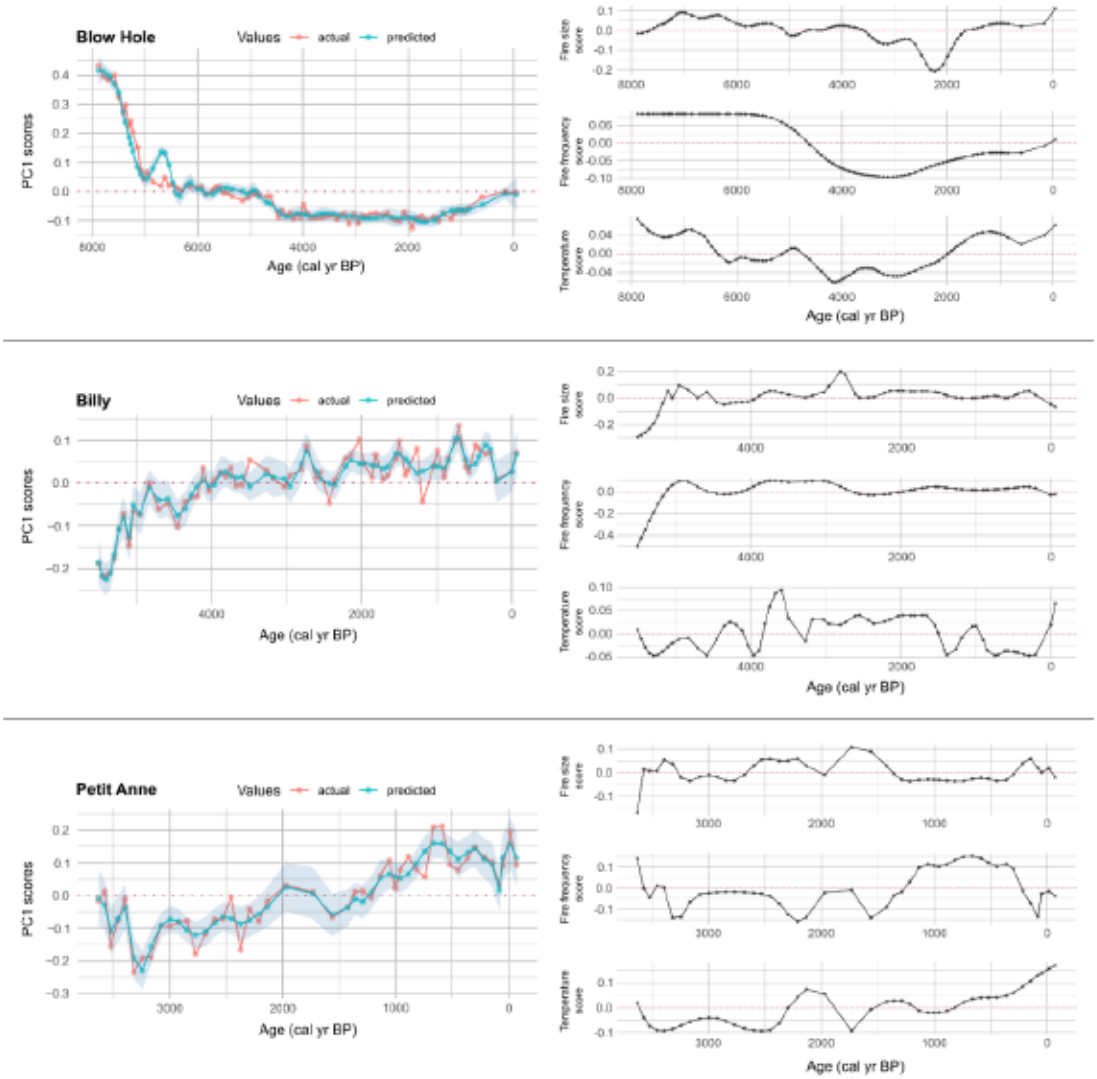

Figure 27
Temporal dynamics of the contribution of the three environmental variables to PC1 score estimates of each study site. Left panels represent observed and predicted values of PC1 scores, right panels refer to the contribution of three proxy used.

4.6 Discussion

4.6.1 Latitudinal variability of fire-climate-vegetation interactions in eastern Quebec and Labrador

Undoubtedly, summer temperature, fire frequency and fire size represent major drivers of vegetation dynamics in eastern Québec, Labrador and elsewhere (Ali et al., 2009b; Remy et al., 2017b; Feussom Tcheumeleu et al., 2023). Our results partially support our first hypothesis, indicating that air temperature represent a key driver of vegetation dynamics in the forest tundra of the Labrador coast. However, forest fires have been proved to also play a pivotal role (Figure 25), despite their low frequency in these environments. Ecosystems near the treeline are known for their high sensitivity to temperature fluctuations (Sirois, 2000; Lloyd et al., 2005). The interplay between summer temperature and fire frequency thus emerges as a pivotal factor driving vegetation dynamics during warm periods (Figure 26 and 27). A pronounced rise in *Picea mariana* abundance during the Holocene Thermal Maximum (*ca*. 4500-3200 yr cal BP, Lesven et al., *in prep.*) indicated conditions highly conducive to its development, contributing to a gradual densification of the treeline. This trend is corroborated by findings from the western Quebec treeline region between *ca*. 4000 and 1500 yr cal BP, where similar warm conditions and increased fire frequencies were observed (Gajewski, 2019; Gajewski et al., 2021). The increased abundance of *Picea mariana*, known for its high flammability (Rogers et al., 2015), in conjunction with the warm and dry conditions of the Holocene Thermal Maximum likely increased fire ignition, leading to more frequent fires than previously recorded (Figure 24). *Picea mariana* exhibits serotinous cones, using wildfires as a means of reproduction under favorable climatic conditions (Splawinski et al., 2022). This increase in fire frequency induced a positive feedback on *Picea mariana* abundance (Remy et al., 2017a), promoting its densification in these northern environments.

However, these conditions appear to shift during colder intervals, particularly over the last 1300 yr cal BP. Within this interval, the influence of summer temperature on vegetation dynamics was relatively low (Figure 27). Conversely, fire frequency, and to a lesser extent fire size, emerged as the predominant factors driving these dynamics (Figure 27). Indeed, despite the temperature decline which did not strongly alter

vegetation dynamics, *Picea mariana* can persist during cold periods through vegetative reproduction by layering. However, fire likely played a pivotal role. Despite the infrequent nature of fires during this period, their increasing size likely contributed to removing *Picea mariana* in the landscape, leading to a gradual decline in its abundance over time (Asselin and Payette, 2005; Gajewski, 2019). These findings corroborate the deforestation hypothesis proposed by Payette and Gagnon (1985), suggesting that fire events in the forest tundra led to landscape opening under suboptimal conditions. Conversely, this opening of the forest tundra appeared to favor early-successional taxa such as *Betula* and *Alnus alnobetula* ssp. *crispa* (Gajewski et al., 2021), owing to their enhanced dispersal and reproductive capabilities even during colder periods.

Surprisingly, our study shows that the influence of temperature on vegetation dynamics does not linearly decrease across the latitudinal spectrum studied. Indeed, our findings reveal that summer temperature also played a major role towards the south of our transect (Petit Anne site), where we hypothesised their impact was minor. Interestingly, this relationship appears less pronounced in ecosystems at intermediate latitudes (Figure 25). At Petit Anne site, our results show that the coldest period of the record was particularly favorable to the development of *Picea mariana*, during which fire frequency was the highest of the record (Figure 26 and 27). However, summer temperature appeared to play the most important role during this period (Figure 27). Indeed, the gradual decrease in temperature characteristic of the Neoglacial period induced a progressive coniferization of the landscape due to cold climatic conditions, while broadleaf taxa were particularly disadvantaged. This gradual decline in broadleaf taxa in favour of serotinous conifers has also been shown in similar environments in both western (Fréchette et al., 2018) and eastern Quebec (Feussom Tcheumeleu et al., 2023). This transition to an environment characterised by high *Picea mariana* values likely led to a progressive rise in fire frequency, potentially inducing a positive feedback due to its high flammability (Remy et al., 2019). The limited fire size along all the record may also be related to the uneven topography of eastern Québec, favoring fire ignition but limiting their spread over large areas (Parisien and Moritz,

2009; Remy et al., 2017a). In contrast, the warmest period of the record was marked by the highest abundance of deciduous taxa such as *Betula* or *Alnus incana* ssp. *rugosa*, and the lowest fire frequencies. During this period, summer temperature and fire frequency were the main forcings of vegetation dynamics. More particularly, warm summer temperature and moderate fire frequency during this period favored the development of deciduous trees such as *Betula* spp. in the landscape surrounding Lac Petit Anne. Particularly, *Betula papyrifera* might have been favored in post-fire environments (Gajewski et al., 1993), therefore contributing to its high representation.

However, in the open-crown lichen woodlands in the mid-latitudes of our transect (Billy site), the variance partitioning indicated a minimal influence of summer temperature on vegetation, implying that wildfires predominantly drive long-term vegetation trajectories in these regions, as recently suggested by Remy et al., (2017b) close to our study site. Nonetheless, the authors suggested that fire size rather than fire frequency exert a pronounced influence on changes in forest composition. Given that our dataset enables to disentangle the contribution of fire frequency and size on vegetation dynamics, it provides new insights into the trajectories of vegetation in the lichen woodlands of eastern Quebec and Labrador. Fire size was the most explanatory factor at the beginning of the record, suggesting that this variable played a pivotal role in shaping vegetation dynamics during this period (Figure 27). The prevalence of high *Betula* values towards the end of the Holocene Thermal Maximum had been previously noted by Remy et al., (2017b) in close proximity to our study site, indicating that large fires during this period likely facilitated landscape opening and subsequently fostered *Betula* development (Gajewski et al., 1993). Indeed, broadleaf tree species are typically found in young stands regenerated after fire, mostly *Betula papyrifera* (Foster and King, 1986), which is strongly represented in our study area (Baldwin et al., 2020). After *ca*. 5200 yr cal BP, the increased *Picea mariana* abundance appeared to be predominantly driven by both fire frequency and size (Figure 27). More specifically, the rise in fire frequency and decline in fire size from this period suggests that numerous small fires favored *Picea mariana* over *Betula*. The gradual decrease in fire-intolerant *Abies balsamea* over time further underscores the influence of forest

fires on vegetation dynamics. This decline is attributed to the regional shift away from fire-intolerant *Abies balsamea* stands, supplanted by *Picea mariana* that is more prone to fire (de Lafontaine and Payette, 2010, 2012). Surprisingly, Remy et al., (2017b) found that its decrease was more linked to increased fire size, underlining the fact that further studies in these regions are needed to better understand the drivers of vegetation dynamics. These conditions characterised by high fire frequencies and small fires persisted until recent times, with both fire variables making a substantial contribution (Figure 27). The poor influence of summer temperature on vegetation may be explained by the fact that these ecosystems are situated well further south than the treeline, in environments where temperature is not constraining for the sexual reproduction of *Picea mariana*. Concurrently, they are located within environments sufficiently northern to limit the expansion of deciduous trees, enabling the predominant growth of conifers. We hypothesize that the combination of these conditions, characterised by moderately cold temperature, results in a muted response to temperature fluctuations within these ecosystems, whose dynamics are predominantly governed by disturbance regimes and particularly fire (Splawinski et al., 2019a).

4.6.2 Recent changes in vegetation trajectories and fire regimes

Several studies have drawn attention to the recent opening of boreal forests in western and central Quebec, attributed to a diminished resilience stemming from increasing disturbance regimes (see (Asselin and Payette, 2005; Girard et al., 2008; Splawinski et al., 2019a). These changes are typically characterised by a decrease in the relative abundance of trees, notably *Picea mariana*, alongside a general increase in herbaceous and shrubby species as evidenced by pollen records (Gajewski et al., 2021), and a general rise in exotic species in sediment records (Remy et al., 2017b). Although the vegetation of eastern Quebec has received far less attention, the longer fire return intervals in eastern Quebec and Labrador may imply greater resilience due to less frequent disturbances. Consequently, recent declines in tree cover in our records should not be observed.

Towards the north of our transect, Blow Hole record reveals a substantial *Picea mariana* decline from *ca*. 1300 yr cal BP. As previously discussed, this is induced by decreasing Neoglacial temperatures and probably associated with the large fire size during this period, eliminating trees incapable of regenerating post-fire. However, a second increase in the fire size, surpassing the initial one, occurred from *ca*. 300 yr cal BP (Figure 24), yet did not appear to be correlated with major vegetation changes. Only a notable increase in dwarf shrubs, evident in the positive values of PC1, is visible during this period (Figures 25 and 27), coinciding with a positive contribution from fire size (Figure 27). This suggests that the forest tundra of coastal Labrador has undergone a sharp increase in fire size over the last few centuries, but that this has not led to any major changes in the composition of the vegetation. This rising fire size in eastern Canada is also evident in Billy and Petit Anne records, indicating recent alterations in disturbance regimes in eastern Quebec and Labrador.

Several studies on the Canadian boreal forest have documented a recent decrease in fire frequency after the industrial revolution (Larsen, 1996; Weir et al., 2000; Bergeron et al., 2001), attributed to increased humidity from rising temperatures (Bergeron and Archambault, 1993). Other studies have corroborated similar findings but also noted a recent increase in fire size, driven by drier spring climatic conditions compared to the past (Ali et al., 2012). Consequently, the differentiation of marginal effects indicated that over the past few centuries, the contribution of fire frequency has strongly declined at Billy and Petit Anne, while that of fire size has markedly increased (Figure 27). Simultaneously, the contribution of summer temperature has notably risen in the recent period, underscoring the constraint imposed by the cold temperatures of the Neoglacial period on vegetation. Ordinations and pollen diagrams reveal a pronounced decrease in *Picea mariana* over the recent period at Billy and Petit Anne (Figure 24), accompanied by a rapid increase in non-arboreal taxa, particularly *Alnus alnobetula* spp. *crispa*. This taxa, indicative of open environments, especially post-large fires, could imply a recent reduction in stand density in eastern Quebec and Labrador. The continual input of exotic pollen species (data not shown) also attests to this recent opening in these regions. It is likely that the decrease in Neoglacial

temperatures and the recent increase in fire size in eastern Quebec and Labrador have led to additional stress on the vegetation, consequently leading to a decline in *Picea mariana* in favor of non-arboreal taxa. The fact that these changes in vegetation are still fairly small highlights the need for rapid adaptation measures in eastern Canada, in order to counter the effects of future climate change.

4.7 Conclusion

This study explored how vegetation responded to changes in climate and fire along a north-south transect in eastern Quebec and Labrador Peninsula. It uses variation partitioning and GAMs to decipher the respective impact of temperature, fire frequency and fire size, on pollen assemblages over time. Our findings unveil notable latitudinal disparities. In the forest tundra of eastern Labrador, warm periods fostered vegetation densification through fires, while colder periods prompt landscape openness, as *Picea mariana* was forced to reproduce vegetatively. Within closed-crown spruce-moss forests, temperature exerted a substantial influence on vegetation dynamics, interacting with fire regimes. In these regions, warm temperatures correlated with increase deciduous tree abundance, whereas temperature declines corresponded to higher proportions of coniferous trees. Conversely, open-crown lichen-woodlands predominantly responded to variations in fire frequency and size, while temperature played a minor role. We hypothesize that their geographical positioning, too far south for vegetative reproduction yet too far north for deciduous trees to thrive easily, accentuates the importance of fire in these ecosystems.

Additionally, recent observations indicated a reduction in fire frequency across all study sites, accompanied by a notable increase in fire size. Consequently, our records registered a heightened contribution from fire size to pollen assemblages. Southernmost sites exhibited slight landscape openings and an increase in non-arboreal taxa. Consequently, with rising temperature and intensified fire regimes, the forest tundra will probably undergo a densification in the next decades. Conversely, closed- and open-crown spruce forests will potentially face negative impacts, including

gradual landscape openings similar to those observed further west. This study may serve as a warning for the ecosystems of eastern Quebec and the Labrador Peninsula, underscoring the pressing need to implement conservation strategies in these regions to ensure their long-term viability under the expected climate changes.

4.8 Author statements

4.8.1 Competing interests statement

The authors declare there are no competing interests.

4.8.2 Author contribution statement

Jonathan A. Lesven: Conceptualization, Methodology, Software, Investigation, Data curation, Writing - original draft, Writing - review & editing, Visualization, Project administration; François Gillet: Conceptualization, Methodology, Software, Data curation, Writing - review & editing, Visualization, Supervision, Project administration; Yves Bergeron: Conceptualization, Methodology, Writing - review & editing, Supervision, Project administration, Funding acquisition; André Arsenault: Conceptualization, Methodology, Writing - review & editing, Supervision, Project administration; Adam A. Ali: Writing - review & editing, Supervision; Milva Druguet Dayras: Investigation, Writing - review & editing; Laurent Millet: Investigation, Writing - review & editing, Supervision; Cécile C. Remy: Software, Data curation, Writing - review & editing; Damien Rius: Conceptualization, Methodology, Investigation, Writing - review & editing, Supervision, Project administration, Funding acquisition.

4.9 Funding statement

This work was supported by grants from the ANR Interarctic, the Nich-Arctic Project, the PEPS-INEE EPIDERME program, the Mitacs Globalink program, and the International Research Project “Cold forest”.

CONCLUSION GÉNÉRALE

L'objectif général de cette thèse de doctorat était de documenter l'impact des modifications climatiques et des régimes de perturbations sur les trajectoires des forêts boréales du Québec et au Labrador au cours de l'Holocène, en se concentrant particulièrement sur l'épinette noire. Ces travaux de recherche ont permis de mettre en lumière l'importante variabilité spatiale et temporelle du climat à l'est du Canada, ainsi que ses liens étroits avec l'activité des feux de forêt et de la composition végétale. En outre, cette thèse de doctorat souligne l'importance des interactions entre les températures estivales de l'air, les fréquences de feu et la superficie brûlée sur la végétation nord-est canadienne au cours de l'Holocène, et témoigne d'une forte variabilité latitudinale dans la réponse de la végétation aux fluctuations des variables environnementales. Cette première documentation de la dynamique à long terme de cette région à partir d'une approche multisite et multi-indicatrice nous permet ainsi d'approfondir nos connaissances sur les trajectoires des écosystèmes boréaux, données précieuses afin de mieux anticiper leur réponse aux changements climatiques en cours.

Plus spécifiquement, cette thèse s'est articulée autour de deux axes principaux, tous deux destinés à approfondir notre compréhension de l'impact potentiel des changements climatiques sur les pessières fermées du Canada. Le premier axe abordait une approche synthétique, dressant un état des connaissances de l'impact des changements climatiques sur la croissance et les taux de mortalité de l'épinette noire à l'horizon 2100, à travers l'ensemble de son aire de répartition. Le second adoptait une approche rétrospective, divisée en trois chapitres, visant à décrypter les rôles respectifs des feux de forêt, du climat, ainsi que de leurs interactions, dans la dynamique long terme des écosystèmes boréaux le long d'un transect nord-sud de carottes sédimentaires lacustres situées à l'est du Québec et au Labrador. Le premier de ces chapitres visait à acquérir les données de feux à partir d'une méthodologie novatrice, en développant une nouvelle approche automatisée pour quantifier et mesurer la surface des macrocharbons dans les échantillons sédimentaires. Le deuxième chapitre avait pour objectif de fournir les données de températures estivales

de l'air, tout en améliorant notre compréhension de l'histoire climatique holocène du Québec-Labrador à partir des assemblages polliniques et de chironomes. Enfin, le dernier chapitre utilisait l'ensemble des données recueillies afin de discuter des impacts respectifs du climat et des feux de forêt sur la dynamique millénaire de la végétation dans ces régions peu étudiées. Prises dans leur ensemble, les informations issues des quatre chapitres du corps de cette thèse (chapitres I à IV) permettent d'obtenir une vision plus éclairée que précédemment de l'impact des changements climatiques futurs sur les forêts boréales est-canadiennes.

Apports de la paléoécologie dans la compréhension des interactions feux-climat-végétation au Québec-Labrador au cours de l'Holocène. ***Histoire climatique holocène du Québec-Labrador.*** Alors que la plupart des études paléoclimatiques holocènes dans l'est de l'Amérique du Nord se basent sur l'analyse du pollen (*e.g.* Kerwin et al., 2004; Viau et Gajewski, 2009; Fréchette et al., 2018, 2021), le chapitre III de cette thèse met en évidence un potentiel biais dans certains enregistrements polliniques. Celui-ci peut résulter de modifications dans les assemblages polliniques sous l'influence de facteurs internes tels que les feux de forêt, ou être induit par la surreprésentation de taxons dont la dynamique est peu sensible aux variations de température de l'air. Bien que sensible à d'autres variables, en particulier aux facteurs internes des lacs (acidité, présence de macrophytes), la comparaison avec les capsules céphaliques de chironomes permet d'apporter une perspective plus complète sur l'histoire climatique holocène du Québec-Labrador.

L'Holocène a débuté il y a 11700 ans. Cependant, la présence de la calotte laurentide dans les régions du Québec-Labrador jusqu'à environ 5700 ans cal BP (Dalton et al., 2020) a entraîné une variabilité climatique régionale marquée (Renssen et al., 2009). La déglaciation se produit *ca.* 10300 ans cal BP à Mista, et *ca.* 9600 ans cal BP à Blow Hole et Aurélie, respectivement (Dalton et al., 2020). Comme la majorité des autres reconstitutions régionales (Viau et Gajewski, 2009; Gajewski, 2015; Fréchette et al., 2018, 2021), ces trois sites montrent les températures estivales de l'air les plus

froides au début des enregistrements. Celles-ci sont associées à la circulation atmosphérique anticyclonique résultant des vents catabatiques froids (Ullman et al., 2016b) liés à la persistance de la calotte laurentide à proximité des sites d'étude (Renssen et al., 2009), compensant l'insolation estivale élevée de cette période (Kaplan et Wolfe, 2006). Après cet épisode froid, les trois sites ont enregistré une forte augmentation des températures estivales de l'air de 4 à 6°C (chapitre III), marquant le début du maximum thermique de l'Holocène (HTM) sous l'effet d'un important forçage radiatif (Berger et Loutre, 1991). Comme l'ont souligné de nombreuses études (*e.g.* Gajewski et Atkinson, 2003; Kaufman, 2004; Miller et al., 2010), le début et la durée des températures maximales varient considérablement dans l'est de l'Amérique du Nord. En effet, la durée du Maximum Thermique de l'Holocène en Amérique du Nord dépend largement des forçages externes comme internes, notamment l'insolation estivale, la distance à la calotte laurentide, la concentration atmosphérique en gaz à effet de serre (Renssen et al., 2009, 2012), mais aussi les changements de la circulation océanique dans la mer du Labrador et la baie de Baffin (Briner et al., 2016b). Par conséquent, ces sites ont montré d'importantes disparités régionales (chapitre III). À Aurélie, les températures estivales de l'air maximales (15-17,2 °C) ont été observées avant 8000 ans cal BP, alors qu'à Mista, les températures maximales (14-16°C) ont été observées *ca.* 8000-7800 ans cal BP. Sur la côte du Labrador, le site de Blow Hole a montré un réchauffement en deux phases : une stagnation modérée des températures estivales de l'air entre *ca.* 7000 et 4500 ans cal BP (8-11°C), suivie d'une phase de températures maximales après cette période (9.5-12°C). Ce schéma correspond étroitement aux reconstitutions basées sur le pollen réalisées par Kelly et Funder (1974) et Gajewski (2015) dans l'Arctique canadien et le sud du Groenland, montrant un Maximum Thermique de l'Holocène retardé entre *ca.* 5200 et 3200 ans cal BP autour de la mer du Labrador. Ces trois séquences mettent en évidence l'importante variabilité climatique de l'est de l'Amérique du Nord au cours de l'Holocène.

Après le Maximum Thermique de l'Holocène, la plupart des enregistrements révèlent un refroidissement progressif jusqu'à nos jours, caractérisé par une variabilité

prononcée. Ce processus de refroidissement marque la transition d'un optimum thermique chaud à une période néoglaciaire plus froide, coïncidant avec la diminution de l'insolation estivale suite à la récession des derniers vestiges de la calotte laurentide (Kaplan et Wolfe, 2006; Fréchette et al., 2021). Bien que les températures estivales aient commencé à baisser *ca.* 5000 ans cal BP à Aurélie, cette tendance n'est pas observée avant *ca.* 4200 ans cal BP à Mista, malgré des changements notables dans la végétation, caractérisés par la densification de l'épinette noire due à une augmentation importante de la taille des feux après *ca.* 5000 ans cal BP. Sur la côte du Labrador, le schéma est moins clair. Alors que les chironomes suggèrent une diminution nette des températures estivales à partir de *ca.* 3200 ans cal BP jusqu'à nos jours, les données basées sur le pollen ne montrent pas ce schéma avant *ca.* 1500 ans cal BP (chapitre III). Les études menées par Gajewski (2015) et Viau et Gajewski (2009) ont reconstitué les températures maximales au Québec-Labrador jusqu'à environ 1500 ans cal BP, tandis que celle de Kelly et Funder (1974) concorde davantage avec nos données sur les chironomes. D'autres études sont donc nécessaires pour améliorer notre compréhension de la dynamique climatique récente autour de la mer du Labrador. Le refroidissement néoglaciaire est également perceptible dans les reconstitutions polliniques des sites de Billy et Petit Anne (chapitre III), probablement marqués par divers événements séculaires tels que la période chaude romaine, l'anomalie climatique médiévale ou le petit âge glaciaire. Bien que certains de ces événements puissent être observables dans nos enregistrements, leurs variations se situent généralement dans les marges d'erreur des inférences de températures, et n'ont donc pas été interprétées dans cette étude.

Interactions feu-climat-végétation au Québec-Labrador durant l'Holocène. L'analyse rétrospective des sites a mis en lumière une réponse contrastée de la végétation aux fluctuations des températures et des feux de forêt au cours de l'Holocène. Comme déjà suggéré par Burton et al., (2008) et Kasischke et Turetsky (2006), il est clair que les interactions entre ces trois compartiments majeurs ne peuvent être généralisées à large échelle spatiale.

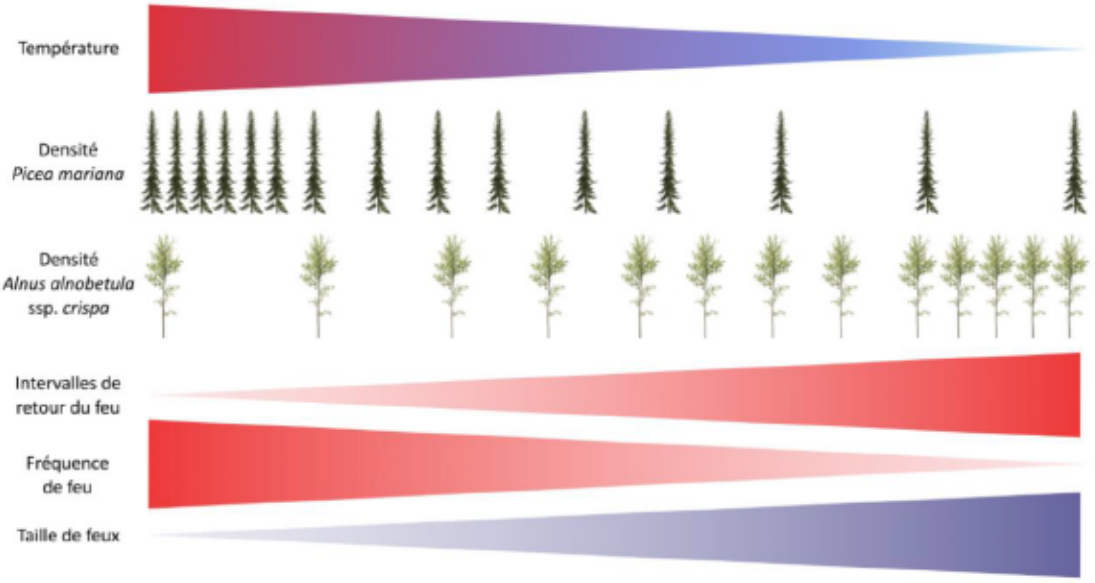

Figure 28
Schéma conceptuel de la dynamique de la végétation et des feux de forêt en fonction de la température estivale de l'air dans la toundra forestière du Labrador (site Blow Hole). La pointe des triangles représente les valeurs les plus faibles.

Les températures estivales de l'air se sont révélées être un facteur crucial contrôlant la dynamique de végétation dans la toundra forestière de la côte du Labrador, interagissant avec des feux de fréquence et de taille variées (chapitre III). En accord avec les résultats de Gajewski (2019) et Gajewski et al., (2021) dans l'ouest du Québec, les périodes les plus chaudes ont été associées à un développement rapide et prononcé de l'épinette noire (Figure 6.1). En effet, le dépassement d'un seuil de température (~10°C, chapitre III) semble autoriser la mise en place d'une reproduction sexuée de l'épinette noire. Ainsi, les feux de forêt favorisent une densification des peuplements grâce aux cônes faiblement sérotineux de cette espèce. En retour, l'augmentation de la densité des peuplements génère probablement une rétroaction positive en raison de la forte inflammabilité de l'épinette noire, entrainant une augmentation de la fréquence des feux de forêt. Comme le suggéraient Gajewski et al., (2021), les incendies entrainent à l'inverse une ouverture des peuplements durant

les périodes les plus froides, car la baisse des températures limite la production de graines et de cônes (Sirois, 2000), n'autorisant qu'une reproduction par marcottage. Par conséquent, les feux de forêt deviennent létaux pour l'épinette noire et entraînent une déforestation conduisant à une ouverture progressive des peuplements. À l'inverse, l'aulne crispé, avec sa forte affinité pour les milieux ouverts, voit son abondance augmenter dans les milieux post-feux.

Dans les pessières ouvertes (site Billy), le feu s'est révélé être le facteur de structuration majeur des trajectoires de végétation, corroborant en partie l'étude de Remy et al., (2017b). Cependant, notre étude montre que si la superficie brûlée explique effectivement la majeure partie de la variance des assemblages polliniques, la fréquence des feux joue également un rôle majeur dans ces environnements (Figure 6.2). Les plus grands feux de la séquence du lac Billy se sont produits à la fin du Maximum Thermique de l'Holocène. Cette période a été caractérisée par la forte abondance du bouleau (Chapitre IV; Remy et al., 2017b), suggérant que les grands feux ont facilité l'ouverture des paysages et induit un développement important des feuillus, en particulier le bouleau et l'aulne crispé. L'augmentation de la fréquence des feux jusqu'aux derniers siècles avant aujourd'hui (chapitres II et IV) et la diminution progressive de la superficie brûlée suggèrent que de nombreux petits feux ont ensuite favorisé le développement progressif de l'épinette noire dans le paysage. En parallèle, la diminution progressive du sapin baumier dans le paysage laisse à penser que cette espèce, intolérante au feu et retrouvée en fin de succession (Sirois, 1997), a été graduellement remplacée par l'épinette noire, plus adaptée aux feux de forêt (de Lafontaine et Payette, 2010, 2012).

Similairement à la région du lac Blow Hole, les températures estivales de l'air se sont révélées être un forçage majeur de la dynamique de végétation dans les pessières fermées du sud du transect, bien que l'enregistrement du site Petit Anne présente une couverture temporelle plus limitée. Contrairement aux écosystèmes de la toundra forestière, les périodes les plus chaudes ont été associées aux plus faibles abondances de l'épinette noire et aux abondances les plus élevées des feuillus, tels que le bouleau (Figure 6.3). Les fréquences de feu élevées durant cette période ont

probablement contribué en particulier à l'augmentation du bouleau à papier dans les environnements post-feux (Gajewski et al., 1993). De même, les températures élevées ont probablement favorisé leur développement, conduisant à la formation de forêts mixtes dans des environnements typiques de l'actuelle sapinière à bouleau blanc au sud du Québec. La diminution des températures caractéristique de la période néoglaciaire a ensuite favorisé les conifères, alors que les feuillus ont été désavantagés. Cette conifériSation des paysages dans une période plus froide et humide que précédemment a déjà été observée dans l'est du Québec (Feussom Tcheumeleu et al., 2023). Comme dans la toundra forestière, l'accroissement des taxons sérotineux a entrainé une boucle de rétroaction permettant leur maintien dans le paysage.

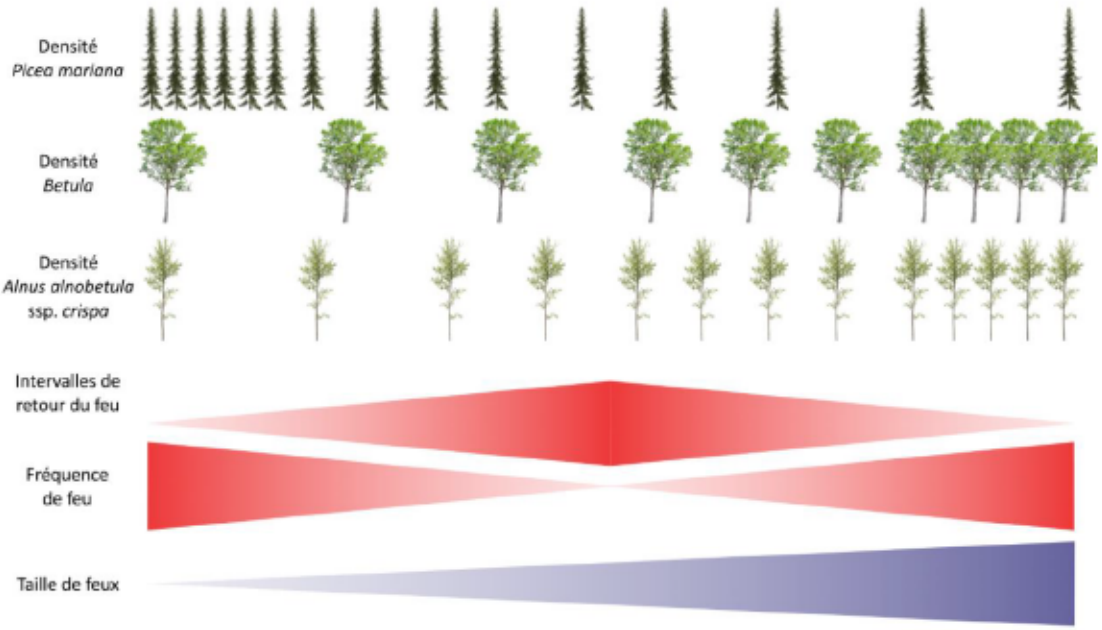

Figure 29
Schéma conceptuel de la dynamique de la végétation et des feux de forêt dans les pessières ouvertes (site Billy). La pointe des triangles représente les valeurs les plus faibles.

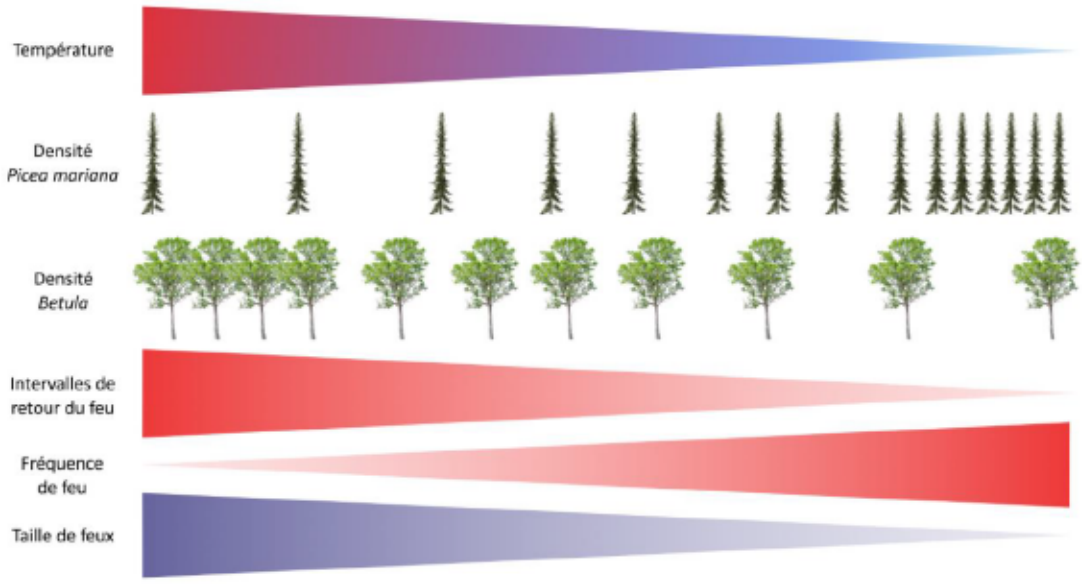

Figure 30
Schéma conceptuel de la dynamique de la végétation et des feux de forêt en fonction de la température estivale de l'air dans les pessières fermées (site Petit Anne). La pointe des triangles représente les valeurs les plus faibles.

Trajectoires futures en contexte de changements climatiques à l'est du Québec et au Labrador. Les concentrations atmosphériques en dioxyde de carbone ont évolué de 310 ppm (partie par million) en 1950 à 424 ppm en 2024, principalement en raison de la combustion des combustibles fossiles par les activités humaines. Selon les projections les plus récentes, ces émissions pourraient demeurer stables (RCP2.6[1]), augmenter de manière modérée à 670 ppm (RCP6.0), voire atteindre jusqu'à 936 ppm (RCP8.5) d'ici à 2100 (IPCC, 2022). Cependant, des projections récentes suggèrent que les deux derniers scénarios sont actuellement les plus probables (Capellán-Pérez et al., 2016), présageant une augmentation des températures mondiales entre *ca.* 2.5 et 4.8°C (IPCC, 2022). Le biome boréal se réchauffant environ deux fois plus rapidement que la moyenne mondiale, les

[1] Les scénarios *Representative Concentration Pathways*, ou RCP (« profils représentatifs d'évolution de concentration » en français), représentent les trajectoires possibles du forçage radiatif à l'horizon 2100.

projections récentes estiment donc une augmentation des températures entre *ca*. 4°C et 11°C d'ici à la fin du siècle dans le biome boréal (Gauthier et al., 2015). Ces modifications climatiques auront des répercussions majeures sur les écosystèmes boréaux nord-est américains, parmi lesquels l'est du Québec et le Labrador seront également largement impactés. L'ensemble des données acquises au cours de cette thèse nous permet d'établir différentes hypothèses sur les trajectoires futures de la végétation au sein des trois zones de végétation étudiées (Figure 6.4).

Toundra forestière. Les différents chapitres de cette thèse ont révélé que la toundra forestière du nord-est du Québec-Labrador, actuellement dominée par les épinettes noires et blanches, l'aulne crispé et le bouleau, pourrait subir d'importantes modifications d'ici la fin du siècle. Ces changements devraient inclure des températures qui se rapprocheront progressivement de celles observées pendant le maximum de température de l'Holocène – après *ca*. 4500 ans cal BP – estimées 3-5°C supérieures à celles d'aujourd'hui (chapitre III). Certaines études synthétisées dans le chapitre I ont mis en lumière que l'augmentation parallèle des précipitations devrait suffire à compenser l'évapotranspiration croissante associée aux condit ions plus chaudes à ces latitudes, suggérant que ces environnements ne seront pas limités par la disponibilité en eau, même sous le scénario RCP8.5 (D'Orangeville et al., 2016, 2018). De plus, l'augmentation des températures de l'air, de la concentration atmosphérique en CO_2, de la minéralisation de l'azote et de la nitrification – entre autres – devraient bénéficier à la croissance de l'épinette noire à ces latitudes (chapitre I, Moore et al., 1999; Messaoud et Chen, 2011; Huang et al., 2013). Il convient de noter que la fonte progressive du pergélisol discontinu et la possible propagation de maladies dans des zones où elles étaient précédemment limitées par la température pourraient *a contrario* contrebalancer ces effets bénéfiques pour l'épinette noire et amener à d'importants épisodes de mortalité (Haynes et al., 2021; Gray et al., 2021), bien que des gains notables de croissance soient tout de même attendus à ces latitudes (D'Orangeville et al., 2016, 2018). Cette augmentation des températures devrait mener au développement de formes érigées de l'épinette noire (chapitre I), ainsi qu'à la production de cônes facilitant sa reproduction sexuée

(Gamache and Payette, 2004). Cette évolution sera probablement associée à une augmentation progressive de la fréquence des feux (Girardin et Mudelsee, 2008; Wotton et al., 2010) et de la surface brûlée (Flannigan et al., 2009), ayant été identifiés comme des forçages importants de la dynamique de ces écosystèmes (chapitre IV). Cette modification des régimes de feux devrait résulter de l'augmentation des températures et d'un combustible progressivement plus sec (Flannigan et al., 2009), ainsi que de la rétroaction positive induite par le développement de l'épinette noire (chapitre IV). Cette amélioration des conditions climatiques, associée à une plus grande inflammabilité des paysages, devrait par conséquent conduire à une densification progressive de la toundra forestière dans les décennies à venir, tandis que les taxons typiques des milieux ouverts, tels que l'aulne crispé, devraient diminuer progressivement en abondance.

Pessières ouvertes. Dans les pessières ouvertes (site Billy), les modifications climatiques attendues devraient induire une réponse plus complexe. De manière similaire à la toundra forestière (site Blow Hole), l'augmentation des précipitations devrait être suffisante pour compenser l'augmentation des températures, même dans les scénarios les plus pessimistes, créant ainsi des conditions propices à la croissance de l'épinette noire au niveau individuel (chapitre I, Huang et al., 2013; D'Orangeville et al., 2016, 2018). L'augmentation des températures du sol, des concentrations atmosphériques en CO_2 et du couvert nival devrait également favoriser sa croissance par rapport aux conditions actuelles (chapitre I). Ces effets bénéfiques pourraient cependant être contrebalancés par l'accroissement des épidémies de tordeuse du bourgeon de l'épinette (*Choristoneura fumiferana* Clemens) vers des positions plus septentrionales (Gray, 2008), bien que la faible densité des peuplements d'épinette noire à ces latitudes – potentiellement exacerbée par les feux de forêt – pourrait limiter leur expansion vers le Nord (Régnière et al., 2012). Parallèlement, la fonte progressive du pergélisol discontinu et la plausible évolution de maladies ou parasite vers des positions plus septentrionales pourraient également entraîner d'importants épisodes de mortalité. Le degré d'importance des facteurs bénéfiques comme délétères reste

donc à déterminer, mais il est probable qu'à ces latitudes les effets restent bénéfiques pour la croissance de l'épinette noire même sous le scénario RCP8.5 (chapitre I).

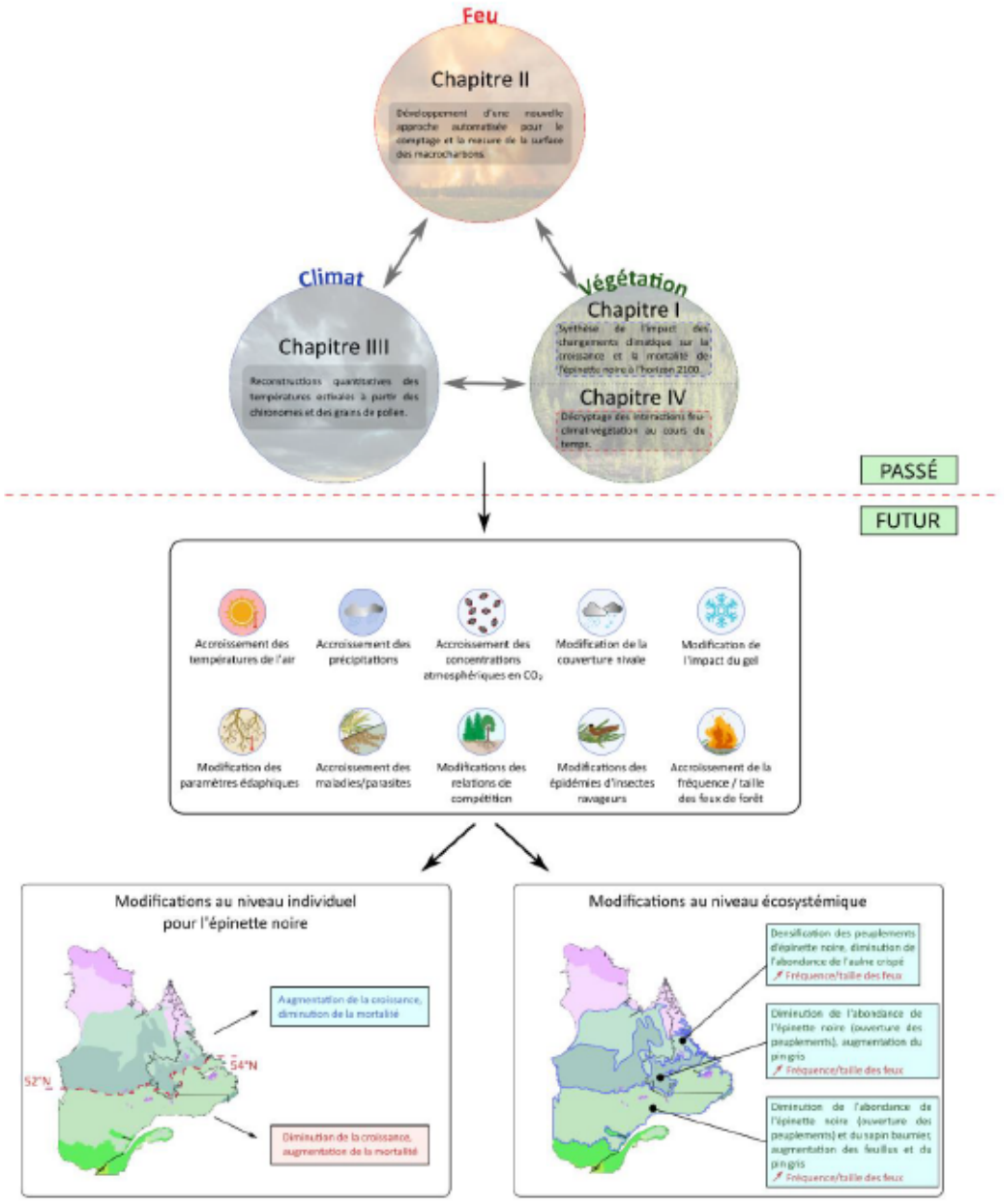

Figure 31
Schéma conceptuel résumant les impacts futurs possibles des changements climatiques sur les écosystèmes boréaux de l'est du Québec et du Labrador.

Au regard de nos résultats, les écosystèmes situés à l'écotone entre pessières à mousses et pessières à lichen pourraient subir de profondes modifications d'ici la fin du siècle. Les projections climatiques restant incertaines à ces latitudes, différentes hypothèses peuvent être formulées. Si l'augmentation des précipitations suffit à compenser l'élévation des températures, il est relativement probable que la fréquence et la taille des feux de forêt augmenteront peu. Par conséquent, les paysages actuels pourraient demeurer semblables à ceux de la période néoglaciaire, c'est-à-dire marqués par la dominance de l'épinette noire (chapitre IV, Remy et al., 2017b), ainsi que, dans une moindre mesure, du bouleau, de l'épinette blanche et du sapin baumier. L'augmentation des températures pourrait également mener à une densification progressive du sapin baumier à des latitudes plus élevées qu'actuellement (Messaoud et al., 2007; Bouchard et al., 2008). À l'inverse, si comme cela est plus probable l'accroissement des températures se conjuguait à une faible augmentation des précipitations, ces conditions devraient conduire à une augmentation de la fréquence (Girardin et Mudelsee, 2008; Wotton et al., 2010) et de la taille des feux (Flannigan et al., 2009), ces variables s'étant révélées comme les forçages principaux de la dynamique de végétation dans ces environnements (chapitre IV). Nos données ont révélé une récente diminution de l'abondance de l'épinette noire sous l'effet de l'augmentation de la taille des feux de forêt, et inversement une augmentation marquée de l'abondance de l'aulne crispé. Ce dernier a une forte affinité pour les milieux ouverts (Gajewski et al., 1993), soulignant que les régimes de feu peuvent largement influencer le potentiel de régénération des conifères boréaux, en particulier l'épinette noire, et par conséquent modifier la densité des peuplements forestiers (Van Bogaert et al., 2015; Splawinski et al., 2019a) à l'est du Québec et au Labrador (Figure 6.4). Avec le réchauffement des températures et l'accroissement de la fréquence et de la taille des feux, le couvert végétal pourrait également favoriser progressivement le pin gris dans des zones où il était auparavant inadapté en raison d'intervalles de retour du feu trop longs ou des feux de trop faible superficie (Remy et al., 2017b; Baltzer et al., 2021).

Pessières fermées. Les écosystèmes situés dans les régions les plus méridionales des forêts boréales du Canada devraient subir des changements prononcés dans leur croissance, leur mortalité et leurs trajectoires écologiques en raison des changements climatiques anticipés. Au sud du Québec, l'accroissement des précipitations ne devrait plus être suffisant pour compenser l'augmentation des températures, menant à un bilan hydrique négatif (Price et al., 2013). Cette situation devrait conduire à des épisodes plus fréquents de sécheresse, mettant en péril la croissance de l'épinette noire et exacerbant les risques de mortalité (chapitre I, D'Orangeville et al., 2016, 2018). Bien que l'enrichissement atmosphérique en CO_2 et l'augmentation des températures du sol puissent au contraire être bénéfiques à la croissance de l'épinette noire dans ces forêts fermées, la diminution de la couverture neigeuse plus tôt dans l'année devrait accroître les dommages dus aux épisodes de gel tardifs (chapitre I, Marquis et al., 2021; Girardin et al., 2022), accroitre l'impact des épidémies de tordeuse du bourgeon de l'épinette (Régnière et al., 2012; Fuentealba et al., 2017; Bellemin-Noël et al., 2021) comme des maladies et parasites (Westwood et al., 2012). En conséquence, d'importantes diminutions de la croissance de l'épinette noire et épisodes de mortalité sont attendus dans ces régions (chapitre I).

De plus, le chapitre IV a mis en évidence une augmentation récente de la taille des feux, une tendance qui devrait largement s'accentuer dans les prochaines décennies (Flannigan et al., 2009), de même que leur fréquence (Girardin et Mudelsee, 2008; Wotton et al., 2010) et la durée de la saison de feux (Wotton et Flannigan, 1993). Similairement aux écosystèmes plus septentrionaux, le chapitre IV a montré une diminution récente de l'abondance de l'épinette noire et une augmentation de l'aulne crispé. Bien que ces différences restent ténues, l'importance des feux de forêt sur les transitions entre les pessières fermées et ouvertes a déjà été montrée par différentes études proches de notre site d'étude (voir Remy et al., 2017a, 2017b), mais également à l'ouest du Québec (Girard et al., 2008; Splawinski et al., 2019a; Baltzer et al., 2021). La transformation des forêts fermées en forêts ouvertes moins productives est une conséquence directe de ces changements. Cependant, différents paramètres doivent être ajoutés dans ces scénarios futurs. L'accroissement des températures et les

modifications des régimes de feu dans ces régions pourraient entraîner des conditions proches de celles observées *ca.* 3000 yr cal BP, et par conséquent augmenter la proportion d'espèces décidues comme le bouleau dans les paysages, induisant une rétroaction négative sur les incendies (Hély et al., 2001; Johnstone et Chapin, 2006b; Terrier et al., 2013). Ces modifications pourraient entraîner le développement du pin gris dans ces régions où il était auparavant limité par des intervalles de retour du feu trop longs, en particulier sur les sols secs, sableux et pauvres en nutriments (Desponts et Payette, 1992; Payette, 1993). Similairement à notre étude, il a été montré que la dynamique du sapin baumier est majoritairement contrôlée par les régimes de feux (Messaoud et al., 2007; Ali et al., 2008). L'augmentation prévue de la fréquence et de la taille des incendies dans le futur pourrait ainsi entraîner un déclin progressif de son abondance, avec un maintien dans le paysage résultant du relief vallonné de la région offrant des zones refuges pour cette espèce (De Grandpré et al., 2000; Cyr et al., 2007).

Limites de l'étude des interactions feu-climat-végétation à partir des archives sédimentaires lacustres. Comme démontré précédemment, les archives sédimentaires lacustres représentent une source d'information majeure pour la compréhension des écosystèmes passés. Elles ne représentent cependant pas une réalité écologique parfaite, en réalité de la simplification des processus écologiques complexes jouants sur la dynamique de ces forêts, induite par l'étude des sédiments. En effet, comme souligné dans le chapitre III, les variations de température ne représentent qu'une partie de la réalité climatique, de par l'importance de la variabilité hydrologique régionale (précipitations/évapotranspiration) que ces études ne permettent pas d'intégrer. Elles ignorent également la forte variabilité des paramètres édaphiques, la topographie ainsi que la fragmentation forestière, représentant chacun une importance majeure dans ces environnements (Gavin et al., 2006; Ali et al., 2009a).

Dans les environnements de haute latitude où la production de biomasse reste généralement faible, les reconstitutions des feux de forêt requièrent cependant quelques précautions. En premier lieu, la résolution d'étude doit être suffisamment fine afin de pouvoir discerner des évènements de feux plus ou moins rapprochés dans le temps. Alors qu'à l'ouest du Québec les feux fréquents (intervalles de retour du feu de 80-150 ans; Lesieur et al., 2002) obligent une résolution temporelle élevée des séries anthracologiques, l'est du Québec et le Labrador sont marqués par les intervalles de retour du feu parmi les plus longs du Canada (intervalles de retour du feu de 250-5000 ans; Coops et al., 2018; Couillard et al., 2021). En conséquence, la résolution temporelle nécessaire peut être plus faible, c'est pourquoi nos séquences ont été échantillonnées tous les cm (chapitre II). Ceci nous a permis d'obtenir une résolution temporelle généralement comprise entre 50 et 70 ans (chapitre II), suffisante pour la détection d'évènements de feux peu récurrents.

Dans les études anthracologiques, la résolution d'étude doit également permettre la détection d'évènements de feux sur l'ensemble des séquences. Cependant, celle-ci varie souvent largement entre les sédiments d'interface et basaux (de 7 à 130 ans.cm^{-1} dans le chapitre II). Le calcul des fréquences de feu inclut généralement un rééchantilonnage à la résolution temporelle médiane des échantillons afin de limiter, entre autres, les biais taphonomiques (Higuera, 2009). En cas de non-homogénéité des séries, les échantillons basaux risquent d'être divisés en plusieurs échantillons, alors que l'effort d'échantillonnage sera masqué dans les échantillons d'interface, car plusieurs échantillons seront rassemblés. Pour atténuer ce biais, les sédiments récents peuvent être traités à partir de la résolution médiane des sédiments d'interface (Brossier et al., 2014). Cela s'est avéré nécessaire en particulier pour la séquence du lac Billy (chapitre II).

Enfin, à la différence de nombreuses études, nos reconstitutions des régimes de feux ne combinent pas plusieurs sites dans chaque zone de végétation. Bien que nous soyons confiants que les différences latitudinales aient été bien reflétées par notre étude, l'utilisation d'un seul site par zone de végétation ne permet pas de limiter les biais inhérents aux processus taphonomiques locaux (Remy et al., 2018). En

conséquence, nos séries peuvent ne pas refléter les tendances de feux à l'échelle régionale, même si le chapitre II a révélé que la combinaison des différents sites reflétait bien les tendances connues de l'est du Québec et du Labrador (*e.g.* Remy et al., 2017a, 2017b).

Perspectives de recherche et mot de fin. En conclusion, cette thèse de doctorat démontre que les changements de régime de feux (fréquence/taille), les modifications climatiques ainsi que leurs interactions respectives peuvent largement modifier la composition des forêts boréales de l'est du Québec et du Labrador, bien que leur impact diffère latitudinalement. Elle a apporté une base importante pour une meilleure compréhension de l'impact des changements climatiques sur les forêts boréales du nord-est du Canada, et plus largement a permis de compléter les connaissances acquises à l'échelle de l'Amérique du Nord sur les interactions feu-climat-végétation à l'échelle plurimillénaire (*e.g.* Ali et al., 2012; Kelly et al., 2013; Remy et al., 2017a; Bastianelli, 2018; Gaboriau et al., 2020, 2023; Feussom Tcheumeleu et al., 2023). Cette thèse s'inscrit dans un travail de recherche ancré dans une volonté de compréhension de la trajectoire évolutive des écosystèmes, initié il y a plusieurs décennies. Elle ne représente par conséquent qu'une brique supplémentaire à l'édifice complexe de la compréhension du fonctionnement des écosystèmes boréaux et de leurs réponses aux variations du climat. Son importance réside dans sa contribution à un corpus croissant de connaissances, visant à éclairer les voies d'adaptation et de gestion forestière durable, nécessaires pour préserver ces écosystèmes cruciaux dans un contexte de changement climatique. Ces travaux ne doivent par conséquent par être vus comme une finalité, mais comme l'ouverture sur d'autres études visant à approfondir notre compréhension de processus écologiques complexes, et ultimement à élaborer des stratégies de gestion adaptative pour préserver la biodiversité et la résilience des écosystèmes boréaux face aux défis climatiques à venir.

Vers des perspectives méthodologiques innovantes. Bien que les feux de forêt représentent un facteur de perturbation majeur dans les forêts boréales nord-américaines, il est important de rappeler que de nombreuses autres perturbations (épidémies d'insectes ravageurs, chablis, maladies) influent également de manière importante sur la dynamique et la structure des écosystèmes forestiers boréaux. Parmi ceux-ci, la tordeuse du bourgeon de l'épinette se nourrit des jeunes aiguilles de sapin (*Abies* spp.) et d'épinette (*Picea* spp.), provoquant des dommages aux arbres pouvant aller d'une simple réduction de la croissance annuelle à la mort de vastes peuplements après plusieurs années de défoliation importante (Chen et al., 2017). Ces épidémies, survenant de manière cyclique au cours du temps (Royama, 1984; Boulanger et Arseneault, 2004), ont des répercussions considérables sur la composition spécifique des forêts, la régénération des pessières boréales (Bouchard et al., 2006), mais pourraient également influer sur la fréquence et l'intensité des feux de forêt (Fleming et al., 2002). Cependant, la reconstitution des épidémies à des échelles plurimillénaires reste aujourd'hui un verrou méthodologique important. De nombreuses approches intégrant la dendrochronologie sur arbres vivants (Morin et Laprise, 1990), morts (Boulanger et Arseneault, 2004) ou subfossiles (Sonia et al., 2011), l'étude des capsules céphaliques (Lavoie et al., 2009) ou des fèces des chenilles (Simard et al., 2006), ou encore le comptage des écailles chitineuses des ailes des imagos dans les sédiments lacustres (Navarro et al., 2017; Montoro Girona et al., 2018) ont été envisagées pour pallier ce problème. Cependant, elles se sont révélées comme étant trop coûteuses en temps, trop onéreuses, ou ayant une portée chronologie trop limitée dans le temps. Des approches nouvelles permettraient par conséquent d'améliorer notre compréhension des liens entre les régimes de perturbations, le climat et la dynamique de la végétation à des échelles de temps plurimillénaires, et par conséquent de couvrir une plus large gamme de variation qu'au cours des derniers siècles. En particulier, la détection de l'ADN environnemental préservé dans les sédiments lacustres pourrait constituer une avancée majeure dans ce domaine afin de mieux caractériser l'impact des insectes sur la dynamique forestière passée. Plus largement, cet outil pourrait permettre l'étude conjointe d'autres insectes ravageurs (*e.g. Malacosoma disstria* Hübner, la livrée des forêts)

sévissant actuellement dans les forêts boréales est-canadiennes. Une compréhension approfondie de l'interaction entre les épidémies d'insectes ravageurs et les feux de forêt pourrait ainsi fournir des informations précieuses afin d'élaborer des stratégies de gestion intégrée, prenant en compte davantage de facteurs de perturbation majeurs des forêts boréales est-canadiennes aux échelles plurimillénaires.

Vers une compréhension accrue des variations et forçages climatiques. Au travers de cette thèse de doctorat, les capsules céphaliques de chironomes ont montré une grande sensibilité aux températures moyennes estivales de l'air le long de notre transect. Bien que les études palynologiques soient nombreuses à l'est du Canada et offrent une large représentation spatiale de la dynamique climatique holocène (*e.g.* Kerwin et al., 2004; Viau et Gajewski, 2009; Fréchette et al., 2018, 2021; Gajewski et al., 2021), les études basées sur les chironomes permettent de réduire les biais inhérents aux variations hydrologiques et aux régimes de perturbations au cours du temps. Cependant, seules quelques études (Bajolle et al., 2018; Feussom Tcheumeleu et al., 2023) basées sur ces indicateurs en pessières boréales ont actuellement été réalisées dans ces régions. En conséquence, une multiplication des sites d'étude à l'échelle du Québec-Labrador est nécessaire afin d'améliorer notre caractérisation des évènements climatiques majeurs de l'Holocène, en termes d'amplitude comme de durée. De plus, d'importants efforts doivent être déployés afin d'améliorer notre compréhension à plus large échelle des forçages climatiques de cette région. La province du Québec et la région du Labrador se situent au cœur de téléconnexions complexes entre l'océan et l'atmosphère, de par leur position entre les moyennes et les hautes latitudes de l'Atlantique Nord. Plus particulièrement, le courant du Labrador est un courant orienté vers le sud, modulant largement le climat de l'hémisphère nord en apportant de l'eau douce de l'Arctique et de l'est du Groenland aux latitudes moyennes de l'Atlantique Nord (Thornalley et al., 2018; Lippold et al., 2019), avant de se diviser en deux parties près de la pointe des Grands Bancs, où la branche ouest rencontre les eaux chaudes du Gulf Stream (Jutras et al., 2023). En conséquence, Li et Piper (2015) ont pu montrer un lien étroit

entre une vigueur accrue du courant du Labrador et des périodes de refroidissement bien connues du Quaternaire, à savoir l'événement de Heinrich 1 (17,5 - 15 ka cal BP) et le Dryas Récent (12,8 - 11,6 ka cal BP). Ce courant froid pourrait donc jouer un rôle clé dans la modulation de la variabilité climatique holocène aux échelles millénaire ou séculaire. L'utilisation de la paléocéanographie, et plus largement les reconstitutions de la température et de la salinité de surface autour du Québec et du Labrador pourraient permettre d'améliorer notre compréhension de l'histoire climatique holocène de ces régions, et leur lien avec l'évolution des régimes de perturbations et de la végétation. Enfin, comme montré dans le Chapitre III, les chironomes sont sensibles aux conditions environnementales locales et peuvent présenter des variations prononcées d'un site à l'autre en fonction de forçages internes affectant les conditions du lac étudié. La réplicabilité des sites revêt par conséquent une importance majeure, car elle garantit la robustesse et la validité des reconstitutions paléoclimatiques. Il est par conséquent essentiel de disposer de multiples sites de référence représentatifs de différentes conditions environnementales, afin d'obtenir une image précise, temporellement et spatialement représentative des variations climatiques passées. En outre, la réplicabilité des sites facilite la comparabilité entre les études menées dans des régions géographiquement distinctes, contribuant ainsi à établir des modèles climatiques plus robustes et à affiner les projections futures.

Vers une meilleure robustesse des études paléoécologiques. Bien que l'histoire de la végétation, du climat et des régimes de perturbations apporte des informations essentielles sur le fonctionnement des écosystèmes, certaines conclusions restent conjecturales dans la mesure où elles ne peuvent pas être formellement vérifiées à des échelles de temps plurimillénaires. La robustesse des études paléoécologiques dépend par conséquent largement de la concordance des preuves issues de sources variées. Dans ce contexte, il est souhaitable d'étudier autant d'indicateurs que possibles afin d'obtenir une vision plus complète et intégrative que celle qui pourrait être obtenue à partir d'un seul (Birks et Birks, 2006; Smol, 2009). Ainsi, l'utilisation d'indicateurs paléoécologiques complémentaires comme la géophysique ou la

géochimie pourrait permettre d'apporter des informations complémentaires quant aux mécanismes de résilience des écosystèmes boréaux est-canadiens. Ces indicateurs sont des marqueurs tangibles des changements climatiques, des variations dans les régimes de feu, de l'évolution des sols, et plus largement des processus environnementaux ayant façonné les écosystèmes au fil du temps. Par exemple, Bastianelli et al., (2017) ont montré des différences des cations basiques (particulièrement Ca^{2+} et Mg^{2+}), du ratio C/N et des taux d'accumulation de carbone entre les pessières ouvertes et fermées du centre du Québec. L'utilisation de ces marqueurs en lien avec les régimes de feu et l'évolution du climat à l'est du Canada pourrait ainsi permettre d'apporter des informations nouvelles quant aux mécanismes de résilience des pessières boréales à l'est du Canada. Le ratio carbone/azote (Verneaux et al., 1991), le carbone organique total (Jarvie, 1991), la susceptibilité magnétique (Thompson et al., 1975), la perte au feu des échantillons sédimentaires (Dean, 1974; Heiri et al., 2001), ainsi que la spectrométrie de fluorescence des rayons X (Revenko, 2002) constituent autant d'indicateurs paléolimnologiques permettant d'améliorer notre compréhension du fonctionnement et des conditions des lacs étudiés, ainsi que des processus sédimentologiques étant survenus dans leur bassin versant (Ewing et Nater, 2002). Ainsi, la combinaison de ces données géophysiques et géochimiques avec les différents indicateurs étudiés dans le cadre de cette thèse permettrait d'obtenir une vision plus complète et détaillée de l'histoire environnementale des écosystèmes boréaux (Bastianelli et al., 2017), et donc une meilleure compréhension de leur réponse aux changements environnementaux à long terme.

Vers une vision plus intégrée : collaboration interdisciplinaire et modélisation mécaniste pour la gestion durable des forêts boréales est-canadiennes. Bien que les leçons tirées des expériences passées offrent des perspectives intéressantes sur la dynamique, la résistance et la résilience des écosystèmes forestiers au cours du temps, elles ne sont aujourd'hui pas suffisantes pour prédire l'avenir des forêts boréales est-canadiennes. Pour aborder ces défis, les collaborations

interdisciplinaires entre paléoécologues et modélisateurs sont essentielles. Elles permettent de combiner les connaissances des deux disciplines pour apporter des informations sur le futur, et par conséquent de proposer des recommandations de gestion forestière durable. Ces mesures pourraient permettre d'améliorer la résistance des écosystèmes aux échelles individuelles comme écosystémiques, mais également de renforcer leur capacité de résilience face aux conditions climatiques futures (Foley et al., 2005). En conséquence, l'utilisation de modèles mécanistes, par exemple les modèles dynamiques de végétation globale (DGVM, *Dynamic Global Vegetation Models*), pourrait permettre d'inclure les interactions feu-climat-végétation traitées dans cette thèse sous divers scénarios de changements climatiques futurs. Ce type de modèle, utilisé récemment à l'ouest du Canada (*e.g.* Gaboriau et al., 2023), pourrait ainsi permettre de mieux caractériser notre représentation du fonctionnement de ces écosystèmes (Hantson et al., 2016; Walker et al., 2020), et par conséquent d'implémenter des stratégies de gestion forestière durable.

Mot de fin. Finalement, ce travail de thèse démontre le potentiel et l'intérêt de l'utilisation des études rétrospectives pour offrir une vision intégrée sur les dynamiques passées et présentes des écosystèmes boréaux. Bien que les pistes d'amélioration soient nombreuses, l'ensemble de cette thèse de doctorat apporte de nouveaux aspects sur la réponse des forêts boréales du nord-est de l'Amérique du Nord aux variations climatiques, mais représente également une base de réflexion essentielle pour orienter les futurs travaux scientifiques et les actions de gestion. Plus largement, elle souligne l'importance de la recherche scientifique et de la collaboration interdisciplinaire pour aborder les défis complexes auxquels nous sommes confrontés. En tirant parti des outils et des connaissances à notre disposition, nous sommes en mesure de mieux comprendre les écosystèmes forestiers boréaux et de concevoir des stratégies de gestion adaptées et durables pour assurer leur préservation et leur résilience face aux défis à venir. Cette thèse aspire ainsi à contribuer à l'avancement des connaissances scientifiques, mais surtout à la protection et à la gestion responsable de ces écosystèmes essentiels pour les générations actuelles et futures.

ANNEXE A – BACKGROUND CORRECTION TO GET HOMOGENOUS SERIES OF PICTURES

In order to analyze an image to specifically determine charcoal particles from minerals or plant debris, it is important to be able to compare images within a series (TRE, BIL, BLH…) or between series. However, some images within a series, or even full series (BLH) can display a background luminosity very different from other pictures, because contrast was automatically adjusted during the acquisition. Images need to be compared altogether to determine specific colorimetric parameters corresponding to the nature of charcoal particles. In that purpose, luminosity has to be adjusted to display similar background for every image from the different series.

Intensity of split red (R), green (G), and blue (B) channels were measured on the background top left region (960*960 px). R_{bk}, G_{bk} , B_{bk} data were extracted and saved as tables. Data analysis performed on Excel revealed similar red and green mean intensity distribution for every series, and it appeared a significative difference of intensity for the blue channel only, red and green channels displaying a similar distribution for the three series. A blue channel correction coefficient was defined as follow for each image:

B correction coefficient = $\frac{R_{bk}/1.08 + G_{bk}/1.04}{2} - B_{bk}$

This value (which can either be positive or negative) is added to blue channel to correct its global intensity.

ANNEXE B – FILTRE DEFINITION ON TRE AND BIL CALIBRATION SERIES

Manual annotation was performed on the selected particles from the following images spread along the core: TRE_07, TRE_19_TRE_31, TRE_43, TRE_55, TRE_67, TRE_79, TRE_383, TRE_395 (TRE calibration series), and BIL_121, BIL_127, BIL_139, BIL_143, BIL_166, BIL_01, BIL_11 (BIL calibration series). Particles identified by at least one operator as a charcoal was labeled as well. The comparison of data generated by the annotation and manual counting for the calibration series showed a similar number of particles, suggesting that charcoal particles were globally detected.

According to that correlation, several colorimetric parameters were compared between charcoal and non-charcoal populations: Rmean, Gmean, Bmean, R+Gmean, R+G-Bmean, R/Gmean, R/Bmean, Rmin, Bmin, Rmax- Rmin, Bmax- Bmin. A colorimetric score was defined as $(R+(R+G-B))*R/G*R/B$, and a contrast score as $G\_min*B\_min+\Delta G\_(max-min)*\Delta B\_(max-min)$.

Distribution histograms were performed for every parameter, at first for each image, then data were combined for a calibration series, and finally for the whole dataset of calibration images: R/B [0.95-1.50], R/G [0.95-1,20], R [47-84], R+G-B [50-89], colorimetric score [112-280], contrast score [3300-∞]

R/B		R/G		R		R+G-B		Colorimetric score		Contrast score
min	max	min	max	min	max	min	max	min	max	min
0.95	1.50	0.95	1.20	47	84	50	89	112	280	3300

Every single image chosen for calibrating the filter was finely analyzed to determine which particle was kept or rejected by the filter. Statistical analysis was performed on particles annotated as charcoal to determine the selectivity of the filter. 60-70% of

charcoals particles are detected among the selected particles, and the global number of filtered particles is in the same order than charcoals manually estimated. The percentage of recovery is even closer concerning area estimation, based on a comparison with the estimated area of particles annotated as charcoals.

ANNEXE C – SCRIPT IMAGEJ

```
run("Clear Results");
dir=getDirectory("select folder containing images to get analyzed");
folder=getFileList(dir);

Threshold_value=75;

total_list_final=newArray(0);
nb_final=newArray(0);
total_area_final=newArray(0);


for (h=0;h<folder.length;h++)
{
if (startsWith(folder[h], "image"))
{

dir1=dir+File.separator+folder[h];
list = getFileList(dir1);
nl=list.length;

File.makeDirectory(dir+File.separator+"Analysis_filter");


index_0=lastIndexOf(list[0],".tif");
t1=substring(list[0],2,index_0);
index_n=lastIndexOf(list[nl-1],".tif");
t2=substring(list[nl-1],2,index_n);

fichier_final=newArray(0);
particule_final=newArray(0);
unfiltered_rank_final=newArray(0);
area_final=newArray(0);
L_ellipse_final=newArray(0);
l_ellipse_final=newArray(0);
L_feret_final=newArray(0);
l_feret_final=newArray(0);
Aspect_ratio_ellipse_final=newArray(0);
Aspect_ratio_feret_final=newArray(0);
calc_value_final=newArray(0);
R_value_final=newArray(0);
G_value_final=newArray(0);
B_value_final=newArray(0);
RGB_value_final=newArray(0);
X_final=newArray(0);
```

```
Y_final=newArray(0);
R_Min_final=newArray(0);
G_Min_final=newArray(0);
B_Min_final=newArray(0);
R_Max_final=newArray(0);
G_Max_final=newArray(0);
B_Max_final=newArray(0);

particle_account=newArray(nl);
total_area=newArray(nl);

filter=newArray(0.975,1.525,1.04,1.25,47,84,50,89,115,280,450000,0.015);

for (j=0;j<nl;j++)
{
	open (dir1+"//"+list[j]);
	title1=File.nameWithoutExtension();
	title2=getTitle();
	selectWindow(title2);
	w=getWidth();
	if (w>9761)
	{
		run("Size...", "width=9761 height=10440 depth=1 constrain average
interpolation=Bilinear");
	}
	selectWindow(title2);
	l=getRedScale();
	run("Set Scale...", "distance=l known=1 pixel=1 unit=mm");

	selectWindow(title2);
	run("Duplicate...", " ");
	run("Split Channels");

	corr=CorrB(title1);
	corrB[j]=corr;

	imageCalculator("Add create 32-bit", title1+"-1.tif (red)",title1+"-1.tif (green)");
	selectWindow("Result of "+title1+"-1.tif (red)");
	rename(title1+"_R+G.tif");
	imageCalculator("Subtract create 32-bit", title1+"_R+G.tif",title1+"-1.tif
(blue)");
	rename(title1+"_R+G-B.tif");

	selectWindow(title1+"_R+G-B.tif");
	run("Duplicate...", " ");
	setOption("ScaleConversions", true);
```

```
	run("8-bit");
	setThreshold(0, Threshold_value);
	run("Analyze Particles...", "size=0.0046-Infinity exclude clear add");


	m=roiManager("count");
	false_measure=newArray(m);
	unfiltered_rank=newArray(m);

	for (i=0;i<m;i++)
	{
		selectWindow(title1+"-1.tif (red)");
		roiManager("select", i);
		area=getValue("Area");
		R=getValue("Mean");
		Rmin=getValue("Min");
		Rmax=getValue("Max");
		selectWindow(title1+"-1.tif (green)");
		roiManager("select", i);
		G=getValue("Mean");
		Gmin=getValue("Min");
		Gmax=getValue("Max");
		selectWindow(title1+"-1.tif (blue)");
		roiManager("select", i);
		B=getValue("Mean");
		Bmin=getValue("Min");
		Bmax=getValue("Max");
		selectWindow(title1+"_R+G-B.tif");
		roiManager("select", i);
		RG=getValue("Mean");

	false_measure[i]=ROIscore(R,G,B,RG,Rmin,Rmax,Gmin,Gmax,Bmin,Bmax,a
rea,filter);
		unfiltered_rank[i]=i+1;
	}


	for (i=m-1;i>-1;i--)
	{
		if (false_measure[i]>0)
		{
			unfiltered_rank=Array.deleteIndex(unfiltered_rank,i);
			roiManager("select", i);
			roiManager("delete");
		}
	}
```

```
n=roiManager("count");

if (n>0)
{
	fichier=newArray(n);
	particule=newArray(n);
	area=newArray(n);
	L_ellipse=newArray(n);
	l_ellipse=newArray(n);
	L_feret=newArray(n);
	l_feret=newArray(n);
	Aspect_ratio_ellipse=newArray(n);
	Aspect_ratio_feret=newArray(n);
	calc_value=newArray(n);
	R_value=newArray(n);
	G_value=newArray(n);
	B_value=newArray(n);
	RGB_value=newArray(n);
	X=newArray(n);
	Y=newArray(n);
	R_Min=newArray(n);
	G_Min=newArray(n);
	B_Min=newArray(n);
	R_Max=newArray(n);
	G_Max=newArray(n);
	B_Max=newArray(n);

	selectWindow(title1+"_R+G-B.tif");
	for (i=0;i<n;i++)
	{
		fichier[i]=title1;
		particule[i]=i+1;
		roiManager("select", i);
		area[i]=getValue("Area");
		L_ellipse[i]=getValue("Major");
		l_ellipse[i]=getValue("Minor");
		L_feret[i]=getValue("Feret");
		l_feret[i]=getValue("MinFeret");
		Aspect_ratio_ellipse[i]=L_ellipse[i]/l_ellipse[i];
		Aspect_ratio_feret[i]=L_feret[i]/l_feret[i];
		calc_value[i]=getValue("Mean");
		X[i]=getValue("XM");
		Y[i]=getValue("YM");
	}
```

```
		selectWindow(title1+"-1.tif (red)");
		for (i=0;i<n;i++)
		{
			roiManager("select", i);
			R_value[i]=getValue("Mean");
			R_Min[i]=getValue("Min");
			R_Max[i]=getValue("Max");
		}
		selectWindow(title1+"-1.tif (green)");
		for (i=0;i<n;i++)
		{
			roiManager("select", i);
			G_value[i]=getValue("Mean");
			G_Min[i]=getValue("Min");
			G_Max[i]=getValue("Max");

		}
		selectWindow(title1+"-1.tif (blue)");
		for (i=0;i<n;i++)
		{
			roiManager("select", i);
			B_value[i]=getValue("Mean");
			B_Min[i]=getValue("Min");
			B_Max[i]=getValue("Max");
			RGB_value[i]=R_value[i]+G_value[i]+B_value[i];
		}

		Array.getStatistics(area,min, max, mean, std);
		total_area[j]=mean*n;
		particle_account[j]=n;

		print (list[j]+" : "+total_area[j]+"mm² "+particle_account[j]+"
charcoals");

	}
	else
	{
		fichier=newArray(title1);
		particule=newArray(0,0);
		area=newArray(0,0);
		L_ellipse=newArray("NA");
		l_ellipse=newArray("NA");
		L_feret=newArray("NA");
		l_feret=newArray("NA");
		Aspect_ratio_ellipse=newArray("NA");
		Aspect_ratio_feret=newArray("NA");
```

```
                calc_value=newArray("NA");
                R_value=newArray("NA");
                G_value=newArray("NA");
                B_value=newArray("NA");
                RGB_value=newArray("NA");
                X=newArray("NA");
                Y=newArray("NA");
                R_Min=newArray("NA");
                G_Min=newArray("NA");
                B_Min=newArray("NA");
                R_Max=newArray("NA");
                G_Max=newArray("NA");
                B_Max=newArray("NA");
                total_area[j]=0;
                particle_account[j]=0;

                print (list[j]+" : "+total_area[j]+"mm² "+particle_account[j]+"
charcoals");
        }



        Array.show("final
"+title1,particule,area,L_ellipse,l_ellipse,L_feret,l_feret,Aspect_ratio_ellipse,Aspect_r
atio_feret,calc_value,R_value,G_value,B_value,RGB_value,X,Y,R_Min,G_Min,B_Mi
n,R_Max,B_Max,G_Max,unfiltered_rank);
        Table.save(dir+File.separator+"Analysis_filter"+File.separator+title1+"_filter.c
sv");
        run("Close");

        fichier_final=Array.concat(fichier_final,fichier);
        particule_final=Array.concat(particule_final,particule);
        area_final=Array.concat(area_final,area);
        L_ellipse_final=Array.concat(L_ellipse_final,L_ellipse);
        l_ellipse_final=Array.concat(l_ellipse_final,l_ellipse);
        L_feret_final=Array.concat(L_feret_final,L_feret);
        l_feret_final=Array.concat(l_feret_final,l_feret);
        Aspect_ratio_ellipse_final=Array.concat(Aspect_ratio_ellipse_final,Aspect_rat
io_ellipse);
        Aspect_ratio_feret_final=Array.concat(Aspect_ratio_feret_final,Aspect_ratio_f
eret);
        calc_value_final=Array.concat(calc_value_final,calc_value);
        R_value_final=Array.concat(R_value_final,R_value);
        G_value_final=Array.concat(G_value_final,G_value);
        B_value_final=Array.concat(B_value_final,B_value);
        RGB_value_final=Array.concat(RGB_value_final,RGB_value);
```

```
        X_final=Array.concat(X_final,X);
        Y_final=Array.concat(Y_final,Y);
        R_Min_final=Array.concat(R_Min_final,R_Min);
        G_Min_final=Array.concat(G_Min_final,G_Min);
        B_Min_final=Array.concat(B_Min_final,B_Min);
        R_Max_final=Array.concat(R_Max_final,R_Max);
        G_Max_final=Array.concat(G_Max_final,G_Max);
        B_Max_final=Array.concat(B_Max_final,B_Max);
        unfiltered_rank_final=Array.concat(unfiltered_rank_final,unfiltered_rank);

        shape="yes"; //yes/no
        if (shape=="yes")
        {
                selectWindow(title2);
                run("Duplicate...", " ");
                setFont("SanSerif", 120, "antialiased");
                setJustification("right");
                odd=1;
                for (i=0;i<n;i++)
                {
                        if (odd==1)
                        {
                                label_color="yellow";//odd number
                                odd=0;
                        }
                        else
                        {
                                label_color="cyan";//even number
                                odd=1;
                        }
                        setColor(label_color);
                        roiManager("select", i);
                        Overlay.addSelection(label_color,10);
                        Overlay.drawString(i+1,(X[i]-0.35)*l,(Y[i]+0.15)*l);
                        Overlay.show;
                }
                Overlay.flatten;
                rename(title1+"shape.tif");     unfiltered_rank=newArray(m);

        saveAs("tiff",dir+File.separator+"Analysis_filter"+File.separator+title1+"_shap
e");
        }
        close("*");
}

Array.show("total",list,total_area,particle_account);
```

```
Table.save(dir+File.separator+"Analysis_filter"+File.separator+"total_filter"+".csv");
Array.show("final",fichier_final,particule_final,area_final,L_ellipse_final,l_ellipse_final,
L_feret_final,l_feret_final,Aspect_ratio_ellipse_final,Aspect_ratio_feret_final,calc_val
ue_final,R_value_final,G_value_final,B_value_final,RGB_value_final,X_final,Y_final,
R_Min_final,G_Min_final,B_Min_final,R_Max_final,G_Max_final,B_Max_final,unfilter
ed_rank_final);
Table.save(dir+File.separator+"Analysis_filter"+File.separator+"results_folder_filter"+
".csv");

File.rename(dir+File.separator+"Analysis_filter",dir+File.separator+"Analysis_filter
"+t1+"-"+t2);
File.rename(dir1,dir+File.separator+"images - performed analysis - "+t1+"-"+t2);


        }
}

function CorrB(title1)
{
        n=1200;
        N=300;

        selectWindow(title1+".tif");
        makeRectangle(0, 0, N, N);
        color=getValue("Mean");

        if (color==0)
        {
                x1=getWidth()-n;
                y1=N;
                x2=n*0.7;
                y2=n*0.7;
                print("dark square !!!");
        }
        else
        {
                x1=N;
                y1=N;
                x2=n*0.7;
                y2=n*0.7;
        }

        selectWindow(title1+"-1.tif (red)");
        makeRectangle(x1, y1, x2, y2);
        R=getValue("Mean");
```

```
	selectWindow(title1+"-1.tif (green)");
	makeRectangle(x1, y1, x2, y2);
	G=getValue("Mean");

	selectWindow(title1+"-1.tif (blue)");
	makeRectangle(x1, y1, x2, y2);
	B=getValue("Mean");


	corr1=G/1.04-B;
	corr2=R/1.08-B;
	corr=(corr1+corr2)/2;
	return corr;
}

function getRedScale()
{
	n=1200;
	run("Duplicate...", " ");
	makeRectangle(getWidth()-n, getHeight()-n, n*0.8, n*0.8);
	run("Crop");
	run("8-bit");
	setThreshold(0,85);
	run("Analyze Particles...", "clear add");
	roiManager("select",0);
	run("Crop");
	n1=getWidth();
	k=1;
	for (i=0;i<n1;i++)
	{
		if (k==1)
		{
			if (getValue(i,0)>110)
			{
				x=i;
				k=0;
			}
		}
	}
	close();
	if (x>n1/2)
	{
		l=n1-(n1-x)*2;
	}
	else
```

```
        {
                l=n1-x*2;
        }
        return l;
}

function ROIscore(R,G,B,RG,Rmin,Rmax,Gmin,Gmax,Bmin,Bmax,area,filter)
{
        k=0;
        if (R/B<filter[0])
        {
                k=k+1;
        }
        if (R/B>filter[1])
        {
                k=k+1;
        }
        if (R/G<filter[2])
        {
                k=k+1;
        }
        if (R/G>filter[3])
        {
                k=k+1;
        }
        if (R<filter[4])
        {
                k=k+1;
        }
        if (R>filter[5])
        {
                k=k+1;
        }
        if (RG<filter[6])
        {
                k=k+1;
        }
        if (RG>filter[7])
        {
                k=k+1;
        }
        if ((R+RG)*R/B*R/G<filter[8])
        {
                k=k+1;
        }
        if ((R+RG)*R/B*R/G>filter[9])
```

```
        {
                k=k+1;
        }
                if ((Bmin+Gmin)*(Bmax-Bmin+Gmax-
Gmin)*((Rmax/3+Gmax/3+Bmax/3))<filter[10])
        {
                k=k+1;
        }
        if (area<filter[11])
        {
                k=k+1;
        }
        return k;
}
```

ANNEXE D – RANKS OBTAINED FOR EACH PARAMETER TESTED WITH A DCA, PCA AND CA. ONLY THE TOP 10 RANKS ARE DISPLAYED. FOR THE LEGEND OF THE PARAMETERS, THE READER MAY REFER TO WHITMORE ET AL., (2005)

Parameters	Rank obtained with DCA (R squared)	Rank obtained with PCA (R squared)	Rank obtained with CA (R squared)	Final rank (total score)
tjja	1 (0.8690)	2 (0.7897)	4 (0.8875)	**1** (7)
apetptdc	5 (0.8578)	3 (0.7893)	2 (0.8976)	**2** (10)
tjun	6 (0.8552)	1 (0.7949)	5 (0.8853)	**3** (12)
mtwa	2 (0.8673)	6 (0.7863)	6 (0.8803)	**4** (14)
apetpt	9 (0.8440)	4 (0.7890)	1 (0.8976)	**5** (14)
tjul	3 (0.8669)	5 (0.7885)	8 (0.8799)	**6** (16)
taug	4 (0.8651)	12 (0.7679)	9 (0.8786)	**7** (25)
tmax	7 (0.8497)	8 (0.7778)	15 (0.8324)	**8** (30)
gdd0	14 (0.8167)	11 (0.7696)	7 (0.8800)	**9** (32)
gdd5	15 (0.7906)	7 (0.7830)	11 (0.8740)	**10** (33)

ANNEXE E – AGE-DEPTH MODEL OF BLOW HOLE, BILLY, PETIT ANNE, MISTA AND AURÉLIE LAKES FROM 'RBACON' OUTPUT. FOR EACH MODEL, UPPER LEFT PANELS DESCRIBE THE MARKOV CHAIN MONTE CARLO ITERATIONS, UPPER MIDDLE PANELS DISPLAY THE DISTRIBUTION OF SEDIMENT ACCUMULATION RATES, AND UPPER RIGHT PANELS SHOW THE MEMORY CORRESPONDING TO THE VARIATION OF SEDIMENT ACCUMULATION RATE IN TIME. BOTTOM PANELS REPRESENT THE CALIBRATED RADIOCARBON DATES (SEE TABLE 5 FOR DETAILS) AND AGE-DEPTH MODELS WITH 95% CONFIDENCE INTERVALS

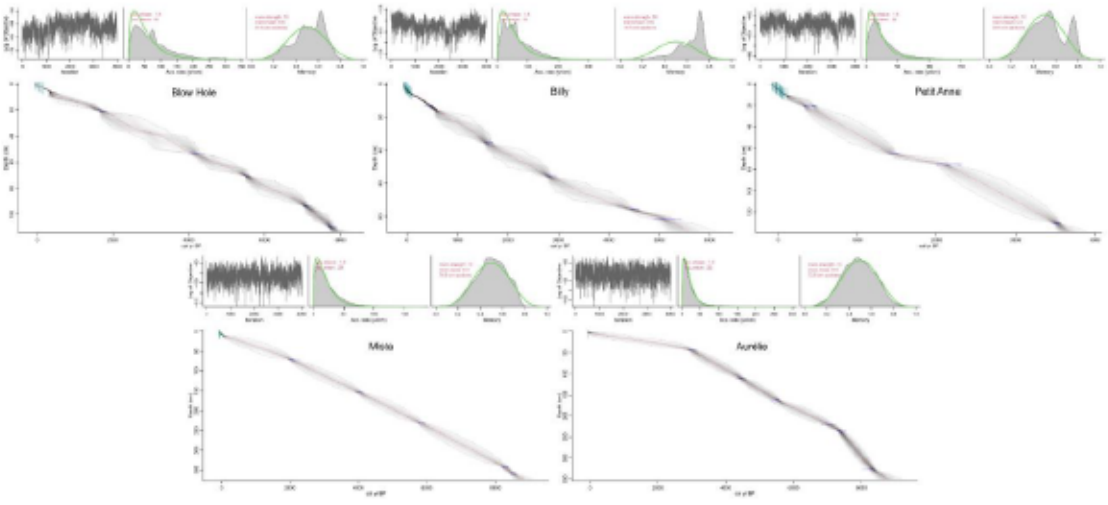

ANNEXE F – LOCATION OF MODERN DATABASE SITES AND ANALOGUES FOR POLLEN GRAINS (MAPS A TO E) AND CHIRONOMIDS (MAP F) IN NORTHEASTERN NORTH AMERICA. CIRCLES REPRESENT MODERN DATABASE SITES. THE COLORED CIRCLES REPRESENT THE ANALOGUES SELECTED FOR MSAT INFERENCES VIA MAT USING POLLEN GRAINS (SIZE AND COLOR INTENSITY VARY ACCORDING TO THE AGE OF THE ANALOGUES) FOR (A) BLOW HOLE, (B) BILLY, (C) PETIT ANNE, (D) MISTA AND (E) AURÉLIE. THE FIVE SITES STUDIED ARE REPRESENTED BY YELLOW STARS. THE CANADIAN PROVINCES OF QUEBEC AND NEWFOUNDLAND AND LABRADOR ARE SHOWN IN LIGHT GREEN

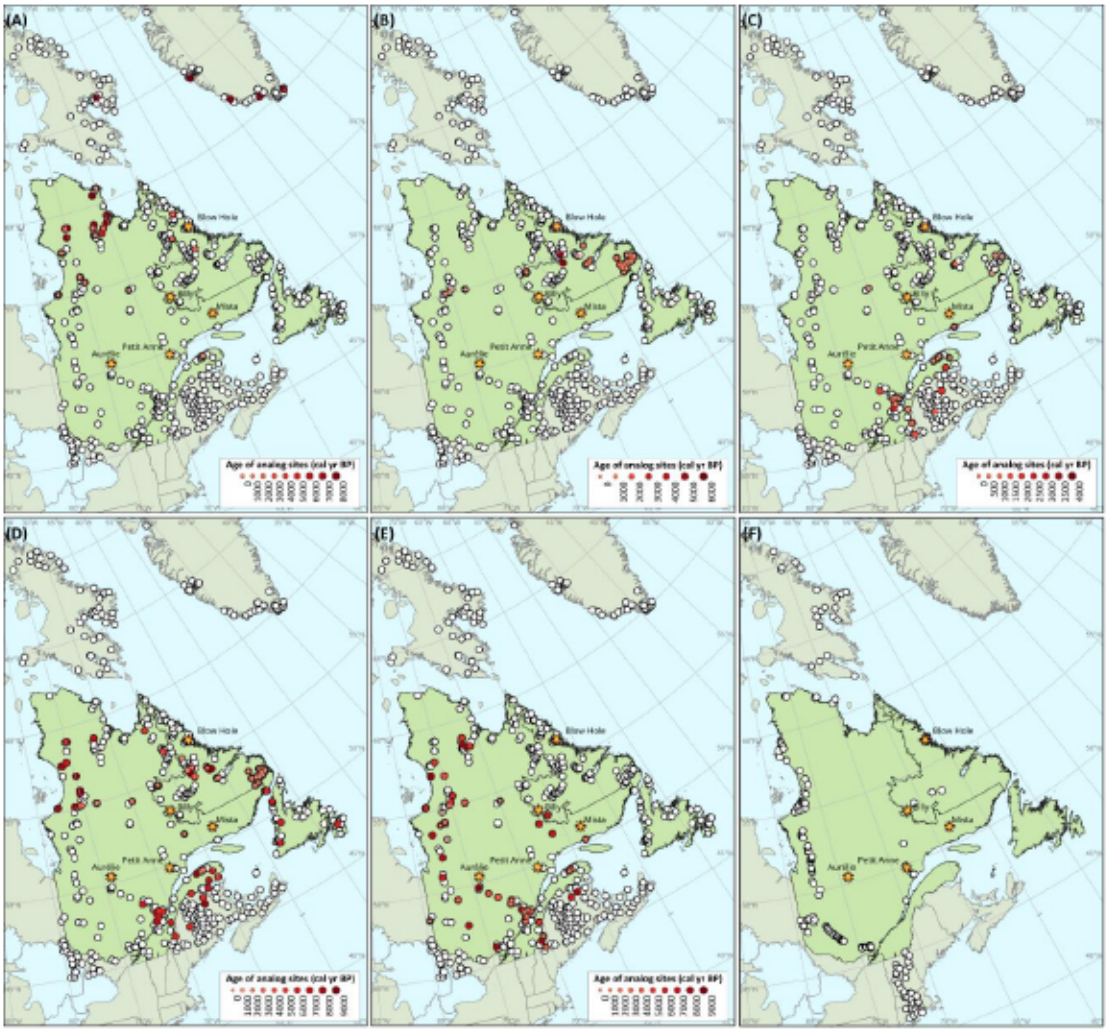

ANNEXE G – SIMPLIFIED POLLEN AND CHIRONOMID PERCENTAGE DIAGRAMS FOR BLOW HOLE LAKE WITH MSAT INFERENCES AND SIGNIFICANT ASSEMBLAGE ZONES FOR BOTH PROXIES. IN THE POLLEN DIAGRAM, ARBOREAL POLLEN ARE DISPLAYED IN GREEN, AND NON ARBOREAL POLLEN IN BROWN. PALE COLORS REPRESENT THE X5 EXAGGERATION CURVES. ONLY POLLEN GRAINS WHOSE PERCENTAGE EXCEEDS 0.5% AT LEAST ONCE ARE SHOWN

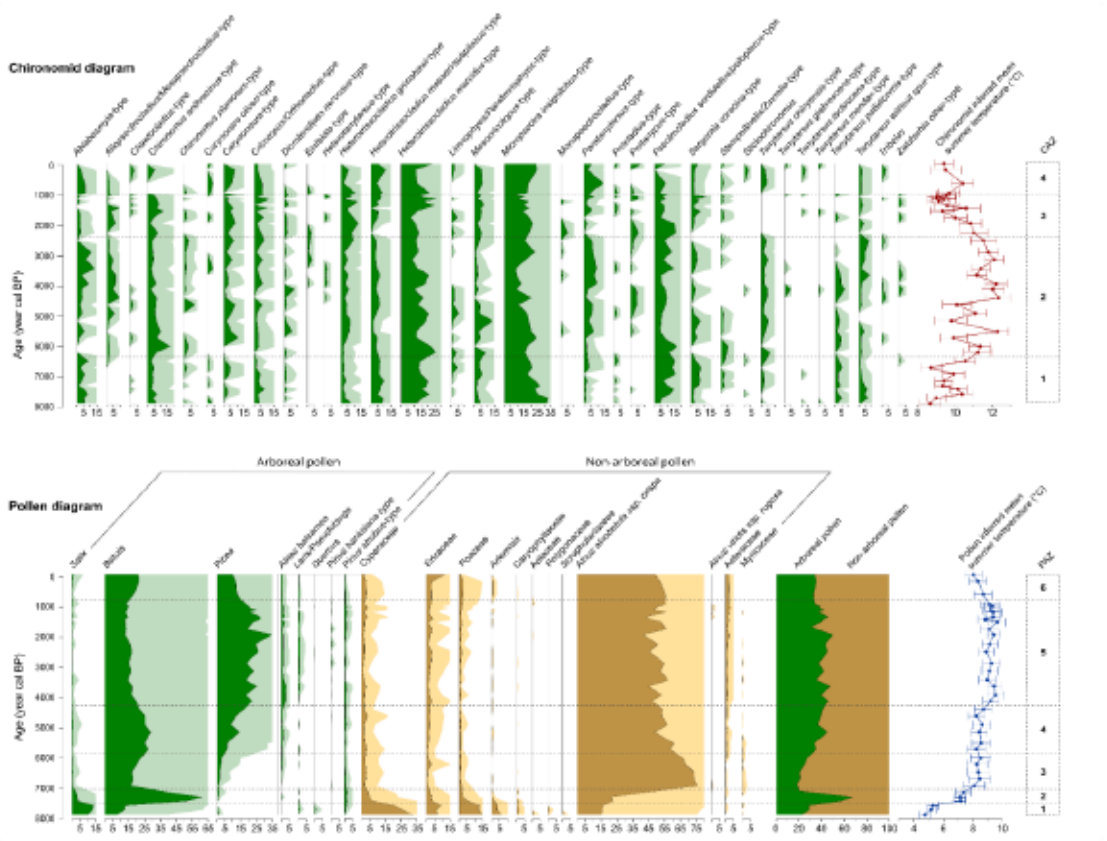

ANNEXE H – SIMPLIFIED POLLEN AND CHIRONOMID PERCENTAGE DIAGRAMS FOR BLOW HOLE LAKE WITH MSAT INFERENCES AND SIGNIFICANT ASSEMBLAGE ZONES FOR BOTH PROXIES. IN THE POLLEN DIAGRAM, ARBOREAL POLLEN ARE DISPLAYED IN GREEN, AND NON ARBOREAL POLLEN IN BROWN. PALE COLORS REPRESENT THE X5 EXAGGERATION CURVES. ONLY POLLEN GRAINS WHOSE PERCENTAGE EXCEEDS 0.5% AT LEAST ONCE ARE SHOWN

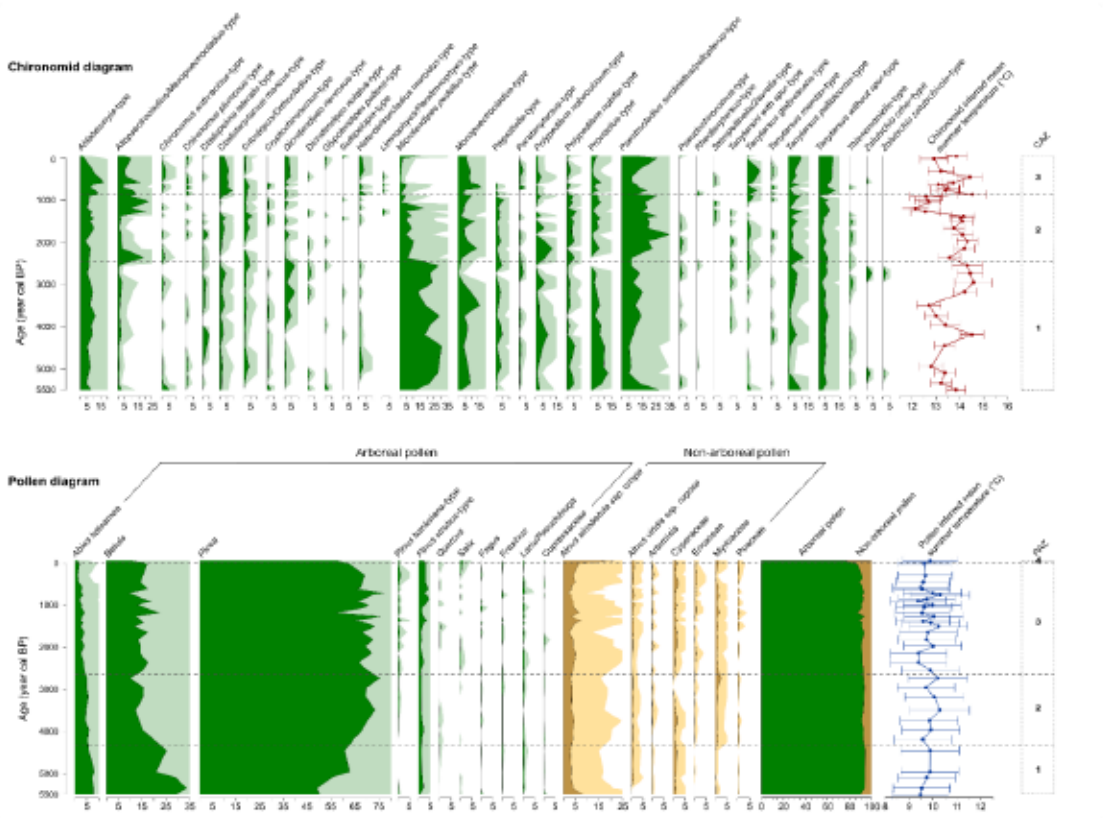

ANNEXE I – SIMPLIFIED POLLEN AND CHIRONOMID PERCENTAGE DIAGRAMS FOR PETIT ANNE LAKE WITH MSAT INFERENCES AND SIGNIFICANT ASSEMBLAGE ZONES FOR BOTH PROXIES. IN THE POLLEN DIAGRAM, ARBOREAL POLLEN ARE DISPLAYED IN GREEN, AND NON ARBOREAL POLLEN IN BROWN. PALE COLORS REPRESENT THE X5 EXAGGERATION CURVES. ONLY POLLEN GRAINS WHOSE PERCENTAGE EXCEEDS 0.5% AT LEAST ONCE ARE SHOWN

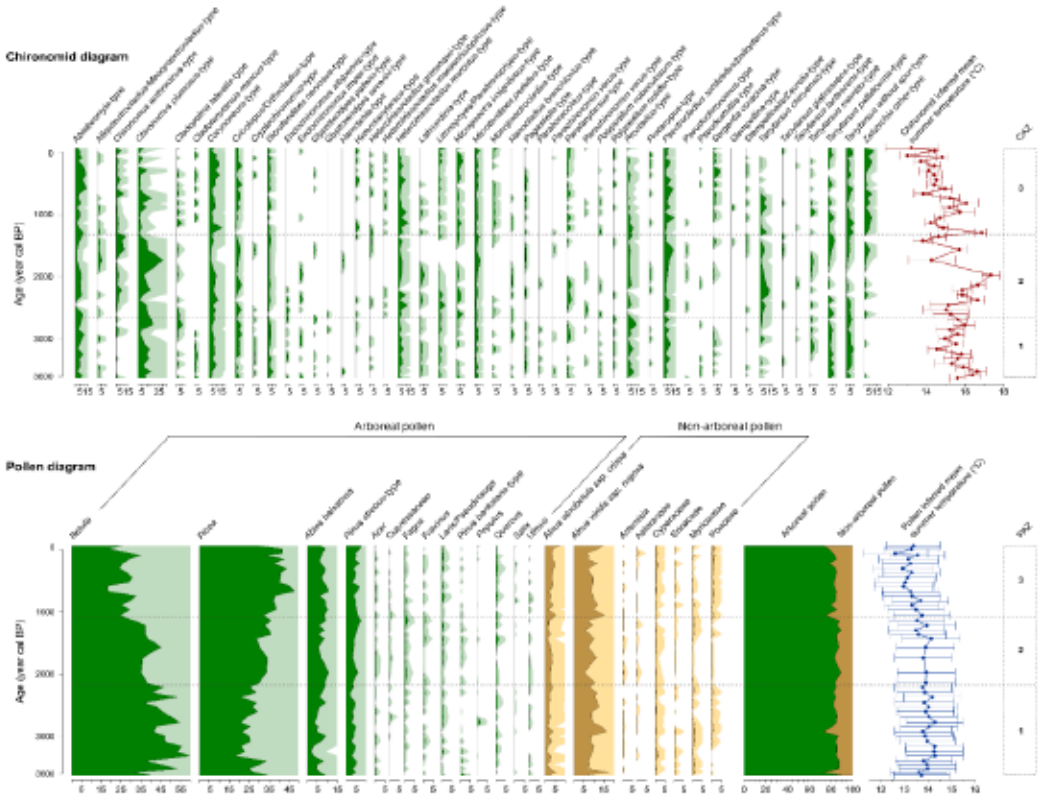

ANNEXE J – SIMPLIFIED POLLEN AND CHIRONOMID PERCENTAGE DIAGRAMS FOR MISTA LAKE WITH MSAT INFERENCES AND SIGNIFICANT ASSEMBLAGE ZONES FOR BOTH PROXIES. IN THE POLLEN DIAGRAM, ARBOREAL POLLEN ARE DISPLAYED IN GREEN, AND NON ARBOREAL POLLEN IN BROWN. PALE COLORS REPRESENT THE X5 EXAGGERATION CURVES. ONLY POLLEN GRAINS WHOSE PERCENTAGE EXCEEDS 0.5% AT LEAST ONCE ARE SHOWN

ANNEXE K – SIMPLIFIED POLLEN AND CHIRONOMID PERCENTAGE DIAGRAMS FOR AURÉLIE LAKE WITH MSAT INFERENCES AND SIGNIFICANT ASSEMBLAGE ZONES FOR BOTH PROXIES. IN THE POLLEN DIAGRAM, ARBOREAL POLLEN ARE DISPLAYED IN GREEN, AND NON ARBOREAL POLLEN IN BROWN. PALE COLORS REPRESENT THE X5 EXAGGERATION CURVES. ONLY POLLEN GRAINS WHOSE PERCENTAGE EXCEEDS 0.5% AT LEAST ONCE ARE SHOWN

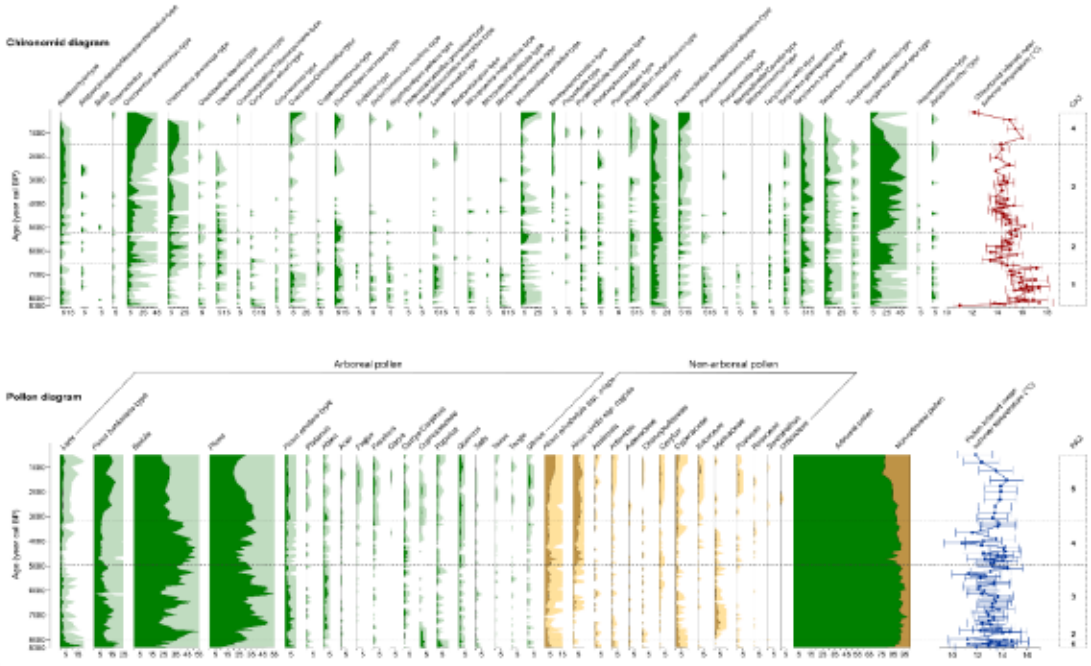

ANNEXE L – MEAN SUMMER AIR TEMPERATURE INFERENCES BASED ON CHIRONOMID ASSEMBLAGES. BLOW HOLE LAKE

CAZ1 (*ca*. 7900-6200 yr cal BP) was characterised by the prevalence of cold stenothermic species such as *Micropsectra insignilobus*-type, *Heterotrissocladius marcidus*-type, *Heterotrissocladius maeaeri/subpilosus*-type, and *Sergentia coracina*-type (Brooks et al., 2007; Medeiros et al., 2022) (Annexe G). The inferred MSAT during this period were relatively cold (8.8-10.6°C), although there was a simultaneous presence of more thermophilic taxa such as *Ablabesmyia* spp., *Chironomus anthracinus*-type, and *Psectrocladius sordidellus/psilopterus*-type (Brundin, 1949; Brooks et al., 2007). CAZ2 (*ca*. 6200-2300 yr cal BP) was marked by a two-step increase in MSAT. From *ca*. 6200 to 4500 yr cal BP, MSAT increased slightly, driven by a reduction of cold stenotherms (*Heterotrissocladius maeaeri/subpilosus*-type, *Micropsectra insignilobus*-type) and an increase in taxa with higher optima like *Corynoneura* spp., *Chironomus anthracinus*-type, and *Paratanytarsus* spp. (Brodersen et al., 2001). Then, from *ca*. 4500 to 2300 yr cal BP, there was a notable rise in taxa with high air temperature optima, including *Ablabesmyia* spp., *Tanytarsus* without spur-type, Tanytarsus *pallidicornis*-type, *Allopsectrocladius/Mesopsectrocladius* spp., coupled with a notable decrease in cold stenotherms such as *Mesocricotopus* spp., *Sergentia coracina*-type, and *Heterotrissocladius marcidus*-type (Walker and MacDonald, 1995; Brooks et al., 2007). As a result, inferred MSAT indicated a sharp rise of approximately 3°C. CAZ3 (*ca*. 2300 to 900 yr cal BP) was characterised by a gradual decrease in MSAT. This decline was attributed to the resurgence of taxa with a cold optimum, including *Mesocricotopus* spp., *Heterotrissocladius grimshawi*-type, *Heterotrissocladius maeaeri/subpilosus*-type, and *Corynocera oliveri*-type. Conversely, taxa with higher optima (*Psectrocladius sordidellus/psilopterus*-type, *Tanytarsus* without spur-type, *Ablabesmyia* spp.) exhibited a decreasing trend during this period. Finally, CAZ4 (*ca*. 900 yr cal BP to present) is marked by a slight increase of taxa with a low temperature optimum such as *Paratanytarsus* spp., *Heterotrissocladius maeaeri/subpilosus*-type and *Micropsectra insignilobus*-type (Brodin, 1986; Walker and MacDonald, 1995;

Brooks et al., 2007). At the same type, more thermophilic taxa such as *Ablabesmyia* spp. or *Tanytarsus chinyensis*-type (Brodin, 1986; Brooks et al., 2007) also increased in abundance, leading to slightly warmer MSAT inferences at the beginning of the zone, while the two more recent samples remained as low as those of CAZ3.

ANNEXE M – MEAN SUMMER AIR TEMPERATURE INFERENCES INFERENCES BASED ON CHIRONOMID ASSEMBLAGES. BILLY LAKE

CAZ1 (*ca*. 5500-2400 yr cal BP) was characterised by the large prevalence of *Microtendipes pedellus*-type (13-36%) (Annexe H). Additionally, taxa such as *Ablabesmyia* spp. and *Psectrocladius sordidellus/psilopterus*-type were extensively represented. Despite indicating relatively warm conditions, these taxa are also associated with acidophilic and productive environments (Larocque et al., 2006; Brooks et al., 2007; Fortin et al., 2015), suggesting that factors other than MSAT may have played a role in shaping chironomid assemblages. This zone exhibited notable climatic fluctuations, ranging from 12.7 to 14.6°C. CAZ2 (*ca*. 2400-900 yr cal BP), and was marked by the shift from a dominance of *Microtendipes pedellus*-type to *Psectrocladius sordidellus/psilopterus*-type and *Allopsectrocladius/Mesopsectrocladius* spp. The thermophilic taxa *Tanytarsus pallidicornis*-type and *Tanytarsus* without spur-type (Brodin, 1986; Brooks et al., 2007) were also present, each averaging ~5% in abundance. Although MSAT remained consistently high during this period, a notable cooling event occurred between 1300 and 900 yr cal BP, coinciding with a major increase in *Allopsectrocladius/Mesopsectrocladius* spp. These genera are typically found in macrophyte-rich, acidophilic lakes (Pinder and Morley, 1995; Brodersen et al., 2001; Brooks et al., 2007), suggesting a decrease in lake pH during this period. Finally, PAZ3 (*ca*. 900 yr cal BP to the present) was still characterised by the dominance of *Psectrocladius sordidellus/psilopterus*-type, along with an increase in taxa typical of warm, acidic lakes and littoral zones, such as *Ablabesmyia* spp., *Cladotanytarsus mancus*-type, *Dicrotendipes nervosus*-type, and *Tanytarsus glabrescens*-type. This zone was marked by an initial increase in inferred MSAT compared to the previous zone, followed by a decrease until the present day.

ANNEXE N – MEAN SUMMER AIR TEMPERATURE INFERENCES INFERENCES BASED ON CHIRONOMID ASSEMBLAGES. PETIT ANNE LAKE

CAZ1 (*ca*. 3600-2700 yr cal BP) was characterised by the prevalence of numerous thermophilic taxa, albeit in low abundance, including *Ablabesmyia* spp., *Chironomus plumosus*-type, *Tanytarsus pallidicornis*-type, and *Zalutschia* other-type (Brodin, 1986; Olander et al., 1997; Brooks et al., 2007), along with the presence of taxa with lower thermal optima such as *Heterotrissocladius marcidus*-type or *Sergentia coracina*-type (Brodin, 1986; Walker and MacDonald, 1995; Brooks et al., 2007) (Annexe I). The reconstructed MSAT during this period were relatively high, ranging from 14.5 to 16.7°C. In CAZ2 (*ca*. 2700-1300 yr cal BP), MSAT peaked at a maximum of 17.3°C *ca*. 2000 yr cal BP, before exhibiting a downward trend. The initial phase was marked by an increase in the abundance of thermophilic taxa like *Tanytarsus chinyensis*-type, *Microtendipes pedellus*-type, *Chironomus plumosus*-type, and *Ablabesmyia* spp. Subsequently, *Psectrocladius sordidellus/psilopterus*-type, *Chironomus plumosus*-type, *Chironomus anthracinus*-type, and *Zalutschia* other-type became dominant. Finally, CAZ3 (*ca*. 1300 yr cal BP to present) was marked by a sharp increase in cold-optimum taxa, including *Sergentia coracina*-type, *Heterotrissocladius marcidus*-type and *Heterotrissocladius maeaeri/subpilosus*-type. The inferred MSAT show a clear decreasing trend, although some thermophilic taxa such as *Ablabesmyia* spp., *Psectrocladius sordidellus/psilopterus*-type, and *Zalutschia* other-type remained largely represented.

ANNEXE O – MEAN SUMMER AIR TEMPERATURE INFERENCES INFERENCES BASED ON CHIRONOMID ASSEMBLAGES. MISTA LAKE

CAZ1 (*ca*. 8700-8100 yr cal BP) was characterised by the prevalence of cold stenotherms, including *Sergentia coracina*-type, *Corynocera oliveri*-type, *Micropsectra insignilobus*-type, and *Heterotrissocladius marcidus*-type (Annexe J). Consequently, reconstructed MSAT were relatively low, ranging from 8.1 to 12.3°C. In CAZ2 (*ca*. 8100-3800 yr cal BP), there was a notable decrease in the abundance of cold stenotherms and an increase in more thermophilic taxa such as *Ablabesmyia* spp., *Tanytarsus chinyensis*-type, *Microtendipes pedellus*-type, *Psectrocladius sordidellus/psilopterus*-type, and *Polypedilum nubeculosum*-type became more prevalent. The two latter are often associated with macrophytes or lake acidification (Brooks et al., 2007; Millet et al., 2012; Feussom Tcheumeleu et al., 2023), suggesting a potential impact on MSAT inferences. This shift was reflected in a MSAT increase (15-17°C) compared to the preceding period. CAZ3 (*ca*. 3800-1200 yr cal BP) was characterised by a substantial increase in *Sergentia coracina*-type, *Chironomus anthracinus*-type, and *Corynocera oliveri*-type taxa, indicative of cold mesotrophic lakes. Despite an overall decrease in MSAT compared to the previous zone, a slight upward trend was observed between *ca*. 2500 and *ca*. 1900 yr cal BP, coinciding with an increase in more thermophilic taxa such as *Ablabesmyia* spp. and *Tanytarsus* without spur-type. Finally, in CAZ4 (*ca*. 1200 yr cal BP to the present), there was a sharp increase in the cold stenotherm *Micropsectra insignilobus*-type (Brooks et al., 2007). Other taxa characteristic of similar environments, such as *Corynocera oliveri*-type, *Sergentia coracina*-type, and *Paratanytarsus* spp., were also well represented. Consequently, the reconstructions indicated a downward MSAT trend compared to the preceding period, with cold oligotrophic conditions in the lake (Brooks et al., 2007; Feussom Tcheumeleu et al., 2023).

ANNEXE P – MEAN SUMMER AIR TEMPERATURE INFERENCES INFERENCES BASED ON CHIRONOMID ASSEMBLAGES. AURELIE LAKE

CAZ1 (*ca*. 8300-6600 yr cal BP) was characterised by the dominance of thermophilic taxa such as *Dicrotendipes nervosus*-type, *Procladius* spp., *Polypedilum nubeculosum*-type, *Tanytarsus mendax*-type, *Pseudochironomus* spp., and *Lauterborniella* spp. (Brooks et al., 2007), indicating warm MSAT and potentially oligotrophic conditions in the lake during this period (Annexe K). However, the three oldest samples in the sequence, dominated by cold-optima taxa like *Chironomus anthracinus*-type, *Corynocera oliveri*-type, and *Micropsectra radialis*-type (Brodin, 1986; Brooks et al., 2007), reflected cold conditions following the deglaciation (Dalton et al., 2020). CAZ2 (*ca*. 6600-5100 yr cal BP) was marked by a substantial increase in *Tanytarsus* without spur-type (25-45%), along with taxa exhibiting low MSAT optima such as *Chironomus anthracinus*-type and *Tanytarsus lugens*-type. Concurrently, taxa with higher optima like *Chironomus plumosus*-type and *Cladotanytarsus mancus*-type (Brodin, 1986; Brooks et al., 2007) were also present, reflecting unstable climatic conditions during this period (Bajolle et al., 2018). As a result, reconstructed MSAT showed more variability than the previous zone, with slightly cooler MSAT. CAZ3 (*ca*. 5100-1500 yr cal BP) was marked by the resurgence of *Tanytarsus* without spur-type. Reconstructed MSAT were slightly cooler than the previous period due to an increase of cold stenotherms such as *Tanytarsus lugens*-type. Finally, CAZ4 (*ca*. 1500 yr cal BP to the present) was characterised by the replacement of *Tanytarsus* without spur-type dominance (correlated with *Tanytarsus lugens*-type in this record) by *Chironomus anthracinus*-type and *Chironomus plumosus*-type, indicating an improvement of climatic conditions but also a possible increase in lake eutrophication (Hofmann, 1988; Brooks et al., 2007; Bajolle et al., 2018). The latest sample showed a further increase in cold taxa (*Cricotopus*/*Orthocladius* spp., *Heterotrissocladius marcidus*-type) and a sharp decrease in reconstructed MSAT.

ANNEXE Q – MEAN SUMMER AIR TEMPERATURE INFERENCES INFERENCES BASED ON POLLEN ASSEMBLAGES. BLOW HOLE LAKE

Following the deglaciation (PAZ1, *ca*. 7900-7500 yr cal BP), the landscape was dominated by a tundra vegetation, made of herbaceous (*e.g*. Cyperaceae, Poaceae, Artemisia, Caryophyllaceae) and dwarf-shrub (Ericaceae) taxa, along with Salix (Annexe G). This composition led to inferred cold MSAT ranging from 4.3 to 5.3°C. These taxa sharply declined in abundance as afforestation began, accompanied by a rapid increase in *Betula* spp., reaching nearly 65% relative abundance during PAZ2 (*ca*. 7500-7000 yr cal BP). This shift was reflected in a pronounced increase in MSAT, ranging between 6 and 8°C. In PAZ3 (*ca*. 7000-5900 yr cal BP), *Alnus alnobetula* ssp. *crispa* replaced *Betula* spp., and *Picea* began to develop. This led to high MSAT inference, which showed a stagnation between 8 and 8.5°C in this zone. During PAZ4 (*ca*. 5900-4200 yr cal BP), *Picea* and *Betula* experienced rapid increases in percentage (reaching 29 and 25% relative abundance, respectively), while *Alnus alnobetula* ssp. *crispa* showed an opposite trend, resulting in a slight increase in MSAT. At the beginning of PAZ5 (*ca*. 4200-800 yr cal BP), *Picea* and *Abies* increased in abundance, while *Betula* spp. decreased and stabilised at around 15% relative abundance. These changes led to a ~1°C increase in summer temperature inference in the first part of this zone. Subsequently, MSAT declined towards the end of the zone, a tendency continuing into PAZ6 (*ca*. 800 yr cal BP to present). This decrease in MSAT coincided with a reduction in *Picea* abundance and an increase in *Betula* spp., herbaceous taxa and Ericaceae over the same period.

ANNEXE R – MEAN SUMMER AIR TEMPERATURE INFERENCES INFERENCES BASED ON POLLEN ASSEMBLAGES. BILLY LAKE

PAZ1 (*ca*. 5500-4300 yr cal BP) was marked by the highest abundances of *Abies* (~8%) and *Betula* (~34%) of the sequence (Annexe H). Conversely, *Picea* exhibited its lowest abundance (~50%), leading to MSAT inference of 9.5-10°C. In PAZ2 (*ca*. 4300-2700 yr cal BP), both *Abies* and *Betula* spp. experienced a decline in abundance (to 5 and 10% relative abundance, respectively), while *Picea* underwent a rapid increase, surpassing 70% in abundance. Throughout this period, MSAT inferences showed minor changes compared to the preceding zone. During PAZ3 (*ca*. 2700-0 yr cal BP), the abundance of *Picea* and *Betula* remained relatively constant, whereas that of *Abies* continued to decrease. In parallel, *Pinus strobus*-type increased rapidly in abundance, from 2% in PAZ2 to 5% in PAZ3. Despite greater variability than before, MSAT reconstructed remained relatively constant during this phase. PAZ4, (*ca*. 0 yr cal BP to present), represented only the most recent sample. During this phase, there was a notable decline in *Picea* and *Betula*, accompanied by a sharp increase in *Alnus alnobetula* spp. *crispa* (from 6 to 22% relative abundance). Despite these vegetation changes, temperature inference showed no major change compared to the previous pollen zone.

ANNEXE S – MEAN SUMMER AIR TEMPERATURE INFERENCES INFERENCES BASED ON POLLEN ASSEMBLAGES. PETIT ANNE LAKE

PAZ1 (*ca*. 3600-2150 yr cal BP) was characterised by a high abundance of *Betula* (35-60% relative abundance) and *Picea* (20-35% relative abundance) (Annexe I). *Abies*, *Pinus strobus*-type, *Alnus alnobetula* ssp. *crispa* and *Alnus viridis* ssp. *rugosa* were also represented although in lesser proportions. Inferences remained relatively stable throughout this period, indicating MSAT between 13.5 and 15°C. Then, PAZ2 (*ca*. 2150-1100 yr cal BP) showed a gradual decrease in *Betula* spp. from 40 to 27% relative abundance, and an increase in *Picea* (from 27 to 34% relative abundance), while the other taxa remained in similar proportions. This was reflected by a slight decline in MSAT reconstructed during this period. Finally, CAZ3 (*ca*. 1100 yr cal BP to present) was marked by the lowest percentages of *Betula* spp. in the sequence (18-35% relative abundance) and the highest percentages of *Picea* (30-48% relative abundance), *Abies* (6-11% relative abundance) and herbaceous taxa. Temperature inference indicated a gradual decrease in MSAT by about 1.5°C over this period.

ANNEXE T – MEAN SUMMER AIR TEMPERATURE INFERENCES INFERENCES BASED ON POLLEN ASSEMBLAGES. MISTA LAKE

Following the deglaciation, PAZ1 (*ca.* 8700-8100 yr cal BP) was characterised by a progressive afforestation, marked by high percentages of *Picea* along with representations of *Betula*, *Alnus alnobetula* ssp. *crispa*, and *Populus* spp. (Annexe J). Inferences showed cold temperature, ranging from 8.5 to 10°C. PAZ2 (*ca.* 8100-7900 yr cal BP) was marked by a drastic decrease in *Picea* percentages (~20% relative abundance), accompanied by a sharp increase in *Abies* (from 0 to 46% relative abundance) and *Betula* spp., as well as *Carpinus*/*Ostrya*. MSAT during this period rose by approximately 4°C. *Picea* percentages reached their minimum (5-16% relative abundance) in PAZ3 (*ca.* 7900-6800 yr cal BP), while those of *Betula* increased sharply, and many thermophilic taxa (*Ostrya*/*Carpinus*, *Corylus*, *Fraxinus*, *Alnus viridis* ssp. *rugosa*) reached a maximum. Despite a slight decrease at the beginning of the zone, MSAT remained high during this period. PAZ4 (*ca.* 6800-4900 yr cal BP) was characterised by the highest percentages of *Betula* (66% relative abundance) in the sequence, accompanied by a sharp increase in *Picea*, from 11 to 38% relative abundance. Conversely, thermophilic taxa from PAZ3 sharply decreased. Temperature inference showed MSAT ranging between 11 and 15°C, with high-amplitude intersample difference. PAZ5 (*ca.* 4900-1800 yr cal BP) was marked by a rapid increase in *Picea* abundance, along with a parallel increase in *Alnus alnobetula* ssp. *crispa* and a decrease in *Betula* from 45 to 15% relative abundance. At the beginning of PAZ5, MSAT reconstructed by the MAT sharply fell (9.5-10°C) before stabilising in PAZ6. In this zone (*ca.* 1800-300 yr cal BP), *Picea* decreased again, while *Betula*, *Abies*, *Carya*, and *Alnus alnobetula* ssp. *crispa* increased in abundance. MSAT reconstructed also rose slightly during the second half of this phase. Finally, PAZ7 (*ca.* 300 yr cal BP to present) showed a sharp increase in *Picea*, reaching its maximum abundance of the sequence (~84%), while *Betula* spp., *Abies*, *Carya*, and *Alnus alnobetula* ssp. *crispa* reached their minimum. Reconstructed MSAT remained relatively stable during this period.

ANNEXE U – MEAN SUMMER AIR TEMPERATURE INFERENCES INFERENCES BASED ON POLLEN ASSEMBLAGES. AURELIE LAKE

PAZ1 (*ca*. 8300-8000 yr cal BP) was characterised by the prevalence of *Larix*, *Pinus banksiana*-type, *Betula* spp., and *Picea*, with additional presence of *Pinus strobus*-type, *Populus*, *Alnus alnobetula* ssp. *crispa*, and Cyperaceae in smaller proportions (Annexe K). Temperature inferences showed low MSAT, but with high inter-sample variability. In PAZ2 (*ca*. 8000-7400 yr cal BP), there was a notable decline in *Larix*, *Pinus banksiana*-type, and *Populus*, while *Betula* spp. and *Picea* exhibited a simultaneous sharp increase, reaching 55% and 37% in abundance, respectively. Reconstructions for this period closely resemble those of the preceding zone. In PAZ3 (*ca*. 7400-5000 yr cal BP), *Picea* reached its maximum abundance (50%) but displayed sharp fluctuations, as well as *Betula* and *Pinus banksiana*-type. *Myrica* also experienced a sharp increase (from 0 to 5% relative abundance), and MAT reconstruction provided very close MSAT estimates (12-13.8°C) compared to the previous PAZ, but with lower intersample variability. PAZ4 (*ca*. 5000-3100 yr cal BP) was characterised by a pronounced increase in *Betula* and a concurrent decrease in conifers (*Larix*, *Pinus strobus*-type and *Pinus banksiana*-type, *Picea*), resulting in a slight MSAT increase compared to PAZ4. In contrast, PAZ5 (*ca*. 3500 yr cal BP to present) was marked by further expansion of conifers and *Alnus alnobetula* ssp. *crispa*, accompanied by a slight decrease in *Betula*. Temperature reconstruction indicated a slight MSAT increase during the first half of PAZ5, before decreasing until the current period.

ANNEXE V – COMPARISON OF R-SQUARES FOR MSAT IN EACH MONTH OF THE YEAR OBTAINED USING DCA, PCA AND CA

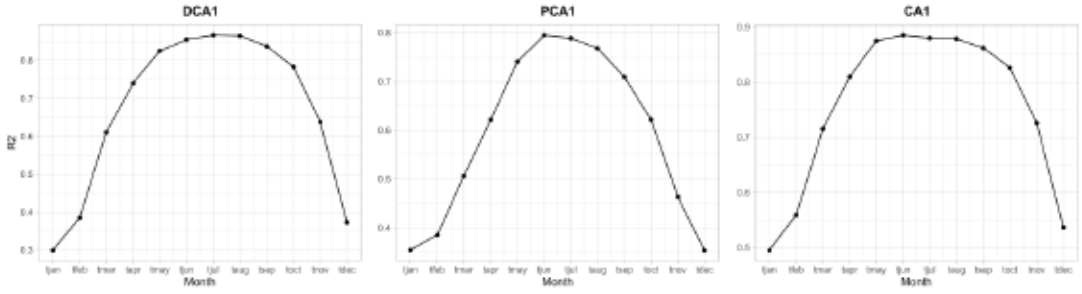

LISTE DE RÉFÉRENCES

Aakala, T. et al., 2018, Multiscale variation in drought controlled historical forest fire activity in the boreal forests of eastern Fennoscandia: Ecological Monographs, v. 88, p. 74–91, doi:10.1002/ecm.1276.

Abràmoff, M.D., Magalhães, P.J., and Ram, S.J., 2004, Image Processing with ImageJ: Biophotonics international, v. 11, p. 36–42.

Aleman, J.C. et al., 2013, Tracking land-cover changes with sedimentary charcoal in the Afrotropics: The Holocene, v. 23, p. 1853–1862, doi:10.1177/0959683613508159.

Ali, A.A. et al., 2012, Control of the multimillennial wildfire size in boreal North America by spring climatic conditions: Proceedings of the National Academy of Sciences, v. 109, p. 20966–20970, doi:10.1073/pnas.1203467109.

Ali, A.A., Asselin, H., Larouche, A.C., Bergeron, Y., Carcaillet, C., and Richard, P.J.H., 2008, Changes in fire regime explain the Holocene rise and fall of Abies balsamea in the coniferous forests of western Québec, Canada: The Holocene, v. 18, p. 693–703, doi:10.1177/0959683608091780.

Ali, A.A., Carcaillet, C., and Bergeron, Y., 2009a, Long-term fire frequency variability in the eastern Canadian boreal forest: the influences of climate vs. local factors: Global Change Biology, v. 15, p. 1230–1241, doi:10.1111/j.1365-2486.2009.01842.x.

Ali, A.A., Higuera, P.E., Bergeron, Y., and Carcaillet, C., 2009b, Comparing fire-history interpretations based on area, number and estimated volume of macroscopic charcoal in lake sediments: Quaternary Research, v. 72, p. 462–468, doi:10.1016/j.yqres.2009.07.002.

Allen, C.R., Angeler, D.G., Garmestani, A.S., Gunderson, L.H., and Holling, C.S., 2014, Panarchy: Theory and Application: Ecosystems, v. 17, p. 578–589, doi:10.1007/s10021-013-9744-2.

Alvarez-Uria, P., and Körner, C., 2007, Low temperature limits of root growth in deciduous and evergreen temperate tree species: Functional ecology, v. 21, p. 211–218, doi:10.1111/j.1365-2435.2007.01231.x.

Ameray, A., Cavard, X., and Bergeron, Y., 2023, Climate change may increase Quebec boreal forest productivity in high latitudes by shifting its current composition: Frontiers in Forests and Global Change, v. 6, p. 1020305, doi:10.3389/ffgc.2023.1020305.

Anderson, T.W., Levac, E., and Lewis, C.F.M., 2007, Cooling in the Gulf of St. Lawrence and estuary region at 9.7 to 7.2 14C ka (11.2–8.0 cal ka): Palynological response to the PBO and 8.2 cal ka cold events, Laurentide Ice Sheet air-mass circulation and enhanced freshwater runoff: Palaeogeography, Palaeoclimatology, Palaeoecology, v. 246, p. 75–100, doi:10.1016/j.palaeo.2006.10.028.

Appleby, P.G., Oldfield, F., Thompson, R., Huttunen, P., and Tolonen, K., 1979, 210Pb dating of annually laminated lake sediments from Finland: Nature, v. 280, p. 53–55, doi:10.1038/280053a0.

Arrhenius, S., 1896, XXXI. On the influence of carbonic acid in the air upon the temperature of the ground: The London, Edinburgh, and Dublin Philosophical Magazine and Journal of Science, v. 41, p. 237–276, doi:10.1080/14786449608620846.

Asselin, H., and Payette, S., 2005, Late Holocene Opening of the Forest Tundra Landscape in Northern Québec, Canada: Global Ecology and Biogeography, v. 14, p. 307–313, doi:10.1111/j.1466-822x.2005.00157.x.

Asselin, H., Payette, S., Fortin, M.-J., and Vallée, S., 2003, The northern limit of Pinus banksiana Lamb. in Canada: explaining the difference between the eastern and western distributions: Journal of Biogeography, v. 30, p. 1709–1718, doi:10.1046/j.1365-2699.2003.00935.x.

Astrup, R., Bernier, P.Y., Genet, H., Lutz, D.A., and Bright, R.M., 2018, A sensible climate solution for the boreal forest: Nature Climate Change, v. 8, p. 11–12, doi:10.1038/s41558-017-0043-3.

Augustin, F., Girardin, M.P., Terrier, A., Grondin, P., Lambert, M.-C., Leduc, A., and Bergeron, Y., 2022, Projected changes in fire activity and severity feedback in the spruce–feather moss forest of western Quebec, Canada: Trees, Forests and People, v. 8, p. 100229, doi:10.1016/j.tfp.2022.100229.

Axford, Y., Briner, J.P., Cooke, C.A., Francis, D.R., Michelutti, N., Miller, G.H., Smol, J.P., Thomas, E.K., Wilson, C.R., and Wolfe, A.P., 2009, Recent changes in a remote Arctic lake are unique within the past 200,000 years: Proceedings of the National Academy of Sciences, v. 106, p. 18443–18446, doi:10.1073/pnas.0907094106.

Bajolle, L., Larocque-Tobler, I., Ali, A.A., Lavoie, M., Bergeron, Y., and Gandouin, E., 2019, A chironomid-inferred Holocene temperature record from a shallow Canadian boreal lake: potentials and pitfalls: Journal of Paleolimnology, v. 61, p. 69–84, doi:10.1007/s10933-018-0045-9.

Bajolle, L., Larocque-Tobler, I., Gandouin, E., Lavoie, M., Bergeron, Y., and Ali, A.A., 2018, Major postglacial summer temperature changes in the central

coniferous boreal forest of Quebec (Canada) inferred using chironomid assemblages: Journal of Quaternary Science, v. 33, p. 409–420, doi:10.1002/jqs.3022.

Baldwin, K. et al., 2020, Zones de végétation du Canada: une perspective biogéoclimatique:, https://epe.lac-bac.gc.ca/100/201/301/weekly_acquisitions_list-ef/2022/22-04/publications.gc.ca/collections/collection_2022/rncan-nrcan/Fo123-2-25-2020-fra.pdf (accessed April 2022).

Baltzer, J.L. et al., 2021, Increasing fire and the decline of fire adapted black spruce in the boreal forest: Proceedings of the National Academy of Sciences, v. 118, p. e2024872118, doi:10.1073/pnas.2024872118.

Baltzer, J.L., Veness, T., Chasmer, L.E., Sniderhan, A.E., and Quinton, W.L., 2014, Forests on thawing permafrost: fragmentation, edge effects, and net forest loss: Global Change Biology, v. 20, p. 824–834, doi:10.1111/gcb.12349.

Barber, K., Maddy, D., Rose, N., Stevenson, A., Stoneman, R., and Thompson, R., 2000, Replicated proxy-climate signals over the last 2000 yr from two distant UK peat bogs: new evidence for regional palaeoclimate teleconnections: Quaternary Science Reviews, v. 19, p. 481–487.

Bastianelli, C., 2018, Changements globaux et dynamiques forestières des pessières du Québec au cours des 8000 dernières années à partir d'approches paléoécologiques et biogéochimiques [These de doctorat]: Paris Sciences et Lettres (ComUE), https://www.theses.fr/2018PSLEP044 (accessed February 2024).

Bastianelli, C., Ali, A.A., Beguin, J., Bergeron, Y., Grondin, P., Hély, C., and Paré, D., 2017, Boreal coniferous forest density leads to significant variations in soil physical and geochemical properties: Biogeosciences, v. 14, p. 3445–3459, doi:10.5194/bg-14-3445-2017.

Battarbee, R.W., John Anderson, N., Jeppesen, E., and Leavitt, P.R., 2005, Combining palaeolimnological and limnological approaches in assessing lake ecosystem response to nutrient reduction: Freshwater Biology, v. 50, p. 1772–1780, doi:10.1111/j.1365-2427.2005.01427.x.

Battles, J., Robards, T., Das, A., Waring, K., Gilless, J., Schurr, F., LeBlanc, J., Biging, G., and Simon, C., 2006, Climate change impact on forest resources. A report from: California Climate Change Center.:

Belcher, C.M., New, S.L., Santín, C., Doerr, S.H., Dewhirst, R.A., Grosvenor, M.J., and Hudspith, V.A., 2018, What Can Charcoal Reflectance Tell Us About Energy Release in Wildfires and the Properties of Pyrogenic Carbon? Frontiers in Earth Science, v. 6, p. 169, doi:10.3389/feart.2018.00169.

Bellemin-Noël, B., Bourassa, S., Despland, E., De Grandpré, L., and Pureswaran, D.S., 2021, Improved performance of the eastern spruce budworm on black spruce as warming temperatures disrupt phenological defences: Global Change Biology, v. 27, p. 3358–3366, doi:10.1111/gcb.15643.

Bennett, K.D., 1996, Determination of the number of zones in a biostratigraphical sequence: New Phytologist, v. 132, p. 155–170, doi:10.1111/j.1469-8137.1996.tb04521.x.

Berger, A., and Loutre, M.-F., 1991, Insolation values for the climate of the last 10 million years: Quaternary Science Reviews, v. 10, p. 297–317, doi:https://doi.org/10.1016/0277-3791(91)90033-Q.

Bergeron, Y. et al., 2006, Past, current, and future fire frequencies in Quebec's commercial forests: implications for the cumulative effects of harvesting and fire on age- class structure and natural disturbance-based management1,2: v. 36, p. 8, doi:10.1139/x06-177.

Bergeron, Y., and Archambault, S., 1993, Decreasing frequency of forest fires in the southern boreal zone of Québec and its relation to global warming since the end of the "Little Ice Age": The Holocene, v. 3, p. 255–259, doi:10.1177/095968369300300307.

Bergeron, Y., Gauthier, S., Flannigan, M., and Kafka, V., 2004, Fire regimes at the transition between mixedwood and coniferous boreal forest in northwestern Quebec: Ecology, v. 85, p. 1916–1932, doi:10.1890/02-0716.

Bergeron, Y., Gauthier, S., Kafka, V., Lefort, P., and Lesieur, D., 2001, Natural fire frequency for the eastern Canadian boreal forest: consequences for sustainable forestry: Canadian Journal of Forest Research, v. 31, p. 384–391, doi:10.1139/x00-178.

Bergeron, Y., Leduc, A., Harvey, B., and Gauthier, S., 2002, Natural fire regime: a guide for sustainable management of the Canadian boreal forest: Silva Fennica, v. 36, doi:10.14214/sf.553.

Berkes, F., and Davidson-Hunt, I.J., 2006, Biodiversity, traditional management systems, and cultural landscapes: examples from the boreal forest of Canada: International Social Science Journal, v. 58, p. 35–47, doi:10.1111/j.1468-2451.2006.00605.x.

Beug, H.-J., 1961, Leitfaden der Pollenbestimmung für Mitteleuropa und angrenzende Gebiete:

Bigras, F.J., and Bertrand, A., 2006, Responses of Picea mariana to elevated CO2 concentration during growth, cold hardening and dehardening: phenology,

cold tolerance, photosynthesis and growth: Tree Physiology, v. 26, p. 875–888, doi:10.1093/treephys/26.7.875.

Bird, M.I., Ascough, P.L., Young, I.M., Wood, C.V., and Scott, A.C., 2008, X-ray microtomographic imaging of charcoal: Journal of Archaeological Science, v. 35, p. 2698–2706, doi:10.1016/j.jas.2008.04.018.

Birks, H.H., and Birks, H.J.B., 2006, Multi-proxy studies in palaeolimnology: Vegetation History and Archaeobotany, v. 15, p. 235–251, doi:10.1007/s00334-006-0066-6.

Birks, H.J.B., Line, J.M., Juggins, S., Stevenson, A.C., and Braak, C.J.F.T., 1990, Diatoms and pH Reconstruction: Philosophical Transactions of the Royal Society of London. Series B, Biological Sciences, v. 327, p. 263–278, doi:10.1098/rstb.1990.0062.

Blaauw, M., 2010, Methods and code for 'classical' age-modelling of radiocarbon sequences: Quaternary Geochronology, v. 5, p. 512–518, doi:10.1016/j.quageo.2010.01.002.

Blaauw, M., Christen, J.A., Lopez, M.A.A., Vazquez, J.E., Belding, T., Theiler, J., Gough, B., Karney, C., Rcpp, L., and Blaauw, M.M., 2021, Package 'rbacon':

Blarquez, O., Ali, A.A., Girardin, M.P., Grondin, P., Fréchette, B., Bergeron, Y., and Hély, C., 2015, Regional paleofire regimes affected by non-uniform climate, vegetation and human drivers: Scientific Reports, v. 5, p. 13356, doi:10.1038/srep13356.

Blarquez, O., Girardin, M.P., Leys, B., Ali, A.A., Aleman, J.C., Bergeron, Y., and Carcaillet, C., 2013, Paleofire reconstruction based on an ensemble-member strategy applied to sedimentary charcoal: Geophysical Research Letters, v. 40, p. 2667–2672, doi:10.1002/grl.50504.

Blarquez, O., Talbot, J., Paillard, J., Lapointe-Elmrabti, L., Pelletier, N., and Gates St-Pierre, C., 2018, Late Holocene influence of societies on the fire regime in southern Québec temperate forests: Quaternary Science Reviews, v. 180, p. 63–74, doi:10.1016/j.quascirev.2017.11.022.

Blarquez, O., Vannière, B., Marlon, J.R., Daniau, A.-L., Power, M.J., Brewer, S., and Bartlein, P.J., 2014, paleofire: An R package to analyse sedimentary charcoal records from the Global Charcoal Database to reconstruct past biomass burning: Computers & Geosciences, v. 72, p. 255–261, doi:10.1016/j.cageo.2014.07.020.

Bobek, P. et al., 2019, Divergent fire history trajectories in Central European temperate forests revealed a pronounced influence of broadleaved trees on

fire dynamics: Quaternary Science Reviews, v. 222, p. 105865, doi:10.1016/j.quascirev.2019.105865.

Bogdanski, B., 2008, Canada's boreal forest economy: economic and socioeconomic issues and research opportunities. Inf. Rep: BC-X-414. Natural Resources Canada, Canadian Forest Service, Pacific ….

Bond, W.J., Woodward, F.I., and Midgley, G.F., 2005, The global distribution of ecosystems in a world without fire: New Phytologist, v. 165, p. 525–538, doi:10.1111/j.1469-8137.2004.01252.x.

Bonsal, B.R., Wheaton, E.E., Chipanshi, A.C., Lin, C., Sauchyn, D.J., and Wen, L., 2011, Drought research in Canada: A review: Atmosphere-Ocean, v. 49, p. 303–319, doi:10.1080/07055900.2011.555103.

Borcard, D., Gillet, F., Legendre, P., Borcard, D., Gillet, F., and Legendre, P., 2018, Canonical ordination: Numerical ecology with R, p. 203–297.

Borcard, D., Legendre, P., and Drapeau, P., 1992, Partialling out the Spatial Component of Ecological Variation: Ecology, v. 73, p. 1045–1055, doi:10.2307/1940179.

Bouchard, M., Kneeshaw, D., and Bergeron, Y., 2006, Forest Dynamics After Successive Spruce Budworm Outbreaks in Mixedwood Forests: Ecology, v. 87, p. 2319–2329, doi:10.1890/0012-9658(2006)87[2319:FDASSB]2.0.CO;2.

Bouchard, M., Pothier, D., and Gauthier, S., 2008, Fire return intervals and tree species succession in the North Shore region of eastern Quebec: Canadian Journal of Forest Research, v. 38, p. 1621–1633, doi:10.1139/X07-201.

Boulanger, Y., and Arseneault, D., 2004, Spruce budworm outbreaks in eastern Quebec over the last 450 years: Canadian Journal of Forest Research, v. 34, p. 1035–1043, doi:10.1139/x03-269.

Boulanger, Y., Girardin, M., Bernier, P.Y., Gauthier, S., Beaudoin, A., and Guindon, L., 2017, Changes in mean forest age in Canada's forests could limit future increases in area burned but compromise potential harvestable conifer volumes: Canadian Journal of Forest Research, v. 47, p. 755–764, doi:10.1139/cjfr-2016-0445.

Boulanger, Y., Gray, D.R., Cooke, B.J., and De Grandpr'e, L., 2016, Model-specification uncertainty in future forest pest outbreak: Global Change Biology, v. 22, p. 1595–1607.

Boulanger, Y., and Pascual Puigdevall, J., 2021, Boreal forests will be more severely affected by projected anthropogenic climate forcing than mixedwood and

northern hardwood forests in eastern Canada: Landscape Ecology, v. 36, p. 1725–1740, doi:https://doi.org/10.1007/s10980-021-01241-7.

Bova, S., Rosenthal, Y., Liu, Z., Godad, S.P., and Yan, M., 2021, Seasonal origin of the thermal maxima at the Holocene and the last interglacial: Nature, v. 589, p. 548–553, doi:10.1038/s41586-020-03155-x.

Boyle, J., Chiverrell, R., Plater, A., Thrasher, I., Bradshaw, E., Birks, H., and Birks, J., 2013, Soil mineral depletion drives early Holocene lake acidification: Geology, v. 41, p. 415–418, doi:10.1130/G33907.1.

ter Braak, C.J.F., and Prentice, I.C., 2004, A Theory of Gradient Analysis, *in* Advances in Ecological Research, Elsevier, v. 34, p. 235–282, doi:10.1016/S0065-2504(03)34003-6.

Bradshaw, R.H.W., 1981, Modern Pollen-Representation Factors for Woods in South-East England: Journal of Ecology, v. 69, p. 45–70, doi:10.2307/2259815.

Brandt, J.P., 1995, Forest Insect-and Disease-caused Impacts to Timber Resources of West-central Canada, 1988-1992: Canadian Forest Service, Northern Forestry Centre, v. 341.

Brandt, J.P., Flannigan, M.D., Maynard, D.G., Thompson, I.D., and Volney, W.J.A., 2013, An introduction to Canada's boreal zone: ecosystem processes, health, sustainability, and environmental issues: v. 21, p. 20, doi:10.1139/er-2013-0040.

Brecka, A.F.J., Shahi, C., and Chen, H.Y.H., 2018, Climate change impacts on boreal forest timber supply: Forest Policy and Economics, v. 92, p. 11–21, doi:10.1016/j.forpol.2018.03.010.

Briner, J.P. et al., 2016a, Holocene climate change in Arctic Canada and Greenland: Quaternary Science Reviews, v. 147, p. 340–364, doi:10.1016/j.quascirev.2016.02.010.

Briner, J.P. et al., 2016b, Holocene climate change in Arctic Canada and Greenland: Quaternary Science Reviews, v. 147, p. 340–364, doi:10.1016/j.quascirev.2016.02.010.

Brodersen, K.P., Odgaard, B.V., Vestergaard, O., and Anderson, N.J., 2001, Chironomid stratigraphy in the shallow and eutrophic Lake Søbygaard, Denmark: chironomid–macrophyte co-occurrence: Freshwater Biology, v. 46, p. 253–267, doi:10.1046/j.1365-2427.2001.00652.x.

Brodin, Y.W., 1986, The postglacial history of Lake Flarken, southern Sweden, interpreted from subfossil insect remains: Internationale Revue der Gesamten

Hydrobiologie und Hydrographie, v. 71, p. 371–432, doi:10.1002/iroh.19860710313.

Bronson, D.R., Gower, S.T., Tanner, M., and Van Herk, I., 2009, Effect of ecosystem warming on boreal black spruce bud burst and shoot growth: Global Change Biology, v. 15, p. 1534–1543, doi:10.1111/j.1365-2486.2009.01845.x.

Brooks, S.J., and Birks, H.J.B., 2001, Chironomid-inferred air temperatures from Lateglacial and Holocene sites in north-west Europe: progress and problems: Quaternary Science Reviews, v. 20, p. 1723–1741, doi:10.1016/S0277-3791(01)00038-5.

Brooks, J.R., Flanagan, L.B., and Ehleringer, J.R., 1998, Responses of boreal conifers to climate fluctuations: indications from tree-ring widths and carbon isotope analyses: Canadian Journal of Forest Research, v. 28, p. 524–533.

Brooks, S.J., Langdon, P.G., and Heiri, O., 2007, The identification and use of Palaearctic Chironomidae larvae in palaeoecology: Quaternary Research Association Technical Guide, p. i–vi.

Brossier, B., Oris, F., Finsinger, W., Asselin, H., Bergeron, Y., and Ali, A.A., 2014, Using tree-ring records to calibrate peak detection in fire reconstructions based on sedimentary charcoal records: The Holocene, v. 24, p. 635–645, doi:10.1177/0959683614526902.

Brown, R.D., and Mote, P.W., 2009, The Response of Northern Hemisphere Snow Cover to a Changing Climate*: Journal of Climate, v. 22, p. 2124–2145, doi:10.1175/2008JCLI2665.1.

Burns, R.M., Honkala, B.H., and others, 1990, Silvics of North America. Volume 1. Conifers.: Agriculture Handbook (Washington),.

Burton, P.J., 2003, Towards sustainable management of the boreal forest: NRC Research Press.

Burton, P., Messier, C., Weetman, G., Prepas, E.E., Adamowicz, L., and Tittler, R., 2003, The current state of boreal forestry and the drive for change, *in* p. 1–40.

Burton, P.J., Parisien, M.-A., Hicke, J.A., Hall, R.J., and Freeburn, J.T., 2008, Large fires as agents of ecological diversity in the North American boreal forest: International Journal of Wildland Fire, v. 17, p. 754, doi:10.1071/WF07149.

Cahoon, S.M.P., Sullivan, P.F., Brownlee, A.H., Pattison, R.R., Andersen, H.-E., Legner, K., and Hollingsworth, T.N., 2018, Contrasting drivers and trends of coniferous and deciduous tree growth in interior Alaska: Ecology, v. 99, p. 1284–1295, doi:10.1002/ecy.2223.

Camill, P., Lynch, J.A., Clark, J.S., Adams, J.B., and Jordan, B., 2001, Changes in biomass, aboveground net primary production, and peat accumulation following permafrost thaw in the boreal peatlands of Manitoba, Canada: Ecosystems, v. 4, p. 461–478.

Campbell, J.L. et al., 2009, Consequences of climate change for biogeochemical cycling in forests of northeastern North AmericaThis article is one of a selection of papers from NE Forests 2100: A Synthesis of Climate Change Impacts on Forests of the Northeastern US and Eastern Canada.: Canadian Journal of Forest Research, v. 39, p. 264–284, doi:10.1139/X08-104.

Campbell, I.D., 1999, Quaternary pollen taphonomy: examples of differential redeposition and differential preservation: Palaeogeography, Palaeoclimatology, Palaeoecology, v. 149, p. 245–256, doi:10.1016/S0031-0182(98)00204-1.

Canadian Forest Service, 2010, The State of Canada's Forests, Annual Report 2010.: Natural Resources Canada, Canadian Forest Service, Headquarters, Ottawa, p. 45.

Capellán-Pérez, I., Arto, I., Polanco-Martínez, J.M., González-Eguino, M., and Neumann, M.B., 2016, Likelihood of climate change pathways under uncertainty on fossil fuel resource availability: Energy & Environmental Science, v. 9, p. 2482–2496, doi:10.1039/C6EE01008C.

Cappuccino, N., Lavertu, D., Bergeron, Y., and Régnière, J., 1998, Spruce budworm impact, abundance and parasitism rate in a patchy landscape: Oecologia, v. 114, p. 236–242, doi:10.1007/s004420050441.

Carcaillet, C., 2007, Charred Particle Analysis: Encyclopedia of Quaternary Science, p. 1582–1593, doi:10.1016/B0-44-452747-8/00187-3.

Carcaillet, C., Bergeron, Y., Richard, P.J.H., Fréchette, B., Gauthier, S., and Prairie, Y.T., 2001, Change of fire frequency in the eastern Canadian boreal forests during the Holocene: does vegetation composition or climate trigger the fire regime?: *Holocene fire frequency changes in Canadian boreal forests*: Journal of Ecology, v. 89, p. 930–946, doi:10.1111/j.1365-2745.2001.00614.x.

Carcaillet, C., and Richard, P., 2000, Holocene changes in seasonal precipitation highlighted by fire incidence in eastern Canada: Climate Dynamics, v. 16, p. 549–559.

Carlson, A.E., LeGrande, A.N., Oppo, D.W., Came, R.E., Schmidt, G.A., Anslow, F.S., Licciardi, J.M., and Obbink, E.A., 2008, Rapid early Holocene deglaciation of the Laurentide ice sheet: Nature Geoscience, v. 1, p. 620–624, doi:10.1038/ngeo285.

Chagnon, C., Wotherspoon, A.R., and Achim, A., 2022, Deciphering the black spruce response to climate variation across eastern Canada using a meta-analysis approach: Forest Ecology and Management, v. 520, p. 120375, doi:10.1016/j.foreco.2022.120375.

Chang, C.Y.-Y., Bräutigam, K., Hüner, N.P.A., and Ensminger, I., 2021, Champions of winter survival: cold acclimation and molecular regulation of cold hardiness in evergreen conifers: New Phytologist, v. 229, p. 675–691, doi:10.1111/nph.16904.

Chapin, F.S., Callaghan, T.V., Bergeron, Y., Fukuda, M., Johnstone, J., Juday, G., and Zimov, S., 2004, Global change and the boreal forest: thresholds, shifting states or gradual change? AMBIO: A Journal of the Human Environment, v. 33, p. 361–365, doi:doi.org/10.1579/0044-7447-33.6.361.

Chasmer, L., and Hopkinson, C., 2017, Threshold loss of discontinuous permafrost and landscape evolution: Global Change Biology, v. 23, p. 2672–2686, doi:10.1111/gcb.13537.

Chaste, E., Girardin, M.P., Kaplan, J.O., Bergeron, Y., and Hély, C., 2019, Increases in heat-induced tree mortality could drive reductions of biomass resources in Canada's managed boreal forest: Landscape Ecology, doi:10.1007/s10980-019-00780-4.

Chavardès, R.D., Balducci, L., Bergeron, Y., Grondin, P., Poirier, V., Morin, H., and Gennaretti, F., 2023, Greater tree species diversity and lower intraspecific competition attenuate impacts from temperature increases and insect epidemics in boreal forests of western Quebec, Canada: Canadian Journal of Forest Research, v. 53, p. 48–59, doi:10.1139/cjfr-2022-0114.

Chavardès, R.D., Gennaretti, F., Grondin, P., Cavard, X., Morin, H., and Bergeron, Y., 2021, Role of Mixed-Species Stands in Attenuating the Vulnerability of Boreal Forests to Climate Change and Insect Epidemics: Frontiers in Plant Science, v. 12, p. 658880, doi:10.3389/fpls.2021.658880.

Chen, C., Weiskittel, A., Bataineh, M., and MacLean, D.A., 2017, Even low levels of spruce budworm defoliation affect mortality and ingrowth but net growth is more driven by competition: Canadian Journal of Forest Research, v. 47, p. 1546–1556, doi:10.1139/cjfr-2017-0012.

Chevalier, M. et al., 2020, Pollen-based climate reconstruction techniques for late Quaternary studies: Earth-Science Reviews, v. 210, p. 103384, doi:10.1016/j.earscirev.2020.103384.

Christoffersen, P., Tulaczyk, S., Wattrus, N.J., Peterson, J., Quintana-Krupinski, N., Clark, C.D., and Sjunneskog, C., 2008, Large subglacial lake beneath the

Laurentide Ice Sheet inferred from sedimentary sequences: Geology, v. 36, p. 563, doi:10.1130/G24628A.1.

Clark, J.S., 1990, Fire and Climate Change During the Last 750 Yr in Northwestern Minnesota: Ecological Monographs, v. 60, p. 135–159, doi:10.2307/1943042.

Clark, J.S., and Hussey, T.C., 1996, Estimating the mass flux of charcoal from sedimentary records: effects of particle size, morphology, and orientation: The Holocene, v. 6, p. 129–144, doi:10.1177/095968369600600201.

Clark, J.S., and Royall, P.D., 1996, Local and Regional Sediment Charcoal Evidence for Fire Regimes in Presettlement North-Eastern North America: The Journal of Ecology, v. 84, p. 365, doi:10.2307/2261199.

Clément, D., 1995, Why is taxonomy utilitarian? Journal of Ethnobiology, v. 15, p. 1–44.

Cleve, K.V., Yarie, J., Erickson, R., and Dyrness, C.T., 1993, Nitrogen mineralization and nitrification in successional ecosystems on the Tanana River floodplain, interior Alaska: Canadian Journal of Forest Research, v. 23, p. 970–978, doi:10.1139/x93-125.

Conedera, M., Tinner, W., Neff, C., Meurer, M., Dickens, A.F., and Krebs, P., 2009, Reconstructing past fire regimes: methods, applications, and relevance to fire management and conservation: Quaternary Science Reviews, v. 28, p. 555–576, doi:10.1016/j.quascirev.2008.11.005.

Coops, N.C., Hermosilla, T., Wulder, M.A., White, J.C., and Bolton, D.K., 2018, A thirty year, fine-scale, characterization of area burned in Canadian forests shows evidence of regionally increasing trends in the last decade (E. G. Lamb, Ed.): PLOS ONE, v. 13, p. e0197218, doi:10.1371/journal.pone.0197218.

Costanza, R., De Groot, R., Sutton, P., Van Der Ploeg, S., Anderson, S.J., Kubiszewski, I., Farber, S., and Turner, R.K., 2014, Changes in the global value of ecosystem services: Global Environmental Change, v. 26, p. 152–158, doi:10.1016/j.gloenvcha.2014.04.002.

Costanza, R., and Limburg, K., 1997, The value of the world's ecosystem: Nature, v. 387, p. 8.

Côté, D., Girard, F., Hébert, F., Bouchard, S., Gagnon, R., and Lord, D., 2013, Is the closed-crown boreal forest resilient after successive stand disturbances? A quantitative demonstration from a case study: Journal of Vegetation Science, v. 24, p. 664–674, doi:10.1111/j.1654-1103.2012.01488.x.

Couillard, P.-L., Payette, S., Lavoie, M., and Frégeau, M., 2021, Precarious resilience of the boreal forest of eastern North America during the Holocene: Forest Ecology and Management, v. 485, p. 118954, doi:10.1016/j.foreco.2021.118954.

Couillard, P.-L., Payette, S., Lavoie, M., and Laflamme, J., 2019, La forêt boréale du Québec : influence du gradient longitudinal: Le Naturaliste canadien, v. 143, p. 18–32, doi:10.7202/1060052ar.

Crawford, A.J., and Belcher, C.M., 2016, Area–volume relationships for fossil charcoal and their relevance for fire history reconstruction: The Holocene, v. 26, p. 822–826, doi:10.1177/0959683615618264.

Cyr, D., Gauthier, S., and Bergeron, Y., 2007, Scale-dependent determinants of heterogeneity in fire frequency in a coniferous boreal forest of eastern Canada: Landscape Ecology, v. 22, p. 1325–1339, doi:10.1007/s10980-007-9109-3.

Cyr, D., Splawinski, T.B., Pascual Puigdevall, J., Valeria, O., Leduc, A., Thiffault, N., Bergeron, Y., and Gauthier, S., 2022, Mitigating post-fire regeneration failure in boreal landscapes with reforestation and variable retention harvesting: At what cost? Canadian Journal of Forest Research, v. 52, p. 568–581, doi:10.1139/cjfr-2021-0180.

Dalton, A.S. et al., 2020, An updated radiocarbon-based ice margin chronology for the last deglaciation of the North American Ice Sheet Complex: Quaternary Science Reviews, v. 234, p. 106223, doi:10.1016/j.quascirev.2020.106223.

D'Arrigo, R., Wilson, R., Liepert, B., and Cherubini, P., 2008, On the 'Divergence Problem' in Northern Forests: A review of the tree-ring evidence and possible causes: Global and Planetary Change, v. 60, p. 289–305, doi:10.1016/j.gloplacha.2007.03.004.

De Grandpré, L., Archambault, L., and Morissette, J., 2000, Early understory successional changes following clearcutting in the balsam fir-yellow birch forest: Écoscience, v. 7, p. 92–100, doi:10.1080/11956860.2000.11682577.

Dean, W.E., 1974, Determination of carbonate and organic matter in calcareous sediments and sedimentary rocks by loss on ignition; comparison with other methods: Journal of Sedimentary Research, v. 44, p. 242–248, doi:10.1306/74D729D2-2B21-11D7-8648000102C1865D.

Denneler, B., Asselin, H., Bergeron, Y., and Begin, Y., 2008, D ecreased fire frequency and increased water levels affect riparian forest dynamics in southwestern boreal Quebec, Canada: Canadian Journal of Forest Research, v. 38, p. 1083–1094.

Desponts, M., and Payette, S., 1992, Recent dynamics of jack pine at its northern distribution limit in northern Quebec: Canadian Journal of Botany, v. 70, p. 1157–1167, doi:10.1139/b92-144.

Djamali, M., and Cilleros, K., 2020, Statistically significant minimum pollen count in Quaternary pollen analysis; the case of pollen-rich lake sediments: Review of Palaeobotany and Palynology, v. 275, p. 104156, doi:10.1016/j.revpalbo.2019.104156.

D'Orangeville, L., Duchesne, L., Houle, D., Kneeshaw, D., Côté, B., and Pederson, N., 2016, Northeastern North America as a potential refugium for boreal forests in a warming climate: Science, v. 352, p. 1452–1455, doi:10.1126/science.aaf4951.

D'Orangeville, L., Houle, D., Duchesne, L., Phillips, R.P., Bergeron, Y., and Kneeshaw, D., 2018, Beneficial effects of climate warming on boreal tree growth may be transitory: Nature Communications, v. 9, p. 3213, doi:10.1038/s41467-018-05705-4.

Drake, B.G., Gonzàlez-Meler, M.A., and Long, S.P., 1997, More efficient plants: A Consequence of Rising Atmospheric CO_2? Annual Review of Plant Physiology and Plant Molecular Biology, v. 48, p. 609–639, doi:10.1146/annurev.arplant.48.1.609.

Drobyshev, I., Simard, M., Bergeron, Y., and Hofgaard, A., 2010, Does Soil Organic Layer Thickness Affect Climate–Growth Relationships in the Black Spruce Boreal Ecosystem? Ecosystems, v. 13, p. 556–574, doi:10.1007/s10021-010-9340-7.

Dukes, J.S. et al., 2009, Responses of insect pests, pathogens, and invasive plant species to climate change in the forests of northeastern North America: What can we predict?This article is one of a selection of papers from NE Forests 2100: A Synthesis of Climate Change Impacts on Forests of the Northeastern US and Eastern Canada.: Canadian Journal of Forest Research, v. 39, p. 231–248, doi:10.1139/X08-171.

Duveneck, M.J., Scheller, R.M., White, M.A., Handler, S.D., and Ravenscroft, C., 2014, Climate change effects on northern Great Lake (USA) forests: A case for preserving diversity: Ecosphere, v. 5, p. art23, doi:10.1890/ES13-00370.1.

Dyke, A.S., 2004, An outline of North American deglaciation with emphasis on central and northern Canada, *in* Developments in Quaternary Sciences, Elsevier, v. 2, p. 373–424, doi:10.1016/S1571-0866(04)80209-4.

Ecological Stratification Working Group, 1995, A national ecological framework for Canada: Centre for Land and Biological Resources Research; Hull, Quebec.

Epler, J., Ekrem, T., and Cranston, P., 2013, The larvae of Chironominae (Diptera: Chironomidae) of the Holarctic region–keys and diagnoses: Andersen, T., Cranston, PS & Epler, JH (Sci. Eds.), The larvae of Chironomidae (Diptera) of the Holarctic Region—Keys and diagnoses. Insect Systematics & Evolution, v. 66, p. 387–556.

Ettinger, A.K., and HilleRisLambers, J., 2013, Climate isn't everything: Competitive interactions and variation by life stage will also affect range shifts in a warming world: American Journal of Botany, v. 100, p. 1344–1355, doi:10.3732/ajb.1200489.

Ewing, H.A., and Nater, E.A., 2002, Holocene Soil Development on Till and Outwash Inferred from Lake-Sediment Geochemistry in Michigan and Wisconsin: Quaternary Research, v. 57, p. 234–243, doi:10.1006/qres.2001.2303.

Faegri, K., Iversen, J., Kaland, P.E., and Krzywinski, K., 1989, Textbook of pollen analysis. Caldwell:

FAO, 2012, Agriculture organization of the United Nations. 2012: FAO statistical yearbook,.

Farrar, J., 1995, Trees in Canada. Fitzhenry & Whiteside Ltd., Markham, Ont., and Canadian Forest Service: Natural Resources Canada, Ottawa, Ont, p. 106–107.

Fenton, N.J., and Bergeron, Y., 2006, Sphagnum Spore Availability in Boreal Forests: The Bryologist, v. 109, p. 173–181, doi:10.1639/0007-2745(2006)109[173:SSAIBF]2.0.CO;2.

Feussom Tcheumeleu, A., Millet, L., Rius, D., Ali, A.A., Bergeron, Y., Grondin, P., Gauthier, S., and Blarquez, O., 2023, An 8500-year history of climate-fire-vegetation interactions in the eastern maritime black spruce–moss bioclimatic domain, Québec, Canada: Écoscience, p. 1–17, doi:10.1080/11956860.2023.2292354.

Field, C.B., Barros, V.R., and IPCC (Eds.), 2014, Climate change 2014: impacts, adaptation, and vulnerability: Working Group II contribution to the fifth assessment report of the Intergovernmental Panel on Climate Change: New York, NY, Cambridge University Press, 1 p.

Fierravanti, A., Cocozza, C., Palombo, C., Rossi, S., Deslauriers, A., and Tognetti, R., 2015, Environmental-mediated relationships between tree growth of black spruce and abundance of spruce budworm along a latitudinal transect in Quebec, Canada: Agricultural and Forest Meteorology, v. 213, p. 53–63, doi:10.1016/j.agrformet.2015.06.014.

Filion, L., Saint-Laurent, D., Desponts, M., and Payette, S., 1991, The late Holocene record of aeolian and fire activity in northern Québec, Canada: The Holocene, v. 1, p. 201–208.

Finsinger, W., and Bonnici, I., 2022, Tapas: An R Package to Perform Trend and Peaks Analysis: Zenodo. Available online: https://hal. inria. fr/hal-03607000/,.

Finsinger, W., Kelly, R., Fevre, J., and Magyari, E.K., 2014, A guide to screening charcoal peaks in macrocharcoal-area records for fire-episode reconstructions: The Holocene, v. 24, p. 1002–1008, doi:10.1177/0959683614534737.

Flannigan, M.D., Krawchuk, M.A., de Groot, W.J., Wotton, B.M., and Gowman, L.M., 2009, Implications of changing climate for global wildland fire: International Journal of Wildland Fire, v. 18, p. 483, doi:10.1071/WF08187.

Flannigan, M.D., Logan, K.A., Amiro, B.D., Skinner, W.R., and Stocks, B.J., 2005, Future Area Burned in Canada: Climatic Change, v. 72, p. 1–16, doi:10.1007/s10584-005-5935-y.

Flannigan, M.D., Stocks, B.J., and Wotton, B.M., 2000, Climate change and forest fires: Science of The Total Environment, v. 262, p. 221–229, doi:10.1016/S0048-9697(00)00524-6.

Flannigan, M.D., and Wotton, B.M., 2001, Climate, weather, and area burned, *in* Forest fires, Elsevier, p. 351–373, https://10.1016/B978-012386660-8/50012-X.

Fleming, R.A., Candau, J.-N., and McAlpine, R.S., 2002, Landscape-scale analysis of interactions between insect defoliation and forest fire in central Canada: Climatic Change, v. 55, p. 251–272, doi:10.1023/A:1020299422491.

Flower, A., and Smith, D.J., 2011, A dendroclimatic reconstruction of June–July mean temperature in the northern Canadian Rocky Mountains: Dendrochronologia, v. 29, p. 55–63, doi:10.1016/j.dendro.2010.10.001.

Foley, J.A. et al., 2005, Global Consequences of Land Use: Science, v. 309, p. 570–574.

Fortin, M.-C., Medeiros, A.S., Gajewski, K., Barley, E.M., Larocque-Tobler, I., Porinchu, D.F., and Wilson, S.E., 2015, Chironomid-environment relations in northern North America: Journal of Paleolimnology, v. 54, p. 223–237, doi:10.1007/s10933-015-9848-0.

Foster, D.R., 1983a, The history and pattern of fire in the boreal forest of southeastern Labrador: Canadian Journal of Botany, v. 61, p. 2459–2471, doi:10.1139/b83-269.

Foster, D.R., 1983b, The Phytosociology, Fire History, and Vegetation Dynamics of the Boreal Forest of Southeastern Labrador, Canada [Ph.D.]: 208 p., https://www.proquest.com/docview/303162317/abstract/30F76EABF11E400DPQ/1 (accessed June 2022).

Foster, D.R., and King, G.A., 1986, Vegetation Pattern and Diversity in S.E. Labrador, Canada: Betula Papyrifera (Birch) Forest Development in Relation to Fire History and Physiography: The Journal of Ecology, v. 74, p. 465, doi:10.2307/2260268.

Fourcade, T., Goñi, M.F.S., Lesven, J., Lahaye, C., and Philippe, A., 2024, Vegetation response in NW Mediterranean borderlands to the millennial-scale climate variability of the last glacial period: Quaternary Science Reviews, v. 334, p. 108722.

Fréchette, B., Ensminger, I., Bergeron, Y., and Berninger, F., 2011, Will changes in root-zone temperature in boreal spring affect recovery of photosynthesis in Picea mariana and Populus tremuloides in a future climate? Tree Physiology, v. 31, p. 1204–1216, doi:doi:10.1093/treephys/tpr102.

Fréchette, B., Richard, P., Grondin, P., Lavoie, M., and Larouche, A., 2018, Histoire postglaciaire de la végétation et du climat des pessières et des sapinières de l'ouest du Québec:

Fréchette, B., Richard, P.J., Lavoie, M., Grondin, P., and Larouche, A.C., 2021, Histoire post glaciaire de la végétation et du climat des pessières et des sapinières de l'est du Québec et du Labrador méridional: Gouvernement du Québec, ministère des Forêts, de la Faune et des Parcs, Direction de la recherche forestière. Mémoire de recherche forestière, p. 170.

Fuentealba, A., Pureswaran, D., Bauce, É., and Despland, E., 2017, How does synchrony with host plant affect the performance of an outbreaking insect defoliator? Oecologia, v. 184, p. 847–857, doi:10.1007/s00442-017-3914-4.

Gaboriau, D.M., Chaste, É., Girardin, M.P., Asselin, H., Ali, A.A., Bergeron, Y., and Hély, C., 2023, Interactions within the climate-vegetation-fire nexus may transform 21st century boreal forests in northwestern Canada: iScience, v. 26, p. 106807, doi:10.1016/j.isci.2023.106807.

Gaboriau, D.M., Remy, C.C., Girardin, M.P., Asselin, H., Hély, C., Bergeron, Y., and Ali, A.A., 2020, Temperature and fuel availability control fire size/severity in the boreal forest of central Northwest Territories, Canada: Quaternary Science Reviews, v. 250, p. 106697, doi:10.1016/j.quascirev.2020.106697.

Gajewski, K., 2019, Environmental history of the northwestern Québec Treeline: Quaternary Science Reviews, v. 206, p. 29–43, doi:10.1016/j.quascirev.2018.12.025.

Gajewski, K., 2015, Quantitative reconstruction of Holocene temperatures across the Canadian Arctic and Greenland: Global and Planetary Change, v. 128, p. 14–23, doi:10.1016/j.gloplacha.2015.02.003.

Gajewski, K., and Atkinson, D.A., 2003, Climatic change in northern Canada: Environmental Reviews, v. 11, p. 69–102, doi:10.1139/a03-006.

Gajewski, K., Grenier, A., and Payette, S., 2021, Climate, fire and vegetation history at treeline east of Hudson Bay, northern Québec: Quaternary Science Reviews, v. 254, p. 106794, doi:10.1016/j.quascirev.2021.106794.

Gajewski, K., Payette, S., and Ritchie, J.C., 1993, Holocene Vegetation History at the Boreal-Forest--Shrub-Tundra Transition in North-Western Quebec: Journal of Ecology, v. 81, p. 433–443, doi:10.2307/2261522.

Gamache, I., and Payette, S., 2004, Height growth response of tree line black spruce to recent climate warming across the forest-tundra of eastern Canada: Journal of Ecology, v. 92, p. 835–845, doi:10.1111/j.0022-0477.2004.00913.x.

Garralla, S., and Gajewski, K., 1992, Holocene vegetation history of the boreal forest near Chibougamau, central Quebec: Canadian Journal of Botany, v. 70, p. 1364–1368.

Gaumont-Guay, D., Black, T.A., Barr, A.G., Jassal, S., and Nesic, Z., 2008, Biophysical controls on rhizospheric and heterotrophic components of soil respiration in a boreal black spruce stand: v. 28.

Gauthier, S., Bernier, P., Kuuluvainen, T., Shvidenko, A.Z., and Schepaschenko, D.G., 2015, Boreal forest health and global change: Science, v. 349, p. 819–822, doi:10.1126/science.aaa9092.

Gavin, D.G., Hallett, D.J., Hu, F.S., Lertzman, K.P., Prichard, S.J., Brown, K.J., Lynch, J.A., Bartlein, P., and Peterson, D.L., 2007, Forest fire and climate change in western North America: insights from sediment charcoal records: , p. 8.

Gavin, D.G., Hu, F.S., Lertzman, K., and Corbett, P., 2006, Weak climatic control of stand-scale fire history during the late holocene: Ecology, v. 87, p. 1722–1732, doi:10.1890/0012-9658(2006)87[1722:WCCOSF]2.0.CO;2.

Gedalof, Z., and Berg, A.A., 2010, Tree ring evidence for limited direct CO2 fertilization of forests over the 20th century: Global Biogeochemical Cycles, v. 24, doi:10.1029/2009GB003699.

Genet, M. et al., 2021, Modern relationships between microscopic charcoal in marine sediments and fire regimes on adjacent landmasses to refine the

interpretation of marine paleofire records: An Iberian case study: Quaternary Science Reviews, v. 270, p. 107148, doi:10.1016/j.quascirev.2021.107148.

Gibson, C.M., Chasmer, L.E., Thompson, D.K., Quinton, W.L., Flannigan, M.D., and Olefeldt, D., 2018, Wildfire as a major driver of recent permafrost thaw in boreal peatlands: Nature Communications, v. 9, p. 3041, doi:10.1038/s41467-018-05457-1.

Gillett, N.P., Weaver, A.J., Zwiers, F.W., and Flannigan, M.D., 2004, Detecting the effect of climate change on Canadian forest fires: Geophysical Research Letters, v. 31, doi:10.1029/2004GL020876.

Giovanni, G., 1994, The effect of fire on soil quality: Soil erosion and degradation as a consequence of forest fires'.(Eds M Sala, JL Rubio) pp, v. 27, p. 15–27, doi:DOI.org (Crossref).

Girard, F., Payette, S., and Gagnon, R., 2008, Rapid expansion of lichen woodlands within the closed-crown boreal forest zone over the last 50 years caused by stand disturbances in eastern Canada: Journal of Biogeography, v. 35, p. 529–537, doi:10.1111/j.1365-2699.2007.01816.x.

Girardin, M.P. et al., 2016a, No growth stimulation of Canada's boreal forest under half-century of combined warming and CO2 fertilization: Proceedings of the National Academy of Sciences, v. 113, p. E8406–E8414, doi:10.1073/pnas.1610156113.

Girardin, M.P., Ali, A.A., Carcaillet, C., Blarquez, O., Hély, C., Terrier, A., Genries, A., and Bergeron, Y., 2013a, Vegetation limits the impact of a warm climate on boreal wildfires: New Phytologist, v. 199, p. 1001–1011, doi:10.1111/nph.12322.

Girardin, M.P., Ali, A.A., Carcaillet, C., Gauthier, S., Hély, C., Le Goff, H., Terrier, A., and Bergeron, Y., 2013b, Fire in managed forests of eastern Canada: Risks and options: Forest Ecology and Management, v. 294, p. 238–249, doi:10.1016/j.foreco.2012.07.005.

Girardin, M.P., Guo, X.J., Gervais, D., Metsaranta, J., Campbell, E.M., Arsenault, A., Isaac-Renton, M., and Hogg, E.H., 2022, Cold-season freeze frequency is a pervasive driver of subcontinental forest growth: Proceedings of the National Academy of Sciences, v. 119, p. e2117464119, doi:10.1073/pnas.2117464119.

Girardin, M.P., Hogg, E.H., Bernier, P.Y., Kurz, W.A., Guo, X.J., and Cyr, G., 2016b, Negative impacts of high temperatures on growth of black spruce forests intensify with the anticipated climate warming: Global Change Biology, v. 22, p. 627–643, doi:10.1111/gcb.13072.

Girardin, M.P., and Mudelsee, M., 2008, Past and Future Changes in Canadian Boreal Wildfire Activity: Ecological Applications, v. 18, p. 391–406, doi:10.1890/07-0747.1.

Girardin, M.P., Portier, J., Remy, C.C., Ali, A.A., Paillard, J., Blarquez, O., Asselin, H., Gauthier, S., Grondin, P., and Bergeron, Y., 2019, Coherent signature of warming-induced extreme sub-continental boreal wildfire activity 4800 and 1100 years BP: Environmental Research Letters, v. 14, p. 124042, doi:10.1088/1748-9326/ab59c9.

Girardin, M.P., Raulier, F., Bernier, P.Y., and Tardif, J.C., 2008, Response of tree growth to a changing climate in boreal central Canada: A comparison of empirical, process-based, and hybrid modelling approaches: Ecological Modelling, v. 213, p. 209–228, doi:10.1016/j.ecolmodel.2007.12.010.

Goetz, S.J., Bunn, A.G., Fiske, G.J., and Houghton, R.A., 2005, Satellite-observed photosynthetic trends across boreal North America associated with climate and fire disturbance: Proceedings of the National Academy of Sciences, v. 102, p. 13521–13525, doi:10.1073/pnas.0506179102.

Gottardini, E., Cristofolini, F., Cristofori, A., Vannini, A., and Ferretti, M., 2009, Sampling bias and sampling errors in pollen counting in aerobiological monitoring in Italy: Journal of environmental monitoring : JEM, v. 11, p. 751–5, doi:10.1039/b818162b.

Government of Canada, S.C., 2023, Natural resources satellite account, indicators:, https://www150.statcan.gc.ca/t1/tbl1/en/tv.action?pid=3810028501 (accessed September 2023).

Gray, D.R., 2008, The relationship between climate and outbreak characteristics of the spruce budworm in eastern Canada: Climatic Change, v. 87, p. 361–383, doi:10.1007/s10584-007-9317-5.

Gray, E.R., Russell, M.B., and Windmuller-Campione, M.A., 2021, The Difficulty of Predicting Eastern Spruce Dwarf Mistletoe in Lowland Black Spruce: Model Benchmarking in Northern Minnesota, USA: Forests, v. 12, p. 843, doi:10.3390/f12070843.

Greene, D.F. et al., 2007, The reduction of organic-layer depth by wildfire in the North American boreal forest and its effect on tree recruitment by seed: Canadian Journal of Forest Research, v. 37, p. 1012–1023, doi:10.1139/X06-245.

Grimm, E.C., 1987, Coniss: A FORTRAN 77 program for stratigraphical constrained cluster analysis by the method of incremental sum of squares: Computers & Geosciences, p. 13–37, doi:10.1016/0098-3004(87)90022-7.

Groffman, P.M., Driscoll, C.T., Fahey, T.J., Hardy, J.P., Fitzhugh, R.D., and Tierney, G.L., 2001, Colder soils in a warmer world: a snow manipulation study in a northern hardwood forest ecosystem: Biogeochemistry, v. 56, p. 135–150, doi:10.1023/A:1013039830323.

de Groot, W.J., Flannigan, M.D., and Cantin, A.S., 2013, Climate change impacts on future boreal fire regimes: Forest Ecology and Management, v. 294, p. 35–44, doi:10.1016/j.foreco.2012.09.027.

Hallett, D.J., and Walker, R.C., 2000, Paleoecology and its application to fire and vegetation management in Kootenay National Park, British Columbia: Journal of Paleolimnology, v. 24, p. 401–414, doi:10.1023/A:1008110804909.

Halsall, K.M., Ellingsen, V.M., Asplund, J., Bradshaw, R.H., and Ohlson, M., 2018, Fossil charcoal quantification using manual and image analysis approaches: The Holocene, v. 28, p. 1345–1353, doi:10.1177/0959683618771488.

Hamann, A., and Wang, T., 2006, Potential effects of climate change on ecosystem and tree species distribution in British Columbia: Ecology, v. 87, p. 2773–2786, doi:doi.org/10.1890/0012-9658(2006)87[2773:PEOCCO]2.0.CO;2.

Hanes, C.C., Wang, X., Jain, P., Parisien, M.-A., Little, J.M., and Flannigan, M.D., 2019, Fire-regime changes in Canada over the last half century: Canadian Journal of Forest Research, v. 49, p. 256–269, doi:10.1139/cjfr-2018-0293.

Hantson, S. et al., 2016, The status and challenge of global fire modelling: Biogeosciences, v. 13, p. 3359–3375, doi:10.5194/bg-13-3359-2016.

Hart, S.J., Henkelman, J., McLoughlin, P.D., Nielsen, S.E., Truchon-Savard, A., and Johnstone, J.F., 2019, Examining forest resilience to changing fire frequency in a fire-prone region of boreal forest: Global Change Biology, v. 25, p. 869–884, doi:10.1111/gcb.14550.

Hassan, R., Scholes, R., and Ash, N., 2005, Ecosystems and human well-being: current state and trends. Millennium Ecosystem Assessment.: Island press United States of America, v. 1.

Hauer, G., Williamson, T., and Renner, M., 2001, Socioeconomic impacts and adaptive responses to climate change: a Canadian forest sector perspective: v. 110, p. 13055–13060, doi:doi.org/10.1073/pnas.1305069110.

Hausmann, S., Larocque-Tobler, I., Richard, P.J.H., Pienitz, R., St-Onge, G., and Fye, F., 2011, Diatom-inferred wind activity at Lac du Sommet, southern Québec, Canada: A multiproxy paleoclimate reconstruction based on diatoms, chironomids and pollen for the past 9500 years: The Holocene, v. 21, p. 925–938, doi:10.1177/0959683611400199.

Hawthorne, D., and Mitchell, F.J.G., 2016, Identifying past fire regimes throughout the Holocene in Ireland using new and established methods of charcoal analysis: Quaternary Science Reviews, v. 137, p. 45–53, doi:10.1016/j.quascirev.2016.01.027.

Hayhoe, K., Edmonds, J., Kopp, R., LeGrande, A., Sanderson, B., Wehner, M., and Wuebbles, D., 2017, Climate models, scenarios, and projections: Publications, Agencies and Staff of the U.S. Department of Commerce, https://digitalcommons.unl.edu/usdeptcommercepub/589.

Haynes, K.M., Smart, J., Disher, B., Carpino, O., and Quinton, W.L., 2021, The role of hummocks in re-establishing black spruce forest following permafrost thaw: Ecohydrology, v. 14, p. e2273, doi:10.1002/eco.2273.

Hays, J.D., Imbrie, J., and Shackleton, N.J., 1976, Variations in the Earth's Orbit: Pacemaker of the Ice Ages: Science, v. 194, p. 1121–1132, doi:10.1126/science.194.4270.1121.

He, Z., and Pomeroy, J.W., 2023, Assessing hydrological sensitivity to future climate change over the Canadian southern boreal forest: Journal of Hydrology, v. 624, p. 129897, doi:10.1016/j.jhydrol.2023.129897.

Heiri, O., and Lotter, A.F., 2010, How does taxonomic resolution affect chironomid-based temperature reconstruction? Journal of Paleolimnology, v. 44, p. 589–601, doi:10.1007/s10933-010-9439-z.

Heiri, O., Lotter, A.F., Hausmann, S., and Kienast, F., 2003, A chironomid-based Holocene summer air temperature reconstruction from the Swiss Alps: The Holocene, v. 13, p. 477–484, doi:10.1191/0959683603hl640ft.

Heiri, O., Lotter, A.F., and Lemcke, G., 2001, Loss on ignition as a method for estimating organic and carbonate content in sediments: reproducibility and comparability of results: Journal of Paleolimnology, v. 25, p. 101–110, doi:10.1023/A:1008119611481.

Hély, C., Chaste, E., Girardin, M.P., Remy, C.C., Blarquez, O., Bergeron, Y., and Ali, A.A., 2020, A Holocene Perspective of Vegetation Controls on Seasonal Boreal Wildfire Sizes Using Numerical Paleo-Ecology: Frontiers in Forests and Global Change, v. 3, p. 511901, doi:10.3389/ffgc.2020.511901.

Hély, C., Flannigan, M., Bergeron, Y., and McRae, D., 2001, Role of vegetation and weather on fire behavior in the Canadian mixedwood boreal forest using two fire behavior prediction systems: Canadian Journal of Forest Research, v. 31, p. 430–441, doi:10.1139/x00-192.

Hély, C., Girardin, M.P., Ali, A.A., Carcaillet, C., Brewer, S., and Bergeron, Y., 2010, Eastern boreal North American wildfire risk of the past 7000 years: A model-

data comparison: Holocene wildfire risk in boreal forests: Geophysical Research Letters, v. 37, p. n/a-n/a, doi:10.1029/2010GL043706.

Hennebelle, A., Aleman, J.C., Ali, A.A., Bergeron, Y., Carcaillet, C., Grondin, P., Landry, J., and Blarquez, O., 2020, The reconstruction of burned area and fire severity using charcoal from boreal lake sediments: The Holocene, v. 30, p. 1400–1409, doi:10.1177/0959683620932979.

Higuera, P., 2009, CharAnalysis 0.9: Diagnostic and analytical tools for sediment-charcoal analysis: Montana State University: Bozeman, MT, USA, p. 27.

Higuera, P., Peters, M., Brubaker, L., and Gavin, D., 2007, Understanding the origin and analysis of sediment-charcoal records with a simulation model: Quaternary Science Reviews, v. 26, p. 1790–1809, doi:10.1016/j.quascirev.2007.03.010.

Hill, M.O., 1973, Diversity and Evenness: A Unifying Notation and Its Consequences: Ecology, v. 54, p. 427–432, doi:10.2307/1934352.

Hill, M.O., and Gauch Jr, H.G., 1980, Detrended correspondence analysis: an improved ordination technique: Vegetatio, v. 42, p. 47–58, doi:10.1007/BF00048870.

Hofmann, W., 1988, The significance of chironomid analysis (Insecta: Diptera) for paleolimnological research: Palaeogeography, Palaeoclimatology, Palaeoecology, v. 62, p. 501–509, doi:10.1016/0031-0182(88)90070-3.

Hogg, E.H. (Ted), and Bernier, P.Y., 2005, Climate change impacts on drought-prone forests in western Canada: The Forestry Chronicle, v. 81, p. 675–682, doi:10.5558/tfc81675-5.

Holland, M.M., and Bitz, C.M., 2003, Polar amplification of climate change in coupled models: Climate Dynamics, v. 21, p. 221–232, doi:10.1007/s00382-003-0332-6.

Holling, C.S., 1973, Resilience and Stability of Ecological Systems: Annual Review of Ecology and Systematics, v. 4, p. 1–23.

Houle, D., Bouffard, A., Duchesne, L., Logan, T., and Harvey, R., 2012, Projections of Future Soil Temperature and Water Content for Three Southern Quebec Forested Sites: Journal of Climate, v. 25, p. 7690–7701, doi:10.1175/JCLI-D-11-00440.1.

Huang, J.-G., Bergeron, Y., Berninger, F., Zhai, L., Tardif, J.C., and Denneler, B., 2013, Impact of Future Climate on Radial Growth of Four Major Boreal Tree Species in the Eastern Canadian Boreal Forest (B. Bond-Lamberty, Ed.): PLoS ONE, v. 8, p. e56758, doi:10.1371/journal.pone.0056758.

Hudak, J., and Singh, P., 1970, Incidence of Armillaria root rot in balsam fir infested by balsam woolly aphid: , p. 3.

IPCC, 2007, Climate change 2007: The physical science basis: Working group I contribution to the fourth assessment report of the IPCC: Cambridge university press, v. 4.

IPCC, 2022, Climate change 2022: impacts, adaptation and vulnerability.:

Irland, L.C., 2000, Ice storms and forest impacts: Science of the total environment, v. 262, p. 231–242.

Islam, M.A., and Macdonald, S.E., 2004, Ecophysiological adaptations of black spruce (Picea mariana) and tamarack (Larix laricina) seedlings to flooding: Trees - Structure and Function, v. 18, p. 35–42, doi:10.1007/s00468-003-0276-9.

Janssen, T.A.J., Jones, M.W., Finney, D., Van Der Werf, G.R., Van Wees, D., Xu, W., and Veraverbeke, S., 2023, Extratropical forests increasingly at risk due to lightning fires: Nature Geoscience, doi:10.1038/s41561-023-01322-z.

Jardon, Y., Morin, H., and Dutilleul, P., 2003, Périodicité et synchronisme des épidémies de la tordeuse des bourgeons de l'épinette au Québec: Canadian Journal of Forest Research, v. 33, p. 1947–1961, doi:10.1139/x03-108.

Jarvie, D.M., 1991, Total Organic Carbon (TOC) Analysis: Chapter 11: GEOCHEMICAL METHODS AND EXPLORATION: v. 37, p. 113–118.

Jasinski, J.P.P., and Payette, S., 2005, The Creation of Alternative Stable States in the Southern Boreal Forest, Québec, Canada: Ecological Monographs, v. 75, p. 561–583, doi:10.1890/04-1621.

Jayen, K., Leduc, A., and Bergeron, Y., 2006, Effect of fire severity on regeneration success in the boreal forest of northwest Québec, Canada: Écoscience, v. 13, p. 143–151, doi:10.2980/i1195-6860-13-2-143.1.

Jensen, K., Lynch, E.A., Calcote, R., and Hotchkiss, S.C., 2007, Interpretation of charcoal morphotypes in sediments from Ferry Lake, Wisconsin, USA: do different plant fuel sources produce distinctive charcoal morphotypes? The Holocene, v. 17, p. 907–915, doi:10.1177/0959683607082405.

Johnsen, K.H., and Seiler, J.R., 1996, Growth, shoot phenology and physiology of diverse seed sources of black spruce: I. Seedling responses to varied atmospheric CO2 concentrations and photoperiods: Tree Physiology, v. 16, p. 367–373, doi:10.1093/treephys/16.3.367.

Johnson, E.A., 1996, Fire and vegetation dynamics: studies from the North American boreal forest: Cambridge University Press.

Johnson, E.A., and Miyanishi, K., 2012, The boreal forest as a cultural landscape: Annals of the New York Academy of Sciences, v. 1249, p. 151–165, doi:10.1111/j.1749-6632.2011.06312.x.

Johnstone, J.F. et al., 2016, Changing disturbance regimes, ecological memory, and forest resilience: Frontiers in Ecology and the Environment, v. 14, p. 369–378, doi:10.1002/fee.1311.

Johnstone, J., Boby, L., Tissier, E., Mack, M., Verbyla, D., and Walker, X., 2009, Postfire seed rain of black spruce, a semiserotinous conifer, in forests of interior Alaska: Canadian Journal of Forest Research, v. 39, p. 1575–1588, doi:10.1139/X09-068.

Johnstone, J.F., and Chapin, F.S., 2006a, Effects of Soil Burn Severity on Post-Fire Tree Recruitment in Boreal Forest: Ecosystems, v. 9, p. 14–31, doi:10.1007/s10021-004-0042-x.

Johnstone, J.F., and Chapin, F.S., 2006b, Fire Interval Effects on Successional Trajectory in Boreal Forests of Northwest Canada: Ecosystems, v. 9, p. 268–277, doi:10.1007/s10021-005-0061-2.

Johnstone, J.F., Chapin Iii, F.S., Foote, J., Kemmett, S., Price, K., and Viereck, L., 2004, Decadal observations of tree regeneration following fire in boreal forests: Canadian Journal of Forest Research, v. 34, p. 267–273, doi:10.1139/x03-183.

Johnstone, J.F., Hollingsworth, T.N., Chapin Iii, F.S., and Mack, M.C., 2010, Changes in fire regime break the legacy lock on successional trajectories in Alaskan boreal forest: Global Change Biology, v. 16, p. 1281–1295, doi:10.1111/j.1365-2486.2009.02051.x.

Jouzel, J. et al., 2007, Orbital and millennial Antarctic climate variability over the past 800,000 years: science, v. 317, p. 793–796.

Juggins, S., 2015, Rioja: analysis of quaternary science data:

Juggins, S., and Birks, H.J.B., 2012, Quantitative environmental reconstructions from biological data: Tracking environmental change using lake sediments: Data handling and numerical techniques, p. 431–494, doi:10.1007/978-94-007-2745-8_14.

Juggins, S., and Juggins, M.S., 2020, "Package 'rioja'." An R Package for the Analysis of Quaternary Science Data.: v. 0.9 26.

Jutras, M., Dufour, C.O., Mucci, A., and Talbot, L.C., 2023, Large-scale control of the retroflection of the Labrador Current: Nature Communications, v. 14, p. 2623, doi:10.1038/s41467-023-38321-y.

Kaplan, M.R., and Wolfe, A.P., 2006, Spatial and temporal variability of Holocene temperature in the North Atlantic region: Quaternary Research, v. 65, p. 223–231, doi:10.1016/j.yqres.2005.08.020.

Kasischke, E.S., and Turetsky, M.R., 2006, Recent changes in the fire regime across the North American boreal region—Spatial and temporal patterns of burning across Canada and Alaska: Geophysical Research Letters, v. 33, doi:10.1029/2006GL025677.

Kaufman, D., 2004, Holocene thermal maximum in the western Arctic (0–180°W): Quaternary Science Reviews, v. 23, p. 529–560, doi:10.1016/j.quascirev.2003.09.007.

Kelly, R., Chipman, M.L., Higuera, P.E., Stefanova, I., Brubaker, L.B., and Hu, F.S., 2013, Recent burning of boreal forests exceeds fire regime limits of the past 10,000 years: Proceedings of the National Academy of Sciences, v. 110, p. 13055–13060, doi:10.1073/pnas.1305069110.

Kelly, M., and Funder, S., 1974, The pollen stratigraphy of late Quaternary lake sediments of South-West Greenland: Rapport Grønlands Geologiske Undersøgelse, v. 64, p. 1–26, doi:10.34194/rapggu.v64.7374.

Kelly, R.F., Higuera, P.E., Barrett, C.M., and Hu, F.S., 2011, A signal-to-noise index to quantify the potential for peak detection in sediment–charcoal records: Quaternary Research, v. 75, p. 11–17, doi:10.1016/j.yqres.2010.07.011.

Kerwin, M.W., Overpeck, J.T., Webb, R.S., and Anderson, K.H., 2004, Pollen-based summer temperature reconstructions for the eastern Canadian boreal forest, subarctic, and Arctic: Quaternary Science Reviews, v. 23, p. 1901–1924, doi:10.1016/j.quascirev.2004.03.013.

Kliejunas, J.T., Geils, B.W., Glaeser, J.M., Goheen, E.M., Hennon, P., Kim, M.-S., Kope, H., Stone, J., Sturrock, R., and Frankel, S.J., 2009, Review of literature on climate change and forest diseases of western North America: U.S. Department of Agriculture, Forest Service, Pacific Southwest Research Station PSW-GTR-225, PSW-GTR-225 p., doi:10.2737/PSW-GTR-225.

Kljun, N., Black, T.A., Griffis, T.J., Barr, A.G., Gaumont-Guay, D., Morgenstern, K., McCaughey, J.H., and Nesic, Z., 2006, Response of Net Ecosystem Productivity of Three Boreal Forest Stands to Drought: Ecosystems, v. 9, p. 1128–1144, doi:10.1007/s10021-005-0082-x.

Kneeshaw, D.D., and Bergeron, Y., 1998, Canopy and gap characteristics and tree replacement in the southeastern boreal forest: Ecology, v. 79, p. 783–794, doi:10.1890/0012-9658(1998)079[0783:CGCATR]2.0.CO;2.

Kneeshaw, D., Bergeron, Y., and Kuuluvainen, T., 2011, Forest ecosystem structure and disturbance dynamics across the circumboreal forest: The Sage Handbook of Biogeography. Sage, Los Angeles, p. 263–280.

Kolling, H., Schneider, R., Gross, F., Hamann, C., Kienast, M., Kienast, S., Doering, K., Fahl, K., and Stein, R., 2023, Biomarker Records of Environmental Shifts on the Labrador Shelf During the Holocene: Paleoceanography and Paleoclimatology, v. 38, p. e2022PA004578, doi:10.1029/2022PA004578.

Kurz, W.A., Stinson, G., Rampley, G.J., Dymond, C.C., and Neilson, E.T., 2008, Risk of natural disturbances makes future contribution of Canada's forests to the global carbon cycle highly uncertain: Proceedings of the National Academy of Sciences, v. 105, p. 1551–1555, doi:10.1073/pnas.0708133105.

Kusunoki, S., Ose, T., and Hosaka, M., 2020, Emergence of unprecedented climate change in projected future precipitation: Scientific Reports, v. 10, p. 4802, doi:10.1038/s41598-020-61792-8.

Kuuluvainen, T., and Aakala, T., 2011, Natural forest dynamics in boreal Fennoscandia: a review and classification: Silva Fennica, v. 45, doi:10.14214/sf.73.

Lafleur, B., Fenton, N.J., and Bergeron, Y., 2015, Forecasting the development of boreal paludified forests in response to climate change: a case study using Ontario ecosite classification: Forest Ecosystems, v. 2, p. 3, doi:10.1186/s40663-015-0027-6.

de Lafontaine, G., and Payette, S., 2012, Long-term fire and forest history of subalpine balsam fir (*Abies balsamea*) and white spruce (*Picea glauca*) stands in eastern Canada inferred from soil charcoal analysis: The Holocene, v. 22, p. 191–201, doi:10.1177/0959683611414931.

de Lafontaine, G., and Payette, S., 2010, The Origin and Dynamics of Subalpine White Spruce and Balsam Fir Stands in Boreal Eastern North America: Ecosystems, v. 13, p. 932–947, doi:10.1007/s10021-010-9366-x.

Larocque, I., 2001, How many chironomid head capsules are enough? A statistical approach to determine sample size for palaeoclimatic reconstructions: Palaeogeography, Palaeoclimatology, Palaeoecology, v. 172, p. 133–142, doi:10.1016/S0031-0182(01)00278-4.

Larocque, I., Grosjean, M., Heiri, O., Bigler, C., and Blass, A., 2009, Comparison between chironomid-inferred July temperatures and meteorological data AD

1850–2001 from varved Lake Silvaplana, Switzerland: Journal of Paleolimnology, v. 41, p. 329–342, doi:10.1007/s10933-008-9228-0.

Larocque, I., Pienitz, R., and Rolland, N., 2006, Factors influencing the distribution of chironomids in lakes distributed along a latitudinal gradient in northwestern Quebec, Canada: Canadian Journal of Fisheries and Aquatic Sciences, v. 63, p. 1286–1297, doi:10.1139/f06-020.

Larocque-Tobler, I., 2010, Reconstructing temperature at Egelsee, Switzerland, using North American and Swedish chironomid transfer functions: potential and pitfalls: Journal of Paleolimnology, v. 44, p. 243–251, doi:10.1007/s10933-009-9400-1.

Larocque-Tobler, I., Filipiak, J., Tylmann, W., Bonk, A., and Grosjean, M., 2015, Comparison between chironomid-inferred mean-August temperature from varved Lake Żabińskie (Poland) and instrumental data since 1896 AD: Quaternary Science Reviews, v. 111, p. 35–50, doi:10.1016/j.quascirev.2015.01.001.

Larsen, C.P.S., 1996, Fire and climate dynamics in the boreal forest of northern Alberta, Canada, from AD 1850 to 1989: The Holocene, v. 6, p. 449–456, doi:10.1177/095968369600600407.

Larsson, J., Godfrey, A.J.R., Gustafsson, P., Eberly, D.H., Huber, E., Slowikowski, K., Privé, F., and Larsson, M.J., 2016, Package 'eulerr':

Lavoie, C., and Arseneault, D., 2001, Late Holocene Climate of the James Bay Area, Quebec, Canada, Reconstructed Using Fossil Beetles: Arctic, Antarctic, and Alpine Research, v. 33, p. 13–18, doi:10.1080/15230430.2001.12003399.

Lavoie, M., Filion, L., and Robert, É.C., 2009, Boreal peatland margins as repository sites of long-term natural disturbances of balsam fir/spruce forests: Quaternary Research, v. 71, p. 295–306, doi:10.1016/j.yqres.2009.01.005.

Le Roux, G., and Marshall, W.A., 2011, Constructing recent peat accumulation chronologies using atmospheric fall-out radionuclides: Mires and Peat, v. 7, p. 14.

Lebreton, V., Messager, E., Marquer, L., and Renault-Miskovsky, J., 2010, A neotaphonomic experiment in pollen oxidation and its implications for archaeopalynology: Review of Palaeobotany and Palynology, v. 162, p. 29–38, doi:10.1016/j.revpalbo.2010.05.002.

Lefort, P., Gauthier, S., and Bergeron, Y., 2003, The influence of fire weather and land use on the fire activity of the Lake Abitibi area, eastern Canada: Forest science, v. 49, p. 509–521, doi:10.1093/forestscience/49.4.509.

Légaré, S., Paré, D., and Bergeron, Y., 2004, The responses of black spruce growth to an increased proportion of aspen in mixed stands: Canadian Journal of Forest Research, v. 34, p. 405–416, doi:10.1139/x03-251.

Legendre, P., and Gallagher, E.D., 2001, Ecologically meaningful transformations for ordination of species data: Oecologia, v. 129, p. 271–280, doi:10.1007/s004420100716.

Lenton, T.M., Held, H., Kriegler, E., Hall, J.W., Lucht, W., Rahmstorf, S., and Schellnhuber, H.J., 2008, Tipping elements in the Earth's climate system: Proceedings of the National Academy of Sciences, v. 105, p. 1786–1793, doi:10.1073/pnas.0705414105.

Lesieur, D., Gauthier, S., and Bergeron, Y., 2002, Fire frequency and vegetation dynamics for the south-central boreal forest of Quebec, Canada: Canadian Journal of Forest Research, v. 32, p. 1996–2009, doi:10.1139/x02-113.

Lestienne, M., Jouffroy-Bapicot, I., Leyssenne, D., Sabatier, P., Debret, M., Albertini, P.-J., Colombaroli, D., Didier, J., Hély, C., and Vannière, B., 2020, Fires and human activities as key factors in the high diversity of Corsican vegetation: The Holocene, v. 30, p. 244–257, doi:10.1177/0959683619883025.

Lesven, J., Druguet Dayras, M., Borne, R., Remy, C.C., Gillet, F., Bergeron, Y., Arsenault, A., Millet, L., and Rius, D., 2022, Testing a new automated macrocharcoal detection method applied to a transect of lacustrine sediment cores in eastern Canada: Quaternary Science Reviews, v. 295, p. 107780, doi:10.1016/j.quascirev.2022.107780.

Lesven, J.A., Druguet Dayras, M., Cazabonne, J., Gillet, F., Arsenault, A., Rius, D., and Bergeron, Y., 2024, Future impacts of climate change on black spruce growth and mortality: Review and challenges: Environmental Reviews, p. er-2023-0075, doi:10.1139/er-2023-0075.

Leys, B., Carcaillet, C., Dezileau, L., Ali, A.A., and Bradshaw, R.H.W., 2013, A comparison of charcoal measurements for reconstruction of Mediterranean paleo-fire frequency in the mountains of Corsica: Quaternary Research, v. 79, p. 337–349, doi:10.1016/j.yqres.2013.01.003.

Leys, B.A., Commerford, J.L., and McLauchlan, K.K., 2017, Reconstructing grassland fire history using sedimentary charcoal: Considering count, size and shape (C. Carcaillet, Ed.): PLOS ONE, v. 12, p. e0176445, doi:10.1371/journal.pone.0176445.

Li, J., Dang, Q.-L., and Man, R., 2015, Photoperiod and Nitrogen Supply Limit the Scope of Northward Migration and Seed Transfer of Black Spruce in a Future Climate Associated with Doubled Atmospheric CO2 Concentration: American Journal of Plant Sciences, v. 06, p. 189–200, doi:10.4236/ajps.2015.61022.

Li, G., and Piper, D.J.W., 2015, The influence of meltwater on the Labrador Current in Heinrich event 1 and the Younger Dryas: Quaternary Science Reviews, v. 107, p. 129–137, doi:10.1016/j.quascirev.2014.10.021.

Lieffers, V., and Rothwell, R., 1987, Rooting of peatland black spruce and tamarack in relation to depth of water table: Canadian Journal of Botany, v. 65, p. 817–821.

Lindbladh, M., Fraver, S., Edvardsson, J., and Felton, A., 2013, Past forest composition, structures and processes – How paleoecology can contribute to forest conservation: Biological Conservation, v. 168, p. 116–127, doi:10.1016/j.biocon.2013.09.021.

Lippold, J. et al., 2019, Constraining the Variability of the Atlantic Meridional Overturning Circulation During the Holocene: Geophysical Research Letters, v. 46, p. 11338–11346, doi:10.1029/2019GL084988.

Lisiecki, L.E., and Raymo, M.E., 2005, A Pliocene-Pleistocene stack of 57 globally distributed benthic δ18O records: Paleoceanography, v. 20.

Liu, K.-B., 1990, Holocene Paleoecology of the Boreal Forest and Great Lakes-St. Lawrence Forest in Northern Ontario: Ecological Monographs, v. 60, p. 179–212, doi:10.2307/1943044.

Liu, Q., Piao, S., Janssens, I.A., Fu, Y., Peng, S., Lian, X., Ciais, P., Myneni, R.B., Peñuelas, J., and Wang, T., 2018, Extension of the growing season increases vegetation exposure to frost: Nature communications, v. 9, p. 1–8, doi:10.1038/s41467-017-02690-y.

Liu, M., Shen, Y., González-Sampériz, P., Gil-Romera, G., ter Braak, C.J.F., Prentice, I.C., and Harrison, S.P., 2023, Holocene climates of the Iberian Peninsula: pollen-based reconstructions of changes in the west–east gradient of temperature and moisture: Climate of the Past, v. 19, p. 803–834, doi:10.5194/cp-19-803-2023.

Lloyd, A., Wilson, A., Fastie, C., and Landis, R., 2005, Population dynamics of black spruce and white spruce near the arctic tree line in the southern Brooks Range, Alaska: Canadian Journal of Forest Research-revue Canadienne De Recherche Forestiere - CAN J FOREST RES, v. 35, p. 2073–2081, doi:10.1139/x05-119.

Long, S.P., Ainsworth, E.A., Rogers, A., and Ort, D.R., 2004, RISING ATMOSPHERIC CARBON DIOXIDE: Plants FACE the Future: Annual Review of Plant Biology, v. 55, p. 591–628, doi:10.1146/annurev.arplant.55.031903.141610.

Long, C.J., and Whitlock, C., 2002, Fire and Vegetation History from the Coastal Rain Forest of the Western Oregon Coast Range: Quaternary Research, v. 58, p. 215–225, doi:10.1006/qres.2002.2378.

Long, C.J., Whitlock, C., Bartlein, P.J., and Millspaugh, S.H., 1998, A 9000-year fire history from the Oregon Coast Range, based on a high-resolution charcoal study: Canadian Journal of Forest Research, v. 28, p. 14, doi:doi.org/10.1139/x04-071.

Lupi, C., Morin, H., Deslauriers, A., and Rossi, S., 2012, Xylogenesis in black spruce: does soil temperature matter? Tree Physiology, v. 32, p. 74–82, doi:10.1093/treephys/tpr132.

Lynch, J.A., Clark, J.S., Bigelow, N.H., Edwards, M.E., and Finney, B.P., 2002, Geographic and temporal variations in fire history in boreal ecosystems of Alaska: Journal of Geophysical Research, v. 108, p. 8152, doi:10.1029/2001JD000332.

Lynch, J.A., Clark, J.S., and Stocks, B.J., 2004, Charcoal production, dispersal, and deposition from the Fort Providence experimental fire: interpreting fire regimes from charcoal records in boreal forests: Canadian Journal of Forest Research, v. 34, p. 1642–1656, doi:doi.org/10.1139/x04-071.

Ma, Q., Huang, J.-G., Hänninen, H., and Berninger, F., 2019, Divergent trends in the risk of spring frost damage to trees in Europe with recent warming: Global change biology, v. 25, p. 351–360, doi:10.1111/gcb.14479.

Ma, Z., Peng, C., Zhu, Q., Chen, H., Yu, G., Li, W., Zhou, X., Wang, W., and Zhang, W., 2012, Regional drought-induced reduction in the biomass carbon sink of Canada's boreal forests: Proceedings of the National Academy of Sciences, v. 109, p. 2423–2427, doi:10.1073/pnas.1111576109.

MacDonald, G.M., Szeicz, J.M., Claricoates, J., and Dale, K.A., 1998, Response of the Central Canadian Treeline to Recent Climatic Changes: Annals of the Association of American Geographers, v. 88, p. 183–208, doi:10.1111/1467-8306.00090.

Mack, M.C., Walker, X.J., Johnstone, J.F., Alexander, H.D., Melvin, A.M., Jean, M., and Miller, S.N., 2021, Carbon loss from boreal forest wildfires offset by increased dominance of deciduous trees: Science, v. 372, p. 280–283, doi:10.1126/science.abf3903.

Mackay, H., Amesbury, M.J., Langdon, P.G., Charman, D.J., Magnan, G., Van Bellen, S., Garneau, M., Bainbridge, R., and Hughes, P.D.M., 2021, Spatial variation of hydroclimate in north-eastern North America during the last millennium: Quaternary Science Reviews, v. 256, p. 106813, doi:10.1016/j.quascirev.2021.106813.

Magnan, G., and Garneau, M., 2014, Climatic and autogenic control on Holocene carbon sequestration in ombrotrophic peatlands of maritime Quebec, eastern Canada: The Holocene, v. 24, p. 1054–1062, doi:10.1177/0959683614540727.

Magne, G., Brossier, B., Gandouin, E., Paradis, L., Drobyshev, I., Kryshen, A., Hély, C., Alleaume, S., and Ali, A.A., 2020, Lacustrine charcoal peaks provide an accurate record of surface wildfires in a North European boreal forest: The Holocene, v. 30, p. 380–388, doi:10.1177/0959683619887420.

Maher, C.T., Nelson, C.R., and Larson, A.J., 2020, Winter damage is more important than summer temperature for maintaining the krummholz growth form above alpine treeline: Journal of Ecology, v. 108, p. 1074–1087, doi:10.1111/1365-2745.13315.

Mallik, A., and Bloom, R., 2005, Seedbed allelopathy and species regeneration strategy, destabilizing black spruce-Kalmia community in eastern Canada, *in* Proceedings of the 4th World Congress on Allelopathy, p. 21–26.

Man, R., Lu, P., and Dang, Q.-L., 2021, Cold tolerance of black spruce, white spruce, jack pine, and lodgepole pine seedlings at different stages of spring dehardening: New Forests, v. 52, p. 317–328, doi:10.1007/s11056-020-09796-0.

Marchand, W., Girardin, M.P., Hartmann, H., Lévesque, M., Gauthier, S., and Bergeron, Y., 2021, Contrasting life-history traits of black spruce and jack pine influence their physiological response to drought and growth recovery in northeastern boreal Canada: Science of The Total Environment, v. 794, p. 148514, doi:10.1016/j.scitotenv.2021.148514.

Marquis, B., Bergeron, Y., Houle, D., Leduc, M., and Rossi, S., 2022, Variability in frost occurrence under climate change and consequent risk of damage to trees of western Quebec, Canada: Scientific Reports, v. 12, p. 7220, doi:10.1038/s41598-022-11105-y.

Marquis, B., Duval, P., Bergeron, Y., Simard, M., Thiffault, N., and Tremblay, F., 2021, Height growth stagnation of planted spruce in boreal mixedwoods: Importance of landscape, microsite, and growing-season frosts: Forest Ecology and Management, v. 479, p. 118533, doi:10.1016/j.foreco.2020.118533.

McAndrews, J.H., 1973, Key to the Quaternary pollen and spores of the Great Lakes region: Life sciences miscellaneous publications, https://agris.fao.org/search/en/providers/122376/records/65119dc2511bdb9a50701074 (accessed August 2024).

McBeath, A.V., Smernik, R.J., and Krull, E.S., 2013, A demonstration of the high variability of chars produced from wood in bushfires: Organic geochemistry, v. 55, p. 38–44.

McCullough, D.G., Werner, R.A., and Neumann, D., 1998, Fire and Insects in Northern and Boreal Forest Ecosystems of North America: Annual Review of Entomology, v. 43, p. 107–127, doi:10.1146/annurev.ento.43.1.107.

McDowell, N.G. et al., 2020, Pervasive shifts in forest dynamics in a changing world: Science, v. 368, p. eaaz9463, doi:10.1126/science.aaz9463.

Medeiros, A.S. et al., 2022, A continental-scale chironomid training set for reconstructing Arctic temperatures: Quaternary Science Reviews, v. 294, p. 107728, doi:10.1016/j.quascirev.2022.107728.

Mery, G., Katila, P., Galloway, G., Alfaro, R.I., Kanninen, M., Lobovikov, M., Varjo, J., and others, 2010, Forests and society-responding to global drivers of change, *in* IUFRO Vienna.

Messaoud, Y., Bergeron, Y., and Leduc, A., 2007, Ecological factors explaining the location of the boundary between the mixedwood and coniferous bioclimatic zones in the boreal biome of eastern North America: Global Ecology and Biogeography, v. 16, p. 90–102, doi:doi.org/10.1111/j.1466-8238.2006.00277.x.

Messaoud, Y., and Chen, H.Y.H., 2011, The Influence of Recent Climate Change on Tree Height Growth Differs with Species and Spatial Environment: PLOS ONE, v. 6, p. e14691, doi:10.1371/journal.pone.0014691.

Meunier, C., Sirois, L., and Bégin, Y., 2007, Climate and Picea Mariana Seed Maturation Relationships: A Multi-Scale Perspective: Ecological Monographs, v. 77, p. 361–376, doi:10.1890/06-1543.1.

Milankovitch, M., 1941, Canon of insolation and the iceage problem: Koniglich Serbische Akademice Beograd Special Publication, v. 132.

Miller, G.H. et al., 2010, Temperature and precipitation history of the Arctic: Quaternary Science Reviews, v. 29, p. 1679–1715, doi:10.1016/j.quascirev.2010.03.001.

Millet, L., Arnaud, F., Heiri, O., Magny, M., Verneaux, V., and Desmet, M., 2009, Late-Holocene summer temperature reconstruction from chironomid assemblages of Lake Anterne, northern French Alps: The Holocene, v. 19, p. 317–328, doi:10.1177/0959683608100576.

Millet, L., Rius, D., Galop, D., Heiri, O., and Brooks, S.J., 2012, Chironomid-based reconstruction of Lateglacial summer temperatures from the Ech palaeolake

record (French western Pyrenees): Palaeogeography, Palaeoclimatology, Palaeoecology, v. 315–316, p. 86–99, doi:10.1016/j.palaeo.2011.11.014.

Ministère des Ressources naturelles et de la Faune, 2008, Sustainable Management in the Boreal Forest: A Real Response to Environmental Challenges:

Miranda, B.R., Sturtevant, B.R., Schmelzer, I., Doyon, F., and Wolter, P., 2016, Vegetation recovery following fire and harvest disturbance in central Labrador — a landscape perspective: Canadian Journal of Forest Research, v. 46, p. 1009–1018, doi:10.1139/cjfr-2015-0516.

Molina, E., Valeria, O., De Grandpre, L., Ramirez, J.A., Cyr, D., and Boulanger, Y., 2021, Projecting future aboveground biomass and productivity of managed eastern Canadian mixedwood boreal forest in response to climate change: Forest Ecology and Management, v. 487, p. 119016.

Montoro Girona, M., Navarro, L., and Morin, H., 2018, A Secret Hidden in the Sediments: Lepidoptera Scales: Frontiers in Ecology and Evolution, v. 6, https://www.frontiersin.org/articles/10.3389/fevo.2018.00002 (accessed February 2024).

Montoro Girona, M., Rossi, S., Lussier, J.-M., Walsh, D., and Morin, H., 2017, Understanding tree growth responses after partial cuttings: A new approach: PLoS One, v. 12, p. e0172653.

Moore, T.R. et al., 1999, Litter decomposition rates in Canadian forests: Global Change Biology, v. 5, p. 75–82, doi:10.1046/j.1365-2486.1998.00224.x.

Moore, P.D., Webb, J.A., Collison, M.E., and others, 1991, Pollen analysis.: Blackwell scientific publications.

Morin, H., and Laprise, D., 1990, Histoire récente des épidémies de la Tordeuse des bourgeons de l'épinette au nord du lac Saint-Jean (Québec): une analyse dendrochronologique: Canadian Journal of Forest Research, v. 20, p. 1–8, doi:10.1139/x90-001.

Mudelsee, M., Börngen, M., Tetzlaff, G., and Grünewald, U., 2004, Extreme floods in central Europe over the past 500 years: Role of cyclone pathway "Zugstrasse Vb": extreme floods in central europe: Journal of Geophysical Research: Atmospheres, v. 109, doi:10.1029/2004JD005034.

Natural Resources Canada, 2022a, Canada, Permafrost. National Atlas of Canada: v. 4177, https://ouvert.canada.ca/data/fr/dataset/d1e2048b-ccff-5852-aaa5-b861bd55c367.

Natural Resources Canada, 2010, Historical data, Environment and natural resources:, https://climat.meteo.gc.ca/climate_normals/.

Natural Resources Canada, 2022b, The State of Canada's Forests Annual Report 2013:

Navarro, L., Harvey, A.-É., and Morin, H., 2017, Lepidoptera wing scales: a new paleoecological indicator for reconstructing spruce budworm abundance1: Canadian Journal of Forest Research, doi:10.1139/cjfr-2017-0009.

Nealis, V.G., and Régnière, J., 2004, Insect–host relationships influencing disturbance by the spruce budworm in a boreal mixedwood forest: v. 34, p. 13, doi:10.1139/x04-061.

Nicklen, E.F., Roland, C.A., Ruess, R.W., Scharnweber, T., and Wilmking, M., 2021, Divergent responses to permafrost and precipitation reveal mechanisms for the spatial variation of two sympatric spruce: Ecosphere, v. 12, p. e03622, doi:10.1002/ecs2.3622.

Niemelä, J., 1999, Ecology and urban planning: Biodiversity & Conservation, v. 8, p. 119–131, doi:10.1023/A:1008817325994.

Norby, R.J., Warren, J.M., Iversen, C.M., Medlyn, B.E., and McMurtrie, R.E., 2010, CO2 enhancement of forest productivity constrained by limited nitrogen availability: Proceedings of the National Academy of Sciences, v. 107, p. 19368–19373.

Oberndorfer, E., 2020, What the Blazes!? A People's History of Fire in Labrador: Journal of the North Atlantic, v. 2020, p. 1–16, doi:10.3721/037.006.4001.

Oboite, F.O., and Comeau, P.G., 2020, The interactive effect of competition and climate on growth of boreal tree species in western Canada and Alaska: Canadian Journal of Forest Research, v. 50, p. 457–464, doi:10.1139/cjfr-2019-0319.

Oksanen, J., 2015, Vegan: an introduction to ordination:

Olander, H., Korhola, A., and Blom, T., 1997, Surface sediment Chironomidae (Insecta: Diptera) distributions along an ecotonal transect in subarctic Fennoscandia: developing a tool for palaeotemperature reconstructions: Journal of Paleolimnology, v. 18, p. 45–59, doi:10.1023/A:1007906609155.

Olefeldt, D., Heffernan, L., Jones, M., Sannel, A., Treat, C., and Turetsky, M., 2021, Permafrost Thaw in Northern Peatlands: Rapid Changes in Ecosystem and Landscape Functions, *in* p. 27–67, doi:10.1007/978-3-030-71330-0_3.

Ols, C., Hofgaard, A., Bergeron, Y., and Drobyshev, I., 2016, Previous growing season climate controls the occurrence of black spruce growth anomalies in boreal forests of Eastern Canada: Canadian Journal of Forest Research, v. 46, p. 696–705, doi:10.1139/cjfr-2015-0404.

Oris, F., Ali, A.A., Asselin, H., Paradis, L., Bergeron, Y., and Finsinger, W., 2014a, Charcoal dispersion and deposition in boreal lakes from 3 years of monitoring: Differences between local and regional fires: Monitoring charcoal deposition in lakes: Geophysical Research Letters, v. 41, p. 6743–6752, doi:10.1002/2014GL060984.

Oris, F., Asselin, H., Ali, A.A., Finsinger, W., and Bergeron, Y., 2014b, Effect of increased fire activity on global warming in the boreal forest: Environmental Reviews, v. 22, p. 206–219, doi:10.1139/er-2013-0062.

Ostry, M.E., and Nicholls, T.H., 1979, Eastern dwarf mistletoe on black spruce: Department of Agriculture, Forest Service, v. 158.

Overpeck, J.T., Webb, T., and Prentice, I.C., 1985, Quantitative Interpretation of Fossil Pollen Spectra: Dissimilarity Coefficients and the Method of Modern Analogs: Quaternary Research, v. 23, p. 87–108, doi:10.1016/0033-5894(85)90074-2.

PAGES, P.I.W.G. of, 2016, Interglacials of the last 800,000 years: Reviews of Geophysics, v. 54, p. 162–219.

Pan, Y. et al., 2011, A large and persistent carbon sink in the world's forests: Science, v. 333, p. 988–993, doi:10.1126/science.1201609.

Pardi, M.I., and Smith, F.A., 2012, Paleoecology in an Era of Climate Change: How the Past Can Provide Insights into the Future, *in* Louys, J. ed., Paleontology in Ecology and Conservation, Berlin, Heidelberg, Springer, Springer Earth System Sciences, p. 93–116, doi:10.1007/978-3-642-25038-5_6.

Parisien, M.-A., and Moritz, M.A., 2009, Environmental controls on the distribution of wildfire at multiple spatial scales: Ecological Monographs, v. 79, p. 127–154, doi:10.1890/07-1289.1.

Pau, M., Gauthier, S., Chavardès, R.D., Girardin, M.P., Marchand, W., and Bergeron, Y., 2022, Site index as a predictor of the effect of climate warming on boreal tree growth: Global Change Biology, v. 28, p. 1903–1918, doi:10.1111/gcb.16030.

Payette, S., 1992, Fire as a controlling process in the North American boreal forest: A systems analysis of the global boreal forest: Canadian Journal of Forest Research, v. 30, p. 144–169, doi:doi.org/10.1139/x99-207.

Payette, S., 1993, The range limit of boreal tree species in Qu6bec-Labrador: an ecological and palaeoecological interpretation:

Payette, S., Bhiry, N., Delwaide, A., and Simard, M., 2000, Origin of the lichen woodland at its southern range limit in eastern Canada: the catastrophic impact of insect defoliators and fire on the spruce–moss forest: v. 30, p. 18.

Payette, S., and Delwaide, A., 2018, Tamm review: The North-American lichen woodland: Forest Ecology and Management, v. 417, p. 167–183, doi:10.1016/j.foreco.2018.02.043.

Payette, S., Delwalde, A., Morneau, C., and Lavole, C., 1995, Patterns of tree stem decline along a snow-drift gradient at treeline: A case study using stem analysis: Canadian Journal of Botany, v. 74, p. 1671–1683, doi:10.1139/b96-203.

Payette, S., and Gagnon, R., 1985, Late Holocene deforestation and tree regeneration in the forest–tundra of Québec: Nature, v. 313, p. 570–572, doi:10.1038/313570a0.

Pearce, D.W., 2001, The Economic Value of Forest Ecosystems: Ecosystem Health, v. 7, p. 284–296, doi:10.1046/j.1526-0992.2001.01037.x.

Pelletier, M., Allard, M., and Levesque, E., 2019, Ecosystem changes across a gradient of permafrost degradation in subarctic Québec (Tasiapik Valley, Nunavik, Canada): Arctic Science, v. 5, p. 1–26, doi:10.1139/as-2016-0049.

Peng, C., Ma, Z., Lei, X., Zhu, Q., Chen, H., Wang, W., Liu, S., Li, W., Fang, X., and Zhou, X., 2011, A drought-induced pervasive increase in tree mortality across Canada's boreal forests: Nature Climate Change, v. 1, p. 467–471, doi:10.1038/nclimate1293.

Peyron, O., Bégeot, C., Brewer, S., Heiri, O., Magny, M., Millet, L., Ruffaldi, P., Van Campo, E., and Yu, G., 2005, Late-Glacial climatic changes in Eastern France (Lake Lautrey) from pollen, lake-levels, and chironomids: Quaternary Research, v. 64, p. 197–211, doi:10.1016/j.yqres.2005.01.006.

Pinder, L., and Morley, D., 1995, Chironomidae as indicators of water quality with a comparison of the chironomid faunas of a series of contrasting Cumbrian Tarns:

Pörtner, H.O. et al., 2022, Climate change 2022: impacts, adaptation and vulnerability:, doi:doi:10.1017/9781009325844.

Power, M.J. et al., 2008, Changes in fire regimes since the Last Glacial Maximum: an assessment based on a global synthesis and analysis of charcoal data: Climate Dynamics, v. 30, p. 887–907, doi:10.1007/s00382-007-0334-x.

Prasad, A., Pedlar, J., Peters, M., McKenney, D., Iverson, L., Matthews, S., and Adams, B., 2020, Combining US and Canadian forest inventories to assess

habitat suitability and migration potential of 25 tree species under climate change: Diversity and Distributions, v. 26, p. 1142–1159, doi:10.1111/ddi.13078.

Previdi, M., Smith, K.L., and Polvani, L.M., 2021, Arctic amplification of climate change: a review of underlying mechanisms: Environmental Research Letters, v. 16, p. 093003, doi:10.1088/1748-9326/ac1c29.

Price, D.T. et al., 2013, Anticipating the consequences of climate change for Canada's boreal forest ecosystems: Environmental Reviews, v. 21, p. 322–365, doi:10.1139/er-2013-0042.

Pureswaran, D.S., De Grandpré, L., Paré, D., Taylor, A., Barrette, M., Morin, H., Régnière, J., and Kneeshaw, D.D., 2015, Climate-induced changes in host tree–insect phenology may drive ecological state-shift in boreal forests: Ecology, v. 96, p. 1480–1491, doi:10.1890/13-2366.1.

Pureswaran, D.S., Neau, M., Marchand, M., De Grandpré, L., and Kneeshaw, D., 2019, Phenological synchrony between eastern spruce budworm and its host trees increases with warmer temperatures in the boreal forest: Ecology and Evolution, v. 9, p. 576–586, doi:10.1002/ece3.4779.

Quinlan, R., and Smol, J.P., 2001, Setting minimum head capsule abundance and taxa deletion criteria in chironomid-based inference models: Journal of Paleolimnology, v. 26, p. 327–342, doi:10.1023/A:1017546821591.

R Core Team, 2023, R: A language and environment for statistical computing. R Foundation for Statistical Computing, Vienna, Austria. 2012:

R Core Team R: A language and environment for statistical computing. R Foundation for Statistical Computing, Vienna, Austria. Available online at https://www.R-project.org/: 2018,.

Rao, M.P. et al., 2023, Approaching a thermal tipping point in the Eurasian boreal forest at its southern margin: Communications Earth & Environment, v. 4, p. 247, doi:10.1038/s43247-023-00910-6.

Régnière, J., St-Amant, R., and Duval, P., 2012, Predicting insect distributions under climate change from physiological responses: spruce budworm as an example: Biological Invasions, v. 14, p. 1571–1586, doi:10.1007/s10530-010-9918-1.

Reille, M., 1995, Pollen et spores d'Europe et d'Afrique du Nord: Laboratoire de Botanique historique et Palynologie, v. 2.

Reimer, P.J. et al., 2020, The IntCal20 Northern Hemisphere Radiocarbon Age Calibration Curve (0–55 cal kBP): Radiocarbon, v. 62, p. 725–757, doi:10.1017/RDC.2020.41.

Remy, C.C. et al., 2018, Guidelines for the use and interpretation of palaeofire reconstructions based on various archives and proxies: Quaternary Science Reviews, v. 193, p. 312–322.

Remy, C.C., Hély, C., Blarquez, O., Magnan, G., Bergeron, Y., Lavoie, M., and Ali, A.A., 2017a, Different regional climatic drivers of Holocene large wildfires in boreal forests of northeastern America: Environmental Research Letters, v. 12, p. 035005, doi:10.1088/1748-9326/aa5aff.

Remy, C.C., Lavoie, M., Girardin, M.P., Hély, C., Bergeron, Y., Grondin, P., Oris, F., Asselin, H., and Ali, A.A., 2017b, Wildfire size alters long-term vegetation trajectories in boreal forests of eastern North America: Journal of Biogeography, v. 44, p. 1268–1279, doi:10.1111/jbi.12921.

Remy, C.C., Senici, D., Chen, H.Y.H., Bergeron, Y., Lavoie, M., Paradis, L., and Ali, A.A., 2019, Coniferization of the mixed-wood boreal forests under warm climate: Journal of Quaternary Science, v. 34, p. 509–518, doi:10.1002/jqs.3136.

Renssen, H., Seppä, H., Crosta, X., Goosse, H., and Roche, D.M., 2012, Global characterization of the Holocene Thermal Maximum: Quaternary Science Reviews, v. 48, p. 7–19, doi:10.1016/j.quascirev.2012.05.022.

Renssen, H., Seppä, H., Heiri, O., Roche, D.M., Goosse, H., and Fichefet, T., 2009, The spatial and temporal complexity of the Holocene thermal maximum: Nature Geoscience, v. 2, p. 411–414, doi:10.1038/ngeo513.

Revenko, A.G., 2002, X-ray fluorescence analysis of rocks, soils and sediments: X-Ray Spectrometry, v. 31, p. 264–273, doi:10.1002/xrs.564.

Rhodes, A.N., 1998, A method for the preparation and quantification of microscopic charcoal from terrestrial and lacustrine sediment cores: The Holocene, v. 8, p. 113–117, doi:10.1191/095968398671104653.

Richard, P., 1970, Atlas pollinique des arbres et de quelques arbustes indigenes du Quebec. IV. Angiospermes (Rosacees, Anacardiacees, Aceracees, Rhamnacees, Tiliacees, Cornacees, Oleacees, Caprifoliacees): Natur Can,.

Richard, P., 1980, Histoire postglaciaire de la végétation au sud du lac Abitibi, Ontario et Québec: Géographie physique et Quaternaire, v. 34, p. 77–94, doi:10.7202/1000385ar.

Rius, D., Vanniére, B., and Galop, D., 2012, Holocene history of fire, vegetation and land use from the central Pyrenees (France): Quaternary Research, v. 77, p. 54–64, doi:10.1016/j.yqres.2011.09.009.

Roberts, B.A., Simon, N.P., and Deering, K.W., 2006, The forests and woodlands of Labrador, Canada: ecology, distribution and future management: Ecological Research, v. 21, p. 868–880, doi:doi.org/10.1007/s11284-006-0051-7.

Rockström, J. et al., 2009, Planetary Boundaries: Exploring the Safe Operating Space for Humanity: Ecology and Society, v. 14, p. art32, doi:10.5751/ES-03180-140232.

Rogers, B.M., Soja, A.J., Goulden, M.L., and Randerson, J.T., 2015, Influence of tree species on continental differences in boreal fires and climate feedbacks: Nature Geoscience, v. 8, p. 228–234, doi:10.1038/ngeo2352.

Rouhani, H., and Leconte, R., 2018, A methodological framework to assess PMP and PMF in snow-dominated watersheds under changing climate conditions – A case study of three watersheds in Québec (Canada): Journal of Hydrology, v. 561, p. 796–809, doi:10.1016/j.jhydrol.2018.04.047.

Royama, T., 1984, Population Dynamics of the Spruce Budworm Choristoneura Fumiferana: Ecological Monographs, v. 54, p. 429–462, doi:10.2307/1942595.

Ruddiman, W.F., 2006, Orbital changes and climate: Quaternary Science Reviews, v. 25, p. 3092–3112.

Rull, V., 2010, Ecology and Palaeoecology: Two Approaches, One Objective: The Open Ecology Journal, v. 3, p. 1–5, doi:10.2174/1874213001003020001.

Rustad, L., Campbell, J., Marion, G., Norby, R., Mitchell, M., Hartley, A., Cornelissen, J., Gurevitch, J., and GCTE-NEWS, 2001, A meta-analysis of the response of soil respiration, net nitrogen mineralization, and aboveground plant growth to experimental ecosystem warming: Oecologia, v. 126, p. 543–562, doi:10.1007/s004420000544.

Sánchez Goñi, M.F., Fourcade, T., Salonen, S., Lesven, J., Frigola, J., Swingedouw, D., and Sierro, F.J., 2021, Muted cooling and drying of NW Mediterranean in response to the strongest last glacial North American ice surges: GSA Bulletin, v. 133, p. 451–460, doi:10.1130/B35736.1.

Saucier, J., Robitaille, A., Bergeron, J., and Gosselin, J., 2011, Les Régions Écologiques du Québec Méridional (4ème version). Carte à L'échelle de 1/1250000: Direction des inventaires forestiers, Ministère des Ressources naturelles et de la Faune du Québec,.

Scheffer, M., Hirota, M., Holmgren, M., Van Nes, E.H., and Chapin, F.S., 2012, Thresholds for boreal biome transitions: Proceedings of the National Academy of Sciences, v. 109, p. 21384–21389, doi:10.1073/pnas.1219844110.

Senici, D., Chen, H.Y.H., Bergeron, Y., and Ali, A.A., 2015, The effects of forest fuel connectivity on spatiotemporal dynamics of Holocene fire regimes in the central boreal forest of North America: Forest fuel connectivity controls on boreal forest fire regimes: Journal of Quaternary Science, v. 30, p. 365–375, doi:10.1002/jqs.2790.

Senici, D., Lucas, A., Chen, H.Y.H., Bergeron, Y., Larouche, A., Brossier, B., Blarquez, O., and Ali, A.A., 2013, Multi-millennial fire frequency and tree abundance differ between xeric and mesic boreal forests in central Canada (P. Bellingham, Ed.): Journal of Ecology, v. 101, p. 356–367, doi:10.1111/1365-2745.12047.

Shackleton, N.J., and Opdyke, N.D., 1973, Oxygen Isotope and Palaeomagnetic Stratigraphy of Equatorial Pacific Core V28-238: Oxygen Isotope Temperatures and Ice Volumes on a 10: Quaternary Research, v. 3, p. 39–55, doi:10.1016/0033-5894(73)90052-5.

Shala, S., Helmens, K.F., Luoto, T.P., Salonen, J.S., Väliranta, M., and Weckström, J., 2017, Comparison of quantitative Holocene temperature reconstructions using multiple proxies from a northern boreal lake: The Holocene, v. 27, p. 1745–1755, doi:10.1177/0959683617708442.

Shorohova, E., Kneeshaw, D., Kuuluvainen, T., and Gauthier, S., 2011, Variability and dynamics of old-growth forests in the circumboreal zone: implications for conservation, restoration and management: Silva Fennica, p. 22, doi:10.14214/sf.72.

Shvidenko, A., and Schepaschenko, D., 2013, Climate change and wildfires in Russia: Contemporary Problems of Ecology, v. 6, p. 683–692, doi:10.1134/S199542551307010X.

Sienkiewicz, E., 2016, Post-glacial acidification of two alpine lakes (Sudetes Mts., SW Poland), as inferred from diatom analyses: Acta Palaeobotanica, v. 56, p. 65–77, doi:10.1515/acpa-2016-0002.

Simard, I., Morin, H., and Lavoie, C., 2006, A millennial-scale reconstruction of spruce budworm abundance in Saguenay, Québec, Canada: The Holocene, v. 16, p. 31–37, doi:10.1191/0959683606hl904rp.

Simpson, G.L., 2007, Analogue Methods in Palaeoecology: Using the **analogue** Package: Journal of Statistical Software, v. 22, doi:10.18637/jss.v022.i02.

Simpson, G.L., and Anderson, N.J., 2009, Deciphering the effect of climate change and separating the influence of confounding factors in sediment core records using additive models: Limnology and Oceanography, v. 54, p. 2529–2541, doi:10.4319/lo.2009.54.6_part_2.2529.

Sirois, L., 1997, Distribution and dynamics of balsam fir (Abies balsamea [L.] Mill.) at its northern limit in the James Bay area: Écoscience, https://www.tandfonline.com/doi/abs/10.1080/11956860.1997.11682413 (accessed March 2024).

Sirois, L., 2000, Spatiotemporal variation in black spruce cone and seed crops along a boreal forest – tree line transect: v. 30, p. 10, doi:10.1139/x00-015.

Skay, R., Windmuller-Campione, M.A., Russell, M.B., and Reuling, L.F., 2021, Influence of eastern spruce dwarf mistletoe on stand structure and composition in northern Minnesota: Forest Ecology and Management, v. 481, p. 118712, doi:10.1016/j.foreco.2020.118712.

Smol, J.P., 2009, Pollution of Lakes and Rivers: A Paleoenvironmental Perspective: John Wiley & Sons, 401 p.

Smol, J.P., and Cumming, B.F., 2000, Tracking Long-Term Changes in Climate Using Algal Indicators in Lake Sediments: Journal of Phycology, v. 36, p. 986–1011, doi:10.1046/j.1529-8817.2000.00049.x.

Sniderhan, A.E., 2018, Growth dynamics of black spruce (Picea mariana) across northwestern North America: , p. 200.

Sniderhan, A.E., Mamet, S.D., and Baltzer, J.L., 2021, Non-uniform growth dynamics of a dominant boreal tree species (*Picea mariana*) in the face of rapid climate change: Canadian Journal of Forest Research, v. 51, p. 565–572, doi:10.1139/cjfr-2020-0188.

Snyder, P.K., Delire, C., and Foley, J.A., 2004, Evaluating the influence of different vegetation biomes on the global climate: Climate Dynamics, v. 23, p. 279–302, doi:10.1007/s00382-004-0430-0.

Soja, A.J., Tchebakova, N.M., French, N.H., Flannigan, M.D., Shugart, H.H., Stocks, B.J., Sukhinin, A.I., Parfenova, E., Chapin III, F.S., and Stackhouse Jr, P.W., 2007, Climate-induced boreal forest change: predictions versus current observations: Global and Planetary Change, v. 56, p. 274–296, doi:doi.org/10.1016/j.gloplacha.2006.07.028.

Sonia, S., Morin, H., and Krause, C., 2011, Long-term spruce budworm outbreak dynamics reconstructed from subfossil trees: Journal of Quaternary Science, v. 26, p. 734–738, doi:10.1002/jqs.1492.

Sperry, J.S., and Robson, D.J., 2001, Xylem Cavitation and Freezing in Conifers, *in* Bigras, F.J. and Colombo, S.J. eds., Conifer Cold Hardiness, Dordrecht, Springer Netherlands, Tree Physiology, p. 121–136, doi:10.1007/978-94-015-9650-3_5.

Splawinski, T.B., Boucher, Y., Bouchard, M., Greene, D.F., Gauthier, S., Auger, I., Sirois, L., Valeria, O., and Bergeron, Y., 2022, Factors influencing black spruce reproductive potential in the northern boreal forest of Quebec: Canadian Journal of Forest Research, v. 52, p. 1499–1512, doi:10.1139/cjfr-2022-0092.

Splawinski, T.B., Cyr, D., Gauthier, S., Jetté, J.-P., and Bergeron, Y., 2019a, Analyzing risk of regeneration failure in the managed boreal forest of northwestern Quebec: Canadian Journal of Forest Research, v. 49, p. 680–691, doi:10.1139/cjfr-2018-0278.

Splawinski, T., Schab, A., Leduc, A., Valeria, O., Cyr, D., Pascual Puigdevall, J., Gauthier, S., and Bergeron, Y., 2019b, Ajustement des stratégies de production de bois dans certaines portions sensibles de la forêt boréale: Rapport présenté au Ministère des Forêts, de la Faune et des Parcs par la Chaire industrielle CRSNG UQAT-UQAM en aménagement forestier durable, p. 1–120.

Stocks, B. et al., 2002, Large forest fires in Canada, 1959–1997: Journal of Geophysical Research: Atmospheres, v. 107, p. FFR-5, doi:10.1029/2001JD000484.

Strömgren, M., and Linder, S., 2002, Effects of nutrition and soil warming on stemwood production in a boreal Norway spruce stand: Global Change Biology, v. 8, p. 1194–1204, doi:10.1046/j.1365-2486.2002.00546.x.

Subedi, N., and Sharma, M., 2013, Climate-diameter growth relationships of black spruce and jack pine trees in boreal Ontario, Canada: Global Change Biology, v. 19, p. 505–516, doi:10.1111/gcb.12033.

Suding, K.N., Gross, K.L., and Houseman, G.R., 2004, Alternative states and positive feedbacks in restoration ecology: Trends in Ecology & Evolution, v. 19, p. 46–53, doi:10.1016/j.tree.2003.10.005.

Suding, K.N., and Hobbs, R.J., 2009, Threshold models in restoration and conservation: a developing framework: Trends in Ecology & Evolution, v. 24, p. 271–279, doi:10.1016/j.tree.2008.11.012.

Swain, A.M., 1973, A History of Fire and Vegetation in Northeastern Minnesota as Recorded in Lake Sediments: Quaternary research, v. 3, p. 383–396, doi:10.1016/0033-5894(73)90004-5.

Tam, B., Szeto, K., Bonsal, B., Flato, G., Cannon, A., and Rong, R., 2018, CMIP5 drought projections in Canada based on the Standardized Precipitation Evapotranspiration Index: Canadian Water Resources Journal / Revue canadienne des ressources hydriques, v. 44, p. 1–18, doi:10.1080/07011784.2018.1537812.

Teitelbaum, S., Asselin, H., Bissonnette, J.-F., and Blouin, D., 2023, Governance in the Boreal Forest: What Role for Local and Indigenous Communities?, *in* Girona, M.M., Morin, H., Gauthier, S., and Bergeron, Y. eds., Boreal Forests in the Face of Climate Change: Sustainable Management, Cham, Springer International Publishing, Advances in Global Change Research, p. 513–532, doi:10.1007/978-3-031-15988-6_20.

Telford, R.J., and Birks, H.J.B., 2011, Effect of uneven sampling along an environmental gradient on transfer-function performance: Journal of Paleolimnology, v. 46, p. 99–106, doi:10.1007/s10933-011-9523-z.

Telford, R.J., and Birks, H.J.B., 2005, The secret assumption of transfer functions: problems with spatial autocorrelation in evaluating model performance: Quaternary Science Reviews, v. 24, p. 2173–2179, doi:10.1016/j.quascirev.2005.05.001.

Ter Braak, C.J.F., 1986, Canonical Correspondence Analysis: A New Eigenvector Technique for Multivariate Direct Gradient Analysis: Ecology, v. 67, p. 1167–1179, doi:10.2307/1938672.

Ter Braak, C.J.F., and Prentice, I.C., 1988, A Theory of Gradient Analysis, *in* Begon, M., Fitter, A.H., Ford, E.D., and Macfadyen, A. eds., Advances in Ecological Research, Academic Press, v. 18, p. 271–317, doi:10.1016/S0065-2504(08)60183-X.

Terrier, A., Girardin, M.P., Périé, C., Legendre, P., and Bergeron, Y., 2013, Potential changes in forest composition could reduce impacts of climate change on boreal wildfires: Ecological Applications, v. 23, p. 21–35, doi:10.1890/12-0425.1.

Thompson, I.D. (Ed.), 2009, Forest resilience, biodiversity, and climate change: a synthesis of the biodiversity / resiliende / stability relationship in forest ecosystems: Montreal, Secretariat of the Convention on Biological Diversity, CBD technical series 43, 67 p.

Thompson, R., Battarbee, R.W., O'sullivan, P., and Oldfield, F., 1975, Magnetic susceptibility of lake sediments: Limnology and Oceanography, v. 20, p. 687–698.

Thornalley, D.J.R. et al., 2018, Anomalously weak Labrador Sea convection and Atlantic overturning during the past 150 years: Nature, v. 556, p. 227–230, doi:10.1038/s41586-018-0007-4.

Tinner, W., and Hu, F.S., 2003, Size parameters, size-class distribution and area-number relationship of microscopic charcoal: relevance for fire reconstruction: The Holocene, v. 13, p. 499–505, doi:10.1191/0959683603hl615rp.

Truchon-Savard, A., Jean, M., and Payette, S., 2019, Black spruce (Picea mariana) colonization of subarctic snowpatches in response to warmer climate: Journal of Ecology, v. 107, p. 1154–1166, doi:10.1111/1365-2745.13123.

Trugman, A.T., Medvigy, D., Anderegg, W.R.L., and Pacala, S.W., 2018, Differential declines in Alaskan boreal forest vitality related to climate and competition: Global Change Biology, v. 24, p. 1097–1107, doi:10.1111/gcb.13952.

Trumbore, S., Brando, P., and Hartmann, H., 2015, Forest health and global change: Science, v. 349, p. 814–818.

Turetsky, M.R., Kane, E.S., Harden, J.W., Ottmar, R.D., Manies, K.L., Hoy, E., and Kasischke, E.S., 2011, Recent acceleration of biomass burning and carbon losses in Alaskan forests and peatlands: Nature Geoscience, v. 4, p. 27–31, doi:10.1038/ngeo1027.

Tymstra, C., Flannigan, M.D., Armitage, O.B., and Logan, K., 2007, Impact of climate change on area burned in Alberta's boreal forest: International Journal of Wildland Fire, v. 16, p. 153, doi:10.1071/WF06084.

Tzedakis, P., Hooghiemstra, H., and Pälike, H., 2006, The last 1.35 million years at Tenaghi Philippon: revised chronostratigraphy and long-term vegetation trends: Quaternary Science Reviews, v. 25, p. 3416–3430.

Ullman, D.J., Carlson, A.E., Hostetler, S.W., Clark, P.U., Cuzzone, J., Milne, G.A., Winsor, K., and Caffee, M., 2016a, Final Laurentide ice-sheet deglaciation and Holocene climate-sea level change: Quaternary Science Reviews, v. 152, p. 49–59, doi:10.1016/j.quascirev.2016.09.014.

Ullman, D.J., Carlson, A.E., Hostetler, S.W., Clark, P.U., Cuzzone, J., Milne, G.A., Winsor, K., and Caffee, M., 2016b, Final Laurentide ice-sheet deglaciation and Holocene climate-sea level change: Quaternary Science Reviews, v. 152, p. 49–59, doi:10.1016/j.quascirev.2016.09.014.

Van Bogaert, R., Gauthier, S., Drobyshev, I., Jayen, K., Greene, D.F., and Bergeron, Y., 2015, Prolonged Absence of Disturbance Associated with Increased Environmental Stress May Lead to Reduced Seedbank Size in Picea mariana in Boreal Eastern North America: Ecosystems, v. 18, p. 1135–1150, doi:10.1007/s10021-015-9888-3.

Van Cleve, K., Oechel, W.C., and Hom, J.L., 1990, Response of black spruce (Picea mariana) ecosystems to soil temperature modification in interior Alaska: Canadian Journal of Forest Research, v. 20, p. 1530–1535, doi:10.1139/x90-203.

Veilleux-Nolin, M., and Payette, S., 2012, Influence of recent fire season and severity on black spruce regeneration in spruce–moss forests of Quebec, Canada [1] This article is one of a selection of papers from the 7th International Conference on Disturbance Dynamics in Boreal Forests.: Canadian Journal of Forest Research, v. 42, p. 1316–1327, doi:10.1139/x2012-098.

Velle, G., Brodersen, K.P., Birks, H.J.B., and Willassen, E., 2010, Midges as quantitative temperature indicator species: Lessons for palaeoecology: The Holocene, v. 20, p. 989–1002, doi:10.1177/0959683610365933.

Velle, G., Brooks, S.J., Birks, H.J.B., and Willassen, E., 2005, Chironomids as a tool for inferring Holocene climate: an assessment based on six sites in southern Scandinavia: Quaternary Science Reviews, v. 24, p. 1429–1462, doi:10.1016/j.quascirev.2004.10.010.

de Vernal, A., Guiot, J., and Turon, J.-L., 1993, Late and Postglacial Paleoenvironments of the Gulf of St. Lawrence: Marine and Terrestrial Palynological Evidence: Géographie physique et Quaternaire, v. 47, p. 167–180, doi:10.7202/032946ar.

Verneaux, J., Vidonne, A., Remy, F., and Guyard, A., 1991, Particules organiques et rapport C/N des sédiments des lacs du Jura: Annales de Limnologie - International Journal of Limnology, v. 27, p. 175–190, doi:10.1051/limn/1991014.

Viau, A.E., and Gajewski, K., 2009, Reconstructing Millennial-Scale, Regional Paleoclimates of Boreal Canada during the Holocene: Journal of Climate, v. 22, p. 316–330, doi:10.1175/2008JCLI2342.1.

Viereck, L.A., Johnston, W.F., Burns, R.M., and Honkala, B.H., 1990, Silvics of North America. Picea mariana (Mill.) BSP, black spruce.: U.S.D.A. Forest Service Agriculture Handbook 654, Washington, DC, v. 1, Conifers, 227–237 p.

Vogel, M.F., Asselin, H., Joannin, S., Bergeron, Y., Leclercq, S., Latapy, C., and Ali, A.A., 2023, Early afforestation on islands of proglacial Lake Ojibway as evidence of post-glacial migration outposts: The Holocene, v. 33, p. 975–985, doi:10.1177/09596836231169988.

van Vuuren, D.P. et al., 2011, The representative concentration pathways: an overview: Climatic Change, v. 109, p. 5, doi:10.1007/s10584-011-0148-z.

Walker, X.J. et al., 2020, Fuel availability not fire weather controls boreal wildfire severity and carbon emissions: Nature Climate Change, v. 10, p. 1130–1136, doi:10.1038/s41558-020-00920-8.

Walker, X.J. et al., 2019, Increasing wildfires threaten historic carbon sink of boreal forest soils: Nature, v. 572, p. 520–523, doi:10.1038/s41586-019-1474-y.

Walker, X., and Johnstone, J.F., 2014, Widespread negative correlations between black spruce growth and temperature across topographic moisture gradients in the boreal forest: Environmental Research Letters, v. 9, p. 064016, doi:10.1088/1748-9326/9/6/064016.

Walker, I.R., and MacDonald, G.M., 1995, Distributions of Chironomidae (Insecta: Diptera) and other freshwater midges with respect to treeline, Northwest Territories, Canada: Arctic and Alpine Research, v. 27, p. 258–263, doi:10.1080/00040851.1995.12003120.

Walker, X.J., Mack, M.C., and Johnstone, J.F., 2017, Predicting Ecosystem Resilience to Fire from Tree Ring Analysis in Black Spruce Forests: Ecosystems, v. 20, p. 1137–1150, doi:10.1007/s10021-016-0097-5.

Walker, X.J., Mack, M.C., and Johnstone, J.F., 2015, Stable carbon isotope analysis reveals widespread drought stress in boreal black spruce forests: Global Change Biology, v. 21, p. 3102–3113, doi:10.1111/gcb.12893.

Walker, I.R., and Mathewes, R.W., 1987, Chironomids, Lake Trophic Status, and Climate: Quaternary Research, v. 28, p. 431–437, doi:10.1016/0033-5894(87)90010-X.

Wang, X., Parisien, M.-A., Taylor, S.W., Candau, J.-N., Stralberg, D., Marshall, G.A., Little, J.M., and Flannigan, M.D., 2017, Projected changes in daily fire spread across Canada over the next century: Environmental Research Letters, v. 12, p. 025005, doi:10.1088/1748-9326/aa5835.

Webb, T., 1986, Is vegetation in equilibrium with climate? How to interpret late-Quaternary pollen data: Vegetatio, v. 67, p. 75–91, doi:10.1007/BF00037359.

Weir, J.M.H., Johnson, E.A., and Miyanishi, K., 2000, Fire Frequency and the Spatial Age Mosaic of the Mixed-Wood Boreal Forest in Western Canada: Ecological Applications, v. 10, p. 1162–1177, doi:10.1890/1051-0761(2000)010[1162:FFATSA]2.0.CO;2.

Weltzin, J.F., Belote, R.T., and Sanders, N.J., 2003, Biological invaders in a greenhouse world: will elevated CO2 fuel plant invasions? Frontiers in Ecology and the Environment, v. 1, p. 146–153, doi:10.1890/1540-9295(2003)001[0146:BIIAGW]2.0.CO;2.

Weng, C., 2005, An improved method for quantifying sedimentary charcoal via a volume proxy: The Holocene, v. 15, p. 298–301, doi:10.1191/0959683605hl795rr.

Westwood, A.R., Conciatori, F., Tardif, J.C., and Knowles, K., 2012, Effects of Armillaria root disease on the growth of Picea mariana trees in the boreal plains of central Canada: Forest Ecology and Management, v. 266, p. 1–10, doi:10.1016/j.foreco.2011.11.005.

Whitlock, C., and Larsen, C., 2002, Charcoal as a fire proxy, *in* Tracking environmental change using lake sediments, Springer, p. 75–97.

Whitmore, J. et al., 2005, Modern pollen data from North America and Greenland for multi-scale paleoenvironmental applications: Quaternary Science Reviews, v. 24, p. 1828–1848, doi:10.1016/j.quascirev.2005.03.005.

Wiederholm, T., 1983, Chironomidae of the Holarctic region. Keys and diagnoses. Part 1: Larvae: Entomologica scandinavica. Supplementum, v. 34, p. 532.

Wilmking, M., Juday, G.P., Barber, V.A., and Zald, H.S.J., 2004, Recent climate warming forces contrasting growth responses of white spruce at treeline in Alaska through temperature thresholds: Global Change Biology, v. 10, p. 1724–1736, doi:10.1111/j.1365-2486.2004.00826.x.

Wold, S., Esbensen, K., and Geladi, P., 1987, Principal component analysis: Chemometrics and intelligent laboratory systems, v. 2, p. 37–52.

Wolkovich, E.M. et al., 2012, Warming experiments underpredict plant phenological responses to climate change: Nature, v. 485, p. 494–497, doi:10.1038/nature11014.

Wood, S.N., 2017, Generalized additive models: an introduction with R: Boca Raton, CRC Press/Taylor & Francis Group, Chapman & Hall/CRC texts in statistical science, 476 p.

Wood, S., and Wood, M.S., 2015, Package 'mgcv': R package version, v. 1, p. 729.

Wotton, B.M., and Flannigan, M.D., 1993, Length of the fire season in a changing climate: The Forestry Chronicle, v. 69, p. 187–192, doi:10.5558/tfc69187-2.

Wotton, B.M., Flannigan, M.D., and Marshall, G.A., 2017, Potential climate change impacts on fire intensity and key wildfire suppression thresholds in Canada: Environmental Research Letters, v. 12, p. 095003, doi:10.1088/1748-9326/aa7e6e.

Wotton, B.M., Nock, C.A., and Flannigan, M.D., 2010, Forest fire occurrence and climate change in Canada: International Journal of Wildland Fire, v. 19, p. 253, doi:10.1071/WF09002.

Wright, H.A., 1974, Effect of Fire on Southern Mixed Prairie Grasses: Journal of Range Management, v. 27, p. 417, doi:10.2307/3896712.

Yin, Q.Z., and Berger, A., 2012, Individual contribution of insolation and CO 2 to the interglacial climates of the past 800,000 years: Climate dynamics, v. 38, p. 709–724.

Youngblut, D., and Luckman, B., 2008, Maximum June–July temperatures in the southwest Yukon over the last 300 years reconstructed from tree rings: Dendrochronologia, v. 25, p. 153–166, doi:10.1016/j.dendro.2006.11.004.

Zasada, J., Viereck, L., and Foote, M., 1979, Quantity and quality of dispersed seed: Ecological effects of the Wickersham Dome fire near Fairbanks, Alaska. Edited by L. Viereck and CT Dyrness. USDA For. Serv. Gen. Tech. Rep. PNW-90, Portland, Oreg, p. 45–49.

Zhang, T., Barry, R., Knowles, K., Ling, F., and Armstrong, R., 2003, Distribution of seasonally and perennially frozen ground in the Northern Hemisphere, *in* Proceedings of the 8th International Conference on Permafrost, AA Balkema Publishers Zürich, Switzerland, v. 2, p. 1289–1294.

Zhang, Q., and Chen, W., 2007, Fire cycle of the Canada's boreal region and its potential response to global change: Journal of Forestry Research, v. 18, p. 55–61, doi:10.1007/s11676-007-0010-3.

Zhang, P., and Sutton, J., 2011, High temperature, darkness, and drought predispose black spruce seedlings to gray mold: Canadian Journal of Botany, v. 72, p. 135–142, doi:10.1139/b94-018.

Zou, Y., Miao, Y., Yang, S., Zhao, Y., Wang, Z., Tang, G., and Yang, S., 2021, A New Automatic Statistical Microcharcoal Analysis Method Based on Image Processing, Demonstrated in the Weiyuan Section, Northwest China: Frontiers in Earth Science, v. 9, p. 609916, doi:10.3389/feart.2021.609916.